The University Of Sheffield.

The investigation of novel virulence genes in *Porphyromonas gingivalis*

By:

Ashley Frederick Gains

A thesis submitted in partial fulfilment of the requirements for the degree of Doctor of Philosophy

University of Sheffield

Faculty of Medicine, Dentistry and Health

School of Clinical Dentistry

27/09/2021

Summary

This study focuses on *Porphyromonas gingivalis*, a Gram negative anaerobic bacterium and a "Keystone" pathogen involved with the progression of periodontal diseases. *P. gingivalis* produces multiple virulence factors that have been linked to other chronic diseases such as cardiovascular disease and Alzheimer's disease. Through the use of fimbriae, gingipain proteases, lipopolysaccharide, and outer membrane proteins, this bacteria has the ability to interact with its host. These host-pathogen interactions allow *P. gingivalis* to bind and invade host cells, influence an inflammatory response whilst simultaneously suppressing local immune defences. This provides a better niche for the survival of the pathogenic subgingival microbiota that progress the chronic inflammatory conditions of periodontal disease. In this thesis, the virulence of *P. gingivalis* is investigated through the study of three genes indicated to be involved in the invasion of host cells, *ompH1, rfbB* and *PGN2012*, whilst simultaneously attempting to identify human receptors involved with *P. gingivalis* adhesion.

Through knockout mutagenesis, these genes have been disrupted and the characterisation of these mutants through investigating their virulence has been assessed. The outer membrane protein chaperone *OmpH1* mutant resulted in reduced adhesion and invasion of H357 (oral epithelial) cells, and reduced protease activity, providing more evidence that the ompH chaperone proteins have clients involved in host-pathogen interactions. The rhamnose synthesis gene mutant *rfbB* produces a truncated lipopolysaccharide and has demonstrated a decreased virulence in multiple assays including biofilm formation, adhesion and invasion of H357 cells, and protease activity. Finally, it has been demonstrated that the efflux channel protein gene *PGN2012* is involved with heavy metal efflux, specifically Zn^{2+}, Co^{2+} and Cd^{2+}, whilst having no significant role in adhesion and invasion of H357 cells. This indicates that *PGN2012* may have a role in intracellular survival rather than the mechanics of invading host cells.

Overall, we demonstrate the important role of surface components in the host-pathogen interactions of *P. gingivalis*. This work also reveals that the *PGN2012* operon is the CzcCBA heavy metal efflux system in *P. gingivalis*.

Acknowledgements

I would like to thank the University of Sheffield for giving me this opportunity and the funding they have provided to make it possible.

A huge thank you to my brilliant supervisor Professor Graham Stafford, without whom I would not be doing this PhD in the first place. Thank you for always believing in me and pushing me when I needed it, thanks to you I have progressed so much from when I first started my masters project. Your advice and guidance have taught me how to hold myself and my work to a higher standard, without which this thesis would not have been produced. The effort and dedication that you put into your work, and that of your students will always be inspiring to me. I would also like to thank my secondary supervisor Professor Daniel Lambert, for academic guidance, support, encouragement, and brilliant input throughout. I could not have had better supervisors.

Thanks also go to our brilliant technical staff Jason and Brenka. You are the backbone of our labs and an endless source of problem solving know how! The brilliant work ethic you provide, and unending patience have made our labs a great place to work.

I would like to thank the dental school community of PhD students, post docs and supervisors who are always happy to help and teach. The collaborative and friendly environment which is at the heart of our department is what makes it so great. Huge thanks to the collaborative force of microbiologists in the Stafford/Shepherd research group, what a great team to have!

I have been lucky enough to meet multiple post docs who have provided me with, encouragement, enthusiasm, advice, guidance, friendship, and kind words. Special thanks to Liz, Tom, George, Caroline, Natalya, and Toby for always believing in me.

Thank you to Kittie, Beth, Cher, and Anita. What a great group of friends to start my journey with. Your great encouragement and company have helped me through the hardest times of the PhD process, whilst making the good times better!

I am incredibly grateful for the support and encouragement of my parents, thanks mum and dad for always being there for me and keeping me sane.

Finally, I would like to thank my amazing fiancé Hannah, for being my rock through the hard times and always encouraging and believing in me. I could not have done this without you.

Abbreviation's list

ABC - ATP binding cassette

ACPA - Anti-citrullinated protein antibodies

AD - Alzheimer's disease

AI2 - Autoinducer 2

A-LPS - Anionic lipopolysaccharide

Amp - Ampicillin

APS - Anionic polysaccharide

ATP - Adenosine Triphosphate

BAM - Beta barrel assembly machinery

BCA - Bicinchoninic acid assay

BMEC - Brain microvascular endothelial cells

BPE - Bovine pituitary extract

BS3 - Bis(sulfosuccinimidyl)suberate

BSA - Bovine serum albumin

C3/5 - Complement 3/5

CAL - Clinical attachment loss

CD14 - Cluster of differentiation 14

COG - Clusters of orthologous groups

CTD - C-Terminal domain

CVD - Cardiovascular disease

DC - Dendritic cells

DC-SIGN - Dendritic cell specific ICAM-3 grabbing nonintegrin

DMEM - Dulbecco's modified eagle medium

DMS - Dimethyl suberimidate

DSS - Disuccinimidyl suberate

DST - Disuccinimidyl tartrate

DTBP - Dimethyl 3,3'-dithiobispropionimidate

dTDP - Deoxythymidine diphosphate

DTSSP - 3,3′-dithiobis(sulfosuccinimidylpropionate)

ECL - Enhanced chemiluminescence

ECM - Extracellular matrix

EDTA - Ethylenediaminetetraacetic acid

EGF - Epidermal growth factor

ELISA - Enzyme linked immunosorbent assay

EPI - Efflux pump inhibitors

EPS - Extracellular polymeric substance

Ery - Erythromycin

FA - Fastidious anaerobe

FAB - Fastidious anaerobe blood agar

FBS - Foetal bovine serum

FePPIX - Protoporphyrin 9

HME - Heavy metal efflux

HMEC - Human microvascular endothelial cells

HRP - Horse radish peroxidase

IL- Interleukin

IMDM - Iscove's Modified Dulbecco's Medium

IGV - Integrative genomics viewer

KB - Kilobases

KDa - Kilo Dalton

Kgp - Lysine targeting gingipain protease

KSFM - Keratinocyte serum-free media

LB - Luria broth

LBP - Lipopolysaccharide binding protein

LPS - Lipopolysaccharide

MATE - Multidrug and toxin extrusion

MDM - Monocyte derived macrophages

MFP - Membrane fusion protein

MFS - Major facilitator superfamily

MOI - Multiplicity of infection

MS - Mass spectrometry

mTOR - Mechanistic target of rapamycin

NEB - New England Biolabs

OMV - Outer membrane vesicles

OSCC - Oral squamous cell carcinoma

OD - Optical density

PAD - Peptidyl arginine deiminase

PAMP - Pathogen associated molecular pattern

PAR - protease activated receptors

PBS - Phosphate buffered saline

PCR - Polymerase chain reaction

PaβN - Phe-Arg β-naphthylamide

qPCR - Quantitative polymerase chain reaction

RA - Rheumatoid arthritis

RBL - Radiographic bone loss

RE1 - Resolvin E1

Rgp - Arginine targeting gingipain protease

RND - Resistance nodulation division

SDS-PAGE - Sodium dodecyl sulphate polyacrylamide gels

SKP - Seventeen Kilo Dalton protein

SMR - Small multidrug resistance

Sulfo-NHS - N-hydroxysulfosuccinimide

TAE - Tris acetate EDTA buffer

TBS - Tris buffered saline

Tet - Tetracycline

TLCK - Tosyl-L-lysyl-chloromethane hydrochloride

TLR - Toll like receptor

TNFα - Tumor necrosis factor alpha

TPCK - N-α-tosyl-L-phenylalanine chloromethyl ketone

T9SS - Type 9 secretion system

Und-P - Undecaprenyl phosphate

UP - Ultrapure

WHO - World health organisation

Contents

List of Figures

List of tables

Chapter 1. Introduction and literature review

1.1 Periodontal disease

Periodontal diseases are a set of chronic inflammatory diseases such as periodontitis that cause the inflammation and eventual destruction of the periodontium, the supporting structure of the tooth. The periodontium consists of the gingiva, periodontal ligament, and alveolar bone. Periodontal diseases begin when plaque formation that occurs on the tooth surface spreads into the sub-gingiva creating a reversible inflammatory state known as gingivitis. If untreated this inflammation will progress and cause periodontitis creating a niche to develop in the sub-gingiva known as a periodontal pocket, this allows a shift in the oral microbiota from commensal aerobic Gram-positive early colonisers such as streptococci to anaerobic Gram negative pathobionts such as *Porphyromonas gingivalis*, *Tannerella forsythia* and *Treponema denticola*, this shift is known as dysbiosis (Hajishengallis and Lamont, 2012; How, Song and Chan, 2016; Kinane, Stathopoulou and Papapanou, 2017) (Figure 1.1). As the anaerobic Gram negative bacteria populate the periodontal pockets, this progresses the inflammatory response from the host and causes the destruction of the surrounding gingiva and periodontal ligament, whilst also inducing resorption of the alveolar bone, these symptoms are recognised as chronic periodontitis which causes irreversible damage and eventually leads to tooth loss. Although periodontal disease is recognised as a polymicrobial disease (Kinane, Stathopoulou and Papapanou, 2017), there are groups of bacteria recognised as having a greater effect on the progression of periodontal disease. A study by Socransky *et al* (1998) investigated the different bacterial communities in healthy patients and patients with periodontal disease to identify the etiological bacteria involved, it was discovered that the "red complex" of *P. gingivalis, Tannerella forsythia,* and *Treponema denticola* were consistently related to periodontal symptoms such as a large gingival pocket depth and bleeding during gingiva probing. There have been further studies that have provided more evidence to the relationship between the red complex and periodontal disease, such as a study by Colombo *et al* (2013) in which subgingival plaque samples were taken from patients with and without periodontitis. The samples were then separated into healthy, treatable periodontitis, or "refractory" periodontitis (unresponsive to treatment), it was found that there was significantly greater detection of the red complex bacteria in refractory periodontitis than in treatable and healthy patients. It has also been shown that the red complex has a role in apical periodontitis, and has been found in necrotic root pulp (Rôças *et al.*, 2001; Siqueira, Alves and Rôças, 2011). A recent investigation by Na *et al* (2020) into the

microbiome profiles buccal mucosa and supragingival space of periodontitis patients and healthy patients presented similar results, showing significant increase in numbers of the red complex bacteria, but also *Filifactor alocis, Fretibacteria fastidiosum, Prevotella intermedia* and *Treponema maltophilum* in periodontitis*.* However, the role of inflammation in the dysbiosis of subgingival biofilm communities suggest that the progression of periodontal disease is not specific to the overgrowth of the red complex, but a change in the overall microbiome from health associated to disease associated bacteria in response to inflammation (Curtis, Diaz and Van Dyke, 2020).

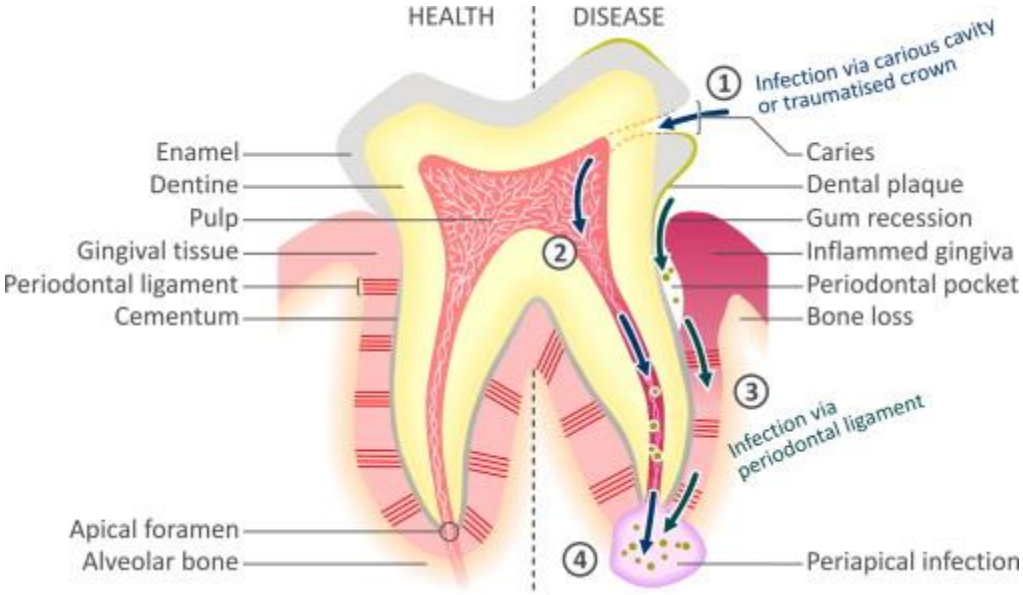

Figure 2.1. Mechanisms of infection in periodontal disease. Periodontal disease such as periodontitis progress through the development of subgingival pockets due to plaque growth into the gingiva. The etiological "red complex" bacteria have also been found to be involved with apical periodontitis travelling through cavities in the tooth (Siqueira, Alves and Rôças, 2011). Taken from the review paper by Douglas *et al* (2014) with permission.

Recently there has been revisions in the clinical identification and grading of periodontitis disease, changing the classification of periodontitis progression to give a greater understanding of the complexity of the disease and the treatment required in a patient dependant manner. In the study by Tonetti *et al* (2018) they proposed a framework grading system for periodontitis. They provide two separate and specific classifications for the stage of periodontitis, and the grade of periodontitis. They suggest four stages (I-IV) of periodontitis which are categorised by increasing severity in clinical attachment loss (CAL), Radiographic bone loss (RBL), tooth loss and descriptions of complexity. This is then supplemented with grading the rate of periodontitis progression in a three grade system (A, B and C). This grading

system takes into consideration the direct evidence of progression (CAL and RBL), indirect evidence of progression (case phenotype), risk factors (smoking and diabetes) and inflammatory burden.

1.2 Bacteriology of Periodontal disease

Bacteria are essential for the progression of chronic periodontal disease, this has been shown in the literature through the lack of alveolar bone loss in germ free mice in comparison to mice with commensal bacteria (George Hajishengallis *et al.*, 2011). The shift of bacteria from healthy commensal bacteria to a dysbiotic pathogenic community is complex and has multiple factors.

1.2.1 Oral biofilm formation

The oral environment is subject to factors that make bacterial colonisation difficult, such as fluid shearing from saliva (Douglas *et al.*, 2014). Therefore, it is important for oral bacteria to be able to form biofilms to protect the growing bacterial community.

The initial development of oral biofilms occur where the gingiva meets the tooth surface, where early colonising bacteria attach themselves to the glycoprotein rich coating of the tooth known as the pellicle (Huang, Li and Gregory, 2011), or inhabit the subgingival environment living on the protein rich gingival crevicular fluid. These early colonisers are often Gram positive species such as *Actinomyces* and S*treptococci*, that can adhere to the proline rich proteins of the pellicle and aggregate other bacteria in the initial biofilm formation (Kolenbrander *et al.*, 2006). These types of early pioneer bacteria are found in abundance in the healthy subgingival environment (Chen *et al.*, 2018). The initial colonising bacteria allow the co-aggregation of other oral bacteria to progress the maturation of the biofilm. The progression of biofilms is stimulated by bacterial cross communication through a process called “quorum sensing”. The communication comes in the form of population dependant secretion of auto-inducers, that signal bacteria to aggregate in communities by inducing gene expression to swap from planktonic to biofilm producing phenotypes (Plančak, Musić and Puhar, 2015). The auto-inducers in Gram negative bacteria are commonly acyl-homoserine lactones like the LuxI/R system described in *Vibrio fischeri* (Schaefer *et al.*, 1996), whereas the auto-inducer system in Gram positive are often peptide based with kinase receptors (Miller and Bassler, 2001). However, subgingival biofilms are complex and are composed of both Gram negative and Gram-positive bacteria, requiring auto-inducers that

can communicate with both types. Auto-inducer 2 (AI2) is an inducer for both Gram negative and positive bacteria that was initially identified in *Vibrio harveyi* (Bassler, Wright and Silverman, 1994). AI2 has been shown to be produced by periodontal pathogens such as *P. gingivalis* and *Fusobacterium nucleatum* (Chung *et al.*, 2001; Frias, Olle and Alsina, 2001; Gerits, Verstraeten and Michiels, 2017).

Quorum sensing attracts multiple species of bacteria to coaggregate to progress the biofilm. This occurs through recognition of specific polysaccharides on bacterial membranes via their respective lectins (Huang, Li and Gregory, 2011). Specific bacteria such as *F. nucleatum* are considered bridging bacteria due to their ability to coaggregate multiple species of bacteria (Bradshaw *et al.*, 1998). With *F. nucleatum* being specifically important for the development of oral biofilms due to the coaggregation of early colonisers such as *S. oralis* and late colonisers such as *P. gingivalis*. Once the biofilms begin to mature through the aggregation of multiple species of bacteria, a extracellular polymeric substance (EPS) matrix is produced consisting of exopolysaccharide, extracellular DNA and proteins (Cugini *et al.*, 2019). This matrix provides structural integrity for the community whilst also acting as a diffusion barrier for harmful chemicals such as antibiotics (Sharma, Misba and Khan, 2019). The oral biofilm formation is a complex system which requires features from the bacteria forming the biofilm, such as adhesins, lectins, pili and fimbriae that allow bacterial coaggregation, whilst also requiring pellicle glycoproteins from the host.

The progression of oral biofilms deeper into the subgingival space leads to a subgingival pocket. This new environmental niche and maturing biofilm is more fit for anaerobic bacteria, leading to a shift towards late colonising anaerobic Gram negative pathogens such as *P. gingivalis* being enriched for in the biofilm community (Bosshardt, 2018).

1.2.2 Dysbiosis and host inflammation in periodontal disease

During the progression of oral biofilm formation and dental plaque, the gingiva begins to recede leading to mild inflammation and bleeding classified as gingivitis. At this point, the symptoms are reversible by good oral hygiene. This was demonstrated by Theilade *et al* (1966), who had subjects with good oral health stop brushing their teeth for up to 21 days, with local gingivitis occurring after 7 days and the gingival index recovering after 1 day when good oral hygiene was returned. However, if gingivitis is not reversed it presents changing

environmental conditions for the bacteria, such as the formation of the periodontal pocket through inflammatory destruction, and the presence of gingival crevicular fluid and blood as nutrient sources (Curtis, Diaz and Van Dyke, 2020).

The colonisation of the periodontal pocket results in a large shift in the subgingival community. This new niche causes the health associated Gram positive bacteria to be outcompeted by the Gram negative anaerobic pathogens such as *P. gingivalis*, *Treponema denticola*, and *Tannerella forsythia* (Socransky *et al.*, 1998), uniquely resulting in a greater biodiversity that is detrimental for the host due to the increase in pathogenic population and virulence leading to greater inflammation (Mombelli, 2018). The inflammatory response of the host to the bacteria is the underlying cause of the destructive symptoms seen in periodontitis, such as bleeding, alveolar bone reabsorption through activation of osteoclasts and periodontium destruction (Scott and Krauss, 2011; Cekici *et al.*, 2014).

There is a relationship between inflammation and the progress of dysbiosis and periodontitis. As bacterial biofilms grow in the subgingival environment they cause an increased pro-inflammatory state, this then provides an environment better suited to that of the anaerobic Gram negative pathogens. This facilitates the change from the health associated bacteria such as *Actinomyces* and *Streptococci*, to disease related bacteria such as *Treponema, Tannerella* and *Porphyromonas* (Curtis, Diaz and Van Dyke, 2020). However, if this inflammation is reversed, so are the effects of periodontitis. In a study by Hasturk *et al* (2006), they discovered that the use of Resolvin E1 (RE1) can prevent the neutrophil mediated destruction of the periodontium in rabbits. RE1 specifically binds to neutrophils and reduces the production of superoxides and the inflammatory affect. The findings of their study was supported by a second investigation (Hasturk *et al.*, 2007), in which rabbit periodontitis models were developed for 6 weeks before treating with RE1. This second investigation demonstrated that the reduction of inflammation by RE1 not only prevented the progression of periodontitis, but it also reversed the destructive effects restoring the gingiva to a healthy state. These results demonstrate the bidirectional relationship between inflammation and periodontal disease progression (Figure 1.2.1). The uncontrolled and destructive inflammatory response is paramount in the symptoms of periodontal disease, therefore controlling this inflammatory response to the bacteria is key when treating periodontal disease.

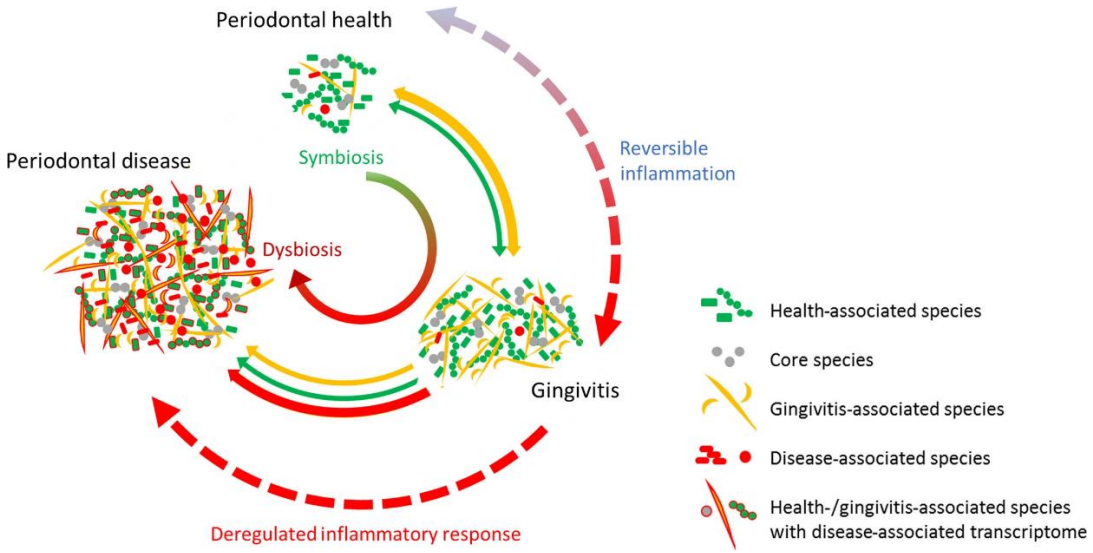

Figure 1.2.1 Bidirectional relationship between inflammation and subgingival bacteria. In healthy conditions the bacterial community is majority composed of health associated species in a symbiotic state. Gingivitis is progressed through greater biomass and increased inflammation, which begins to change the composition and biodiversity of the subgingival microbiota, this is reversible through the reduction of biomass and inflammation. If gingivitis is left untreated an increased inflammatory response and further bacterial biomass causes further dysbiosis. This leads to an increased growth of disease associated bacteria, and the destruction of periodontal tissue seen in periodontal disease. Figure taken from Curtis, Diaz and Van Dyke (2020), and used with permission.

1.3 Systemic disease

The health problems caused by chronic periodontitis have been indicated to have links to many other systemic diseases such as cardiovascular disease (CVD) (Kuramitsu *et al.*, 2001), arthritis (Bingham and Moni, 2013), diabetes (Preshaw *et al.*, 2012), HIV (Ryder *et al.*, 2012) and more recently Alzheimer's disease. One of the major conflicting issues with the connection between periodontal disease and other systemic diseases are the overlapping risk factors, such as; smoking, diet and age (Genco and Borgnakke, 2013).

1.3.1 Cardiovascular disease

Cardiovascular diseases are medical conditions that affect the functionality of the heart or blood vessels. The link between oral health and cardiovascular disease have been investigated in the literature, with studies showing CVD patients having a relationship with periodontal disease, with a trend for the two diseases to be more prevalent together. A study by Stefano *et al* (1994) looked at the relative risk of 9760 subjects of developing cardiovascular disease; it was found that there was a 25% increased risk of coronary heart disease in patients with periodontitis when compared to patients without periodontal disease. Further studies have supported this finding with a meta-analysis by Blaizot *et al* (2009) finding that within 29

studies there was an overall 34% increased risk of cardiovascular disease in periodontitis patients. However, the studies that focus on the trend between periodontitis and CVD are often criticised due to the difficulty to prove a causal relationship. This difficulty in the methodology comes from periodontitis and CVD sharing similar risk factors such as smoking, obesity and diet which are difficult to remove from the studies without drastically reducing the sample size. Although there is a possible connection between cardiovascular disease and periodontal disease, the reason for this link is still not fully understood. There is strong evidence that "red complex" bacteria can exasperate CVD symptoms. A study by Nakano *et al* (2009) investigated the presence of periodontal pathogens in the heart valves of patients undergoing valve replacement surgery through real-time PCR using species specific primers. This study found the presence of many oral bacteria in both heart valves and aneurysmal wall samples, including *Streptococcus mutans* and *P. gingivalis*. This study was further supported by a study by Oliveira *et al* (2015), in which the heart valves of 42 patients with heart valve disease were probed for the presence of *S. mutans*, *P. gingivalis*, *T. forsythia*, and *Prevotella intermedia* by real-time PCR using species specific primers. This study found that all the bacteria that were probed for were detected in the heart valves with *S. mutans* having the greatest detection with 89.3% and *T. forsythia* having the smallest amount of detection at 2.3%. The presence of periodontal pathogens in heart valves indicates the ability of periodontal pathogens to travel via the bloodstream of infected patients. It is then understandable that the inflammatory effects of the periodontal pathogens on the periodontium can also occur within the cardiovascular system. There have been multiple studies showing that *P. gingivalis* can antagonise CVD in murine models (Kuramitsu *et al.*, 2001; Deleon-Pennell, Bras and Lindsey, 2013). In a more recent study by Farrugia, Stafford and Murdoch (2020), they discovered that outer membrane vesicles (OMV) of *P. gingivalis* could increase the permeability of endothelial cell monolayers. This observation was also tested in a zebrafish larvae model and the OMV induced greater vascular disease. This increased vascular permeability was suggested as a gingipain protease specific degradation of PECAM-1 intracellular adhesion molecule.

There is therefore evidence to suggest that periodontal bacteria can potentially antagonise CVD through promoting an inflammatory response and increasing vascular permeability.

However, the difficulty in performing a study to show the causal relationship between periodontitis and CVD is a problem preventing the confirmation of a conclusive connection.

1.3.2 Arthritis

Rheumatoid arthritis (RA) is a chronic inflammatory disease which occurs through the autoimmune response in which the host immune system targets its own cells (Majithia and Geraci, 2007). There is evidence that a link between periodontitis and RA exists with one disease aggravating the other (Bingham and Moni, 2013). There have been many studies comparing RA patients with and without periodontitis and investigating their symptoms. A study by Garib and Qaradaxi (2011) investigated 100 patients with periodontal disease, 50 with RA and 50 without RA. The patients were assessed by multiple methods such as a health association questionnaire and a verbal descriptor pain scale; however, the most convincing results came from the significant difference between the bone loss and tooth loss between the RA group and the control group, with the RA group having a significant increase in both. Recent research has demonstrated the importance of citrullinated peptides and their coinciding anti-citrullinated protein antibodies (ACPA) for the initiation of RA and as a clinical biomarker in the early detection of RA development (van Venrooij and Pruijn, 2000; Farid, Azizi and Mirshafiey, 2013). The host's ACPA initiate an inflammatory response by host immune cells which initiates rheumatoid arthritis (Figure 1.3.1). The study by McGraw *et al* (1999) initially identified that the oral pathogen *P. gingivalis* expresses a peptidyl arginine deiminase (PAD) enzyme that can convert arginine to citrulline when calcium is available, allowing the presence of *P. gingivalis* to potentially produce ACPA and contribute to RA progression. A mouse study by Maresz *et al* (2013) investigated the effect of *P. gingivalis* on collagen induced arthritis, this study found that the presence of *P. gingivalis* significantly increased the effect of arthritis in the infected mice compared to the control, however it was noted that the effect seemed to make no change to the mice's general health or weight indicating that the clinical importance may not have been affected. A more recent study by Gonzalez *et al* (2015), provide evidence that RA patients have increased alveolar bone loss which is a key symptom of periodontitis. In this study 287 RA patients were compared against osteoarthritis patients, and it was found that in RA patients with ACPA present have a significantly higher number of sites with more than 20% alveolar bone loss when compared to the osteoarthritis patients, indicating the importance of ACPA in the progress of

periodontitis. The evidence in the literature suggests a synergistic relationship between periodontitis and RA; in which both inflammatory diseases can exacerbate the symptoms of the other.

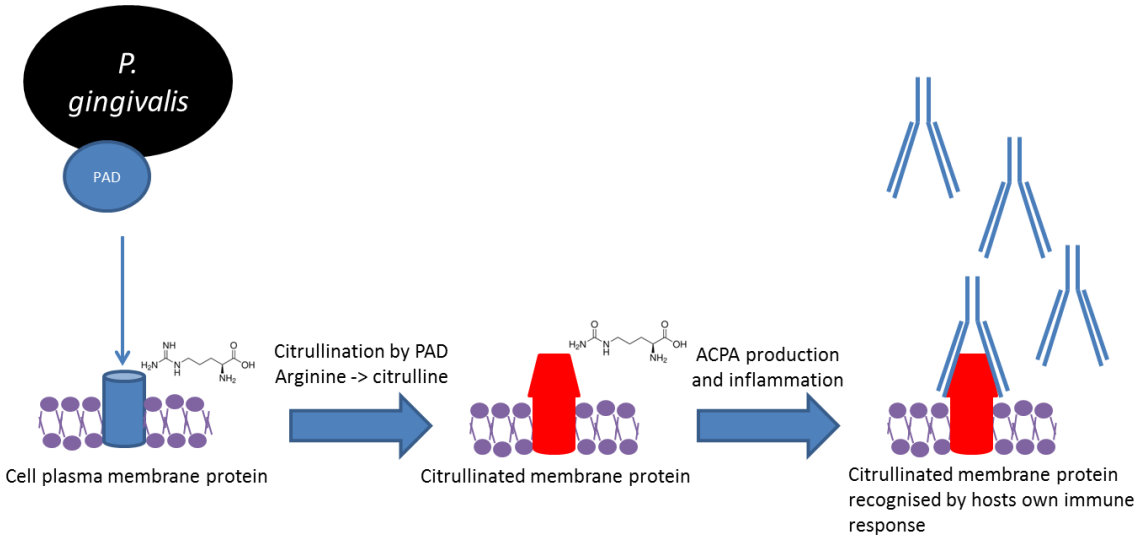

Figure 1.3.1. PAD enzyme citrullinates host proteins and triggers an autoimmune response. The PAD enzyme of *P. gingivalis* can enzymatically alter arginine residues on host proteins to citrulline. This citrullinated protein stimulates the immune response to produce anti-citrullinated protein antibodies. This leads to the recognition of host proteins by the host immune response leading to autoimmune inflammation.

1.3.3 Alzheimer's disease

Alzheimer's disease (AD) is a degenerative neurological disorder which eventually causes the atrophy of the brain through the destruction of brain cells, indicated to be caused through adverse inflammation (Wyss-Coray and Rogers, 2012). This often leads to impaired cognitive abilities and is the most common cause of dementia (Liccardo *et al.*, 2020). The link between periodontal disease and AD has been well studied in the past decade. A long term study by Kaye *et al* (2010), investigated the effect of tooth loss and periodontal progression on cognitive function in five hundred and ninety seven men for up to 32 years. They showed an increased risk of low mini-mental state exam scores and low spatial copying scores when periodontal disease progression and tooth loss occurs. The risk of cognitive decline in response to periodontitis was further supported in a study by Ide *et al* (2016). Ide *et al* performed a 6-month investigation in the effect of periodontitis on the cognitive scores of AD patients. Although a small sample size of 20 periodontitis positive and 32 periodontitis negatives returned for the 6-month check-up, there was a significant decline in cognitive

ability of the periodontitis positive group compared to the negative as assessed by the Alzheimer's disease assessment scale- cognitive score.

One of the keystone periodontal pathogens *P. gingivalis* is considered a potential antagonist of AD, with links to increasing AD marker plaques in mice (Ishida *et al.*, 2017), and one of its major virulence factors LPS being found in the brain sections of people that had AD (Poole *et al.*, 2013). The most compelling case was recently published by Dominy *et al* (2019), who investigated the presence of *P. gingivalis* and one of its major virulence factors the gingipain proteases in human AD brains. Dominy *et al* revealed that the presence of both types of *P. gingivalis* protease (arginine and lysine) were found in significant abundance in the AD brains compared to the healthy controls. It was also discovered that the DNA of *P. gingivalis* was detected in cerebrospinal fluid of AD patients. Upon investigating this further with a mouse model, Dominy et al show that *P. gingivalis* oral infections can spread to the brain and develop AD amyloid plaques. This affect was reduced in the presence of gingipain inhibitors. Their study provides strong evidence to the role of *P. gingivalis* in the antagonization of AD and suggests that the gingipains could be a potential therapeutic target in future AD therapy.

Although there is evidence for a link between periodontal disease and other systemic diseases, there are currently difficulties within the methodology of clinical studies. The overlapping risk factors of periodontal disease and other systemic inflammatory diseases such as CVD and RA create a difficult obstacle to proving a causal relationship even though there are many studies that show a correlation between the diseases. The strongest evidence comes from the study of the microbiology and molecular pathways of the diseases, which are affected by the pathogens present in periodontitis.

1.4 *Porphyromonas gingivalis*

P. gingivalis is a Gram negative anaerobic coccobacillus bacterium of the Bacteroidetes phylum. Originally classified as *Bacteroides gingivalis,* this asaccharolytic member of the "red complex" was renamed to *Porphyromonas* due to its biochemical differences and accumulation of protoporphyrin IX in contrast to conventional *Bacteroides* such as *Bacteroides fragilis* (Shah and Collins, 1988).

1.4.1 The keystone pathogen hypothesis

P. gingivalis is recognised as one of the "red complex" bacteria due to its frequency in patients with periodontitis (Socransky *et al.*, 1998). However, more recently a review by Hajishengallis,

Darveau and Curtis (2012) has given evidence to show that within the progression of periodontal disease *P. gingivalis* acts as a "Keystone pathogen". The "keystone pathogen" hypothesis suggests that *P. gingivalis* is a major factor on the structure and development of periodontal biofilms and periodontitis, and only a small frequency of *P. gingivalis* is required to change the environmental conditions of the oral microbiota and lead to dysbiosis. A study by Hajishengallis *et al* (2011) investigated the role of *P. gingivalis* in biofilm manipulation and periodontitis in mice. This study found that introducing *P. gingivalis* into the oral cavity of mice can cause periodontal bone loss and change the composition of the oral bacterial community, compared to a sham control. There was significant periodontal bone loss between the *P. gingivalis* and sham control, with a reduction of 0.12 mm. This change was brought on with *P. gingivalis* having an abundance of 0.01% relative to the overall community, indicating the "keystone" role *P. gingivalis* plays. However, this study also demonstrated that *P. gingivalis* requires a bacterial community to progress periodontitis. The results of the germ-free mice showed no change in periodontal bone loss.

There is evidence to suggest that *P. gingivalis* creates a more suitable niche for biofilm growth. A study by Darveau *et al* (1998) found that internalising *P. gingivalis* inhibited the production of interleukin-8 (IL-8) a chemokine involved in leukocyte recruitment, this effect was not produced by a non-invasive mutant of *P. gingivalis*. These results were further supported by Bainbridge *et al* (2010) in a study that found the serine phosphatase SerB in *P. gingivalis* inhibits IL-8 secretion from gingival epithelial cells. Using a SerB knockout mutant it was observed that the lack of SerB results in a statistically significant increase in polymorphonuclear neutrophil recruitment, compared to the wild type. The ability for *P. gingivalis* to prevent leukocyte recruitment could allow the progression and growth of biofilms. It is worth noting that this effect does not seem to take place in the periodontal ligament or gingival fibroblasts (Scheres *et al.*, 2011), indicating an initial gingival surface interaction.

P. gingivalis has also been shown to promote the growth of biofilms through the manipulation of gene expression in commensal oral bacteria (Frias-Lopez and Duran-Pinedo, 2012). In the study by Frias-Lopez and Duran Pinedo the presence of *P. gingivalis* in healthy oral community biofilm models increased the expression of many different clusters of orthologous groups (COGs) including genes responsible for growth such as cell wall/membrane biogenesis and

translation, as well as ribosomal structure and biogenesis. However, the study does not look at the presence of *P. gingivalis* alone and these results could also be due to the presence of the other oral pathogen introduced *Aggregatibacter actinomycetemcomitans*.

There is clear evidence to support the hypothesis that *P. gingivalis* is a "keystone" pathogen. *P. gingivalis* can change the microbial composition within a healthy oral biofilm to promote the progression of periodontitis. It has also been observed that *P. gingivalis* is able to manipulate the host and cause chemokine paralysis through gingipain protease degradation whilst creating a more favourable niche to allow biofilm growth. The presence of *P. gingivalis* is also capable of promoting the expression of genes responsible for growth in biofilms. It is therefore understandable that *P. gingivalis* plays an important role in the dysbiosis of the healthy oral microbiota and the progression of periodontitis. However, it is worth noting that although *P. gingivalis* is recognised as a "keystone" pathogen this is not the only factor that is responsible for the progression of periodontitis. The "ecological plaque" hypothesis argues that it is the local environment that leads to the dysbiosis seen in periodontitis, and that specific bacteria are not solely responsible but it is a combination of their virulence traits that progress the symptoms of the disease (Marsh, 2003). It is possible that both theories have merits as the oral environment is diverse and periodontitis is a polymicrobial disease, therefore the local environment is important, however it cannot be denied that *P. gingivalis* has a distinct effect on progressing the symptoms of periodontal disease.

1.4.2 Virulence factors of *P. gingivalis*

P. gingivalis has a plethora of different virulence factors that it produces to allow the infection of oral cells, it is important that these factors are in contact with host cells to be able to interact. These virulence factors can manipulate the host into an inflammatory state, adhere and invade host cells, and manipulate the host innate immune response to avoid detection. The majority of *P. gingivalis* virulence factors are surface components as it is crucial that they are often in direct contact with host cells or other bacteria (Figure 1.4.1).

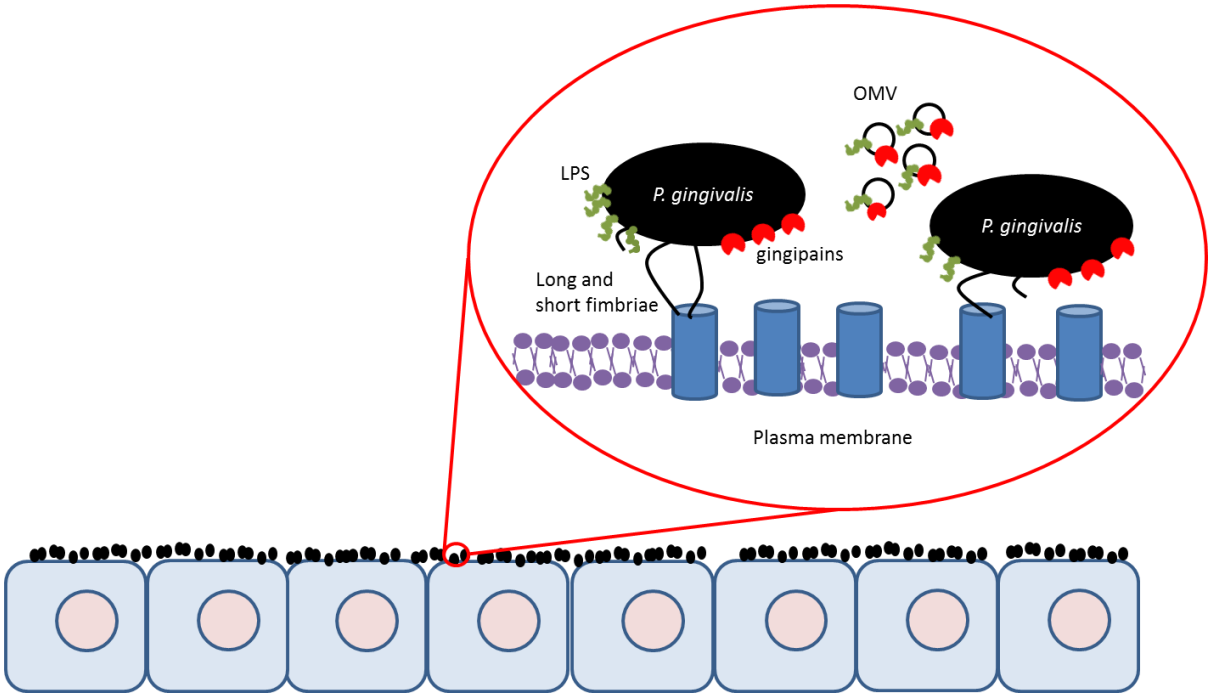

Figure 1.4.1. *P. gingivalis* surface virulence factors. Surface virulence factors are the first contact with host cells and allow *P. gingivalis* to bind and invade the cells whilst manipulating the host immune response.

1.4.2.1 Lipopolysaccharide (LPS)

P. gingivalis is a Gram negative bacteria meaning that its outer membrane has an inner phospholipid layer, and the outer layer consists of LPS. LPS is made of a lipid A section, a core oligosaccharide, and an O- antigen. The LPS provides structural support and a permeability barrier for Gram negative bacteria, whilst also acting as a major inflammatory stimulator (Bertani and Ruiz, 2018). *P. gingivalis* LPS is interesting in that unlike most other Gram negative bacteria the LPS of *P. gingivalis* is heterogeneous and can have multiple forms of lipid A (Darveau *et al.*, 2004) and a LPS with anionic polysaccharide (APS) known as A-LPS (Paramonov *et al.*, 2005). In a study by Rangarajan *et al* (2008), they investigated the two types of LPS from *P. gingivalis* also investigating their lipid-A moieties. Their previous work (Paramonov *et al.*, 2005) demonstrated that the APS of *P. gingivalis* is composed of multiple mannose structures, in comparison to the O-antigen which is composed of a tetrasaccharide repeat of Glucose, rhamnose, acetyl galactosamine and galactose saccharides (Paramonov *et al.*, 2001)(Figure 1.4.2). Further investigation through A-LPS isolation mass spectrometry, revealed that the lipid A of A-LPS is enriched for monophosphorylated penta-acylated lipid A at m/z 1,657 and monophosphorylated tetra-acylated Lipid A at m/z 1,449. These results together suggested that *P. gingivalis* has two unique types of LPS with different O-antigen and Lipid A sections.

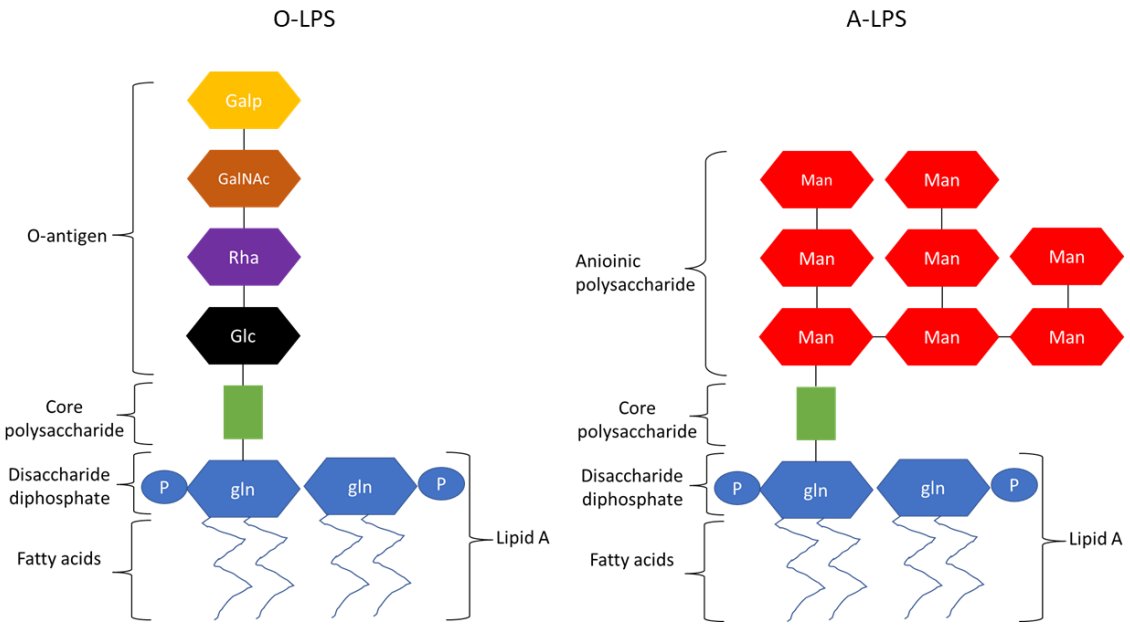

Figure 1.4.2 Structure of O-LPS and A-LPS from *P. gingivalis*. The O-LPS of *P. gingivalis* with an O-antigen consisting of tetrasaccharide repeats of Glucose, Rhamnose, acetyl galactosamine and galactose (Paramonov *et al.*, 2001). Whereas the A-LPS contains an APS instead of an O-antigen which is composed of mannose sugars (Paramonov *et al.*, 2005).

A study by Al-Qutub *et al* (2006) identified that lipid A can be changed from penta-acylated (m/z 1690) to tetra-acylated (m/z 1435/1450) depending on the concentration of hemin. Hemin is available in the periodontal pocket due to the inflammation and bleeding, so it is clinically relevant that the different concentrations of hemin can alter the structure of LPS. Specifically, this is important due to the interactions between LPS and the host cells by interacting with toll-like receptors (TLR's). Toll-like receptors are a set of pathogen associated molecular pattern (PAMP) recognition receptors that are highly conserved in eukaryotic organisms and regulate both the innate immune response and the adaptive immune response. TLR-4 is most commonly associated with recognising the LPS of Gram negative bacteria and promoting an immune response by recruiting neutrophils and expressing cytokines and NF-kβ (Lu, Yeh and Ohashi, 2008). The LPS binds to the LPS binding complex which is recognised by the cluster of differentiation 14 (CD14), the interaction between CD14 and TLR4 then triggers an immune response through the recruitment of leukocytes and expression of cytokines (Jiang *et al.*, 2000). There are conflicting reports on the effect of *P. gingivalis* LPS on TLR's; there are studies that have shown interactions of *P. gingivalis* LPS with TLR2 and TLR4. As the majority of LPS including *E. coli* LPS has been shown to specifically interact with TLR4, the interaction of *P. gingivalis* LPS with TLR-2 is unusual and has been attributed to its heterogeneity (Herath *et al.*, 2013). Darveau *et al*, (2004) demonstrated by

mass spectrometry that within *P. gingivalis* heterogeneous LPS there are different weights due to different acylation. In this study purified tetra-acylated lipid A molecules with mass to charge ratio (m/z) 1435 and 1450 were used on human and mouse cells expressing TLR4, TLR2 or TLR1 and TLR2 and compared to *E. coli* LPS and Pam3CSK4 lipopeptide which is a known agonist of TLR's. It was discovered that *P. gingivalis* lipid-A 1435/1450 could stimulate the cells through TLR2, with 1 μg of LPS causing an 8-fold increase in HEK cell stimulation in a MD-2 independent manner. However, the data suggests that *P. gingivalis* LPS requires MD-2 to stimulate HEK cells through both human and mouse TLR4 activation. A more recent paper by Herath *et al* (2013), supports this finding providing data that shows tetra-acylated LPS from *P. gingivalis* can induce TLR2 expression and weakly affect TLR4 expression whilst penta-acylated LPS can induce both TLR2 and TLR4 in human gingival fibroblasts. The data in this study also indicates that the different acylated LPS activate the cells differently. Penta-acylated LPS increased expression of NF-kβ and cytokines such as IL-6 and IL-8. However, the tetra-acylated LPS result in a reduced expression of NF-kβ and inflammatory cytokines.

A recent study by Nativel *et al* (2017) however, argues that the LPS of *P. gingivalis* is not an agonist of TLR2. In this study a commercially produced ultrapure (UP) *P. gingivalis* LPS was used alongside standard *P. gingivalis* LPS and UP *E. coli* LPS. The data in this paper show that the UP *P. gingivalis* significantly activates TLR4 which is measured by NF-kβ/SEAP activity; however, the TLR2 activation is not present. The authors explain that it is most likely the contamination of LPS by lipoprotein agonists of TLR2 that causes the activation of TLR2 seen in previous papers. However the study by (Darveau *et al.*, 2004), shows a colloidal gold stain of their LPS extraction that clearly show no protein contamination present. The study by Nativel *et al* (2017) also looks for TLR2 activation by NF-kβ/SEAP activity, whereas in the paper by Herath *et al* (2013) their data shows that even though TLR2 is activated, it does not activate the cells through the NF-kβ pathway which explains the lack of activation detected by NF-kβ/SEAP activity.

Although there is some controversy that exists on how the LPS of *P. gingivalis* interacts with host cells, it is clear that the LPS is essential for the inflammatory response required for the progression of periodontal disease and is an important virulence factor.

1.4.2.2 Fimbriae

Fimbriae are thin protein appendages on the outer membrane of bacteria; they have multiple purposes such as adhesion to; cells, surfaces, and other bacteria. They also function as a virulence factor due to being able to bind and invade host cells, as well as helping to form biofilms through coaggregation with bacteria (Enersen, Nakano and Amano, 2013).

P. gingivalis has two main types of fimbriae, long major fimbriae which are composed of FimA proteins expressed by the *FimA* gene, and small minor fimbriae which are composed of Mfa proteins expressed by the *Mfa1* operon. However, a recent study by Nagano *et al* (2015) found a 53 kDa fimbriae like structure in different strains of *P. gingivalis* that is in the same locus as the *Mfa1* gene. In this study the strains found with the 53 kDa gene do not have the *Mfa1* gene. The major fimbriae of *P. gingivalis* are involved with the adherence of the bacteria with other surfaces, bacteria and invasion of cells (Nagano *et al.*, 2012). The minor fimbriae have also been shown to be involved with binding and invasion.

Long fimbriae are classified into 6 types (I, Ib, II, III, IV, V) depending on the DNA sequence variation of the *Fim* genes. These different types have been shown to have different effectiveness at adhering and invading host cells with type II having a more pathogenic phenotype in mice (Nakano *et al.*, 2004), and with types I, II, and IV being found most frequently in clinical studies of periodontitis patients (Beikler *et al.*, 2003). Initial studies into *P. gingivalis* adhesion in the 1980's identified the importance of fimbriae for attachment to epithelial cells (Okuda, Slots and Genco, 1981). Further studies by Amano *et al* (1999) and Nakamura *et al* (1999) identified specific host components which fimbriae bind too such as fibrinogen, fibronectin and elastin which are found in the extracellular matrix (ECM). It was also observed that fimbriae bound to salivary proteins such as proline-rich protein and proline-rich glycoprotein (Amano *et al.*, 1998). In a study by Zheng, Wu and Xie (2011), the authors investigated the different adhesion capabilities of *P. gingivalis* with different long fimbriae types showing that types I and II had greater interaction with saliva and *S. gordonii*. The data from this investigation showed that type I and II fimbriae had a significantly greater ability to interact with both *S. gordonii* and saliva bound microtitre plates than type III and IV. However, when the ratio of binding between the *P. gingivalis* with a specific type of fimbriae and its corresponding fimbriae lacking mutant was compared, it was indicated that type I and II fimbriae are important for the binding as there was a loss in comparison of the number of

mutants bound. On the other hand, the adhesion of the type III and IV fimbriae *P. gingivalis* mutants were not as greatly affected with only a 50% decrease in type IV binding to *S. gordonii*, and no significant decrease in binding of type III fimbriae to saliva coated microtitre plates compared to the mutant indicating that type III fimbriae is not involved in the binding of *P. gingivalis* to saliva.

It has also been shown that the large fimbriae can bind to α5β1 integrin to induce invasion through lipid rafts. A study by Nakagawa *et al* (2002) initially identified the binding capabilities of type II fimbriae with α5β1 integrin, further study by Tsuda *et al* (2005) identified that *P. gingivalis* outer membrane vesicles (OMV) conjugated with fluorescent beads would be surrounded by α5β1 integrin and be internalised into epithelial cells. This effect was inhibited by the addition of methyl-β-cyclodextrin a chemical which breaks down cholesterol indicating the role of lipid rafts in the invasion. Further to this, a continuation study by Tsuda *et al* (2008) identified that the interaction between the fimbriae and α5β1 integrin initiate the invasion of epithelial cells by the formation of lipid rafts and allow entry into the cells through actin remodelling into actin rich phagocytic cups.

Short fimbriae encoded by the *Mfa1* operon have been shown to play similar roles in adhesion. In a study by Park *et al* (2005), they found that Mfa1 fimbriae was essential for binding to *S. gordonii* an early coloniser of oral biofilms. The aggregation was caused by the binding of Mfa1 to the streptococcal surface polypeptide SspB, this binding was lost in the Mfa1 mutant, and the co-aggregation was reduced. It was also found that the short fimbriae are important for the coaggregation of *P. gingivalis* biofilms, Lin, Wu and Xie, (2006) show that a *Mfa1* mutant has a significantly reduced coaggregation demonstrating a reduced binding ability between individual *P. gingivalis*. The Mfa1 fimbriae have also been shown to be involved with the binding and internalisation into dendritic cells (DC). The study by Zeituni *et al* (2009) used dendritic cell specific ICAM-3 grabbing nonintegrin (DC-SIGN) lectin receptor positive and negative cell lines to identify that the minor fimbriae bind specifically to the DC-SIGN and are then internalised. This work was supported by Carrion *et al* (2012) in which they also found that *P. gingivalis* bind to blood DC in a DC-SIGN dependant manner and have an increased intracellular survivability. It is therefore understandable that the outer membrane components such as LPS and fimbriae are important for the interaction with host cells as they are the first point of contact. Recent work by Meghil *et al* (2019), demonstrated that in

dendritic cells the Mfa1 fimbriae of *P. gingivalis* induces the Akt kinase and mechanistic target of rapamycin (mTOR) interaction once internalised, which suppressed autophagy of *P. gingivalis*.

1.4.2.3 Outer membrane vesicles (OMV)

Outer membrane vesicles are sections of bacterial outer membrane that detach from the bacteria and create a small hydrophobic package surrounded by bacterial outer membrane (Kulp and Kuehn, 2010), therefore creating vesicles containing multiple virulence factors in *P. gingivalis* such as, fimbriae, gingipains and LPS (Figure 1.4.3). The production of outer membrane vesicles in Gram negative bacteria is believed to be caused by an accumulation of periplasmic contents that detach the outer membrane from the peptidoglycan, leading to further curvature and eventual "blebbing" of OMV (Zhou *et al.*, 1998; Xie, 2015). Two recent models of Gram negative OMV formation have been proposed. Xie (2015) predicts that the OMV production in *P. gingivalis* could be due to three mechanisms, periplasmic protein accumulation, detachment of peptidoglycan binding lipoproteins, and extracellular signalling causing membrane curvature (Figure 1.4.3). In contrast, Roier *et al* (2016) used a knockout mutant of a phospholipid ABC transporter to investigate the effect of phospholipids in OMV biogenesis. They revealed that the loss of this transporter resulted in the accumulation of phospholipids in the outer membrane, and an increase in OMV produced. They propose a system by which phospholipid integration into the outer membrane provides curvature and eventual budding that leads to the release of OMV's. Both models could potentially work together in Gram negative bacteria OMV production.

The outer membrane surface components and proteins are the major virulence factors of *P. gingivalis* and therefore releasing the outer membrane into the surrounding environment is an important mechanism to deliver *P. gingivalis* virulence factors. In a study by Veith *et al* (2014) used liquid chromatography linked to mass spectrometry to identify 151 OMV proteins from *P. gingivalis* W50. It was discovered that the OMV contain mainly periplasmic and outer membrane proteins including the gingipains Rgp and Kgp and long fimbriae proteins such as fimbrillin. Through the use of an O-antigen ligase mutant (*Waal*$^{-}$), Haurat *et al* (2011) observed that the presence of the gingipain proteases in the OMV depended on O-antigen synthesis indicating a possible role for the O-antigen in OMV production in *P. gingivalis*, however it is worth noting this may be the result of the loss of APS in the O-antigen ligase mutant. Previous

work with a Δ*Waal* mutant by Rangarajan *et* al (2008), demonstrated that the mutant does not produce APS, which is required for gingipain anchoring into the outer membrane. These virulent contents have been shown in the literature to have effects on the inflammatory response of host cells. A study by Duncan *et al* (2004) demonstrated that the treatment of macrophage like U937 cells with *P. gingivalis* OMV caused a loss of the CD14 receptor, which responds to LPS by providing an immune response from the host. This is suggested to be a result of proteolytic degradation by the gingipain cargo of OMV and will reduce the interaction between TLR-4 and CD14 and therefore disrupt the recruitment of macrophages. In a recent study by Cecil *et al* (2017), the authors investigated the effect *P. gingivalis* W50 OMV have on the cytokine production of monocytes and their macrophage like differentiated cells. This study demonstrated that *P. gingivalis* OMV increased the secretion of inflammatory cytokines IL-1β and IL-8, interestingly they also increased the secretion of IL-10 which downregulates other inflammatory cytokines. The production of OMV allow the virulence factors of the outer membrane to reach the host-cells for host pathogen interaction.

One of these host pathogen interactions has been demonstrated recently by Farrugia, Stafford and Murdoch (2020). In their study they isolated OMV from *P. gingivalis* W83 and a W83 mutant known as ΔK/R-ab which produces no gingipain proteases. They used these OMV to investigate the effect of *P. gingivalis* OMV on vascular permeability as a potential link to cardiovascular disease. To do this, they treated human microvascular endothelial cells (HMEC) and zebrafish embryos with OMV from W83 and ΔK/R-ab. There was a significant increase in permeability in the HMEC monolayers after treatment with OMV from W83 that was not seen in the OMV from ΔK/R-ab. Similarly, the zebrafish embryo's developed cardiovascular conditions under treatment with W83 OMV in comparison to ΔK/R-ab OMV. This interaction was investigated, and it was revealed that a cell junction adhesion molecule PECAM-1 was being degraded in HMEC cells in a gingipain dependant manner, potentially causing the membrane permeability seen. This paper shows the importance of OMV cargo in the host-pathogen interactions of *P. gingivalis.*

LPS, Fimbriae and OMV are all surface structures that are the first point of contact with the host cells and therefore play an important role in host-pathogen interaction. However, there are also many major outer membrane proteins that interact with host cells in a virulent manor.

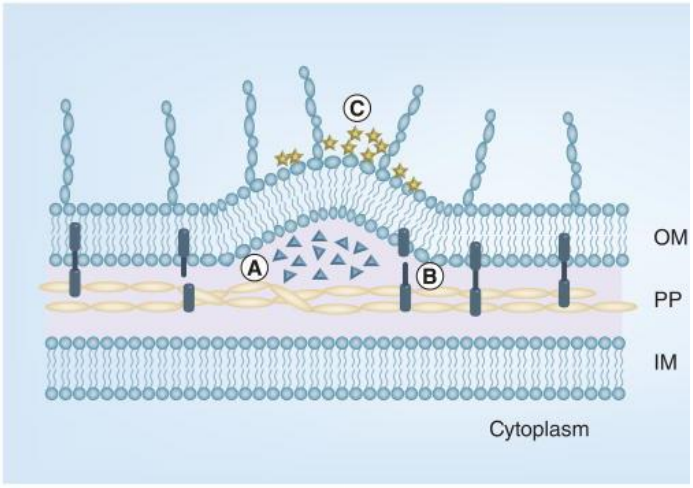

Figure 1.4.3. Outer membrane vesicle production mechanisms. (A) An accumulation of proteins in the periplasm causes the outer membrane to bulge outwards. (B) Lipoproteins connecting the outer membrane to the peptidoglycan are disrupted. (C) Extracellular signalling causes the membrane to curve outwards. Image taken from the review by Xie (2015) with permission.

1.5 Major outer membrane proteins of *P. gingivalis*

P. gingivalis is a Gram negative bacterium and therefore the structure of its membranes consist of an inner phospholipid bilayer membrane, a periplasmic space containing peptidoglycan, and an outer membrane with the inner section consisting of a phospholipid layer and the outer section consisting of an LPS layer. Both membranes also have proteins inserted into them with multiple structures and functions (Brown *et al.*, 2015). The major outer membrane proteins of *P. gingivalis* were initially isolated by Murakami *et al* (2002) and were defined as Pgm1-7. They were later identified as RagA, 75-KDa protein, lysine gingipain, RagB, arginine gingipain and OmpA proteins respectively (Figure 1.5.1). All the major outer membrane proteins have links to virulence which is important as they are the main proteins interacting directly with the host cells.

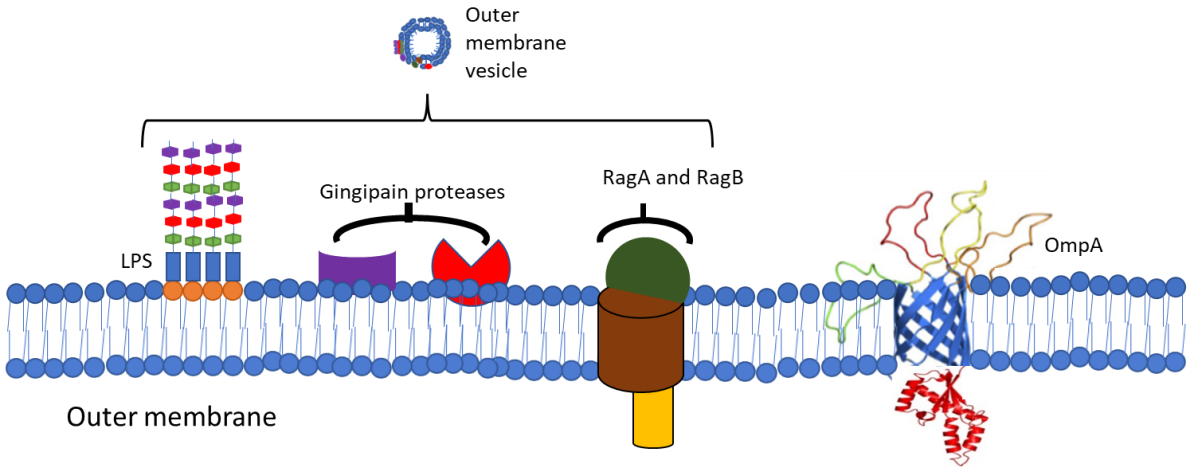

Figure 1.5.1 The outer membrane proteins and LPS are the first point of contact with host cells. The major outer membrane proteins and the LPS of *P. gingivalis* have an important role in host-pathogen interactions. This is achieved through direct contact of *P. gingivalis* with host cells, or through the production of OMV.

1.5.1 Gingipain proteases

Gingipain proteases are trypsin-like cysteine catalysed proteases; *P. gingivalis* can produce two types of gingipains, arginine targeting proteases (Rgp) and lysine targeting proteases (Kgp). The gingipains are outer membrane proteins which are inserted into the outer membrane via the type nine secretion system (T9SS) which recognises C-terminal signal domains of outer membrane proteins (Lasica *et al.*, 2017). The gingipains have roles in chemokine paralysis, cellular and bacterial adhesion, protein processing, haem and peptide acquisition for growth (O-Brien-Simpson *et al.*, 2003). A study by Lewis *et al* (1999) looked at a Kgp knockout mutant and compared the pigmentation and proteolysis to the wild-type *P. gingivalis*. It was observed that the loss of Kgp resulted in a pigmentation change from black to white on FA blood agar plates, indicating the loss of ability to assimilate iron protoporphyrin IX (FePPIX), this was further supported by a reduction in haemolysis and proteolytic activity in the mutant in comparison to the wild type. The ability of *P. gingivalis* to agglutinate and bind to erythrocytes through adhesins also shows the binding capabilities of the gingipain proteases (Chen *et al.*, 2001). In 2007 a study by Kato *et al* (2007) demonstrated that gingipains are also important for the complete maturation of fimbriae. A gingipain-null mutant was successfully fimbriated in the presence of gingipain containing vesicles from wild-type *P. gingivalis.* However, in the presence of foetal calf serum which inhibits gingipain activity the adherence of the gingipain null mutant treated with gingipain containing vesicles was significantly reduced indicating that it is the gingipains that allow fimbriae to mature correctly. Gingipains have also been shown to expose specific binding sites for fimbriae to adhere to on extracellular matrix components (Kontani *et al.*, 1996). In the study by kontani *et al*, the authors purified an arginine gingipain and used it to treat human fibroblasts, this treatment enhanced binding of purified biotinylated *P. gingivalis* fimbriae.

1.5.1.1 Type 9 secretion system and gingipain production

The type 9 secretion system (T9SS) is a mechanism of transport for proteins from the inner membrane to the outer membrane, where they can be secreted into the environment or anchored to the outer membrane (Lasica *et al.*, 2017). Translocation through the inner membrane and periplasm is an important function to produce functioning outer membrane

proteins or secrete functional proteins from the bacteria. There are 11 types of secretion systems, with types 1, 3, 4 and 6 transporting proteins directly from the cytoplasm whilst types 2, 5, 7 and 8 first transport to the periplasm and then to the outer membrane (Douglas *et al.*, 2014), with type 10 and 11 being proposed in the last two years (Grossman *et al.*, 2020; Palmer *et al.*, 2021) . Whilst there are other secretion pathways in bacteria that are used such as the Type 1 secretion system for hemolysin in *E. coli* through the hly gene products (Goebel and Hedgpeth, 1982), or the type 3 secretion system for injectisome and flagella production (Lombardi *et al.*, 2019), the type 9 secretion system is specific to the *Bacteroidetes* phylum.

The T9SS was initially discovered in *P. gingivalis* due to its role in gingipain secretion. Gingipain mutants had been made previously in the literature in which the black pigmentation was lost leading to easy identification (Smalley *et al.*, 1998). In a study by Sato *et al* (2005), they created a mutant of *PorT* which resulted in the loss of black pigment and reduced gingipain activity. Furthermore, gingipains were found in the periplasm of *PorT* mutants in their immature state indicating that *PorT* is involved with the translocation of *P. gingivalis* gingipains. It is now understood that there are at least 16 functional proteins involved in the T9SS, although they are not fully characterised and therefore their roles and functions are not fully understood (Lasica *et al.*, 2017; Gorasia, Veith and Reynolds, 2020). The current pathway of type 9 secretion is proposed by Gorasia, Veith and Reynolds (2020). For a protein to be transported via the T9SS it requires a N-terminal signal peptide for the Sec secretory system, and a C-terminal domain (CTD) that is recognised by the T9SS specifically (Seers *et al.*, 2006). The protein is recognised by SecAB and passed through Sec into the periplasm where it interacts directly with PorM through the CTD signal. The protein is then passed between multiple members of the T9SS due to CTD recognition until it reaches the PorU sortase enzyme that removes the CTD and attaches A-LPS provided by PorZ (Madej *et al.*, 2021) , anchoring the protein into the outer membrane (Figure 1.5.2).

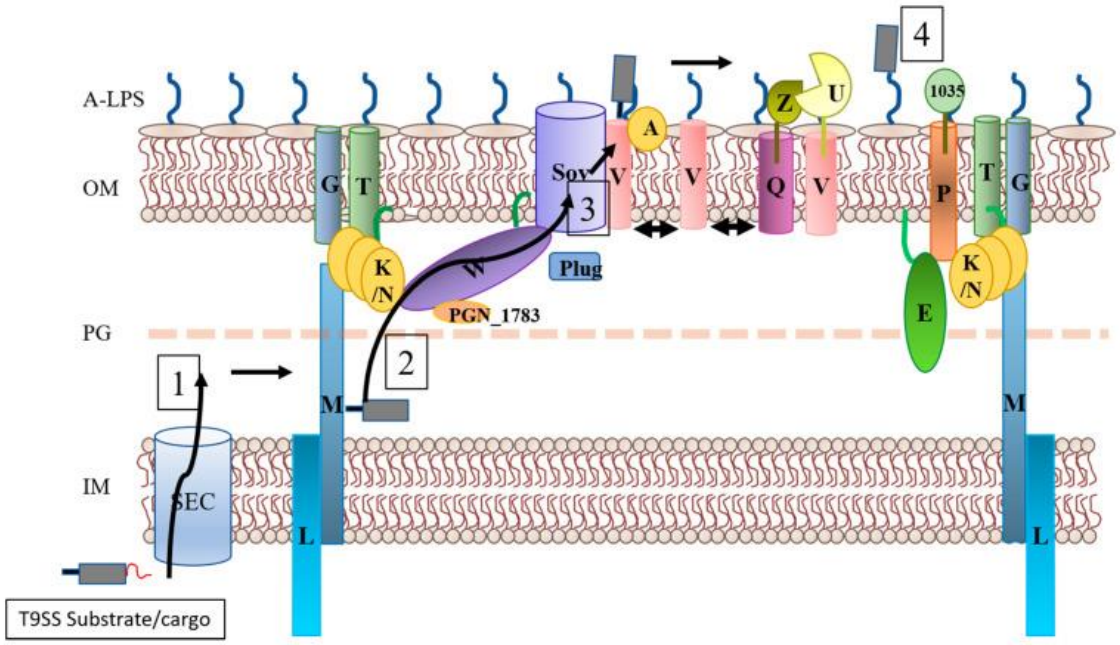

Figure 1.5.2 Predicted process of a T9SS cargo protein being transported and inserted into the Outer membrane. 1. A cargo protein that has a N-terminal signalling peptide is recognised by the Sec secretory system and translocated through the inner membrane, during which the N-terminal signal peptide is cleaved. 2. The cargo protein binds to the PorM via the cargo proteins CTD, this allows transport to PorN and PorW which will move the protein to the Sov translocon. 3. The cargo protein is transported from Sov the PorV, attaching them to the PorU, PorV, PorQ, PorZ complex. 4. The PorU sortase cleaves the CTD and replaces it with A-LPS provided by PorZ. This anchors the cargo protein into the outer membrane via its ALPS, whilst the CTD is released into the environment. This process was predicted by Gorasia, Veith and Reynolds (2020), the figure is taken with permission from their review.

The T9SS has been shown to be essential for the correct production and functionality of gingipains in *P. gingivalis* (Rangarajan *et al.*, 2017).

1.5.1.2 Gingipains in the inflammatory response

Gingipains have been shown to have a conflicting role on the immune response of host cells with the ability to supress the immune response by proteolytic cleavage of important receptors and chemokines; however, there is also evidence to suggest the presence of gingipains also promote the expression of inflammatory interleukins. In a study by Kitamura *et al* (2002) the presence of gingipains within culture medium from *P. gingivalis* was shown to cleave T cell co receptors CD4 and CD8 on human mononuclear cells, although the cleavage of CD8 was less severe. The cleavage was further increased in the presence of 2-mercaptoethanol indicating the cysteine protease activity in the cleavage. The ability of the gingipains to supress the immune system is further evidenced by Tam *et al* (2009), who demonstrate that pro-inflammatory chemokines IL-4 and IL-5 are proteolytically degraded in the presence of gingipains in a dose dependant manner showing complete inactivation at a

1:1 molar ratio. The ability of the gingipains to inactivate interleukins was previously demonstrated by Mikolajczyk-Pawlinska, Travis and Potempa (1998), who identified that RgpA and Kgp treatment resulted in total degradation of IL-8 and prevented the neutrophil recruitment effect of IL-8.

However there is also evidence that gingipains have a role in promoting the inflammatory response, including assisting the chronic inflammatory response responsible for alveolar bone degradation (Akiyama *et al.*, 2014). A study by Lourbakos *et al* (2001) identified that the RgpB gingipain induced IL-6 secretion in the oral epithelial cell line KB. It was found that treating oral epithelial cells with isolated RgpB lead to a threefold increase of IL-6 after an hour incubation, this activation was found to be due to the proteolytic activity of the gingipain, as the addition of an inhibitor prevented the IL-6 production. It is also shown that the RgpB activates protease-activated receptors (PARs) and is indicated that it is this interaction that causes the IL-6 production; this is implied however not strictly tested in this paper. Another study by Oido-Mori *et al* (2001) also demonstrated the effect of gingipains to increase expression of chemokines. In this study human gingival fibroblasts were treated with purified Rgp which resulted in a significant increase of IL-8 mRNA, interestingly the internal IL-8 was significantly increased, however the IL-8 released to the culture medium was decreased indicating the IL-8 that was being released was being degraded by the gingipains which has been observed in other studies.

The complement system of the host immune response is also a target of gingipain protease activity. The complement system is an important part of the immune system, initially named “complement” due to its ability to complement the effect of antibodies in the destruction of bacteria (Varela and Tomlinson, 2015). The complement system is intricate with more than 50 soluble proteins involved in its function. The activation of the complement system leads to the cleavage of complement protein 3 (C3), which in turn leads to the cleavage of complement protein 5 (C5) into C5a and C5b. The cleaved products C5a and C3a are potent inflammatory mediators. *P. gingivalis* gingipains have been shown in the literature to cleave complement proteins such as C5 and C3 into their respective products presenting a method of inflammation (Olsen, Lambris and Hajishengallis, 2017). The work by Hajishengallis *et al* has demonstrated the potential solutions *P. gingivalis* employs to combat the paradox of requiring inflammation for dysbiosis progression, whilst also subverting the immune

response. In a study by Maekawa *et al* (2014), the authors investigated the effect of *P. gingivalis* in neutrophil killing through C5a receptor activation. They found that *P. gingivalis* can activate the inflammatory cytokine production of neutrophils through antagonising the C5a receptor, whilst disrupting *P. gingivalis* killing through neutrophils. This is achieved through the degradation of MyD88, promoting a different C5aR receptor interaction with TLR2 via a kinase which prevented actin rearrangements required for phagocytosis. A similar interaction was seen in a separate study using macrophages, in which the inflammation was increased, but the macrophage killing was reduced. In this study by Liang *et al* (2011), *P. gingivalis* gingipain activity producing C5a developed C5aR-TLR2 signalling which reduced expression of interferon gamma which is required for macrophage priming and intracellular killing of *P. gingivalis*.

There is also evidence to suggest that gingipains continue to interact with cells after *P. gingivalis* has invaded the host cells. In a study by Stafford *et al* (2013) it was found that internalised *P. gingivalis* could manipulate the mammalian target of rapamycin (mTOR) pathways by gingipain degradation. The mTOR is involved with multiple cellular interactions that are responsible for cell survival and growth, including a role in the innate immune system by regulating inflammatory chemokines (Säemann *et al.*, 2009). In the study by Stafford *et al* (2013), their data show that *P. gingivalis* invasion results in the degradation of mTOR, it is also shown using gingipain inhibitors and gingipain lacking mutants that the mTOR degradation was due to gingipain activity.

These studies show an important effect of gingipains to both activate an immune response creating an inflammatory profile required to progress periodontitis, whilst also having the ability to subvert the immune system and thrive via targeted destruction of specific chemokines and T-cell receptors, as well as adhesion and nutrient acquisition through hemagglutinin effects.

1.5.2 RagA/B proteins

The major antigens RagA and RagB proteins are encoded by the rag locus in the DNA of *P.* gingivalis. RagA is a 115 KDa TonB-dependant receptor required for active transport of substrates and ions across the outer membrane and RagB is a 55 KDa major antigen. Both

proteins have been hypothesised to be involved with haem binding (Olczak *et al.*, 2005), but more recently have been shown to have a greater impact in *P. gingivalis* virulence. In a study by Shi *et al* (2007) either *RagA* or *RagB* were inactivated by the replacement of the gene with an erythromycin resistance cassette, it was observed that the deletion of either *RagA* or *RagB* caused the loss of both proteins as shown by Coomassie staining and western blot with a RagB specific monoclonal antibody, western blot was not performed for RagA. The data from this study also suggest that the loss of the Rag proteins had a reduced virulence, as mice survival curves were produced in which the *Rag* mutants had a significantly longer survival time, with one experiment showing no deaths, whilst the second experiment shows a higher survival rate in comparison to the wild type. The virulent effects of the Rag proteins were further supported by Hutcherson *et al* (2015) who found that a *RagB* deletion mutant had a decreased inflammatory response in primary human monocytes which was restored by the complemented mutant. Recombinant RagB had a dose dependant IL-8 response from treated human monocytes, it was also shown that RagB interacts with both TLR-2 and TLR-4 using respective TLR antibodies. Furthermore it was found by Curtis *et al* (1991) that RagB had the greatest antigenic effect out of the outer membrane proteins using the serum from a periodontitis control study when using the most abundant human antibody IgG. This data was supported by Chen *et al* (1995) who also demonstrated that the 55 KDa RagB protein had the greatest interaction with IgG from both the healthy control group used and rapidly progressive periodontitis patients. Further research is finding more functions and interactions of the Rag proteins that are relevant to *P. gingivalis* virulence.

It has been suggested in a recent study that the RagA/B complex is involved in the nutrition acquisition of peptides. *P. gingivalis* is an assacharolytic bacteria, meaning the energy source it uses is not from carbohydrates but often the breakdown of proteins into peptides and eventually acetyl-coa (Hendrickson *et al.*, 2009). In the study by Madej *et al* (2019), they investigated the structure of RagA/B using x ray crystallography, as well as RagA and RagB mutants on growth. In their investigation they discovered that RagA/B forms a dimer structure with RagA forming the β-barrel pore, whilst RagB sits on top acting as a “lid”. Through x ray crystallography they found 3 different conformations of the RagA/B complex indicating it has an open and closed formation. There were also peptides found in the pore of

RagA during crystallography suggesting the role of peptide acquisition, this was further suggested through the reduced growth of RagA and B mutants on bovine serum albumin.

1.5.3 OmpA

The OmpA proteins OmpA1 and OmpA2 are encoded by an operon of *OmpA*1 and *OmpA*2 respectively, the proteins form a heterotrimeric protein structure with an internalised C domain which binds to peptidoglycan and an outer membrane domain with an N -terminal beta barrel with 8 antiparallel beta strands (Smith *et al.*, 2007). The structure of *P. gingivalis* OmpA is homologous to the structure of the *E. coli* OmpA protein which has been more extensively studied and could give insights to potential roles of OmpA in *P. gingivalis* (Nagano *et al.*, 2005; Confer and Ayalew, 2013). In a study by Naylor *et al* (2017) the OmpA proteins of *P. gingivalis* were studied by creating knockout mutants of both *OmpA1* and *OmpA2* as well as a double mutant of both, which were also complemented with plasmids containing the wild type genes to identify if the functionality can be restored. In this study it was found that the deletion of either *OmpA*1 or *OmpA*2 had a significantly reduced biofilm formation, adherence and invasion with the double mutant having the greatest reduction followed by the *OmpA*2 mutant. Naylor *et al* (2017) identified peptide loops on the OmpA2 proteins outer membrane domain, these loops bound to OKF6 cells and treating the OKF6 cells with these peptides reduced binding by *P. gingivalis* indicating that these loops are involved with the binding and invasion process of *P. gingivalis* (Figure 1.5.3). These data suggest an important role of OmpA in the virulence of *P. gingivalis*. Although there are few studies on *P. gingivalis* OmpA proteins there are similarities between the results found by Naylor *et al* (2017) and other studies from OmpA proteins from other Gram negative bacteria. A study by Martinez *et al* (2014) looked at high content multi-phenotypic screening of *Coxiella burnetii* and found that similarly to *P. gingivalis* the *C. burnetii* mutants without OmpA had reduced invasion capabilities, it is also shown that the structure of the OmpA protein has four peptide loops, and that OmpA can bind to and trigger internalisation into A431 non-phagocytic cells. The cellular receptor/s of *P. gingivalis* OmpA is currently unknown; however there have been some suggestions of OmpA receptors in other bacteria. Similar to Naylor *et al* (2017), a study by Prasadarao *et al* (1996) identified that the N-terminal region of *E. coli* OmpA could prevent other *E. coli* from invading brain microvascular endothelial cells (BMEC), indicating that these sections of the OmpA are important for BMEC invasion. Further to this, in 2002 Prasadarao

identified that the OmpA protein of *E. coli* binds to a 95 KDa glycoprotein named Ecgp on the membranes of human brain microvascular endothelial cells.

Although there have been some insights into the possible receptors of *E. coli* OmpA, the receptors of *P. gingivalis* OmpA are still unknown. Using the N-terminal peptide loops of OmpA2, this study attempts to identify the receptors which OmpA2 interacts with on host cells.

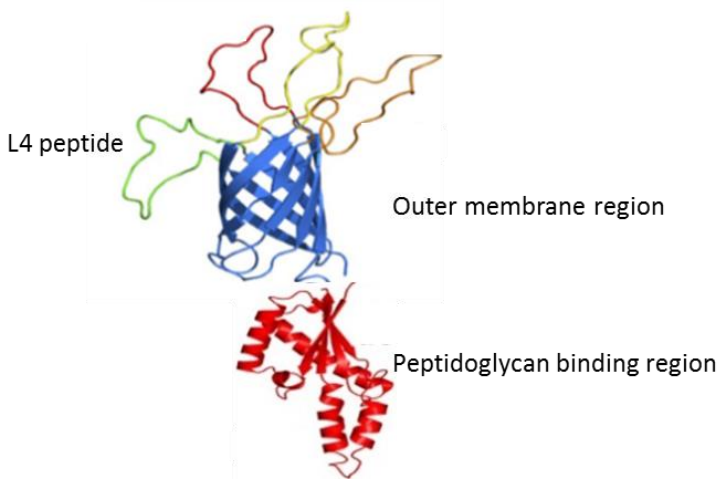

Figure 1.5.3. *P. gingivalis* structural model of OmpA outer membrane beta-barrel (blue) with loop peptides (orange, red, yellow, and green). Image altered from Naylor *et al* (2017) to add predicted peptidoglycan binding region structure (red).

1.6 The hyperinvasive gene set of *P. gingivalis*

Previous work in our lab by Suwannakul *et al* (2010) investigated the adhesion and invasion of *P. gingivalis* in oral epithelial cells. In this study, *P. gingivalis* was incubated with H357 oral epithelial cells to allow invasion, after the bacteria were internalised, the cells were burst and viable intracellular *P. gingivalis* was used to invade fresh H357 cells. It was discovered the bacteria that were previously internalised had a greater adhesion and invasion capability in comparison to fresh *P. gingivalis* (Figure 1.6.1). The stability of this hyperinvasive subpopulation was investigated through multiple passages and the increased invasive capabilities were retained for to 2-3 passages. To investigate potential genes involved with this hyper-invasive phenotype genome microarray analysis was performed multiple times. 19 genes were commonly overexpressed in 4 of the microarray experiments performed, indicating these genes had a role in the invasive capabilities of *P. gingivalis*.

This study will investigate four of the overexpressed genes in this gene set, *ompH*1, *ompH*2, *rfbB,* and *PGN2012*.

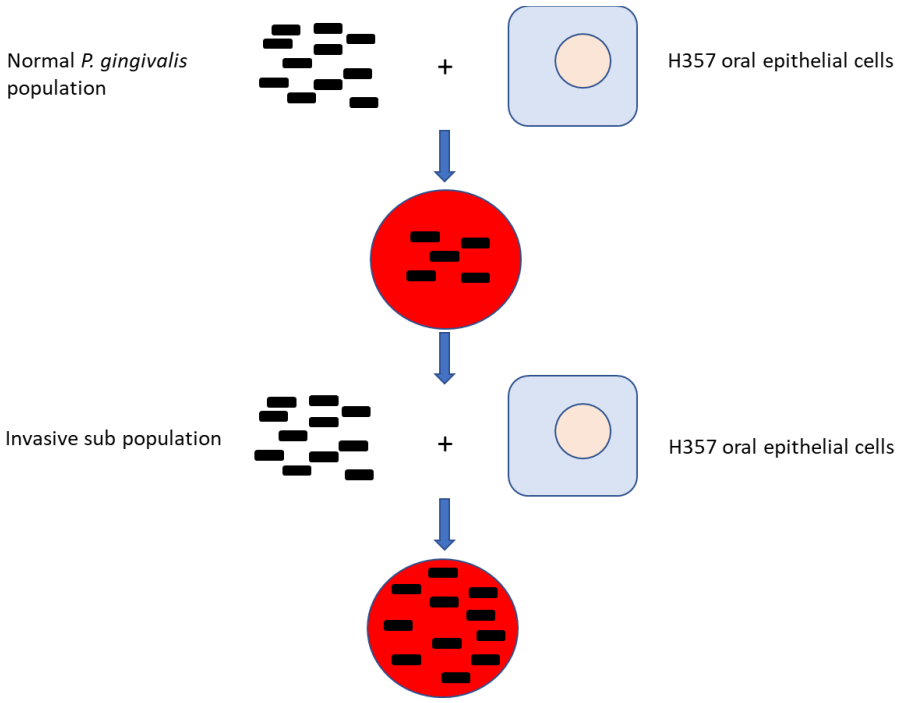

Figure 1.6.1 Enrichment for the hyperinvasive sub population of *P. gingivalis* performed by Suwannakul *et al* (2010). Normal populations of *P. gingivalis* are used to invade H357 human oral epithelial cells. Internalised *P. gingivalis* were recovered and grown on blood agar plates. This *P. gingivalis* population that had previously invaded H357 cells was used for a second invasion assay. The amount of *P. gingivalis* recovered from this second round of invasion was significantly higher than the fresh *P. gingivalis*.

1.6.1 ompH, SKP like chaperone proteins

P. gingivalis produces two Seventeen kilo Dalton protein (Skp) like proteins from an operon consisting of o*mpH*1 and *ompH*2 (also known as PGN_300 and PGN_301), which are responsible for the transport of outer membrane proteins from the inner membrane across the periplasm to the Beta barrel assembly machinery (BAM). There is structural homology between the OmpH proteins and Skp from *E. coli;* however *E. coli* does not produce two different Skp proteins (Taguchi *et al.*, 2015). Skp in *E. coli* forms a hydrophobic cage around unfolded proteins from the SEC machinery in the inner membrane to transport through the hydrophilic periplasm environment to prevent the unfolded protein incorrectly folding (Schiffrin *et al.*, 2016; Noinaj, Gumbart and Buchanan, 2017). This chaperoning has also been shown in *E. coli* to be performed by the SurA chaperone protein and the DegP protease, with SurA being the dominant chaperone (Sklar *et al.*, 2007). The proteins are transported to the BAM and folded correctly before implementing them into the outer membrane (Figure 1.6.2). In a recent study by Taguchi *et al* (2015) the effect of one of the Skp like proteins OmpH1

(named Omp17 in their study) was assessed using a gene knockout mutant which was compared to the wild type. The data from this study show that the loss of the *OmpH*1 gene significantly reduces the gingipain activity and virulence in mice, the gingipain activity was also slightly restored using complementation with the wild-type *OmpH*1 gene. There is also a loss of pigmentation and hemagglutination in the mutant which is expected with the loss of activity of the Kgp gingipain. They also demonstrate that the absence of the *OmpH*1 gene results in the loss of an important T9SS protein PorU from the membrane fraction, although it is still present in the cytoplasmic fractions the correct implementation into the outer membrane is lost. This loss could potentially contribute to the lack of CTD proteins in the outer membrane such as the gingipains. However, there are some inconsistencies within this study such as loss of lysine gingipain via western blot in the culture medium, however it is still present when probed by mass spectrometry of the culture medium. The authors of this study also do not specify whether the genome of the mutant has been checked for other mutations, or incorrect implementations of the knockout. The authors also suggest that *ompH*2 may be essential to viability as a knockout mutant of this gene could not be made. These results suggest that the OmpH1 is important in the virulence of *P. gingivalis* and the correct implementation of gingipain proteins, with a potential role in T9SS. However, the role of *ompH*2 and its client set are unknown. This study will attempt to produce mutants of *ompH*1 and *ompH2* to further investigate their roles in virulence and host-pathogen interactions.

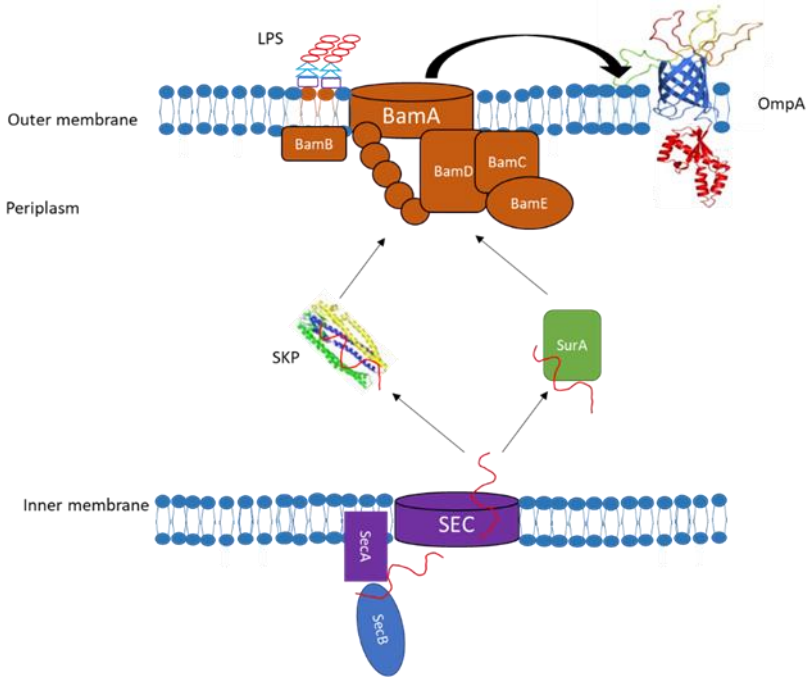

Figure 1.6.2. Skp chaperone protein transporting unfolded outer membrane Beta barrel proteins from the SEC machinery to the BAM complex. Outer membrane proteins are initially translated in the cytoplasm. The N-terminal signal peptide is recognised by the Sec complex and the protein is translocated through the inner membrane and into the periplasm. Chaperone proteins such as SurA or SKP take the unfolded protein safely through the periplasm to the β-Barrel assembly machinery, where the proteins are correctly anchored into the outer membrane.

1.6.2 *RfbB*, rhamnose and its role in LPS production

The most overexpressed gene identified by Suwannakul *et al* (2010) was *rfbB*, the final gene in a putative rhamnose synthesis pathway predicted to be involved in the production of the O-antigen of LPS.

1.6.2.1 LPS production in P. gingivalis

The production of the LPS is important for the function of all Gram negative bacteria, as the LPS plays important roles in structure and protection (Bertani and Ruiz, 2018). However, the process of producing the mixed sugar and fat molecule and transporting it to the outer membrane is quite complex. The production of the LPS can occur through two pathways either the wzy dependant pathway or the ATP binding cassette (ABC) transporter pathway (Kalynych, Morona and Cygler, 2014).

In the wzy dependant pathway the Lipid A is flipped into the periplasm by an ABC transporter, where it waits for the attachment of the core polysaccharide and the O-antigen. Units of O-antigen (O-units) are synthesised by their specific pathways before being anchored onto a lipid carrier such as undecaprenyl phosphate (Und-P) (Jorgenson and Young, 2016), through

glycosyltransferases. The short O-antigen chains are flipped into the periplasm by the flippase enzyme wzx, before being further polymerised to increase the length by an O-antigen polymerase (wzy), the length of which is often controlled by the protein wzz (Murray, Attridge and Morona, 2003). The mature O-antigen is attached to the lipid A core by the O-antigen ligase waal before being transported and inserted into the outer membrane by the lptABCDEFG complex (Dong *et al.*, 2017) (figure 1.6.3).

The ABC transporter pathway begins in a similar manner with the lipid A flipped into the periplasm by an ABC transporter. However, this time the O-antigen is assembled completely in the cytoplasm before being transported to the periplasm by an ABC transporter (wzt and wzm). The fully formed O-antigen is attached to the lipid-A with an O-antigen ligase and transferred to the outer membrane by the lptABCDEFG complex in the same way as the wzy dependant system (Figure 1.6.4).

The system used by *P. gingivalis* has been identified as the wzy dependant pathway by Swietnicki and Caspi (2021). Their study indicates the genome of *P. gingivalis* has homologues for the wzx flippase and wzy O-antigen polymerase, whilst not containing genes seen in the ABC dependent pathway.

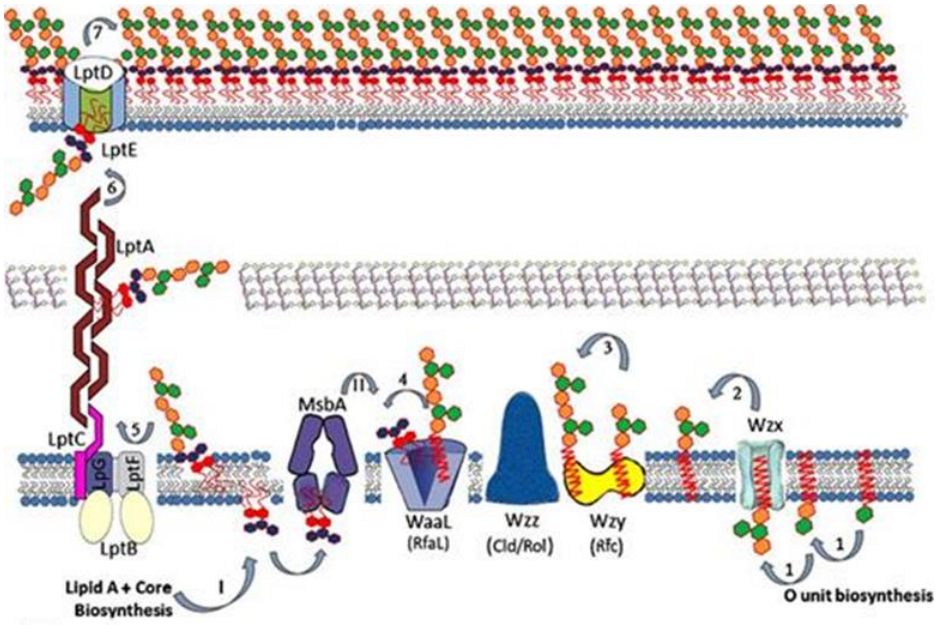

Figure 1.6.3 Wzy dependant LPS biosynthesis. 1. O-units are attached to a lipid anchor and initial O-antigen structures are formed. 2. The O-antigen is flipped into the periplasm by the flippase enzyme wzx. 3. O-antigen structures are polymerised by an O-antigen polymerase (Wzy) with the length of the polymer being controlled by wzz. 4. The O-antigen is attached to the Lipid-A core saccharide. 5. The fully formed LPS is transported via the lptBFG transport system. 6. The LPS is enveloped by LptA and LptC and transferred to LptE. 6. LptE recognises the LPS and anchors it into the outer membrane through LptD. Image taken with permission from Kalynych, Morona and Cygler (2014)

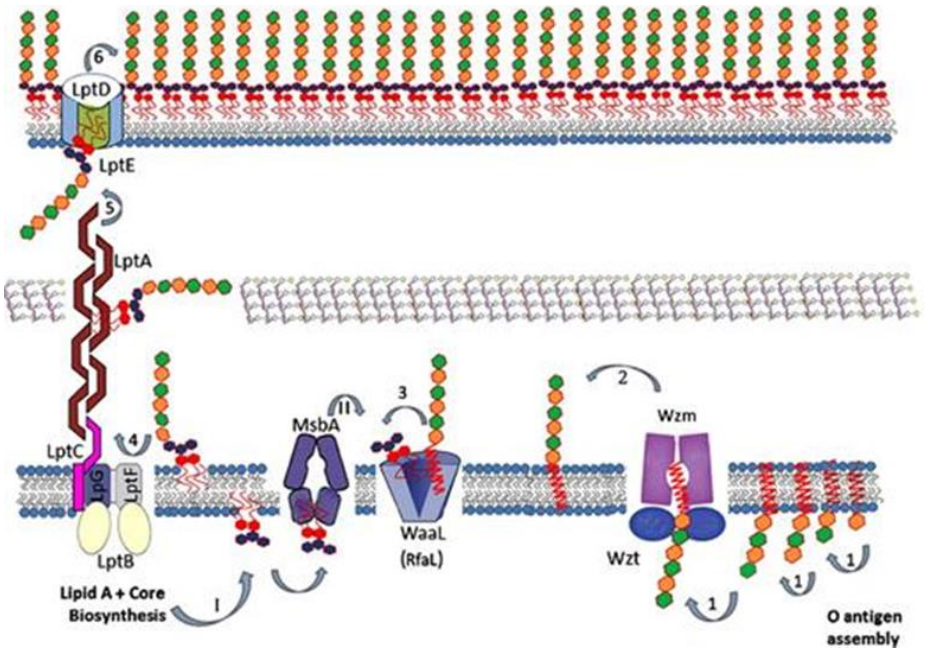

Figure 1.6.4 ABC dependant LPS biosynthesis. 1. O-units are attached to a lipid anchor and mature O-antigen structures are formed synthesised. 2. The O-antigen is moved into the periplasm through an ABC transporter (wzt and wzm). 3. The O-antigen is attached to the Lipid-A core saccharide. 4. The fully formed LPS is transported via the lptBFG transport system. 5. The LPS is enveloped by LptA and LptC and transferred to LptE. 6. LptE recognises the LPS and anchors it into the outer membrane through LptD. Image taken with permission from Kalynych, Morona and Cygler (2014)

1.6.2.2 Rhamnose synthesis and *rfbB*

P. gingivalis O-antigen is a repeating tetrasaccharide composed of glucose, rhamnose, acetyl galactosamine and galactose saccharides with rhamnose being the most abundant in *P. gingivalis* (Bramanti *et al.*, 1989). The synthesis of deoxythymidine diphosphate (dTDP) rhamnose is one of the key steps in O-antigen production in *P. gingivalis* (Swietnicki and Caspi, 2021). The process of dTDP-rhamnose synthesis is well understood and documented in other bacteria (Tsukioka *et al.*, 1997; Dong *et al.*, 2003). Similar to other bacteria *P. gingivalis* has four genes responsible for the rhamnose synthesis pathway, rfbABCD. The synthesis begins with glucose-1-phosphate as a precursor, the addition of deoxy thimydine triphosphate by a thimidylyl transferase (rfbA) produces dTDP-glucose. Two hydrogens and an oxygen molecule are removed by a dehydratase (rfbB) producing dTDP-4-keto-6-deoxy-D-glucose. Spatial rearrangements are then made by an epimerase (rfbC) to give dTDP-4-keto-L-rhamnose. Through final reduction by a reductase (rfbD) the dTDP-4-keto-L-rhamnose is reduced to dTDP-L-rhamnose (Mistou, Sutcliffe and Van Sorge, 2016) (Figure 1.6.5).

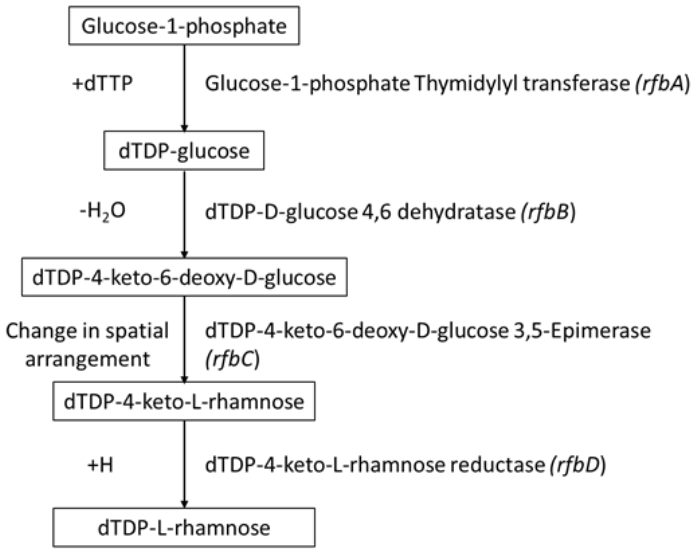

Figure 1.6.5. Rhamnose synthesis pathway in *P. gingivalis*. The precursor sugar glucose-1-phosphate is processed by the four enzymes of the rhamnose synthesis pathway rfbABCD. Producing the final product dTDP-L-rhamnose.

The literature indicates that the rhamnose synthesis pathway is important for the viability of *P. gingivalis*. In a study by Shibata *et al* (1999), they attempted to produce knockout mutants of each of the *rfb* genes (named *rml* in their study). However, no knockout mutants could be made even with multiple attempts, each bacterial strain that they had transformed possessed the mutant gene and the wild type gene indicating strange homologous recombination

events. This essentiality is not seen in other bacteria as mutants of all the rhamnose synthesis pathway have been created for *Streptococcus mutans* (Tsukioka *et al.*, 1997).

In our study we attempt to produce a knockout mutant of *rfbB* to investigate the role of this gene in host-pathogen interactions.

1.6.3 *PGN2012*, a TolC channel protein

The *PGN2012* gene is predicted to be a TolC like channel protein downstream of a putative heavy metal resistance-nodulation-division (RND) efflux pump.

1.6.3.1 TolC channel proteins and multi drug efflux

The TolC protein acts as the only outer membrane channel protein in *E. coli,* functioning in multiple systems. These include the secretion of hemolysin through an ATP binding cassette (ABC) transporter (Wandersman and Delepelaire, 1990), but most famously it is involved with the AcrAB-TolC RND multi drug efflux pump (Du *et al.*, 2014).

Efflux is defined as the removal of substrates from the inside of the bacteria to the environment via an export system. There are multiple types of efflux systems such as ABC family, the major facilitator superfamily (MFS), multidrug and toxin extrusion (MATE) family, the small multidrug resistance (SMR) family and the RND family (Du *et al.*, 2018), however TolC like channel proteins only function with ABC, RND and MFS types (Zgurskaya *et al.*, 2011). RND efflux pumps form tripartite structures with an inner membrane pump which dictates the substrate, periplasmic bound fusion protein and TolC like channel outer membrane protein (Figure 1.6.6). Unlike ABC transporters, ATP is not used as the energy source for the export of substrates, instead there is a proton antiport with the proton entering the cytoplasm and the substrate being exported out of the cell via proton motive force. The role of efflux is a highly relevant topic due to its prominence in multi-drug resistance, and the challenge that puts on the treatment of bacterial infections (World Health Organization (WHO), 2016).

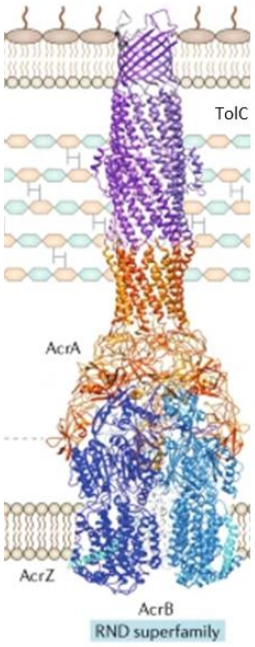

Figure 1.6.6 AcrAB-TolC as an example of an RND tripartite efflux pump. The tripartite formation is seen through the inner membrane pump (AcrB) and the outer membrane channel protein (TolC) being bound together by the membrane fusion protein (AcrA). Image used with permission from Du *et al* (2018).

AcrAB-TolC of *E. coli* and MexAB-OprM in *P. aeruginosa* are the most well characterised RND efflux pumps, both of which are involved with multi-drug resistance (Morita *et al.*, 2001). AcrAB are named after the acriflavine efflux system they belong too, however the number of different substrates that AcrB can export is expansive. An early study by Ma *et al* (1995) investigated the effect of *AcrA* and *AcrB* knockout mutants of *E.coli* and their effect on multiple antibiotics and detergents. Both mutants had a greater susceptibility to multiple antibiotics and detergents such as Novobiocin, erythromycin and sodium dodecyl sulphate. It was also demonstrated that this effect was due to efflux and not membrane permeability, this was observed by investigating the membrane penetration of Cephalothin and seeing no difference between wild type and AcrAB null mutants. This was further supported by Sulavik *et al* (2001), who demonstrated a large range of antibiotics that were substrates of AcrAB through comparing minimal inhibitory concentrations of a AcrAB null mutant and its wild type. This study showed the vast promiscuity of the AcrAB efflux pump, with increased sensitivity to 26 hazardous compounds in the AcrAB null mutant in comparison to the wild type. The promiscuity of RND efflux pumps is what allow the pump to facilitate the resistance to multiple antibiotics and other hazardous materials such as bile salts (Rosenberg *et al.*, 2003). More recent work by Hobbs *et al* (2012), demonstrated another protein with a role in

the AcrAB-TolC system that may be involved with substrate specificity. Their work revealed that an inner membrane protein called AcrZ can interact with the AcrB complex. Further investigation through the knockout of AcrZ displayed increased sensitivity to known substrates of the AcrAB complex but not all of them, this led the authors to hypothesise that AcrZ may have a role in the recognition and export of specific substrates. Further to this, work by Wang *et al* (2017) demonstrated through cryo electron microscopy that AcrZ binds to AcrB, and it is present through multiple conformation changes of AcrAB-TolC when interacting with a substrate. Although AcrZ clearly binds to the substrate specific AcrB protein, there is not enough evidence provided for AcrZ being involved with certain substrate recognition.

Six operons of putative efflux systems including *PGN2012* in *P. gingivalis* have been investigated for their role in the resistance to antibiotics. An initial study by Ikeda and Yoshimura (2002) investigated the operon PGN_1430-1432 (referred to as XepCAB in their study), by creating individual knockout mutants of each gene in the operon. The MIC of each mutant was assessed and an increased sensitivity to ethidium bromide, and multiple antibiotics was observed, individual differences were seen between each mutant. Further to this, Inoue *et al* (2015) investigated six operons predicted to be involved in efflux. To do this, the authors made knockout mutants of the putative membrane fusion proteins (MFP) of each system and investigated the MIC of multiple antibiotics against the mutant and the wild types. All the mutants demonstrated a twofold increase to tetracycline sensitivity, whereas only two mutants became more sensitive to ampicillin, rifampicin and norfloxacin. The mutant of the MFP in the operon of *PGN2012*, demonstrated sensitivity to tetracycline but not the other antibiotics tested.

Antibiotic resistance through multidrug efflux is a challenge for the future of bacterial infection treatment. The acquired resistance of bacteria through horizontal gene transfer of multidrug efflux pumps is progressing the need for different treatments in bacterial infections (Blanco *et al.*, 2016). The ability of a bacteria to export multiple different types of antibacterial chemicals from a single efflux system indicates a potential target for future therapies.

1.6.3.2 Heavy metal efflux and PGN2012

The role of RND efflux systems is not solely the export of antibiotics, but the export of hazardous material. The substrates of RND superfamilies vary to include multiple toxic

compounds, with examples such as bacterial metabolites like enterobactin in *E. coli* (Horiyama and Nishino, 2014), and heavy metals in *Ralstonia metallidurans* (Nies, 2003).

Heavy metal ions are detrimental to bacteria in high concentrations due to their ability to produce oxygen free radicals that can kill bacteria. Investigating a zinc decantation tank led to the discovery of a highly metal resistant bacteria, now known as *R. metallidurans* but originally called *Alcaligenes eutrophus* (Mergeay *et al.*, 1985). Investigation by Mergeay *et al* discovered that *R. metallidurans* contains two plasmids with separate metal resistance operons, pMOL30 contained efflux genes that increased the MIC to Zn^{2+}, Co^{2+} and Cd^{2+} by 50 fold, 33 fold and seven fold respectively. These genes were eventually found to be a tripartite RND efflux pump and named CzcCBA, where CzcA is the RND efflux pump, CzcB is the membrane fusion protein and CzcC is the outer membrane channel (Nies *et al.*, 1987; Saier *et al.*, 1994). Homologues of these proteins have been found in other bacteria such as *P. aeruginosa,* in which they provide a metal resistance to Zn^{2+}, and Cd^{2+} under regulation by specific CzcR/S proteins (Hassan *et al.*, 1999). More information on the regulation of these types of RND efflux pumps are being discovered in other bacteria. In a study by Ducret *et al* (2020) the CzcCBA system of *P. aeruginosa* was shown to be slower to be expressed in the presence of excess Zn^{2+}, in comparison to another zinc exporter CadA. In this study, it was revealed that CadA and its transcriptional regulator CadR were required for expression of fluorescently tagged CzcCBA. The control of excess zinc may also be a virulence trait for *P. aeruginosa*. In the review by Gonzalez *et al* (2019), they describe a potential role of zinc homeostasis in the survival of *P. aeruginosa* upon internalisation from phagocytes. In which zinc that is sequestered during the immune response is released into the phagocyte greatly increasing the zinc concentration.

Like CzcCBA, there is also a RND efflux protein for the resistance of copper known as CusCBA which is best characterised in *E. coli* (Franke *et al.*, 2003). CusCBA also produces a RND tripartite efflux pump with an RND efflux pump (CusA), membrane fusion protein (CusB) and membrane channel protein (CusC) (Alav *et al.*, 2021). The metal resistance seen in CusA also has some promiscuity as is common with RND efflux pumps. In a study by Franke , Grass and Nies (2001) a knockout mutant of *CusA* (named ybdE in their study) was created. Investigating the sensitivity against silver nitrate indicated an increased sensitivity to silver cations.

Similarly, to the studies described here, *PGN2012* is the channel membrane downstream of a CusA/CzcA efflux pump, indicating a role in heavy metal efflux. *PGN2012* was overexpressed in the hyper invasive subpopulation of *P. gingivalis*. Therefore, our study we will investigate the role of *PGN2012* in virulence and efflux.

1.7 Aims

Previous findings from our lab group by Suwannakul *et al* (2010) and Naylor *et al* (2017) displayed novel findings on potential host pathogen interactions. Through reviewing the literature, we found there are gaps in research specifically in the roles of multiple genes from the invasive gene set identified by Suwannakul *et al*. Additionally, although Naylor *et al* gave a novel understanding of the interactions between *P. gingivalis* ompA and human oral epithelial cells, the receptors of these interactions are still unknown. Therefore, the aims of this thesis will be to further investigate the invasive gene set, specifically, *ompH1*, *ompH2*, *rfbB* and *PGN2012* to characterise knockout mutants of these genes and gain a better understanding of their role in adhesion and invasion. Additionally, we will attempt to identify the human oral epithelial cell receptor(s) of the L4 peptide from *P. gingivalis*.

1.7.1 Objectives

- Develop a method using a biotin-streptavidin pulldown immunoprecipitation technique to isolate and identify the receptors of the L4 peptide.
- Probe the receptor peptide interactions through receptor blocking assays, and invasion assays.
- Produce gene knockout mutants of *ompH1, ompH2, rfbB* and *PGN2012*.
- Characterise initial phenotypic changes in the knockout mutants against wild type *P. gingivalis*, including growth curves and biofilm formation.
- Characterise changes to virulence factors between the knockout mutants and wild type *P. gingivalis.*
- Investigate the change to adherence and invasion between the knockout mutants and wild type *P. gingivalis.*
- Investigate the client set of both ompH1 and ompH2 by comparing protein profiles and western blot against the wild type *P. gingivalis*

- Investigate any change to the LPS of the *rfbB* knockout mutant via LPS profiles compared to the wild type. If changes are found, investigate this change on potential inflammatory response of human cells.
- Investigate the metal sensitivity of the *PGN2012* mutant in comparison to the wild type, against the predicted metal cations Zn^{2+}, Co^{2+}, Cd^{2+} and Cu^{2+}.

Chapter 2. Materials and methods

2.1 Manufacturers and suppliers

All equipment, kits and reagents were provided by the suppliers listed in table 2.1. Unless otherwise stated, reagents were supplied by Sigma-Aldrich or ThermoFischer Scientific.

Table 2.1. Suppliers of equipment, kits, and reagents for this project.

Supplier	Location
Agar scientific	Essex (UK)
BD Biosciences	San Jose (US)
Bioline	London (UK)
Biorad laboratories	Hertfordshire (UK)
Cell signalling	London (UK)
Don Whitley Scientific	Shipley (UK)
Expedeon	Swavesey (UK)
GE Lifecare sciences	UK
Gibco	Leicestershire (UK)
Greiner	Kremsmunster (Austria)
iNtRON Biotechnology	Kyungki-Do (Korea)
Invitrogen	Paisley (UK)
Iscabiochemicals	Exeter (UK)
Merck	Darmstadt (Germany)
Millipore	Dorset (UK)
New England Biolabs (NEB)	Hertfordshire (UK)
Oxford Nanopore technologies	Oxford (UK)
Oxoid	Hampshire (UK)

Particle Metrix	Inning am Ammersee (Germany)
Promega	South Hampton (UK)
QIAGEN	West Sussex (UK)
Sigma-Aldrich	Poole (UK)
ThermoFisher scientific	Leicestershire (UK)

2.2 Common buffers and reagents

2.2.1 Phosphate buffered saline

Phosphate buffered saline (PBS) was made by dissolving one tablet of PBS into 200 ml of deionised water to give a PBS solution containing 137 mM NaCl, 2.7 mM KCl and 10 mM phosphate. Solutions made at greater volume were made with a 1 tablet per 200 ml ratio.

2.2.2 Crystal violet stain

A 0.1% (w/v) crystal violet stain was prepared by dissolving 500 mg of crystal violet powder in 500 ml deionised water.

2.3 Bacterial strains, and primers used in this study

2.3.1 *P. gingivalis* strains

Table 2.3.1 shows the *P. gingivalis* strains used in this study. All strains were from the collection of Professor Graham Stafford or generated in this study.

Table 2.3.1 *P. gingivalis* strains used in this study.

***P. gingivalis* strain**	**Description**	**Source**
ATCC 33277	Wild-type strain	Professor Graham Stafford
Δ*ompH1*	*OmpH1* gene replaced with erythromycin cassette in the chromosome of ATCC 33277	This study
Δ*ompH2*	*OmpH2* gene replaced with erythromycin cassette in the chromosome of ATCC 33277	This study

Δ*rfbB*	*Suspected rfbB* gene disrupted by polar effect of upstream erythromycin cassette in the chromosome ATCC 33277	This study
Δ*PG0063*	*PG0063* gene replaced with erythromycin cassette in the chromosome of ATCC 33277	This study

2.3.2 *Escherichia coli* strains

The *E. coli* strain used in this study is the DH5α competent strain supplied by New England Biolabs.

2.3.3 Plasmids used in this study

Details of plasmids used and produced in this study are given in table 2.3.2

Table 2.3.2 Plasmids used in this study.

Plasmid	Insert	Antibiotic resistance	Supplier
pJET 1.2	Empty plasmid used for blunt end cloning and storage	Ampicillin	Thermo Fischer Scientific
pTCOW	Empty plasmid used for the complementation of mutants using sticky end cloning with endonucleases.	Ampicillin/tetracycline	Professor Graham Stafford
pJET 1.2 Δ*ompH1*	An erythromycin resistance cassette (ErmF) replacing the *ompH1* gene with 1000bp 5' and 1000bp 3' flanking DNA. Made by	Ampicillin	This study

	geneart (Thermofischer)		
pJET 1.2 Δ*ompH2*	An erythromycin resistance cassette (ErmF) replacing the *ompH2* gene with 1000bp 5' and 1000bp 3' flanking DNA. Made by geneart (Thermofischer)	Ampicillin	This study
pJET 1.2 Δ*rfbB*	An erythromycin resistance cassette (ErmF) replacing the *rfbB* gene with 1000bp 5' and 1000bp 3' flanking DNA. Made by geneart (Thermofischer)	Ampicillin	This study
pJET 1.2 Δ*PG0063*	An erythromycin resistance cassette (ErmF) replacing the *PG0063* gene with 1000bp 5' and 1000bp 3' flanking DNA. Made by geneart (Thermofischer)	Ampicillin	This study

2.3.4 Primers used in this study

The sequences of primers used for PCR in this study are given in tables 2.3.3, 2.3.4 and 2.3.5.

Table 2.3.3 Primers for cloning confirmation of pJET plasmids.

Primer	Sequence (5'-3')
pJET 1.2 Forward	CGACTCACTATAGGGAGAGCGGC
pJET 1.2 Reverse	AAGAACATCGATTTTCCATGGCAG

Table 2.3.4 Primers for knockout mutation confirmation.

Primer	Sequence (5'-3')
Erythromycin forward	ATGACAAAAAAGAAATTGCCC
Erythromycin reverse	CTACGAAGGATGAAATTTTTC
ΔompH2 upstream flanking forward	TTCTTGTCTGCCGCTCAGAAG
ΔompH2 downstream flanking reverse	TTCTTTTTTAATCGACATGAC
ΔrfbB upstream flanking forward	ACTTAGATATTGACTGGAAAA
ΔrfbB downstream flanking reverse	ATTTGCCCTTCGGCATTGGCA
ΔOmpH1 upstream flanking forward	GCAGTTCTTGGTTCGTATAAT
ΔOmpH1 downstream flanking reverse	CCTTTGCGGTCAAGTCAATAG
ΔPG0063 upstream flanking forward	GGGCAATGACTGTATTACAGA
ΔPG0063 downstream flanking reverse	GCTGCTTTTCAATCAGTTCCG

Table 2.3.5 Primers for qPCR

Primer	Sequence (5'-3')
rfbB forward primer	CCGACGTCATATCCTCATCACC
rfbB reverse primer	CCAGATGAATGACTCCGTCG
16s Forward primer	ACGGGAATAACGGGCGATAC
16s Reverse primer	GCTGACTTACCGAACAACCTAC

2.3.5 Antibiotics

Antibiotics were used in media to select for specific mutations and plasmids where appropriate. Erythromycin and tetracycline were dissolved in ethanol whereas ampicillin was dissolved in deionised water. All antibiotic stocks were stored at -20^{o}C. A list of antibiotics used in this study is given in table 2.3.6.

Table 2.3.6 Antibiotics used in this study.

Antibiotic	Final concentration
Ampicillin	50 µg/ml
Erythromycin	5 µg/ml
Tetracycline	3 µg/ml

2.4 Bacterial culture

Porphyromonas gingivalis ATCC 33277 was cultured on fastidious anaerobic (FA) agar plates supplemented with 10% horse blood (Oxoid) for 72 hours in an anaerobic cabinet (Don Whitley Scientific miniMACs anaerobic workstation) at 37^{o}C with the atmospheric conditions of 10% CO_2, 10% H_2 and 80% N_2 (anaerobic conditions). Liquid cultures were grown for 16 hours in BHI broth supplemented with 0.5% yeast extract, hemin (1 mg/ml), cysteine (250 µg/ml) and vitamin K (1 mg/ml). Culture medium was supplemented to a concentration of 5 µg/ml erythromycin or 3 µg/ml tetracycline as required.

Escherichia coli DH5α was cultured on Luria Broth (LB) agar plates or in 5 ml LB broth at 37°C and agitated using a shaking incubator at 250rpm. For antibiotic selection of plasmids, the culture media was supplemented to a concentration of 50 µg/ml ampicillin as required.

2.4.1 Transformation of bacterial strains

2.4.1.1 *E. coli* transformation

Transformation of DH5α *E. coli* competent bacteria (NEB) was performed by heat shock following manufacturer's instructions. The transformed bacteria were selected for by culturing on LB agar plates supplemented with ampicillin.

2.4.1.2 P. gingivalis transformation

P. gingivalis ATCC 33277 was transformed through a natural competency method (Tribble *et al.*, 2012). To do this an overnight liquid culture of *P. gingivalis* ATCC 33277 was prepared as described in section 2.4. 1 ml of this culture was then pelleted by centrifugation at 16,000 xg for 2 minutes, the supernatant was discarded, and the pellet re-suspended in fresh equilibrated BHI broth with supplements. Plasmid DNA (2000 ng) was then added to the sample before being incubated for 24 hours at 37°C in anaerobic conditions. The culture was pelleted by centrifugation at 16,000 xg for 2 minutes and the pellet resuspended in 200 µl fresh BHI broth. 50 µl of the bacterial culture was then spread on an appropriate antibiotic FA agar plate and incubated at 37°C for one week in anaerobic conditions before being checked for positive transformants.

2.5 Eukaryotic cell culture

The culture of OKF6 (human oral keratinocytes) and H357 (human oral squamous cell carcinoma) cells was performed in a Class II microbiology safety cabinet, sterilised before use through cleaning with 70% industrial methylated spirit (IMS). All items were sterilised with 70% IMS before entering the cabinet. Any media used on the cells was preheated to 37°C in a water bath.

2.5.1 Growth media

OKF6 cells were cultured using keratinocyte serum-free media (KSFM) (Gibco). 500 ml KSFM was supplemented with 25 mg bovine pituitary extract (BPE) and recombinant epidermal growth factor (EGF). Low glucose Dulbecco's modified eagle medium (DMEM) supplemented with 10% foetal bovine serum (FBS) was used to neutralise trypsin during the passage of OKF6 monolayers.

H357 cells were cultured in low glucose DMEM supplemented with 10% FBS, 1% penicillin/streptomycin (1 µg/ml and 1 µg/ml respectively), and L-glutamine (2 mM). The same culture medium was used as neutralising media during the passage of H357 cells.

2.5.2 Cell passaging

Cells were grown to 70-80% confluency before being passaged. To passage the cells, they were first washed 3 times with 10 ml sterile PBS, then 2 ml Trypsin EDTA 1x buffer (2.5 mg/ml Trypsin, 380 µg/ml EDTA) was added and the cells were incubated for 10 minutes at 37^{o}C. Successful cell detachment by the trypsin was confirmed by viewing the cells using a light microscope at 20x magnification. After cell detachment, the Trypsin enzyme activity was neutralised by the addition of 4 ml neutralising media. The cell suspension was then centrifuged at 1250 xg for 5 minutes and the supernatant removed. The cell pellet was re-suspended in 1 ml of the cell growth media before the cell density was calculated. To calculate cell density a Neubaur improved haemocytometer was used and 10 µl of cell suspension was added to each well before being viewed under a light microscope at 20x magnification. Two quadrants of 16 squares were counted before being divided by 2, and then multiplied by 10,000. The equation below shows the calculation required.

Cells/ml= (dilution factor) x (Total number of cells counted/ number of quadrants counted) x 10,000

Cells were then seeded into a new flask or plate at the desired density. T75 cm^2 flasks were used for continual culture of both H357 and OKF6 cell lines.

2.6. Molecular methodologies

2.6.1 Bacterial DNA and RNA extraction

2.6.1.1 Chromosomal and plasmid DNA extraction

Chromosomal DNA was extracted from bacteria overnight liquid cultures using the Wizard Genomic DNA purification kit (Promega) following the manufacturer's instructions. Plasmid DNA was extracted using the Isolate II plasmid miniprep kit (Bioline) following manufacturer's instructions.

2.6.1.2 RNA extraction

RNA was extracted from overnight liquid cultures using the Monarch Total RNA Miniprep Kit (NEB) following manufacturer's instructions.

2.6.2 DNA analysis by agarose gel electrophoresis

2.6.2.1 Tris-Acetate-EDTA buffer (TAE)

TAE was used to make agarose gels and used as the running buffer during electrophoresis. A 50x stock solution was prepared and diluted to 1x final concentration. To make the 50x TAE buffer 242g of Tris(hydroxymethylamine)aminomethane (Tris base) was dissolved in 100 ml of 0.5M ethylenediaminetetraacetic acid (EDTA) (pH 8) and adding 57.1 ml glacial acetic acid before being made up to 1L by adding 842.9 ml deionised water (dH_20) and adjusted to pH8.

2.6.2.2 DNA analysis by Gel electrophoresis

DNA analysis was performed using a 1% agarose gel. Agarose gel powder was added to 1X TAE to make a 1% solution and made molten through microwave heating. 1.5 µl of ethidium bromide was added to the gel just before it was poured into the mould. DNA was then run on the gels using a voltage between 90-110 volts until desired DNA separation was achieved. The DNA was then visualised using UV light.

2.6.3 Polymerase chain reaction (PCR)

PCR was used to amplify selected sequences of DNA for multiple purposes such as mutant confirmation, DNA concentration, plasmid cloning or obtaining a desired area of DNA to use in other experiments. The process of PCR starts by breaking the double stranded DNA into single stranded DNA (denature step), the binding of specific DNA primers selected to produce the desired sequence of DNA (annealing step), and the complementation of the DNA by the extension of the PCR primers which is catalysed by a DNA polymerase enzyme (extension step). The DNA is amplified by increasing the number of cycles of these steps.

The reagents required and used for PCR are found in Table 2.6.1.

Table 2.6.1. Reagents required for performing PCR

Reagent	Volume (µl)
Dreamtaq polymerase master mix X2	10
Forward primer (10 µM)	1
Reverse primer (10 µM)	1
Sample DNA	1

Nuclease free water	7 (make up to the desired total volume)
Total	20

For colony PCR the conditions were the same, but a single colony of bacteria was added to the mixture rather than any DNA. The conditions of the thermocycler are given in table 2.6.2

Table 2.6.2. The thermocycler conditions for PCR using Dreamtaq master mix the temperature of the annealing step and the extension step may change to suit the primers used.

PCR step	Temperature (°C)	Time (Minutes: Seconds)
Initial denature	95	5:00
Denature	95	1:00
Annealing	55	1:00
Extension	72	1:00 (per Kb of DNA)
Final extension	72	7:00
Hold	4	∞

PCR results were then analysed using the methods described in section 2.6.2.2 using agarose gel electrophoresis and visualisation using UV light.

2.6.4 Reverse transcription

Complementary DNA (cDNA) was synthesised from 1 µg of RNA template using the High-Capacity cDNA reverse transcription kit (Thermo Scientific) by following the manufacturer's protocol. The cDNA was either used immediately or stored at -20°C.

2.6.5 Quantitative polymerase chain reaction (qPCR)

qPCR was performed using 2x qPCRbio Sygreen Blue mix Lo-ROX for the quantification of gene expression in *P. gingivalis* cDNA samples. Primers for the 16S gene of *P. gingivalis* ATCC 33277 were used as an internal control for overall DNA quantity (Table 2.3.5). Triplicate samples were prepared using 1 µl of sample cDNA in the total reaction mixture of 20 µl. The temperature cycling was carried out using a 7900 HT Fast Real-Time PCR machine. Quantification was calculated using ΔCT values normalised to the appropriate 16s gene C_T values.

2.6.6 pJET 1.2 blunt cloning

To make the transformation vectors required for *P. gingivalis* gene knockout transformation blunt ended DNA was cloned into the pJET 1.2 holding plasmid. To do this DNA segments were designed with an erythromycin resistance cassette replacing the gene targeted for knockout and this cassette was flanked by 1000bp of upstream and downstream flanking DNA. These DNA fragments were produced commercially by Geneart (Thermo Scientific) and blunt cloned into the pJET 1.2 holding vector following manufacturer's instructions. *E. coli* DH5α (NEB) was then transformed with the blunt cloned product through heat shock transformation following manufacturer's instructions.

2.6.7 pTCOW sticky end cloning

To achieve gene knockout complementation an expression vector was designed to complement the knockout mutants. Complementation inserts were designed before being synthesised commercially by Eurofins Scientific. The pTCOW plasmid was provided by Professor Graham Stafford and isolated using the Isolate II plasmid miniprep kit (Bioline) following manufacturer's instructions. Both the insert and plasmid were cut using the restriction endonucleases *SPHI* (NEB) and *BamHI* (NEB) for 2 hours, the plasmid was treated with 1 µl Antarctic phosphatase for 1 hour after the first hour of restriction cutting. The restriction cut samples were separated by agarose gel electrophoresis as described in section 2.6.2, and the bands of correct size were excised and purified using the PCR and gel clean up kit (Bioline) following manufacturer's instructions. The concentration of the DNA samples was quantified using a nanodrop spectrophotometer. The cut insert and plasmid were ligated using T4 DNA ligase for at least 10 minutes. The ligation solution was used to transform DH5α *E. coli* (Monarch) as described in section 2.4.1, before being spread onto LB agar (100 µg/ml ampicillin) selection plates. Positive colonies were subcultured, before being streaked onto tetracycline supplemented LB agar plates (tetracycline 3 µg/ml). Negative growth on tetracycline selective plates indicated the insertion of the insert into the correct position of pTCOW, these positives were taken further to have their plasmid DNA extracted and sequenced.

2.6.8 Nanopore sequencing

Full genomic sequencing was performed in the laboratory using nanopore sequencing with the MinION and MinIT from Oxford Nanopore Technologies. DNA samples were extracted as described in section 2.6.1; the DNA was checked on an agarose gel for purity before being quantified using Qubit fluorometric quantification (Invitrogen) following manufacturers instruction. Adapters required for the DNA to pass through the MinION were attached to the DNA sample using the ligation sequencing kit (Oxford Nanopore) and cleaned with Ampure XP beads following the manufacturer's instructions. The DNA sample with adapter sequences was then analysed by the MinION following priming using the Flow cell priming kit (Oxford Nanopore) as described by manufacturer's instructions.

2.7.0 Protein methods

2.7.1 Biotinylated L4 peptide receptor pulldown

Biotinylated L4 peptide and a scrambled L4 peptide from the *P. gingivalis* OmpA protein were synthetically produced by ISCAbiochemicals. The scrambled L4 peptide was used as a negative control.

2.7.1.1 Biotinylated peptide binding

2 ml of cells were seeded into 6 well plates at a cell density 250,000 cells/ml and cultured until 80% confluency was achieved. The cells were washed twice with PBS before the addition of 1 ml biotinylated peptide (50 µg/ml in PBS), a negative control of cells with no biotinylated peptide was also used and PBS was used instead of peptide, and a positive control using a biotinylated RGD peptide was also used. The cells were then incubated at 37^{o}C for 5 minutes. Each sample had two wells, with one being crosslinked using 3,3'-dithiobis(sulfosuccinimidylpropionate) (DTSSP). To crosslink the peptide-receptor complexes 1 ml of DSTTP (1 mM in PBS) was added to the crosslinking wells and 1 ml PBS was added to the wells without cross linking before further incubation for 55 minutes at 37^{o}C. All cells were then washed twice with ice cold PBS. After washing the cells were lysed using 200 µl of lysis buffer (2% NP-40, 1% Triton X-100, EDTA free protease inhibitor tablet (Roche) in PBS), the cells were then scraped, and the lysate was either used for streptavidin affinity chromatography pulldown or stored at -20^{o}C until needed.

2.7.1.2 Streptavidin affinity chromatography pulldown

The biotinylated proteins were isolated on Streptavidin coated beads (Amintra) using the following methodology. 20 µl of Streptavidin beads were first equilibrated with the lysis buffer used in the biotinylated peptide binding. The beads were washed by adding 600 µl lysis buffer and pelleting the beads by centrifugation at 2,000 xg for 2 minutes then removing the supernatant, this step was repeated once. The biotinylated complexes were bound to the beads by introducing 150 µl of lysate from each sample to the equilibrated streptavidin beads and incubated and slowly rotated at room temperature for 2 hours using a roller mixer. The beads are then pelleted by centrifugation at 2,000 xg for 2 minutes and the supernatant was discarded. The beads were then washed with 600 µl PBS before being pelleted by centrifugation at 2,000 xg for 2 minutes and the supernatant removed, this wash step was repeated 4 times. After the final wash step the proteins were eluted by re-suspending the beads in 50 µl SDS lysis buffer and boiling them at 95^{o}C for 5 minutes. Samples were then either frozen at -20^{o}C or used for SDS-PAGE analysis and staining with Coomassie instant blue (Expedeon).

2.7.1.3 Streptavidin affinity background optimisation

The H357 cell debris of the lysate was removed by centrifugation at 16,000 xg for 5 minutes; the supernatant was then used for all other steps.

To clear any non-specific binding the H357 cell lysate was cleared with streptavidin beads. To do this the lysate was incubated and slowly rotated on a roller mixer with equilibrated streptavidin beads for 2 hours. The beads were then pelleted, and the supernatant transferred to a new Eppendorf for future steps. This methodology would require the cells to be lysed, and then cleared before exposure to biotinylated peptides and cross linker.

To reduce possible electrostatic interactions of the H357 lysate with the streptavidin resin 300 mM NaCl was added to the PBS used for the streptavidin binding steps in the pulldown assay described in section 2.4.1.2.

If the steps were combined the samples first had the cell debris removed, and then were cleared with streptavidin beads, before finally being washed with PBS containing 300 mM NaCl.

2.7.2 Sodium dodecyl sulphate polyacrylamide gels (SDS-PAGE)

2.7.2.1 SDS-PAGE buffers

The upper buffer for the stacking gel was made by dissolving 6.06g Tris base and 0.4g SDS in 100 ml of dH_2O and the pH was made to 6.8.

The lower buffer for the resolving gel was made by dissolving 18.17g Tris base and 0.4g SDS in 100 ml dH_2O and the pH was adjusted to 8.8.

The running buffer was made by dissolving 12g Tris base, 4g SDS and 57.5g glycine in 1000 ml dH_20. This solution was diluted using 160 ml stock and diluting it with 840ml dH_2O.

The 2x SDS loading buffer was used to boil protein samples in preparation to run on the SDS gels. To make the 2xSDS loading buffer a 50 ml solution was prepared by adding 40 ml 100 mM Tris-HCl, 10 ml of 10% glycerol, 0.1g bromophenol blue, 1g of SDS and 200 mM DTT.

2.7.2.2 SDS-PAGE gels

SDS-Polyacrylamide gels of 10% and 12% were used to separate proteins by size. They were made with a shorter stacking gel and a larger resolving gel using the formulas in table 2.7.1 and 2.7.2.

Table 2.7.1 Reagents and volumes required to make SDS-polyacrylamide resolving gels at 10% and 12% acrylamide.

Reagent	Volume for 10% SDS-polyacrylamide resolving gel	Volume for 12% SDS-polyacrylamide resolving gel requirements
dH_2O	4.825 ml	4.3 ml
Acrylamide	2.475 ml	3 ml
Lower Tris buffer	2.5 ml	2.5 ml
Ammonium persulphate (APS)	350 µl	350 µl
TEMED	5 µl	5 µl

Table 2.7.2 Reagents and volumes required to make the upper stacking gel.

Reagent	Volume
dH_2O	4.725 ml
Acrylamide	0.975 ml
Upper Tris buffer	2.1 ml
Ammonium persulphate (APS)	100 µl
TEMED	17 µl

The TEMED and APS were added last as they catalyse the polymerisation of the gel and need to be added just before pouring as the gel will begin to set. The resolving gel was used to fill a 1 mm or 1.5 mm thick BioRad glass cassette up until a gap was left for the stacking gel and well-comb, isopropanol was then added to the cassette to smooth the top of the resolving gel and remove any air bubbles. After the resolving gel had set the isopropanol was removed. The stacking gel solution was then added to the top of the resolving gel to fill the cassette, the well-comb was then placed into the stacking gel solution and the gel was allowed to set. Once the gel was set, the cassette was placed inside a BioRad protein gel tank (mini PROTEAN Tetra system) and the tank was then filled with SDS running buffer. Protein samples were then boiled in the 2x SDS loading buffer at 95^{o}C for 5 minutes. The well-comb was removed from the gel and 20- 30 µl of each sample was added to the wells and 5 µl of EZ-run protein ladder was added to one of the wells for comparison. The gel was run at 140V until the sample reached the bottom of the gel. The gel was then removed from the tank and cassette and placed in InstantBlue (Expedeon) Coomassie protein stain solution for one hour or overnight to stain the protein bands.

2.7.3 Western blot

2.7.3.1 Western blot common buffers

2.7.3.1.1 Semi dry transfer buffer

Semi-dry transfer buffer was used to transfer the proteins from the SDS-PAGE gel to the nitrocellulose membrane. To make the buffer 5.8 g Tris Base, 2.9 g glycine, 3.7 ml 10% SDS and 200 ml methanol were mixed before being made to 1 L with deionised water.

2.7.3.2 Western blot protocol

Protein samples were first separated by SDS-PAGE (described in section 2.7.2) before being transferred to nitrocellulose paper (GE healthcare life science) by semi-dry transfer. Semi dry transfer was achieved by placing the SDS-PAGE gel onto nitrocellulose paper (GE healthcare life science) that had been soaked in semi dry transfer buffer. The gel and paper were sandwiched between 6 soaked sheets of parchment paper, 3 on either side. The stack was placed nitrocellulose paper side down into a Biorad Trans-blot semi dry transfer cassette (Biorad), and the proteins transferred by running the cassette at 10 A for 25 minutes or until the ladder has visually transferred onto the nitrocellulose paper. The nitrocellulose paper was blocked in TBS (Tris buffered saline) supplemented with 5% milk powder for at least one hour. The nitrocellulose paper was washed 3x for 15 minutes with TBS-Tween (TBS supplemented with 0.1% Tween-20). The primary antibody was prepared according to its specific dilution factor in TBS- 5% milk before being incubated with the nitrocellulose paper for 1 hour. The nitrocellulose paper was washed again 3x for 15 minutes with TBS-Tween. The secondary antibody was prepared in TBS- 5% milk before being incubated with the nitrocellulose paper for 1 hour. The nitrocellulose paper was washed for a final 3x with TBS-Tween. The protein ladder was traced over with an ECL-reactive solution pen (Azure Biosystems) before enhanced chemiluminescence (ECL) solution (Thermo Scientific) was prepared and incubated with the nitrocellulose paper for 10 minutes. The horse radish peroxidase (HRP) conjugated to the secondary antibodies was activated and fluorescence was either observed using light sensitive CL-Xposure film (Thermo Scientific), or a LICOR luminescence scanner.

2.7.3.3 Antibodies

All antibodies used in this study were diluted to their recommended dilution factor in TBS- 5% milk before incubation with the nitrocellulose paper. The antibodies used in this study are listed in table 2.7.3.

Table 2.7.3 Antibodies used in this study; all were prepared to the specified dilution using TBS-5% milk.

Antibody	Type	Dilution	Supplier
Anti-alpha5 integrin	Primary, anti-rabbit	1:1000	Millipore

Anti-FimA	Primary, anti-rabbit	1:2000	Professor Ashu Sharma (University of Buffalo, NY, USA)
Mab1B5 (used for gingipains)	Primary, anti-mouse	1:2000	Professor Mike Curtis (Kings college, London, UK). (Michael A. Curtis *et al.*, 1999)
Anti-rabbit IgG HRP conjugated	Anti-rabbit secondary	1:3000	Cell signalling

2.7.4 Glycoprotein analysis

Glycoprotein profiles were analysed using the Pro-Q Emerald 300 gel stain kit (Invitrogen) following manufacturer's instructions. Protein samples were first separated via SDS-PAGE as described in section 2.7.2 before the SDS-protein gels were incubated agitating overnight in fixing solution (50% methanol, 5% acetic acid in deionised water). The stained gels were visualised using a UV light box.

2.7.5 Enzyme linked immunosorbent assay (ELISA)

Secreted IL-6, IL-8 and TNFα in conditioned media were quantified using BD OptEIA^{TM} ELISA kits (BD biosciences). The conditioned media was diluted either 1:20 or 1:50 for IL-6 and IL-8 whereas for TNFα the media was used neat. The quantification was performed using the manufacturers protocol in 96-well plates (Greiner). Absorbance was read at 450 nm after adding the stop solution. Wavelength was normalised by subtracting the 570 nm absorbance from the 450 nm values, final values were compared as a percentage of quantity in response to wild-type LPS. Multiple comparisons ANOVA were used to identify statistical significance.

2.8 Characterisation methods

2.8.1 LPS gel analysis

2.8.1.1 LPS extraction

A 10 ml overnight culture of *P. gingivalis* was cultured as described in section 2.4 and made to 5 ml of OD_{600} 1. The LPS was then extracted using the iNtRON biotechnologies LPS extraction kit following the manufacturer's instructions.

2.8.1.2 LPS gel

The LPS samples were boiled for 3 minutes in 2xSDS loading buffer before being inserted into the wells of a 1 mm 10% SDS gel. The LPS was the run under the same conditions of an SDS-PAGE gel as described in section 2.4.2.2. The LPS was then stained using the Pro-Q™ Emerald 300 lipopolysaccharide gel stain kit following manufacturer's instructions and visualised using a UV camera box.

2.8.2 LPS treatment of macrophages

Monocyte derived macrophages (MDM) were isolated from peripheral blood mononuclear cells and seeded at $5x10^5$ cells per well in a 6 well plate (Greiner) before being incubated for 9-10 days. The cells were cultured in Iscove's Modified Dulbecco's Medium (IMDM) (Thermo Scientific) supplemented with 2% human AB serum (Sigma) and 1% penicillin/ streptomycin solution. LPS was isolated as described in section 2.8.1.1 and normalised to dry weight before being used in the experiment at 100 ng/mL in 2.5 ml of IMDM (sterile filtered). The MDM were washed twice with 1x PBS before being incubated with LPS supplemented IMDM for 24 hours. The conditioned media was taken and frozen at -20°C for future experiments. The MDM were washed twice with 1x PBS and frozen at -80°C for future RNA isolation.

2.8.3 Total protein profile

The total protein profile of *P. gingivalis* ATCC 33277 and its mutants were visualised using the following method. A 10 ml overnight culture of *P. gingivalis* was prepared as described in section 2.4; the OD600 was then adjusted to 1 by dilution with fresh BHI broth. 1 ml of bacteria culture was then pelleted by centrifugation at 8,000 xg for 5 minutes. The pellet was then re-suspended in 200 µl of 2x SDS loading buffer and boiled for 10 minutes at 95°C before being run on an SDS-PAGE gel and visualised by Coomassie staining.

2.8.4 Outer membrane protein profile

The outer membrane protein profile of *P. gingivalis* ATCC 33277 and its mutants were visualised using the following method modified from Murakami *et al* (2002). A 10 ml overnight culture of *P. gingivalis* was cultured as described in section 2.4 and made to OD_{600} 1. The bacteria were then pelleted by centrifugation at 8,000 xg for 5 minutes in a Beckman Coulter™ J-26 XP. The supernatant was discarded, and the pellet was re-suspended in 2 ml (0.01M HEPES buffer pH 7.4, 2 µl ribonuclease (Promega), 2 µl deoxyribonuclease (Promega)). The bacteria were then lysed by sonication by 5 cycles of 25 second sonication followed by one minute on ice (cycles were continued until the lysate became clear). 2 µl $MgCl_2$ (1 mM) was added to the lysate before centrifugation at 5,000 xg for 5 minutes. The supernatant was then transferred to a glass centrifugation tube and centrifuged at 75,000 xg for 45 minutes at 4°C. The supernatant which contains the periplasmic and cytoplasmic fraction was kept and stored at -20°C. The pellet was then re-suspended in 500 µl of 0.01M HEPES (pH 7.4) with 2% Triton-X100 and incubated at room temperature for 10 minutes, the solution was then pelleted by centrifugation at 75,000 xg for 45 minutes at 4°C. The supernatant was again stored at -20°C as it contains the inner membrane fraction. The pellet was then re-suspended in 500 µl 0.01M HEPES (pH 7.4) and centrifuged at 75,000 xg for 45 minutes. The supernatant was then discarded, and the pellet re-suspended in 50 µl 2x SDS loading buffer (made without DTT) and centrifuged at 16,000 xg for 5 minutes before being boiled at 95°C for 5 minutes and analysed by SDS-PAGE and Coomassie staining.

2.8.5 Biofilm formation assay

P. gingivalis overnight liquid cultures were prepared as described in section 2.4, the cultures were diluted to OD_{600} 0.05 and seeded into a 96 well plate (Greiner). The unused wells were also filled with BHI to avoid loss of broth through evaporation. The bacteria were then grown in anaerobic conditions for 72 hours at 37°C. The total growth was measured by measuring the OD_{600} of the plates using the TECAN infinite M200 plate reader. The wells were washed with PBS 3 times and stained with 100 µl 0.1% crystal violet for 20 minutes. The excess stain was then removed, and the stained biofilms were washed until the PBS became clear before being left to air-dry. The crystal violet in the biofilms were then solubilised using 100 µl ethanol: acetone (80:20) solution and transferred to a new 96 well plate. The crystal violet was quantified by the absorbance at 575 nm using the TECAN plate reader. The biofilm

formation was standardised against growth by dividing the crystal violet absorption by the OD_{600} results.

2.8.6 Outer membrane vesicle quantification

10 ml overnight cultures of *P. gingivalis* ATCC 33277 and its mutants were made as described in section 2.4, and the OD_{600} was measured. The cultures were pelleted by centrifugation at 10,000 xg for 30 minutes and the supernatant was filtered through a 0.22 µM filter. The ZetaView instrument (Particle Metrix) was calibrated using 100 nm polystyrene beads. Supernatants were diluted until in a suitable range for accurate measurement by the ZetaView. 2 ml of diluted supernatant was injected into the fluid cell. Particles were measured at 10 intervals across the fluid cell. Each sample was measured in 3 independent technical repeats to give average particles per millilitre value, the value was then multiplied by the dilution factor and normalised to the OD_{600} of the culture used.

2.8.7 Anaerobic growth curves

Overnight cultures of *P. gingivalis* are prepared as described in section 2.4. The OD600 was measured and made to 0.01 in equilibrated supplemented BHI. Samples were prepared in 9 replicates within a 96 well plate. The well plate was placed inside a Cerillo Stratus plate reader (Cerillo, Virginia) within the anaerobic incubator. The OD600 readings were blanked before being taken every 30 minutes for up to 3 days. The growth curves were then analysed statistically using a multiple comparisons ANOVA.

2.8.8 Metal ion sensitivity assay

Overnight cultures of *P. gingivalis* are prepared as described in section 2.4. The OD600 was measured and made to 0.1 in 1 ml equilibrated BHI supplemented with different concentrations of metal salts ranging from 0.01 mM to 5 mM. The samples were prepared in triplicate for each metal concentration and placed in the wells of a 96 well plate (Greiner). The 96 well plate was placed inside a Cerillo Stratus plate reader (Cerillo, Virginia) within an anaerobic incubator. The plate was incubated anaerobically, and the samples blanked, the OD600 readings were taken every 30 minutes for up to 5 days. Statistical difference was measured using a multiple comparisons ANOVA of the growth curves and Students T-test of specific time points.

2.8.9 Antibiotic protection assay

All antibiotic protections assays were carried out within class II safety cabinets with strict aseptic technique. All media was warmed to 37°C before use. H357 cells were seeded at $8x10^4$ cells/ml in 1 ml of media per replicate and incubated in two 24 well-plates (Greiner) at 37°C, 5% CO_2 until 70-80% confluent (24 to 48 hours). Once the desired confluency had been reached the media was removed from the monolayers and the cells were gently washed with PBS. One of the wells was sacrificed for counting, this was done by adding 500 µl of trypsin-EDTA (Sigma) and incubating at 37°C for 5 minutes until the cells had detached from the well. 500 µl of culture media was introduced to inhibit the trypsin before the cells were counted as described previously. The remaining wells were incubated with 1 ml DMEM supplemented with 2% bovine serum albumin (BSA) for 60 minutes at 37°C, 5% CO_2 to block any non-specific binding. During this incubation period, 3-day old *P. gingivalis* wild type and mutant strains were taken from a blood agar plate and suspended in DMEM. The liquid cultures of bacteria were prepared at a cell/bacteria ratio of 1:100 to make the multiplicity of infection (MOI) 100. After the 60-minute blocking incubation, the cells were washed three times with PBS and incubated with 1 ml of DMEM containing the *P. gingivalis* suspension for 90 minutes at 37°C, 5% CO_2. 6 wells of the 24 well plate without cells were used for the incubation of the bacterial culture to be used to count the viability of the wild type and mutant bacteria (3 wells each) at the end of the experiment. After the 90 minutes of incubation with the *P. gingivalis*, the wells containing both cells and bacteria were washed three times with PBS. One of the 24 well plates with cells and bacteria were incubated for 60 minutes with DMEM supplemented with 200 µM metronidazole to kill the bacteria on the cell surface, allowing the analysis of invaded bacteria. The metronidazole treated plate was then washed 3 times with PBS. Both plates were analysed the same way at this point, 100 µl of deionised water was added to each well and the cells were scraped for 1 minute to lyse the H357 cells. The cell lysate was transferred to a 96 well plate and serially diluted 10-fold down to 10^{-4}, before three replicates of 10 µl samples was spotted onto a FAB plate and grown anaerobically for at least 7 days until colonies can be counted. The viability wells only containing bacteria were also serially diluted and spotted onto FAB plates in the same manor without the addition of water or scraping.

2.8.10 Gingipain protease activity assay

The activity of the two different types of gingipain proteases; arginine and lysine were investigated using either an arginine or lysine substrate attached to the fluorescent 7-amido-

4-methylcourmarin, the fluorescence of which can be measured once cleaved from the substrate.

2.8.10.1 Arginine

Overnight cultures of *P. gingivalis* were prepared as described in section 2.4. The OD 600 was adjusted to 0.01 with equilibrated supplemented BHI. 1 ml of OD_{600} 0.01 culture was pelleted via centrifugation 13,000 xg for 3 minutes, washed and resuspended in 1 ml PBS. To look at arginine gingipain protease activity a substrate of 100 µl PBS containing 1 mM L-cysteine, 200 µM αN-benzoyl-L-arginine-7-amido-4-methylcourmarin was incubated at room temperature for 5 minutes with 50 µl of the sample in triplicate in a 96 well plate. The reaction was then quenched with the addition of 50 µl of 200 µM N-α-tosyl-L-phenylalanine chloromethyl ketone (TPCK), before the fluorescence of the released methylcoumarin was read using a TECAN plate reader with the excitation and emission 365 nm and 460 nm.

2.8.10.2 Lysine

Overnight cultures of *P. gingivalis* were prepared as described in section 2.4. The OD600 was adjusted to 0.01 with equilibrated supplemented BHI. 1 ml of OD_{600} 0.01 culture was pelleted via centrifugation 13,000 xg for 3 minutes, washed and resuspended in 1 ml PBS. For Lysine protease activity a substrate of 100 µl PBS containing 1 mM L-cysteine, 10 µM D-Ala-Leu-Lys-7-amido-4-methylcoumarin (Merck) was incubated for 5 minutes at 37°C with 50 µl of sample in triplicate in a 96 well plate. After the incubation 50 µl of Tosyl-L-lysyl-chloromethane hydrochloride (TLCK) was added and the fluorescence read using a TECAN plate reader with the excitation and emission 365 nm and 460 nm.

2.8.11 Oxidative stress sensitivity assay

Overnight cultures of *P. gingivalis* were prepared as described in section 2.4. The OD600 was adjusted to 0.1 with equilibrated supplemented BHI. The culture was added to 96 well plates in triplicate along with hydrogen peroxide to a final concentration of 0.1 mM and incubated for 5 minutes. Samples were removed and serially diluted 10-fold up to 10^{-4} before 10 µl of each dilution was spotted onto FAB plates in triplicate. The FAB plates were incubated at 37°C in anaerobic conditions until surviving colonies can be counted (usually 7 days). Colonies were then counted and multiplied by 20x the dilution factor to get the number of colonies from each sample.

Chapter 3. Investigation into the human receptors of the *P. gingivalis* OmpA L4 loop peptide

3.1 Introduction

The major outer membrane protein OmpA is present in the majority of Gram negative bacteria, the structure of which is usually conserved with a C-terminal peptidoglycan binding domain and an N-terminal Beta barrel in the external section of the outer membrane with four peptide loops on the outer surface (Smith *et al.*, 2007). The loops on the Beta barrel surface have variable protein sequences which has previously been suggested to be targeted to the specific bacteria's niche and host targets (Hounsome *et al.*, 2011; Confer and Ayalew, 2013). OmpA proteins have multiple roles for Gram negative bacteria, especially within host-pathogen interactions. In *E. coli*, for example, OmpA has been shown to have roles in adhesion and invasion of host cells (Prasadarao *et al.*, 1996; Krishnan and Prasadarao, 2012), this effect is also observed in oral Gram negative bacteria such as *Aggregatibacter actinomycetemcomitans* during invasion of gingival epithelial cells (Kajiya *et al.*, 2011). A study from our group in Sheffield, by Naylor *et al* (2017) investigated the OmpA protein in *P. gingivalis*. They found that the OmpA2 subunit of the *P. gingivalis* OmpA trimer had a significantly greater effect on multiple virulence factors such as biofilm formation and invasive capabilities. It was shown in their study that the peptide loops on the surface of the OmpA2 subunit can bind to OKF6 cells (Figure 3.1.1). Pre-treating the OKF6 cells with the peptide loops before the invasion assays reduced the adherent and invasive ability of the wild type *P. gingivalis,* with the L4 peptide having the greatest effect. This binding therefore indicates that the peptide loops have a role in the adhesion to epithelial cells in order to invade, however the receptor is currently unknown.

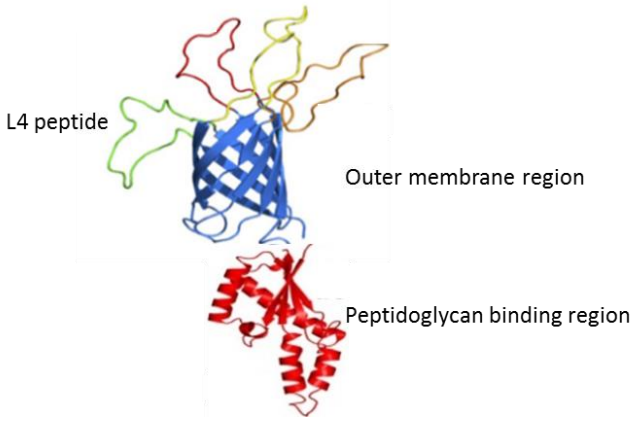

Figure 3.1.1 *P. gingivalis* structural model of OmpA outer membrane beta-barrel (blue) with loop peptides (orange, red, yellow, and green). Image altered from Naylor *et al* (2017) to add predicted peptidoglycan binding region structure (red).

To identify the receptor, in this chapter a biotin-pulldown immunoprecipitation technique was attempted, involving a biotinylated L4 peptide (bait) (used previously by Naylor *et al* (2017)) which it was hoped would bind to the receptors (prey), and allow recovery of peptide-receptor complex can be isolated by affinity chromatography using streptavidin beads In this way we hoped to isolate L4-human receptor complexes and identify the OmpA receptor on human cells.

3.1.1 Aims

The overall aim of this chapter is to investigate the potential host cell receptors of the L4 peptide found on the surface of the *P. gingivalis* OmpA protein. To do this the method of immunoprecipitation using the L4 peptide as bait for the receptors needed to be optimised.

3.2 Results

3.2.1 Design of L4-peptide- receptor complex isolation.

To try and isolate L4-receptor complexes, it was attempted to develop a specific immunoprecipitation/ cross-linking method to isolate complexes. The technique relies on the strong binding affinity between biotin and streptavidin to isolate the peptide-protein receptor complexes, the receptor can then be eluted from the streptavidin beads and analysed by SDS-PAGE. From these gels we hoped to analyse the protein bands representing the receptors by Mass Spectrometry (MS/MS) using a known human proteome using database, e.g., Expasy and Mascot. Similar methods of cell surface protein identification have been used frequently in the literature (Shahan *et al.*, 1999; Schulze and Mann, 2004; Miteva, Budayeva and Cristea, 2013). However, the receptors of the L4 peptide are unknown and therefore the binding affinity of the peptide loop to the receptor is unclear, this presented potential difficulty in lysing the cells to release the receptor/peptide complex as the lysis buffer can disrupt the binding. To provide a better binding in the receptor/peptide complex, a chemical cross linker was used which forms bonds between known lysine amino acids on the peptides and/or receptors. Using chemical cross linkers has provided the ability to isolate receptors with weak interactions with their ligands by providing an ulterior binding mechanism (Corgiat, Nordman and Kabbani, 2014). The planned workflow is outlined in Figure 3.2.1.

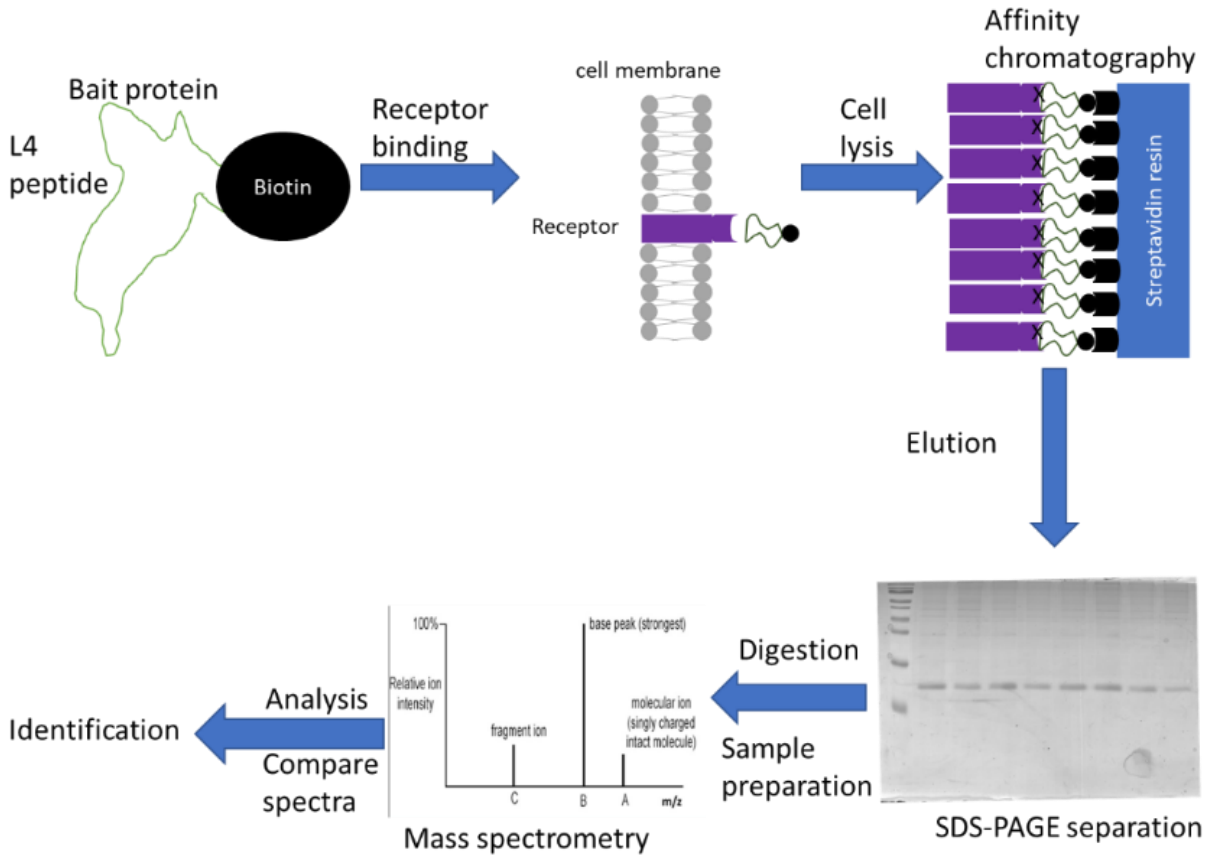

Figure 3.2.1 Immunoprecipitation workflow to identify the human L4 peptide receptor/s. The bait protein consisting of biotinylated L4 peptide is incubated to cell monolayers where it will bind to the receptor/s on the cell surface. The cells are lysed releasing the receptor peptide complex. The receptor peptide complex is isolated through streptavidin affinity chromatography before the receptor is eluted through SDS boiling. The eluted receptors are separated via SDS-PAGE with protein bands of interest being excised for digestion and analysis through mass spectrometry. The mass spectra are compared against the known human proteome through proteome databases.

We investigated multiple potential chemical crosslinkers which can be seen in table 3.2.2. The most important factor when choosing the best crosslinker for our experiments was the crosslinking target. We used a biotinylated recombinant L4 peptide and a biotinylated scrambled version as a control, both of which had multiple primary amines in the form of lysine in their structure (table 3.2.1). Therefore, we only looked at chemical crosslinkers that crosslinked primary amines knowing this should work with our peptides. The other factors we considered are cleavability, solubility, and membrane permeability. The optimal situation would be a crosslinker that is water soluble, cleavable, and not membrane permeable. This would stop the crosslinker from binding to intracellular substrates and focus on the membrane binding, whilst allowing us to separate the receptor peptide complex to analyse.

Out of the 6 primary amine cross linkers we considered, only one fit all our requirements. So, the decision was made to use DTSSP in our future experiments.

Table 3.2.1 Amino acid sequence of L4 peptide and its scrambled counterpart.

L4 peptide	**QAFAGKMNFIGTKRGKADFPVM**
Scrambled peptide	**RINFMAGMPGFADTVGKAKQKF**

Table 3.2.2 Chemical crosslinkers considered for this study. The chosen crosslinker used in this study was DTSSP indicated by the green font.

Cross linker	Spacer arm length (Angstrom)	Crosslinks	Cleavable by	Water soluble	Membrane permeable
Dimethyl 3,3'-dithiobispropionimidate (DTBP)	11.9	Amines to amines (imidoester)	Thiols (100-150 mM DTT at 37°C, 30 min)	Yes	Yes
3,3'-Dithiobis(sulfosuccinimidylpropionate) (DTSSP)	12	Amines to amines (Sulfo-NHS ester)	Thiols (100-150 mM DTT at 37°C, 30 min)	Yes	No
Bis(sulfosuccinimidyl)suberate (BS3)	11.4	Amines to amines (sulfo-NHS ester)	Non	Yes	No
Dimethyl suberimidate (DMS)	11	Amines to amines (imidoester)	Non	Yes	Yes
Disuccinimidyl suberate (DSS)	11.4	Amines to amines (NHS ester)	Non	No	Yes
Disuccinimidyl tartrate (DST)	6.4	Amines to amines (NHS ester)	Sodium meta-periodate	No	Yes

3.2.2 Initial attempts at Biotin-streptavidin pulldown of L4 peptide receptor/s

3.2.2.1 Biotin-streptavidin pulldown of L4 peptide receptor/s on OKF6 cells

Biotinylated L4 peptides were introduced to confluent OKF6 cells in a 6 well plate alongside a biotinylated scrambled L4 peptide negative control and a negative control of just OKF6 cells with PBS. As the receptor is unknown and the binding affinity is unknown a chemical cross-linker DTSSP was also used alongside the peptides in one well for each sample to attempt to trap and maintain any receptor-peptide complexes through the lysis step, in the case that these might be too transient to survive washing protocols. After binding, the cells were lysed, and the lysate was used for streptavidin affinity chromatography before being eluted by boiling in SDS-PAGE sample buffer and separated by SDS-PAGE before the proteins were stained with Coomassie instant blue protein stain. There was no clear difference between the protein bands found with and without the L4 peptide, nor is there any clear difference between the L4 peptide sample and the no peptide and scrambled L4 samples (Figure 3.2.2).

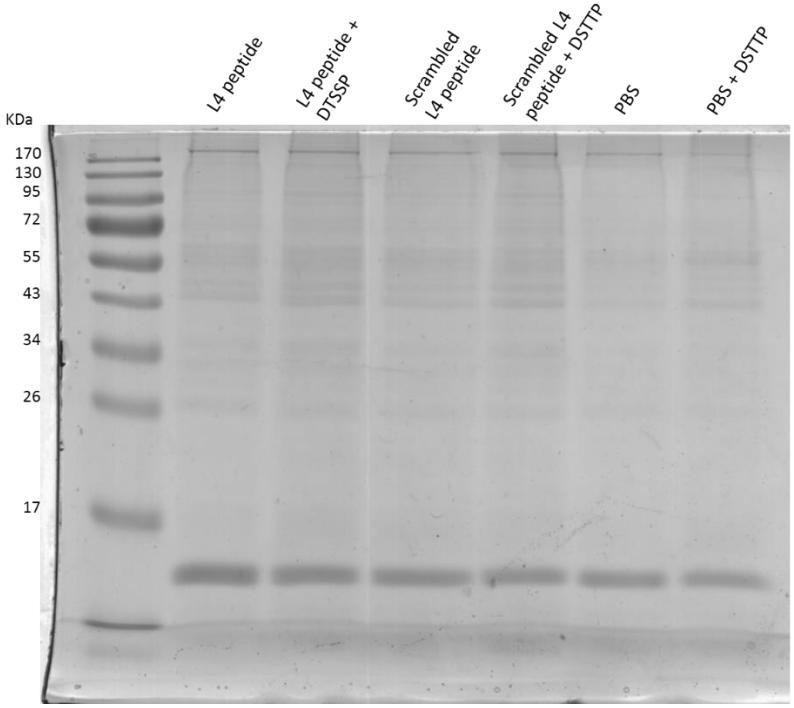

Figure 3.2.2. SDS-PAGE analysis of L4 receptor pulldown assays with OKF6 cells. Confluent OKF6 cells exposed to the L4 peptide, scrambled L4 peptide or PBS with or without DTSSP cross linker were lysed and separated by streptavidin chromatography before being analysed by SDS-PAGE using a 10% acrylamide gel. The gel was stained with Coomassie instant blue.

3.2.2.1 Biotin-streptavidin pulldown of peptide receptor/s on H357 cells

To assess this further the methodology was modified and repeated with a biotinylated RGD-peptide (with or without DTSSP) as a positive control, as RGD binds to integrins on the plasma membrane of human cells (Ruoslahti, 1996). H357 cells were also used instead of OKF6 cells from this point as they grow faster and more reliably, meaning throughput of experiments would be higher. In addition, H357 had been used in previous experiments to show invasion of *P. gingivalis* into human cells. There was still no clear difference between the L4 peptide with or without DTSSP and the other samples, demonstrating a high amount of non-specific binding (Figure 3.2.3). There is a slight increase in the amount of protein in the samples with the chemical cross-linker DTSSP which is more noticeable in the scrambled L4 +DTSSP sample and the PBS + DTSSP samples, which indicates the DTSSP is influencing binding. There was also no difference between the positive control RGD peptide and the negative control of just PBS. This indicated that there is too much non-specific protein binding background so further optimisation experiments were performed to remove the background from the experiment to have a clearer representation of possible binding.

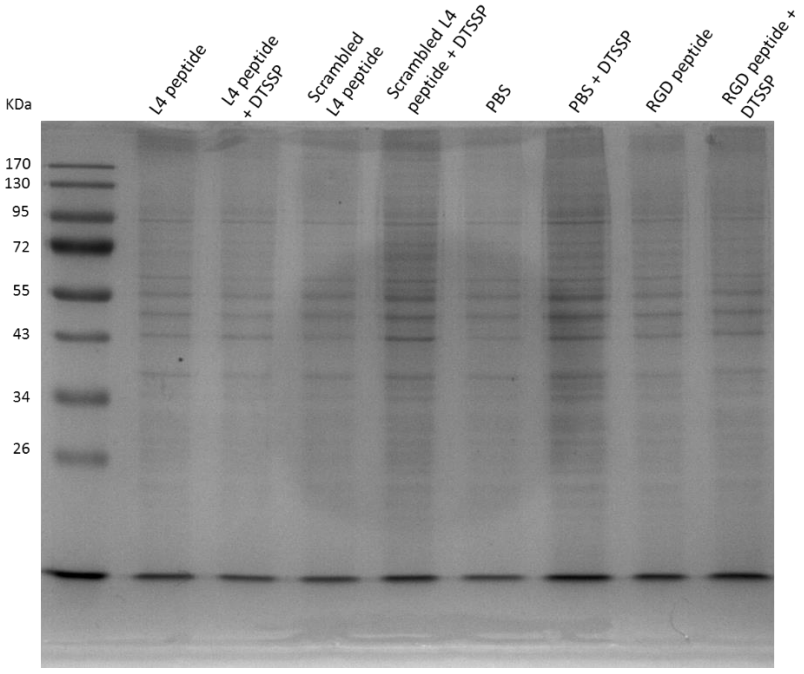

Figure 3.2.3. SDS-PAGE analysis of L4 peptide receptor pulldown assay using H357 cells. Confluent OKF6 cells exposed to the L4 peptide, scrambled L4 peptide, PBS or RGD peptide with or without DTSSP cross linker were lysed and separated by streptavidin chromatography before being analysed by SDS-PAGE using a 10% acrylamide gel. The gel was stained with Coomassie instant blue.

3.2.3 Biotin pull-down assay background optimisation

To attempt to remove the background from the cell lysate, a series of experiments were conducted to reduce non-specific binding as described in method section 2.7.1.3. Confluent H357 cells were lysed and either cleared with streptavidin beads, the cell debris removed, NaCl (300 mM) added to the PBS in the wash step or a combination of the three. There is a clear reduction in non-specific binding background in all the conditions when compared to the H357 control that had no conditions changed from the previous methodology (Figure 3.2.4). The most noticeable differences are the streptavidin cleared conditions (SC+Sa+D, SC+D, SC+Sa and SC) and the samples that have had the cell debris removed (D and Sa+D), whereas the addition of 300 mM NaCl in isolation had the least noticeable effect on non-specific binding.

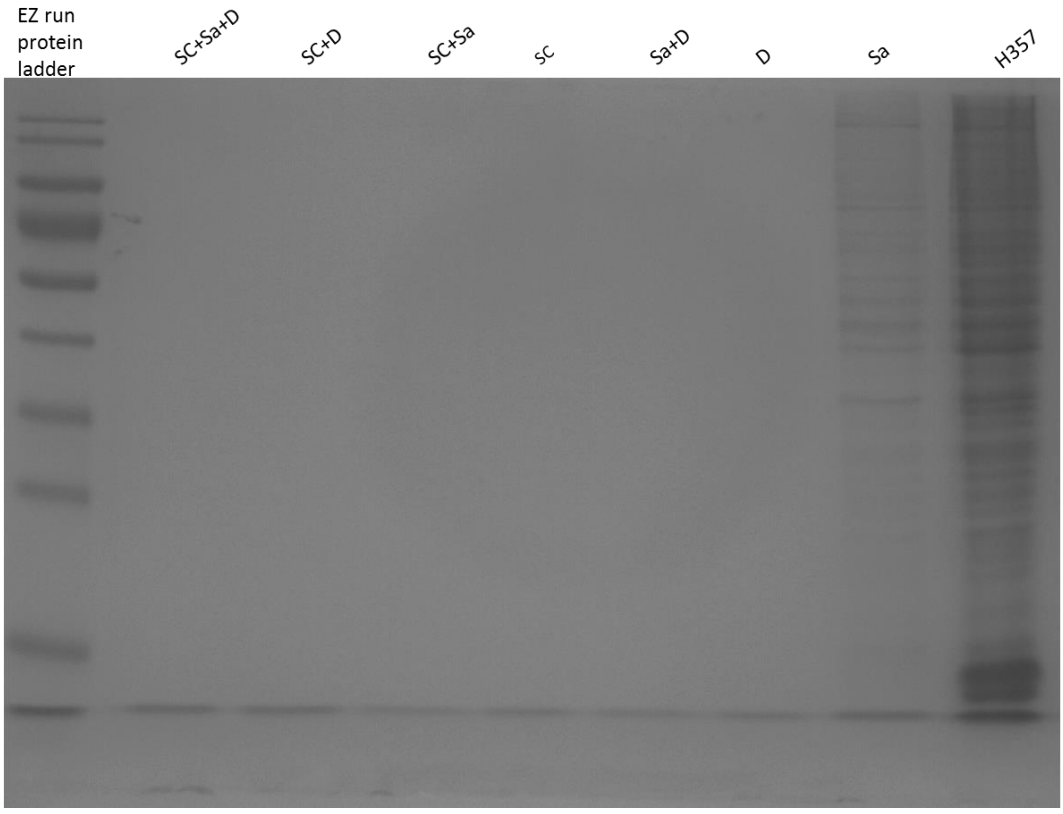

Figure 3.2.4. SDS-PAGE analysis of H357 cell lysate non-specific binding optimisation experiments. Confluent H357 cells were lysed before being and treated by streptavidin clearing (SC), removal of cell debris (D), the addition of 300 mM NaCl in the wash step (Sa) or a combination of the three. The treated lysates were separated by streptavidin affinity chromatography before being analysed by SDS-PAGE using a 10% acrylamide gel which was stained with Coomassie blue protein stain.

To ensure that there is still protein present in the lysate after the streptavidin clearing and the removal of cell debris, a Coomassie stained protein gel (Figure 3.2.5) was analysed with

the cell lysate after the streptavidin clearing step and the debris removal step but before the streptavidin chromatography pulldown assay. There was still protein present in all 3 samples including lysate that had been streptavidin cleared and had the debris removed (SC+D).

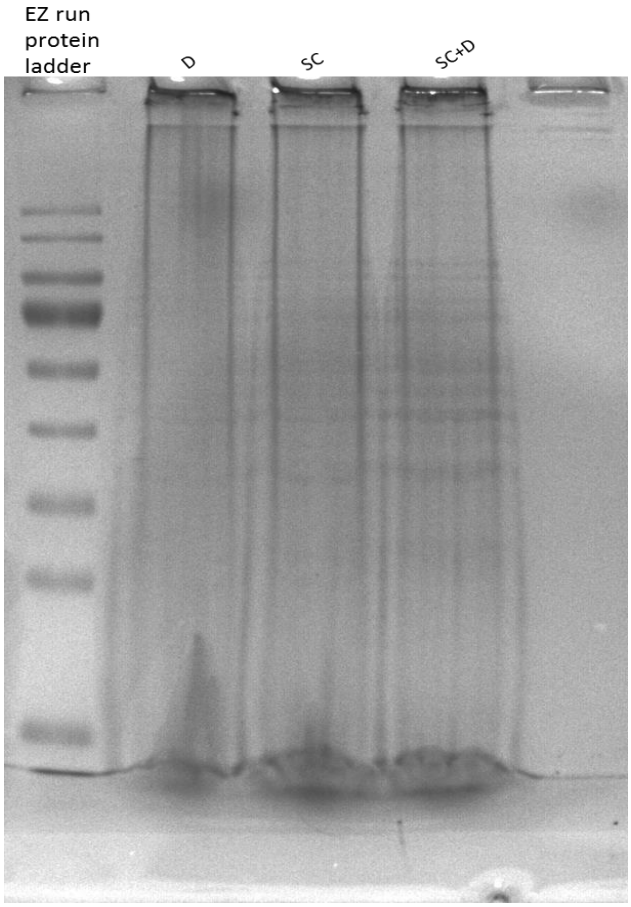

Figure 3.2.5. SDS-PAGE analysis of H357 lysate protein quantity after streptavidin clearing and the removal of cell debris. Confluent H357 cells were lysed before being streptavidin cleared (SC), having the cell debris removed (D), or both streptavidin cleared before the removal of cell debris (SC+D). The lysates were analysed by SDS-PAGE using a 12% acrylamide gel stained with Coomassie instant blue.

For future experiments, the conditions of pelleting cell debris and salt supplemented PBS were used as this had a beneficial effect in background removal, without disrupting the peptide binding methodology.

3.2.4 Optimised Biotin-streptavidin pulldown of L4 peptide receptor/s

After the successful removal of the background signal in the H357 lysate the number of cells used for lysis was increased from a T75 flask to a T175 flask to increase the chance of the receptor quantity being enough to be detected by SDS-PAGE. The biotin-streptavidin pulldown was repeated multiple times with the extra optimisation steps.

Figure 3.2.6 shows the results of the biotin-streptavidin pulldown with the T175 flask. Although the background signal has increased again with the greater number of cells used, two faint bands were seen in the L4 peptide treated sample around ~62 KDa and ~120 KDa.

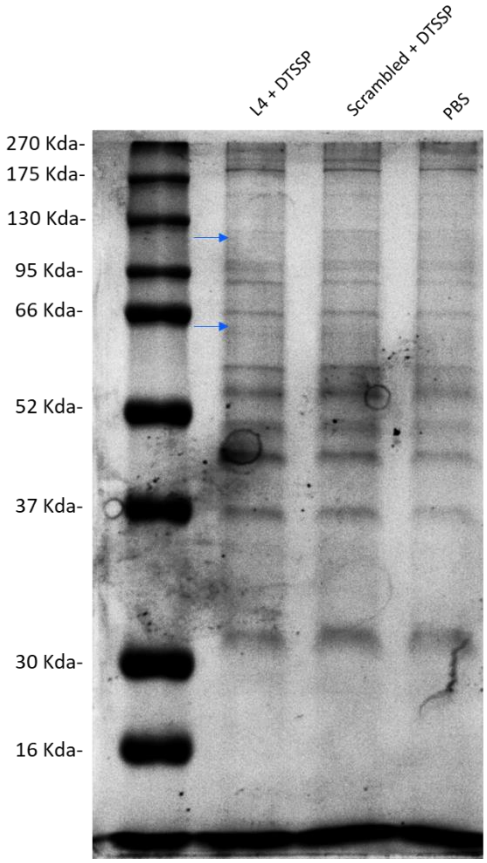

Figure 3.2.6 SDS-PAGE separation of biotin-streptavidin pulldown eluates stained with Coomassie instant blue. Confluent H357cells grown in T175 flasks were exposed to the L4 peptide + DTSSP, scrambled L4 peptide + DTSSP, and PBS. The cells were lysed, and the debris pelleted before samples were separated by streptavidin chromatography. Elutes were analysed by SDS-PAGE using a 10% acrylamide gel. The gel was stained with Coomassie instant blue. Different protein bands are indicated by blue arrows

The pulldown process was repeated two more times (Figure 3.2.7). Although the band at ~62 KDa was not seen in the repeats, the band at ~120 KDa was observed in the second repeat. Along with the ~120 KDa band there were three other bands seen in the second repeat at approximately 150 KDa, 100 KDa and 25 KDa. There was also a band at ~51 KDa seen in both repeats. All the new bands observed in figure 3.2.6 and the same position in the PBS control were excised and sent for digestion and Mass spec analysis. Unfortunately, none of the bands were identified due to low quantities of protein in the excised sections.

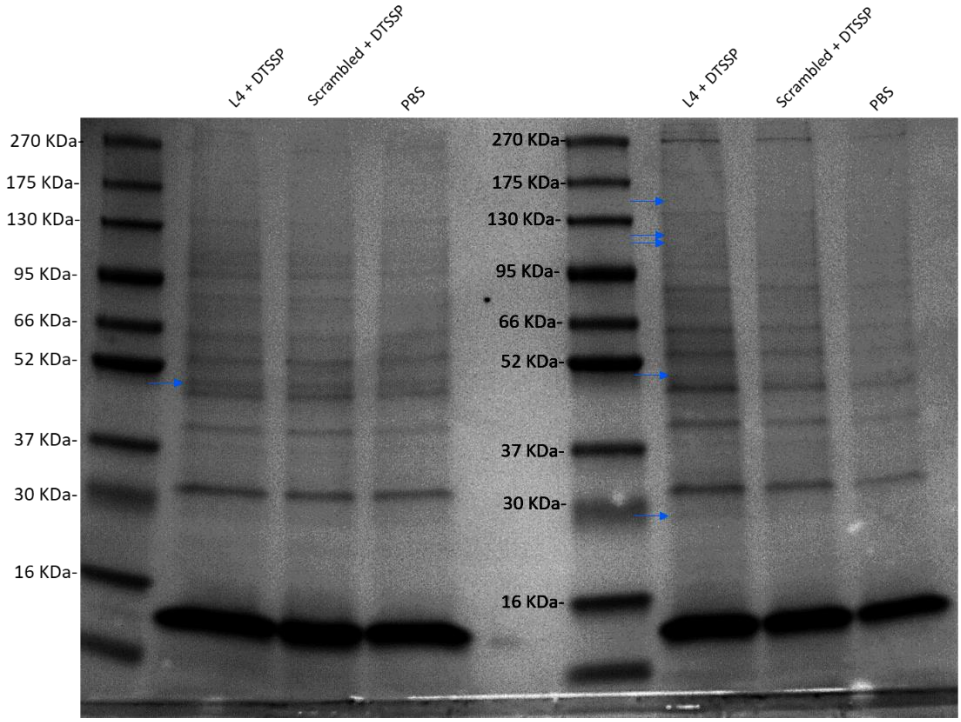

Figure 3.2.7 SDS-PAGE separation of two separate biotin-streptavidin pulldown experiment eluates stained with Coomassie instant blue. Confluent H357cells grown in T175 flasks were exposed to the L4 peptide + DTSSP, scrambled L4 peptide + DTSSP, and PBS. The cells were lysed, and the debris pelleted before samples were separated by streptavidin chromatography. Elutes were analysed by SDS-PAGE using a 10% acrylamide gel. The gel was stained with Coomassie instant blue. Different protein bands are indicated by blue arrows.

3.2.5 biotinylated L4 peptide used as a primary antibody against H357 lysate

To further examine whether the proteins previously seen in section 3.2.4 are actively binding to the L4 peptide we attempted a Far-western blot technique to probe for potential target proteins. To do this a Far-western blot was performed as described in section 2.7.3. In brief, confluent H357 cells from a T175 flask were lysed and the cell debris removed. The lysate was boiled in SDS loading buffer before being separated by SDS-PAGE. The proteins were transferred to nitrocellulose paper through semi-dry transfer. Once transferred the nitrocellulose paper was blocked overnight with TBS supplemented with 5% (W/V) milk powder. The nitrocellulose paper was washed with TBS-Tween before being incubated with L4 peptide for one hour at the same concentration that was used for the pulldown assay. The nitrocellulose was washed again with TBS-Tween before another one hour incubation with the horse radish peroxidase conjugated streptavidin. The nitrocellulose paper was washed again before being incubated with chemiluminescence solution to activate the HRP. The fluorescence was the visualised with the Licor luminescence scanner.

Although this experiment was only performed once, no signal was seen (Figure 3.2.8). Other western blot experiments were planned such as probing the biotin-streptavidin pull down assay elutes for known binding receptors for *P. gingivalis* such as α5β1 integrin, however due to time constraints these were not completed in this study.

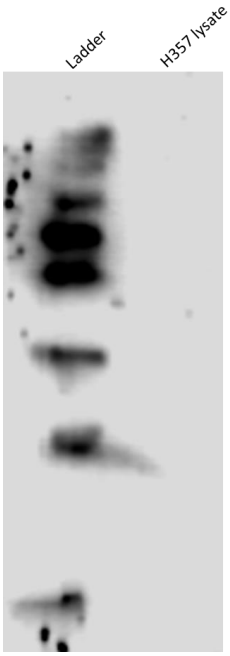

Figure 3.2.8 Western blot using the L4 peptide as the primary antibody against H357 lysate. Confluent H357 cells were lysed and had the cell debris removed before being boiled in 2x SDS lysis buffer. The samples were separated by SDS-PAGE on a 12% acrylamide gel. Proteins were transferred to nitrocellulose paper by semi-dry transfer. Proteins were probed initially with the biotinylated L4 peptide as a primary antibody, then by HRP conjugated streptavidin. HRP was activated using chemiluminescence solution before being visualised with the Licor luminescence scanner.

3.2.6 Glycoprotein stain of L4 peptide biotin-streptavidin pulldown eluates

It is likely that the receptor/s of the L4 peptide is a glycoprotein on the surface of the H357 cells, partly as over 70% of all proteins are glycosylated. Therefore, to visualise whether the L4 peptide might be binding glycoproteins we stained our pulldown samples for glycoproteins using a glycoprotein stain on the eluates of the biotin-streptavidin pulldown assays. To do this the methodology described in section 2.7.4 was used. In brief the process of the biotin-streptavidin pulldown was followed to the point of the eluates being separated by SDS-PAGE. However, instead of Coomassie instant blue protein staining, the glycoproteins were stained using the Pro-Q Emerald 300 gel stain kit (Invitrogen).

No obvious differences were observed in the presence of glycoproteins in either of the L4, scrambled and PBS samples (Figure 3.2.9). Similarly, to the protein stain gels, there is a lot of background which makes it difficult to analyse any subtle changes that may have occurred but does illustrate the number of glycoproteins in these samples as this looks similar to the CBB staining.

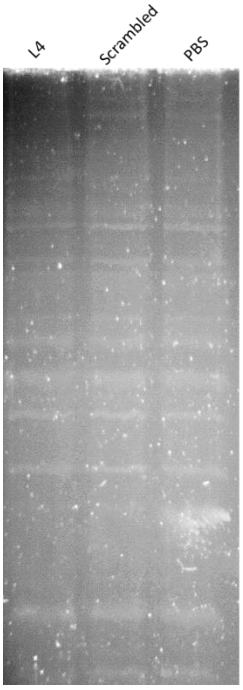

Figure 3.2.9 SDS-PAGE separation of two separate biotin-streptavidin pulldown experiment eluates stained with Coomassie instant blue. Confluent H357cells grown in T175 flasks were exposed to the L4 peptide, scrambled L4 peptide, and PBS. The cells were lysed, and the debris pelleted before samples were separated by streptavidin chromatography. Elutes were analysed by SDS-PAGE using a 10% acrylamide gel. Pro-Q Emerald 300 gel stain kit (Invitrogen) following manufacturer's instructions.

3.3 Discussion

The ompA family of proteins found in Gram negative bacteria are large surface exposed proteins inserted in the outer membrane. The first of these proteins was characterised in *E. coli* by Chai and Foulds (1977) and is the most well characterised. The overall structure of the ompA family of proteins is similar between different bacteria, retaining the peptidoglycan binding domain and outer membrane bound β-barrel with surface loops. However, the loops show the greatest amount of variance with suspected differences being due to interactions with a specific host/niche due to loop sequence changes in similar bacteria from different hosts (Hounsome *et al.*, 2011). OmpA has multiple roles within different bacteria such as; evading the immune response (Kim *et al.*, 2009), antibiotic resistance (Smani *et al.*, 2014; Inomata, Horie and Into, 2018), and the induction of apoptosis (Wang *et al.*, 2020). However, the most common trait of ompA between bacteria is its role in the adhesion and invasion of host cells (Smith, Mahon, M. A. Lambert, *et al.*, 2007). In the study by Naylor *et al* (2017) that investigated the OmpA of *P. gingivalis*, it was observed that knockout mutants of the OmpA genes had significantly reduced adhesion and invasion, specifically the OmpA2 gene. Following on from this it was also shown that the 4 surface loop peptides of OmpA2 had effects on the ability of *P. gingivalis* to invade oral epithelial cells. Specifically, the loop called L4 in their study had the greatest effect on the adhesion and invasion of oral epithelial cells, showing a 5-fold reduction in adhesion and invasion when exposed to the cells before the antibiotic protection assay. Naylor *et al*, also demonstrated that the L4 peptide had the greatest binding to the epithelial cells. The role of the OmpA loops and adhesion/invasion is not specific to *P. gingivalis* and is seen in other pathogenic bacteria. In a study by Prasadarao *et al* (1996) the role of OmpA was investigated in the meningitis related strain of *E. coli* K1 RS218 strain on brain microvascular endothelial cell (BMEC) invasion. Using Δ*ompA* mutants it was found that in the absence of OmpA the *E. coli* the invasion capability of the mutants was 25-50-fold reduced in comparison to the *E. coli* with OmpA, or when the OmpA was complemented into the knockout mutants. Prasadarao *et al* also investigated the OmpA peptide loops on the surface, and like Naylor *et al* found that treating the cells with the loop peptides prior to invasion significantly reduced the invasion by the bacteria. This effect of *E. coli* K1 OmpA loop binding was further evidenced by Shin *et al* (2005) who demonstrated that purified OmpA from *E. coli* K1 lacking its 4 peptide loops would not bind to BMEC whereas purified OmpA with its loops did bind.

The next stage of understanding the interaction between OmpA and host cells is to identify the receptors of which these important peptide loops bind too. Although Naylor *et al* provided strong evidence to show that the L4 peptide has the greatest effect on *P. gingivalis* invasion, how this happens and what the L4 peptide is binding too is currently unknown.

To begin this study, we knew the immunoprecipitation of an unknown receptor-peptide binding complex would be difficult. We know that the L4 peptide binds to the cells surface of oral epithelial cells as it was demonstrated by Naylor *et al*, therefore we know our target is a cell surface receptor. To isolate the cell surface receptor, we would need to use a lysis buffer that would break the receptor away from the cell for isolation through chromatography. The difficulty comes with the fine balance of using a lysis buffer that will be strong enough to release the full receptor complex from the membrane, without being too strong that is breaks the receptor-peptide complex in the process (Miteva, Budayeva and Cristea, 2013). This becomes more difficult when trying to identify an unknown receptor as the binding affinity is unknown. As we used a lysis buffer and cell disruption technique, we used a chemical crosslinker to give the best chance of retaining the peptide-receptor complex during lysis. We opted for DTSSP as our chemical crosslinker of choice. DTSSP contains an N-hydroxysulfosuccinimide (sulfo-NHS) ester at each end of a spacer arm, the sulfo-NHS group forms strong amide bonds with primary amines. This was key for our peptide due to it having three primary amines in its amino acid structure. DTSSP is also non membrane permeable which is optimal for our study as we are focussing on the membrane bound receptors and not internal binding targets. Finally, DTSSP is cleavable by DTT which is present in SDS lysis buffer, this is important to release the receptors from the chromatography media to be analysed. Out of all the chemical crosslinkers we considered DTSSP is the only one that fit all our criteria.

To assess the effect of DTSSP on the L4 peptide binding we planned to repeat a similar experiment to Naylor *et al* (2017). In which fluorescently labelled L4 peptide would be incubated with H357 cells with and without DTSSP with controls including the scrambled peptide. This fluorescence could then be viewed with a fluorescent microscope or measured quantitatively using a TECAN plate reader. However, due to time restraints this was not completed in this study.

The first set of affinity pulldown assays revealed that our protocol produces a lot of background “noise” through non-specific binding during the streptavidin affinity pulldown

step. It was impossible to see any minor changes to the protein profiles due to the amount of excess protein bands present. To combat this, we optimised our methodology to remove as much background as possible. Through this we either lysed the cells and performed streptavidin chromatography on the lysate before peptide treatment (streptavidin clearing), pelleted the lysate before streptavidin affinity pulldown (cell debris removal) or doing the washes with added salt to reduce electrostatic interactions (Shields and Farrah, 1983). Our results show that both streptavidin clearing the lysate or removing the cell debris had the greatest effect on reducing background. This was also the case when combining these processes. Treating the lysate with streptavidin is arguably the best way to remove non-specific protein binding as it is highly specific to our methodology. However, it requires the lysis of the cells before the exposure to the peptides which means that we may be selecting for binding to proteins internal to the cell rather than membrane bound receptors. The removal of cell debris also resulted in a reduction in background. However, there was the potential of losing too much protein in this process, after investigating the amount of protein left in the sample after the pelleting step this was revealed to not be the case. Therefore, we chose to use the cell debris removal and increased salt washes as our optimised methodology.

As the removal of background was successful, we decided to perform future peptide binding steps on confluent cells in T175 flasks instead of 6 well plates to increase the chances of finding the receptor at an observable quantity on a protein gel. Although confluent T175 flasks were used the quantity of protein in the elutes from the affinity chromatography was low giving feint bands in the SDS-PAGE results. Therefore, it took multiple attempts at each stage before visual changes in protein bands were observed. The first successful gel indicated two bands at ~120 KDa and ~62 KDa in the L4 peptide treated cells in comparison to the scrambled and PBS negative controls. After multiple attempts with bands too faint, we produced two gels with visual bands in the L4 peptide that were not in the scrambled or PBS negative. In these two experiments, one only produced a single band at ~51. The second experiment showed 4 bands, 2 of which matched previous experiments at ~120 KDa and ~51 KDA, whereas there were three more at approximately 150 KDa, 100 KDa and 25 KDa. All these bands were unidentifiable by mass spectrometry due to the lack of protein quantity. Given more time we would have repeated these experiments further with multiple T175 flasks as samples which would then be pooled to try and increase the quantity of the observed bands.

The issue with this is that the more overall protein quantity we work with the higher the non-specific background becomes.

Although it is impossible to know for sure what proteins these bands represent, it is interesting to speculate what they could represent. *P. gingivalis* has been shown to interact with the α5β1 integrin of host cells mainly through fimbriae (Yilmaz, Watanabe and Lamont, 2002; Zhang *et al.*, 2013). We observed bands at ~150 KDa and ~120 KDa which are like the bands seen when using α5 and β1 integrin antibodies respectively, with α5 antibody having a smaller band at 19 KDa close to the 25 KDa band seen in our samples. A study by Prasadarao (2002) identified one of the receptors of OmpA from *E. coli* to be a 95 KDa glycoprotein similar to hsp90 termed ecgp in BMEC's. A similar sized band is seen in our sample at ~100 kDa. Although no obvious bands were observed in the glycoprotein staining, this could also be due to the high amount of background.

To investigate these potential receptors further we a performed Far-western blot using the biotinylated L4 peptide as a primary antibody, hoping this would give us a more specific signal and potentially confirm some of the sizes of the potential receptors. There was no signal seen in this western, however this experiment was only performed once and needs further optimisation. As the binding affinity is unknown and the crosslinker was not used in this experiment it is possible that the L4 peptide could not bind strongly to the targets enough to maintain the binding during the washes.

Due to the time-consuming nature of the affinity pulldown and the low quantity of proteins in the pulldown elutes, we also started the process of searching for specific targets in the pulldown samples. Although the specific receptor of the L4 peptide is unknown, we have seen bands of similar size to α5β1 integrin proteins. Therefore, we started the process of using an α5 primary antibody to screen pulldown samples, with plans of doing the same with a β1 primary antibody. Although we could show that α5 could be detected in H357 lysate (not shown) we were not able to conduct this experiment on the pulldown samples in this study.

The receptor(s) of the L4 peptide may also have lectin like mechanisms and bind to carbohydrate groups due to glycosylation of the L4 peptide of *P. gingivalis*. This could potentially be investigated in the future using carbohydrate blocking to potentially prevent the binding of the L4 peptide. Experimentally this could be achieved by treating cells with

different carbohydrates and then probing for adhesion with the L4 peptide bound to streptavidin fluorescent beads.

3.4 Summary

Although the receptor/s of the L4 peptide were not identified in this study, we have further optimised a method with the potential to identify the receptors in future experiments. Our data suggest that there are potentially multiple receptors that L4 may interact with in oral epithelial cells, with bands at ~120 KDa and ~51 KDa being present in multiple experiments.

Chapter 4: Investigation of the role of the OmpH chaperone proteins

4.1 Introduction

The majority of *P. gingivalis* virulence factors such as; gingipain proteases, LPS, fimbriae, and other major proteins such as RagA and RagB are present in or on the outer membrane (Murakami *et al.*, 2002; How, Song and Chan, 2016) and are often the first to interact and elicit a response from the host. Whether that is through direct interaction to the host or via interactions by secreted outer membrane vesicles, the outer membrane plays an important role in the overall virulence of *P. gingivalis*.

In Gram negative bacteria outer membrane proteins are initially translated in the cytoplasm and need to be transported from the cytoplasm to the outer membrane. This process requires the protein to pass the hydrophobic inner membrane and hydrophilic periplasm and arrive at the outer membrane in a fully folded form. This is a difficult task without aggregating the unfolded proteins as they were exposed to these various environments (Rollauer *et al.*, 2015). To achieve this in Gram negative bacteria a translocation system is in place to allow passage across the inner membrane protein being a SecYEG translocon, chaperoning/ folding in the periplasm and assembly into the outer membrane often performed by the β-barrel assembly machinery (BAM) (Noinaj, Gumbart and Buchanan, 2017). The process begins when an outer membrane protein with an OMP signal peptide is recognised by SecAB and inserted into the SecYEG translocon pore powered by ATP (Economou and Wickner, 1994; Papanikou *et al.*, 2004). Once the unfolded protein proceeds through the Sec translocon it will arrive at the periplasm, where chaperone proteins are required to protect and transport the protein to prevent aggregation. In *E. coli* the most well researched of these chaperone proteins are DegP, SurA and SKP. DegP was initially thought to have chaperone activity at low temperatures (Spiess, Beil and Ehrmann, 1999), however a study by Ge *et al* (2014) found very little chaperone activity and concluded the role of DegP is to degrade aggregated OMPs in the periplasm through protease activity . Whereas SurA and SKP bind to the proteins and chaperone them to the BAM complex. The BAM complex then folds and inserts the proteins into the outer membrane (Noinaj, Gumbart and Buchanan, 2017) (Figure 4.1.1). Therefore, the role of the seventeen kilo Dalton protein (SKP) like chaperone proteins *OmpH1* and *OmpH2* may be instrumental in the transportation and correct implementation of many of these virulence factors in the outer membrane.

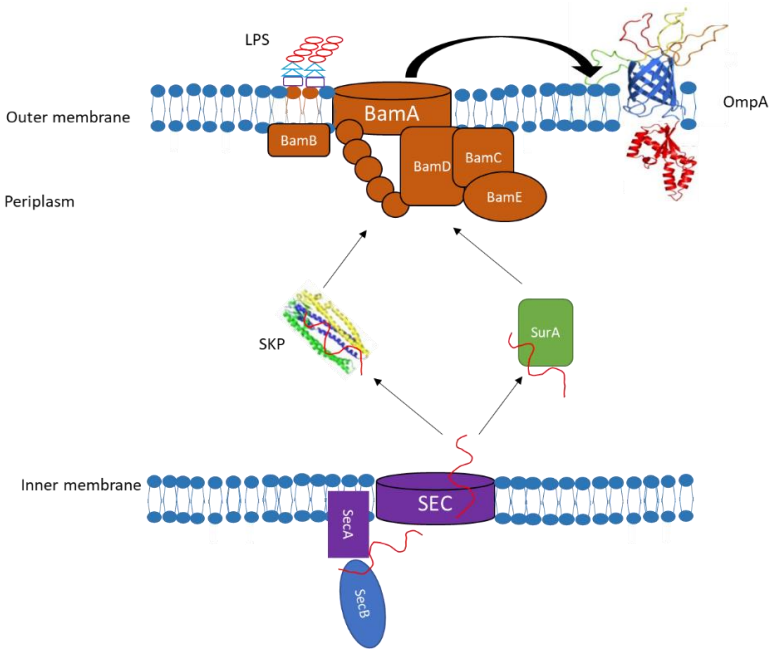

Figure 4.1.1 Schematic diagram of how an OMP is transported to the outer membrane in Gram negative bacteria. Proteins are first translated in the cytoplasm where an OMP signal peptide is recognised by the SecAB complex. SecA inserts itself into the inner membrane and allows passage of the unfolded protein into the Sec translocon. Once through Sec the protein is chaperoned to the BAM complex by chaperone proteins such as SKP and SurA. The BAM complex then folds and inserts the OMP into the outer membrane.

SKP is a chaperone of outer membrane proteins in *E. coli* which transports unfolded proteins from the inner membranes SEC complex to the Beta barrel assembly machinery (BAM) in the outer membrane (Schiffrin *et al.*, 2016). The structure of SKP is essential to its function of a chaperone protein. SKP is a trimeric protein with three α-helical "arms" which reach out 60 Å away from the β-barrel body (Figure 4.1.2). These three "arms" form a hydrophobic cage around the unfolded proteins to stop aggregation in the hydrophilic environment of the periplasm (Walton *et al.*, 2009). In *E. coli* there is only a single copy of the *SKP* gene, however this is not the case for *P. gingivalis* that has two SKP like chaperone proteins next to each other in the genome (Figure 4.1.3), with a conserved locus structure between all known strains of *P. gingivalis*.

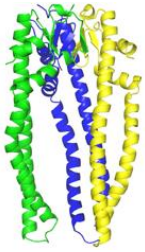

Figure 4.1.2 Three-dimensional structure of SKP from *E. coli*. 3D structure of SKP from *E. coli* showing each of the three 60 Å α-helical "arms". Image taken from Schiffrin *et al* (2016) used with permission.

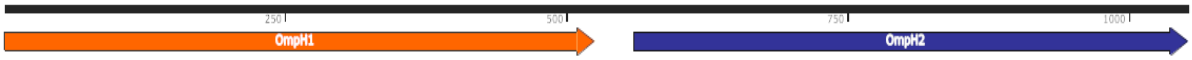

Figure 4.1.3 The operon containing both SKP like chaperone proteins *OmpH1* and *OmpH2*. Sequences for the two OmpH genes were taken from the established ATCC 33277 full genome sequence.

The role of the OmpH proteins are hypothesised to be similar to that of SKP in *E. coli* (Taguchi *et al.*, 2015), however unlike the well-studied SKP protein the role of the OmpH proteins are unknown. In a previous study by Suwannakul *et al* (2010), it was found that the OmpH genes were upregulated in a hyper invasive population of *P. gingivalis*, indicating their role in virulence.

4.1.2 Aims

The aim of this chapter is to investigate the role of the two SKP like chaperone proteins in *P. gingivalis ompH1* and *ompH2* in host-pathogen interactions. This was partially achieved by the knockout mutagenesis of *ompH1,* however Δ*ompH2* was unable to be made for reasons explained further in this chapter. Investigation into Δ*ompH1* was continued and initial characterisation achieved, focussing on virulence traits and invasive capability.

4.2 Results

4.2.1 Knockout mutagenesis attempts of *ompH1* and *ompH2*

Knockout mutagenesis was performed to produce a mutant in which *ompH1* and *ompH2* had been removed and the effects caused by this can be compared to the wild type to investigate the role of these two genes in host-pathogen interactions. An altered gene sequence was commercially produced by Genesynth, with *ompH1* or *ompH2* replaced by an Erythromycin cassette surrounded by 1000 bp of upstream and downstream DNA. These mutant sequences were blunt cloned into pJET1.2 blunt cloning vector for replication and storage. The plasmid DNA was extracted and used to transform *P. gingivalis* ATCC 33277 by natural competency as described in section 2.4.1.2. Positive colonies grown on erythromycin supplemented FAB plates were subcultured and the mutation was initially checked by PCR (Figure 4.2.1).

4.2.1.1 Confirmation PCR of Δ*ompH1* and Δ*ompH2*

Two separate PCR experiments were performed to confirm each mutation. The first used forward and reverse flanking primers to check the mutation had occurred in the desired region. The second experiment used a forward flanking primer and a reverse erythromycin cassette primer to confirm the presence of the erythromycin cassette (Figure 4.2.2).

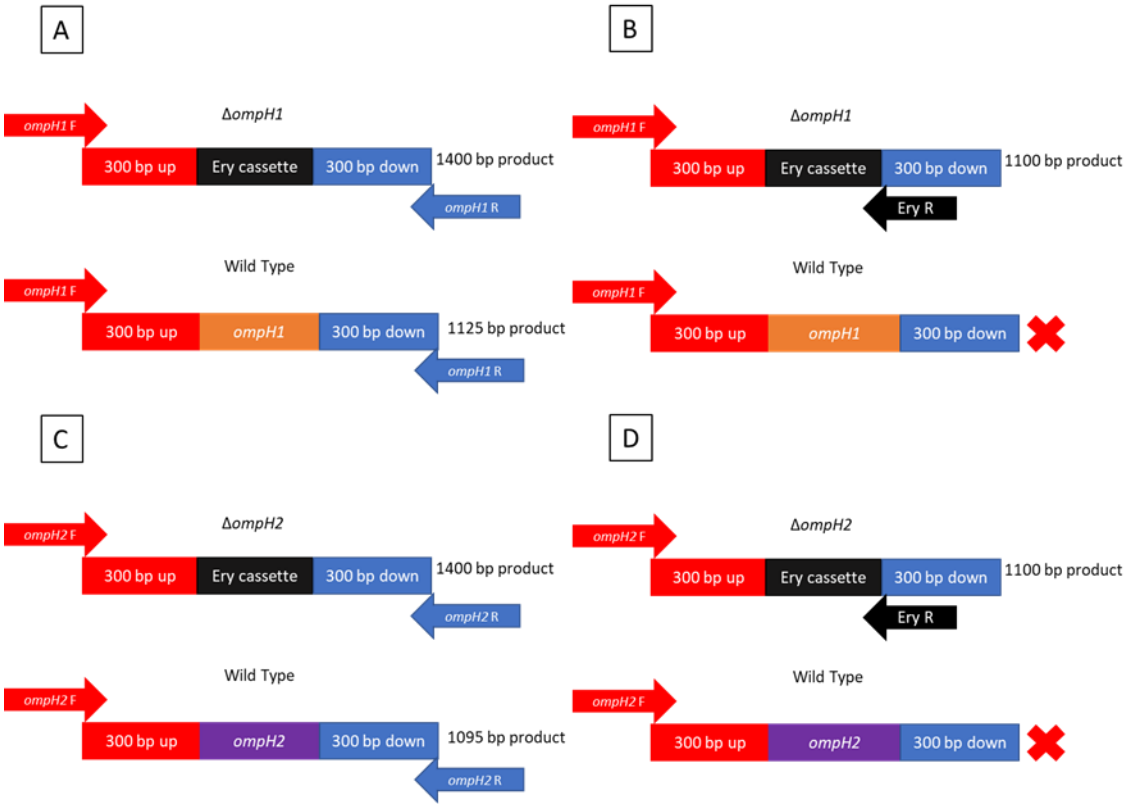

Figure 4.2.1 PCR reactions to confirm the erythromycin resistance cassette insertion for ΔompH1 and ΔompH2. (A) A PCR reaction which will produce a gene sequence that encompasses the ompH1 gene and the upstream and downstream flanking regions, producing a 1125 bp product for the wild type and a 1400 bp product for the mutant due to the shorter Ery cassette. (B) A PCR reaction which will produce a gene product with the upstream flanking region of ompH1 and the erythromycin cassette if correctly inserted, this will not give a product for the wild type. (C) A repeat of the reaction from A but with ompH2 flanking primers, giving a product of 1095 bp for the wild type and 1400 bp for the mutant. (D) A repeat of the reaction from B but using ompH2 forward primers giving a product of 1400bp for the mutant but no product for the wild type.

The confirmation PCR results for Δ*ompH1* are seen in Figure 4.2.2A and B. In figure 4.2.2A upstream and downstream flanking primers were used giving a product in the mutants of ~1400 bp, whereas the wild type has a band of ~1125 bp this difference shows that erythromycin has been inserted in the correct place giving a higher sized product. This is supported by figure 4.2.2B in which a forward flanking primer and erythromycin reverse primer was used, giving bands in the Δ*ompH1* mutants indicating the presence of erythromycin which was not seen in the wild type.

However, for the Δ*ompH2* PCR confirmation the results were different than what was expected in figure 4.2.1. Figure 4.2.2C and D show the confirmation PCR results for Δ*ompH2*. In figure 4.2.2C a single band for the wild type at ~1095 bp which is expected, however the

Δ*ompH2* sample shows two bands, one at the expected 1400 bp but a second unexpected band at ~1095 bp. This result indicates that the mutant gene sequence used for transformation has inserted itself adjacent in the genome of Δ*ompH2,* producing a mutant with the wild type copy of Δ*ompH2* intact but with the mutant gene sequence present as well.

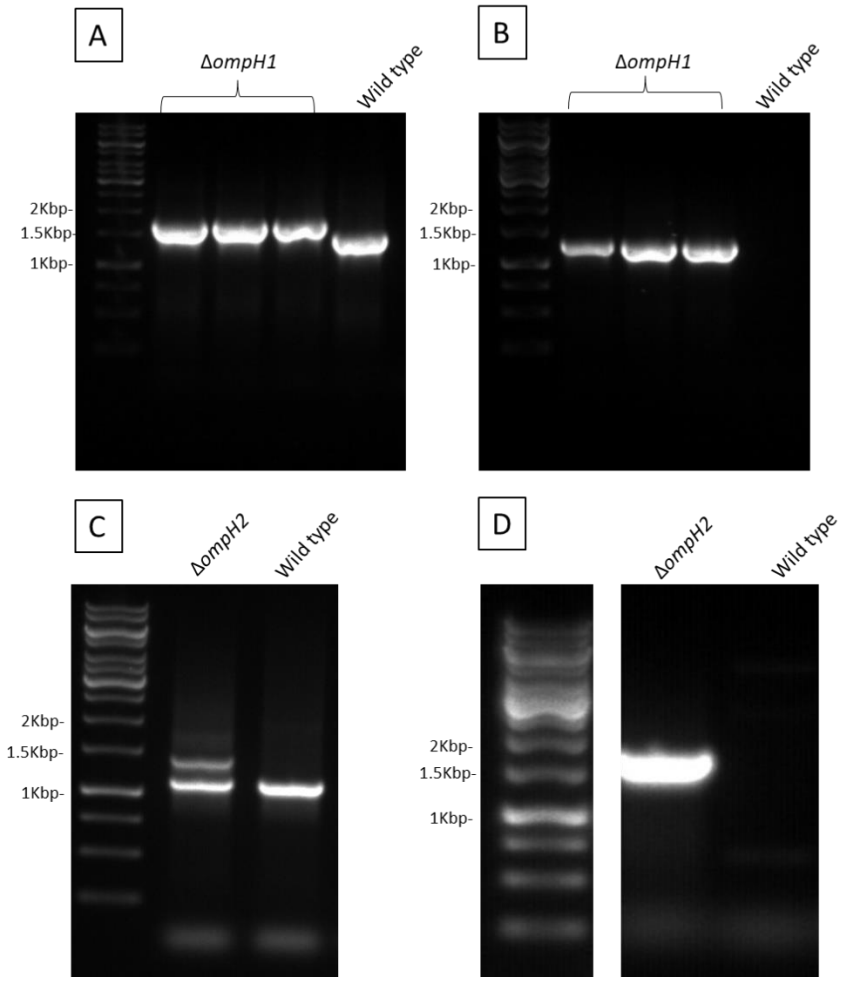

Figure 4.2.2 Confirmation PCR of Wild type, *ΔompH1* and *ΔompH2* chromosomal DNA. (A) Chromosomal DNA of wild type and three Δ*ompH1* mutants was amplified by PCR using upstream and downstream flanking primers as described in figure 6.2.2A. (B) Chromosomal DNA of wild type and three Δ*ompH1* mutants was amplified using an upstream flanking primer and an erythromycin reverse primer as described in figure 6.2.2B. (C) Chromosomal DNA of wild type and Δ*ompH2* was amplified by PCR using upstream and downstream flanking primers as described in figure 6.2.2C. (D) Chromosomal DNA of wild type and Δ*ompH2* was amplified using an upstream flanking primer and an erythromycin reverse primer as described in figure 6.2.2D. All PCR products were separated on a 1% agarose gel supplemented with 0.1% ethidium bromide by electrophoresis. Images were taken in a UV light box.

This data shows that the construct has been inserted into the DNA of the mutant but may have not knocked out the *ompH2* gene. This is rare but can happen during homologous recombination-based mutation when a single crossover event occurs rather than a double

crossover (Kuzminov, 2011). A single crossover event occurs when a construct holds two points of homology however only a single point is crossed over during homologous recombination, this leads to an insertion of the full plasmid rather than the insertion of just the erythromycin knockout region. A single crossover event may also retain the original gene rather than knocking it out, as it will implement the whole plasmid upstream or downstream of the gene of interest at one of the points of homology. To investigate what has happened in the genome of Δ*ompH2* and to further confirm the correct mutation of Δ*ompH1,* we followed these experiments with chromosomal genome sequencing.

4.2.1.2 investigation into the knockout mutation *ompH1* and *ompH2* through Nanopore genomic sequencing

To provide further evidence of correct knockout mutation in Δ*ompH1* and investigate what has happened to Δ*ompH2*, full genomic sequencing was performed to analyse the full sequence of the mutants and confirm mutation. In brief, chromosomal DNA was extracted from overnight cultures of ΔompH1 and Δ*ompH2*. The DNA was checked for purity via gel electrophoresis and cleaned using Ampure XP low fragment binding beads. Protein adaptors for the nanopore were attached to the DNA before being analysed using an Oxford Nanopore technologies minION. The DNA reads were compiled, aligned, and compared against a known *P. gingivalis* ATCC 33277 genome sequence taken from NCBI. Figure 4.2.3 shows the *ompH1* gene region with upstream and downstream flanking areas in Integrative genomics viewer (IGV) as a comparison to the wild type reference. The amount of matching reads to the alignment can be seen by the grey peaks in the top bar in the upstream and downstream flanks, the matching reads can be seen underneath these grey bars as blue or pink bars indicating the direction of the reads. However, in the *ompH1* region there were effectively zero matching reads to the alignment, and the majority of reads in this section match the erythromycin resistance cassette (seen by the multicoloured section). This data in combination with the PCR confirmation show that Δ*ompH1* has lost the original gene and it has been replaced with the erythromycin cassette.

In contrast to Δ*ompH1*, the results from chromosomal sequencing of Δ*ompH2* are more complicated (Figure 4.2.4). There amount of wild type reads of *ompH2* and erythromycin were very similar, indicating that although the erythromycin cassette was present it has not replaced the *ompH2* gene. Further upstream of *ompH2* in this mutant there is plasmid DNA.

This indicates that during mutagenesis there was a single crossover reaction during homologous recombination (Figure 4.2.5). We predict that this single crossover event has integrated the plasmid containing the erythromycin mutant sequence upstream of the original gene, as shown by some of the sequence reads. This explains the double band in the PCR confirmation as both the wild type sequence and mutant sequence are in the genome of Δ*ompH2*. As this double band was seen in multiple mutants made in this process it indicates that there is difficulty in mutating *ompH2* which supports the findings of Taguchi *et al* (2015) who also speculated that *ompH2* may be essential to the bacteria. These data taken together show that *omph1* was successfully knocked out to produce the mutant Δ*ompH1*. However, production of an Δ*ompH2* mutant has been unsuccessful.

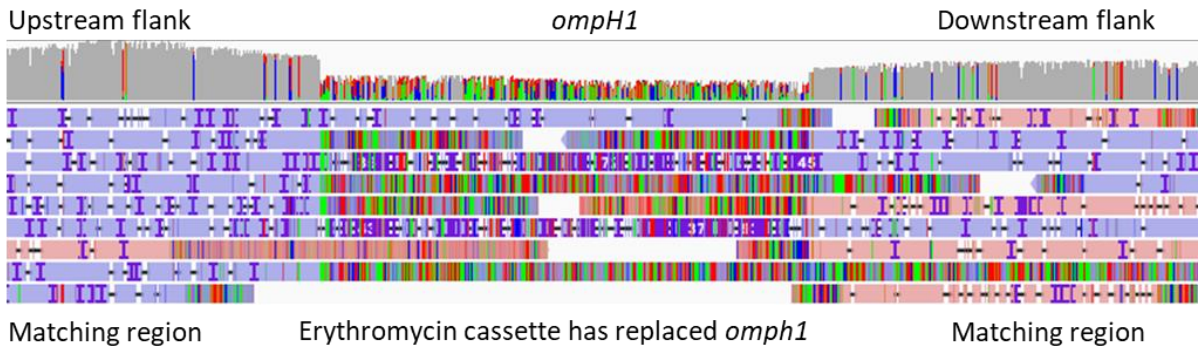

Figure 4.2.3 Change in the *omph1* gene in chromosomal sequencing of Δ*ompH1*. Nanopore chromosomal sequencing was performed on a chromosomal DNA extract of Δ*ompH1*. All the reads were aligned and compared to a previously generated full genomic sequence of *P. gingivalis* ATCC 33277 taken from NCBI. The aligned sequences and the reference sequence were viewed in the Integrative genomics viewer (IGV). Total matching reads are shown in the top bar as grey peaks, with the read data just underneath. Pink or blue bars indicate reads that match the reference genome, whereas multicoloured bars indicate differences to the reference genome.

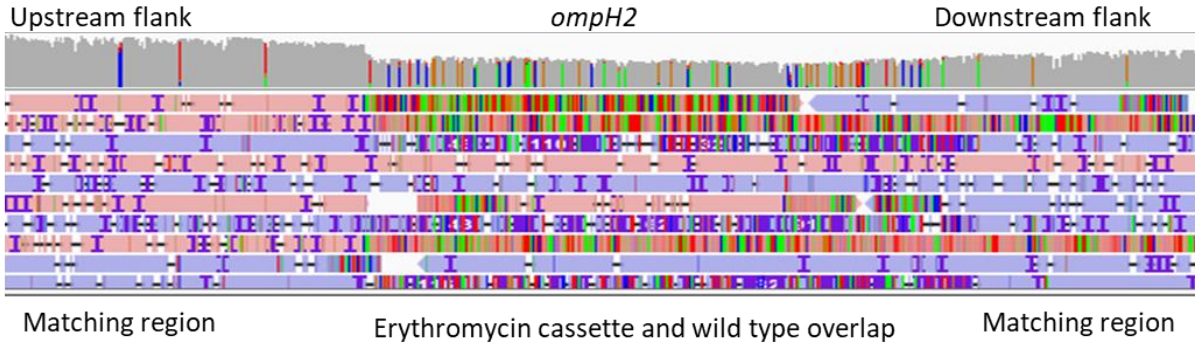

Figure 4.2.4 Change in the *omph2* gene in chromosomal sequencing of Δ*ompH2*. Nanopore chromosomal sequencing was performed on a chromosomal DNA extract of Δ*ompH2*. All the reads were aligned and compared to a previously generated full genomic sequence of *P. gingivalis* ATCC 33277 taken from NCBI. The aligned sequences and the reference sequence were viewed in the Integrative genomics viewer (IGV). Total matching reads are shown in the top bar as grey peaks, with the read data just underneath. Pink or blue bars indicate reads that match the reference genome, whereas multicoloured bars indicate differences to the reference genome.

Figure 4.2.5 Predicted single crossover event resulting in incorrect insertion of erythromycin cassette and plasmid DNA. *OmpH2* and the erythromycin cassette are shown to have both been inserted into the genome, this and the plasmid DNA found in the genome indicates a single crossover. Showing both the OmpH2 and the plasmid DNA being present. This is predicted by the position of the plasmid DNA in the sequence reads from the nanopore DNA sequencing.

4.2.2 Δ*ompH1* has a reduced growth rate in supplemented BHI in comparison to wild type *P. gingivalis*

Outer membrane proteins such as gingipains are important for the growth and nutrition of *P. gingivalis* (Hendrickson *et al.*, 2009), therefore the knockout of one of the transport proteins involved with folding or translocation of OMPs may affect the overall growth of *P. gingivalis* in laboratory conditions. To investigate the effect of Δ*ompH1* in *P. gingivalis* growth, anaerobic growth curves were performed. In brief, overnight cultures of Δ*ompH1* and wild type *P. gingivalis* were grown and normalised to OD_{600} 0.01 in equilibrated supplemented BHI as described in section 2.8.7. The samples were incubated at 37^{o}C in anaerobic conditions for up to 3 days, with the OD_{600} being measured every 30 minutes using a Cerillo stratus plate reader.

Figure 4.2.6 shows the results of the anaerobic growth curve experiments. During the exponential phase between 24.5 and 35 hours there is a significant decrease in rate of growth for Δ*ompH1* in comparison to the wild type. With a mean generation time of 240 minutes in the wild type compared to 375 minutes in Δ*ompH1* ($P< 0.05$). However, there is no significant difference in the stationary phase with the mean OD_{600} of the wild type being 0.941 and Δ*ompH1* being 0.841 with overlapping deviation of the standard error of the mean. This data evidence that the growth rate Δ*ompH1* has been reduced however the overall growth in supplemented BHI has not been reduced. Therefore, indicating that *ompH1* and/or its clients are involved with the growth rate of *P. gingivalis*.

The black pigmentation of this mutant is slowly obtained compared to the wild type indicating a disruption in the gingipains that will be investigated later in this chapter.

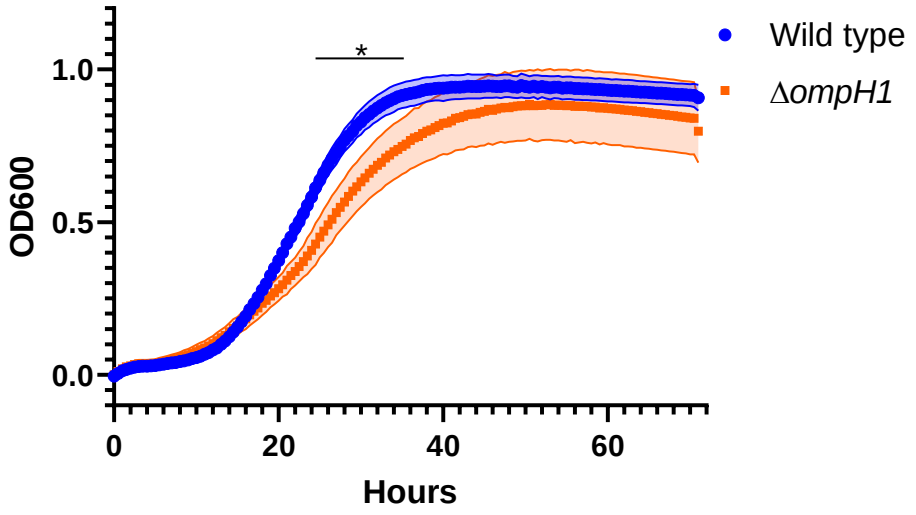

Figure 4.2.6 Anaerobic growth curve of Δ*ompH1* and wild type *P. gingivalis* in supplemented BHI. Wild type and Δ*ompH1 P. gingivalis* were prepared at OD_{600} 0.01 before being incubated at 37°C in anaerobic conditions within a Cerillo stratus plate reader as described in section 2.8.7. OD_{600} was first blanked before being read every 30 minutes for 72 hours. N=3 with 9 technical replicates per biological repeat, Shaded areas represent +/- SEM created on Graphpad prism. Statistical analysis was analysed by 2-way ANOVA comparing the difference of each time point. *p <0.05.

4.2.3 The effect of knocking out *ompH1* on the monoculture biofilm formation of *P. gingivalis*

Biofilm formation is an important virulence factor for the majority of infectious bacteria (Lebeaux, Ghigo and Beloin, 2014). Biofilms allow greater resistance to the environmental stresses surrounding the bacteria as well as providing protection from antibiotics (Larsen, 2002; Sharma, Misba and Khan, 2019) and host immune responses such as phagocytosis (Thurlow *et al.*, 2011). *OmpH1* is predicted to encode an SKP like chaperone protein, which has been indicated to be involved in the chaperoning of outer membrane proteins such as gingipains and potential other proteins such as *OmpA* which has been shown to be important in biofilm formation (Naylor *et al.*, 2017). Therefore, we investigated if *ompH1* had any effect on *P. gingivalis'* ability to form monoculture biofilms. To do this *P. gingivalis* liquid cultures were normalised to OD600 0.01 and incubated at 37°C in anaerobic conditions for 5 days. The OD600 was measured at the end of the experiment to normalise the biofilm formation to growth by dividing crystal violet absorption by OD_{600}, the biofilms were then washed gently with PBS and stained with crystal violet (Section 2.8.5). The biofilms were washed again with PBS to remove excess crystal violet before the crystal violet was dissolved in ethanol: acetone solution and measured in a TECAN plate reader at 575nm.

Figure 4.2.7 shows the results from the biofilm formation assays for Δ*ompH1*. Our data suggests that although there is a small increase of mean absorbance in Δ*ompH1* at 0.627 in comparison to the wild type at 0.42, there is currently no statistical significance in this change due to the variability. The microscopy images arguably show more biofilm formation in the wild type in comparison to *ΔompH1* further evidencing the lack of significance due to variability. This data suggests there are no major changes in monoculture biofilm formation in the absence of a functioning *ompH1* gene.

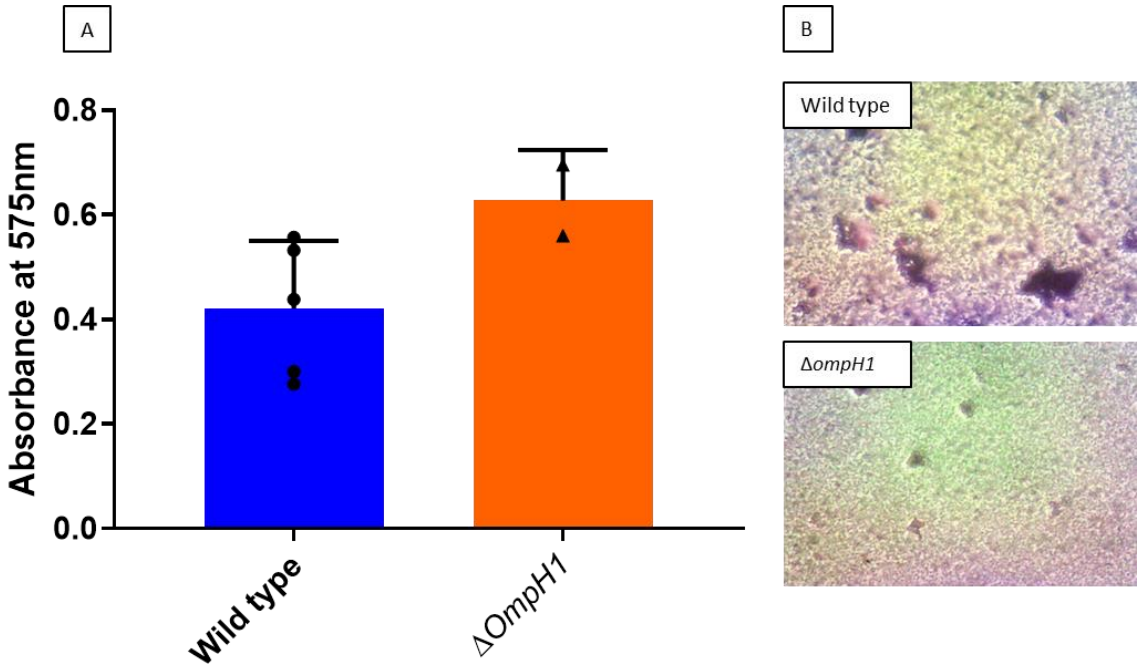

Figure 4.2.7. Biofilm formation assay of wild type and Δ*ompH1 P. gingivalis* after 5 days of growth. (A) Overnight cultures of *P. gingivalis* were made to OD_{600} 0.1 and incubated in a 96-well plate anaerobically at 37°C for 5 days. The OD_{600} was measured using a TECAN plate reader before the biofilms were washed and stained with crystal violet. The crystal violet in the biofilms was solubilised in ethanol: acetone (80:20) and the absorbance measured at 575nm using a TECAN plate reader. The results were normalised to growth by dividing the overall absorbance by the OD_{600} results. Statistical significance was determined by a Students T-test with a p value of <0.05 being significant, no statistical significance was observed, error bars represent +/- SEM. (B) Stained biofilms were washed and dried before images were taken at 100x magnification with an Olympus microscope.

4.2.4 Antibiotic protection assay of Δ*ompH1* in comparison to wild type *P. gingivalis* reveal reduced adhesion and invasion to H357 cells.

In the previously mentioned study by Suwannakul *et al* (2010), *OmpH1* was shown to be overexpressed in a subpopulation of hyper-invasive *P. gingivalis* indicating the gene has a role in the invasive capabilities. To investigate this, we conducted antibiotic protection assays as previously used in the lab (Naylor *et al.*, 2017) which allow the quantitative analysis of the

adhesion and invasion of bacteria to eukaryotic cells, in this case H357 oral squamous carcinoma cells. Briefly, this is accomplished by incubating monolayers of cells with *P. gingivalis* for 90 minutes to allow the bacteria to adhere and invade the cells. Afterwards any planktonic bacteria are washed off with PBS. At this point the cells can be lysed to count the number of bacteria to give total association (adhered and invaded), or the cells can first be treated with the antibiotic metronidazole to kill the adherent bacteria leaving only the invaded bacteria which can then be counted.

Antibiotic protection assays were carried out as described in 2.8.9. The results for total association and invasion are numerated during the experiments by counting the CFU that grow on the FA blood plates after incubation. The adherence was calculated by subtracting the invasion results from the total association results. All results were calculated as a percentage of the bacteria that had survived the conditions of the experiment. The results were then compared to the wild type for each biological repeat, to reduce the error that was caused by slight variations in preparation between the biological repeats.

Figure 4.2.8 shows the results from the antibiotic protection assays of Δ*ompH1*. These results show a significant reduction in total association, adhesion, and invasion for Δ*ompH1* in comparison to the wild type. All three results have a mean reduction of at least 42% with invasion having the greatest reduction of 34% in comparison to the wild type. These data provide further evidence that *ompH1* plays a significant role in the invasive host-pathogen interaction of *P. gingivalis*. To further investigate this, we decided to investigate the presence of some of the major outer membrane proteins in *P. gingivalis* that could be chaperone clients of *ompH1* and influence adhesion/invasion.

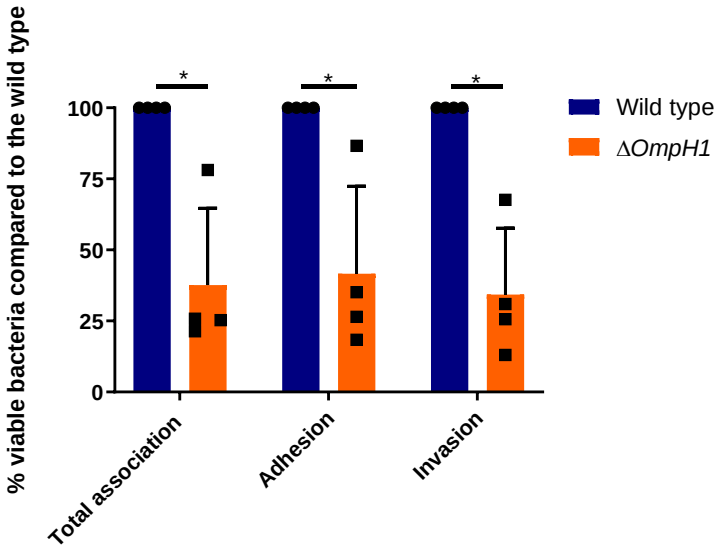

Figure 4.2.8. Antibiotic protection assays of wild type and ΔompH1. Invasion and adhesion were determined using the antibiotic protection assays as described in section 2.8.9. Invasion was determined by the bacteria that survived the metronidazole treatment, as a percentage of overall viable wild type *P. gingivalis*. Total association was determined by admitting the metronidazole killing, therefore counting the number of bacteria that had invaded the cells but also the bacteria that is attached to the surface. Adhesion was calculated by subtracting the invasion data from the total association. All results were then compared to the wild type in each individual experiment to demonstrate the trend seen within the individual experiments that is obscured by the variability between experiments. Error bars are +/- SEM. Statistical analysis was performed using multiple T tests. Antibiotic protection assays were performed with 4 biological repeats, each containing 3 technical replicates.

4.2.5 Investigation into the presence of major outer membrane proteins in Δ*ompH1* and wild type *P. gingivalis*

As *ompH1* is predicted to be an SKP like chaperone involved in the safe transport and correct maturation of outer membrane proteins, it was important to investigate if the presence of some of the major outer membrane proteins of *P. gingivalis* had been altered in the knockout mutant. Specifically, we looked at OmpA a major outer membrane protein shown previously to be important with host-pathogen interactions and invasion (Naylor *et al.*, 2017), fimA the major protein component of *P. gingivalis* fimbriae and the gingipain proteins. To do this, western blot was performed as described in section 2.7.3. In brief, overnight cultures of Δ*ompH1* and wild type *P. gingivalis* were normalised to OD_{600} 1 before being pelleted and boiled in 2X SDS sample buffer. The total protein samples were separated by SDS-PAGE in a 12% acrylamide gel before the proteins were transferred to nitrocellulose paper by semi-dry transfer. The nitrocellulose paper was blocked overnight in TBS with 5% milk before being washed. The nitrocellulose paper was blotted with the appropriate primary antibody before being washed 3x with TBS-Tween. The nitrocellulose was incubated with the secondary

antibody containing a conjugated horse radish peroxidase enzyme. After another wash step the nitrocellulose paper was incubated with chemiluminescence solution to activate the HRP. The fluorescence was visualised by using a Licor luminescence scanner.

Our results seen in figure 4.2.9 show that there has been no loss of either OmpA or FimA in the whole cell samples of Δ*ompH1* in comparison to the wild type *P. gingivalis*, although the OmpA seems to be in greater amounts potentially indicating an accumulation in the periplasm. However, the presence of the arginine gingipain proteases has been reduced in Δ*ompH1* as can be seen using the mab1B5 antibody. We were also interested in investigating if the presence of these proteins changed in the outer membrane fractions of *ΔompH1* in comparison to the wild type. As *ompH1* is responsible for translocation to the outer membrane, it is possible that the proteins are still present in the same amount but not correctly inserted into the outer membrane. However, there were issues in normalising the amount of protein in each sample after the outer membrane protein fraction isolation process was completed. Unfortunately, these issues were not fixed in the time available due to the restrictions caused by the coronavirus pandemic.

Our results indicate that the loss of *ompH1* has resulted in an overall loss of gingipains in Δ*ompH1*. To investigate this further we looked at the protease activity of each type of gingipain protease of Δ*ompH1* in comparison to the wild type.

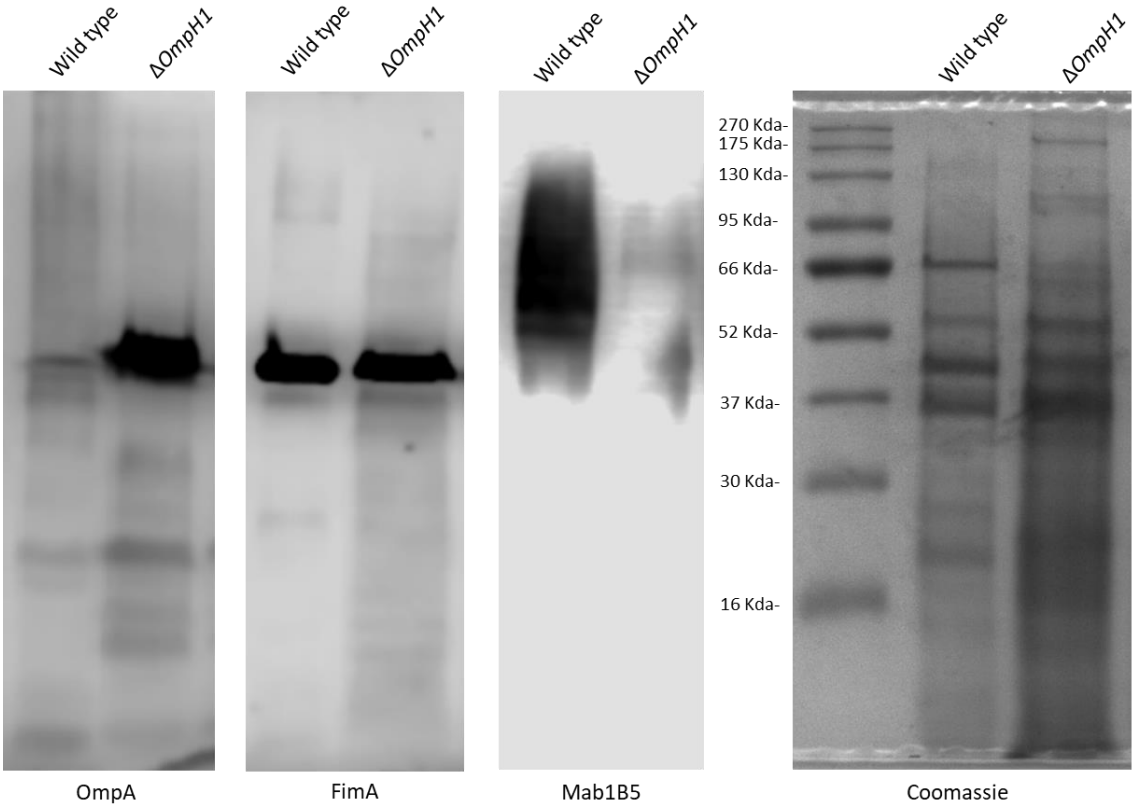

Figure 4.2.9 Western blot for major outer membrane proteins in whole protein samples of wild type and Δ*ompH1* P. gingivalis. Total protein samples were separated by SDS-PAGE and transferred to nitrocellulose paper which underwent western blot using the anti-OmpA, anti-FimA, or MAb1b5 primary antibody, the blot was visualised via fluorescence of HRP-conjugated secondary antibodies using the LICOR luminescence scanner. Total protein samples were also separated via SDS-PAGE and stained using an Instant Blue Coomassie protein stain top show equal loading.

4.2.6 Investigation into the whole cell proteolytic activity of Δ*ompH1* and wild type *P. gingivalis*

Our data suggests the presence of the arginine gingipain proteases has been reduced in the total protein samples of Δ*ompH1* in comparison to the wild type. Gingipain proteases are an important virulence factor for *P. gingivalis* from nutrient acquisition of haem which gives the bacteria its black pigment (O-Brien-Simpson *et al.*, 2003; Olczak *et al.*, 2005), to binding to host cells and manipulating the host immune response (Chen and Duncan, 2004; Guo, K. A. Nguyen and Potempa, 2010). There are two main types of gingipains produced by *P. gingivalis* arginine targeting and lysine targeting. To investigate the activity of these proteases similar experiments were conducted (Section 2.8.10) where a fluorescent conjugated substrate was incubated with whole cell *P. gingivalis*. This releases the fluorescent tag which can be quantified using a TECAN plate reader. The difference between the two experiments is that

the substrates have either an arginine bound fluorescent tag, or a lysine bound fluorescent tag. Both experiments were optimised to measure the fluorescence at a time point where the enzymes were still in an exponential part of their activity.

As can be seen in figure 4.2.10 Δ*ompH1* has significantly reduced arginine with a mean fluorescence unit of 5131 in comparison to 28655 in the wild type. However, the lysine activity has not significantly been changed in comparison to the wild type. This data indicates that *ompH1* may have a role in the transport and correct implementation of the arginine gingipains but not lysine. We were interested in investigating the proteolytic activity of the supernatant as gingipains are on the surface of *P. gingivalis* they are often secreted into the surroundings through outer membrane vesicle biogenesis (Veith *et al.*, 2014) and through the type 9 secretion system (Lasica *et al.*, 2017). However, this was not able to be optimised during this project due to time restrictions due to the coronavirus pandemic.

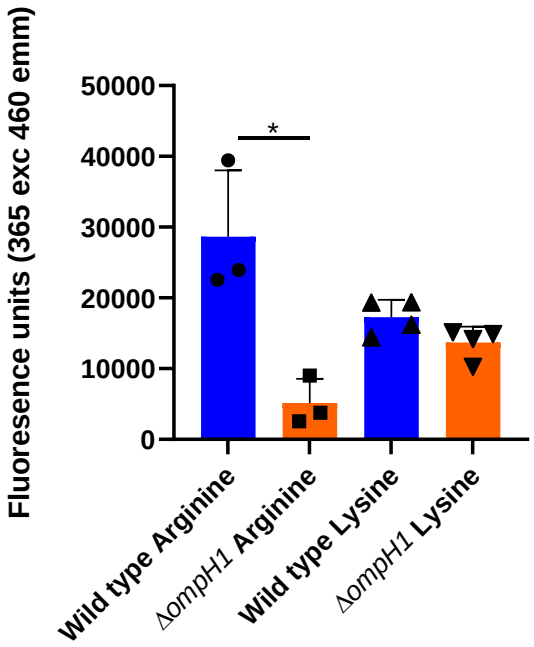

Figure 4.2.10 Arginine gingipain activity of Wild type and Δ*ompH1* P. gingivalis. Overnight cultures of *P. gingivalis* were made to OD600 0.01 before being pelleted and resuspended in PBS, the bacteria were incubated with 100 µl of the arginine or lysine bound methylcoumarin for 5 minutes before the reaction was quenched and the fluorescence was read at 365 excitation and 460 emissions Error bars represent +/- SEM. Statistical analysis was performed using a T-Test. N=3 for arginine and N=4 for lysine each including triplicates of technical repeats.

4.3 Discussion

The translocation of outer membrane proteins across the inner membrane into the periplasm before assembly in the outer membrane is essential for all Gram negative bacteria, this is especially true for *P. gingivalis*, for which several major outer membrane proteins function in multiple host-pathogen interactions as they are the first points of contact with the host (Murakami *et al.*, 2002). Proteins such as RagA/B which act as major antigens and aid in peptide uptake (Curtis *et al.*, 1991; Hutcherson *et al.*, 2015; Madej *et al.*, 2019), OmpA which plays important roles in biofilm formation and invasion of host cells (Naylor *et al.*, 2017), and gingipain proteases. Assembling these proteins in the outer membrane is a multi-step process. After being first translated in the cytoplasm, OMPs need to move through the inner membrane and periplasm to get to the outer membrane. This process would be impossible without assistance due to the different conditions between the hydrophobic membranes and the hydrophilic environment of the periplasm. Without the help of chaperone proteins the unfolded proteins will aggregate in the periplasm where they will get degraded (Entzminger *et al.*, 2012). Therefore, Gram negative bacteria such as *E. coli* have developed translocation pathways. As described in section 4.1, many proteins are recognised by the Sec transport system and passed into the periplasm where the unfolded proteins are chaperoned by SurA or SKP to the BAM where they are correctly folded and inserted into the outer membrane. This system is not unique to *E. coli* and is present in other Gram negative bacteria (Silhavy, Ruiz and Kahne, 2006) including *P. gingivalis*. Previous bioinformatic analysis by Naylor (2017) found related proteins for SecA, SurA, SKP, and BamA (PG0514, PG0415, PG0192/3 and PG0191 respectively), indicating this system is used by *P. gingivalis*. It was shown that the two SKP like proteins in *P. gingivalis* are downstream of a known BamA homologue , and PGN_0297 the gene that encodes PorG which has been shown to be essential in the T9SS (Gorasia *et al.*, 2016; Naito *et al.*, 2019) (Figure 4.3.1). Unlike *E. coli* that only has a single SKP gene, *P. gingivalis* has two in the form of *ompH1* and *ompH2.* There is evidence to suggest that these two proteins have different clients, but it is unknown if they have co-operative functions. This was one of the questions we looked to answer in this study.

Figure 4.3.1 OmpH1 and OmpH2 sequences are positioned downstream of putative BamA and T9SS genes.

Knockout mutation of both *ompH1* and *ompH2* individually was attempted multiple times during this project, eventually producing multiple correct *ΔompH1* mutants whilst Δ*ompH2* was never successfully produced. Even though multiple mutants were produced using the *ompH2* mutant plasmid they all had the double band seen in figure 4.2.2C indicating the knockout was not successful. As this problem occurred multiple times it gives evidence that this result was not down to chance and could possibly be due to *ompH2* being essential for *P. gingivalis* to survive in our current culture methods. This has been previously suggested by Taguchi *et al* (2015) who were also unsuccessful in producing a *ompH2* knockout mutant, however they give no details why or how they came to this conclusion. The ideal situation when studying these genes would have been to make mutants of each individual gene and a double mutant knocking out both genes. This would allow investigation to which gene was responsible to which clients and their overall role in *P. gingivalis*. Within our study we also attempted to produce a mutant of Δ*ompH1+2* which was also unsuccessful, further evidencing the possibility that *ompH2* is essential. Interestingly SKP is not essential in other bacteria where knockout mutants can be made without affecting viability. In a study by Sklar *et al* (2007), growth curves were performed on an *SKP* knockout and the mutant would grow normally as long as SurA was present, this paper also suggests that SurA is responsible for the majority of OMPs with *SKP* playing a more redundant role. In a more recent study by Kapach *et al* (2020) an *SKP* mutant of *Salmonella typhimurium* was made and the growth compared to the wild type in the presence of antibiotic peptides, this mutant had no changes in growth to the wild type in normal conditions. These studies indicate that the role of *ompH2* in *P. gingivalis* is more essential for viability than SKP in other bacteria. In a recent study by Schiffrin *et al* (2016) they used Electrospray ionisation-ion mobility spectrometry-mass spectrometry to investigate and predict the shape and binding of *SKP* when interacting with known clients. Their results predict that for larger OMPs two *SKP* heterotrimers can work together to encapsulate the protein. This raises an interesting question about *ompH1* and *ompH2*. If SKP can work in multiples to accommodate different clients, then potentially *ompH1* and *ompH2* could do the same. This would be an important point to investigate if Δ*ompH2* and Δ*ompH1+2*

can be made in the future, however current evidence points to *ompH2* being essential for *P. gingivalis* viability.

It is also worth noting that as *ompH1* is upstream of *ompH2*, there could be a polar effect disrupting the transcription of *ompH2* which potentially may be responsible for some of the results seen in Δ*ompH1*. This would have been interesting to investigate through QPCR comparing the expression of *ompH2* in Δ*ompH1* and the wild type. Currently this polar effect is unknown, however it is likely to be minimal if not zero as *ompH2* seems to be essential to *P. gingivalis* and the viability of Δ*ompH1* has not changed from the wild type which will be discussed below.

In comparison to the previously mentioned studies Δ*ompH1* had no major changes to viability, which more closely reflects the effect *SKP* knockouts have on other bacteria. The anaerobic growth curves did however show a slower growth rate in Δ*ompH1*, this decrease growth rate was not seen in the SKP mutant of *S. typhimurium* (Kapach *et al.*, 2020) or in *E. coli* (Sklar *et al.*, 2007). A potential explanation for this is the reduction in the proteolytic activity seen in Δ*ompH1. P. gingivalis* is an asaccharolytic bacteria that gets its energy from the metabolism of amino acids as its carbon source rather than complex carbohydrates and sugars (Hendrickson *et al.*, 2009). As the proteolytic activity of the gingipains have been reduced this may have affected the rate of growth for Δ*ompH1*.

The antibiotic protection assays for Δ*ompH1* provide evidence to support the indications made by Suwannakul *et al* (2010) that *ompH1* is involved with an increased invasive phenotype. Both adhesion and invasion were reduced in Δ*ompH1* in comparison to the wild type. However, it is unlikely that the omph protein is directly responsible for this change and more likely that this was caused by the loss/reduction of import client/s. This prompted the question of which clients could be lost that would have a role in the adhesion and invasion of host cells. Initially it was predicted that OmpA may be one of these clients, as *OmpA* and *OmpH* were upregulated in the invasive subpopulation, and OmpA is a client of SKP in *E. coli* (Jarchow *et al.,* 2008). This would explain the decrease in adhesion and invasion as OmpA has been shown previously to play an important role in the invasive capabilities of *P. gingivalis* (Naylor *et al.*, 2017). However, this would be conflicting with the biofilm formation results as the biofilm was not significantly changed whereas biofilm loss was seen in *P. gingivalis* lacking

OmpA. The western blot results for OmpA in the total protein samples also showed no loss. However, it would be better to have a western blot of the outer membrane protein profile as it is possible that OmpA is present in the same amount but has not been inserted into the outer membrane, making it non-functional. This was planned but unfortunately was not able to be completed in this study.

To further probe potential clients of *ompH1* western blots of the gingipains and the major fimbriae protein FimA were performed. There was no difference seen between the western blot of FimA for Δ*ompH1* and wild type *P. gingivalis*. To produce mature fimbriae containing FimA proteins *P. gingivalis* uses outer membrane bound members of the *Fim* operon to help produce and anchor the mature long fimbriae (Nagano *et al.*, 2012). In comparison to our data, a study by Palomino, Marín and Fernández (2011) looked at the role of multiple chaperone proteins including SKP, SurA and DegP in FimD translocation. Palomino, Marín and Fernández (2011) found that single mutants of SKP and DegP had no effect on the presence of FimD in *E. coli* mutants, whereas a complete loss of FimD was observed in the SurA mutant. Indicating that SurA may be solely responsible for the translocation of the Fim proteins. It would be interesting for multiple reasons to use electron microscopy to analyse the cell surface of Δ*ompH1*. TEM images would allow us to visualise the outer membrane surface which can be disrupted when missing outer membrane proteins (Naylor *et al.*, 2017). This would also allow us to visualise the fimbriae proteins and the visual morphology of the bacterial surface.

The western blot of the gingipain proteins using the Mab1B5 antibody showed a reduction in signal in Δ*ompH1* when compared to the wild type *P. gingivalis*. On further investigation into the activity of arginine and lysine gingipain activity we also found that arginine specific activity was significantly reduced in Δ*ompH1* in comparison to the wild type. This was not the case for lysine activity however which was unchanged. In the previously mentioned study by Taguchi *et al* (2015), an *ompH1* knockout mutant was generated and they state major changes to both arginine and lysine gingipains. In their study they state the Δ*ompH1* mutant (named Δ*omp17* in their study) loses all pigment, this is a common phenotype in gingipain null *P. gingivalis* as gingipains are required for the breakdown of haem and assimilation of protoporphyrin IX into the outer membrane which gives the black pigment (Smalley *et al.*, 2004). However, in our study the pigmentation is not lost in Δ*ompH1* but is slower to become black. This is not

surprising as our data suggests that only arginine gingipains have been disrupted by the knockout of *ompH1*, this would explain the pigmentation as mutants lacking only arginine gingipains still present a black pigment whereas disruption to the lysine gingipain causes loss of black pigmentation (Shi *et al.*, 1999; Lasica *et al.*, 2017). This is a point of contrast between our study and Taguchi *et al* (2015), our study shows evidence that only arginine gingipains have been disrupted as the activity of lysine was unaffected by the *ompH1* mutation and no change in the final pigment is observed. However, Taguchi *et al* show a reduction in both arginine and lysine activity in their Δ*ompH1* whole cell samples. There are some strange inconsistencies with their results however such as western blot work for the lysine gingipain showing complete loss in culture medium of Δ*ompH1*, whereas future analysis of the culture medium from Δ*ompH1* by mass spectrometry showed that the lysine gingipain was still present. We had planned to look at the gingipain activity of the supernatant to analyse if gingipains were still being translocated through the periplasm, however unfortunately optimisation of the gingipain assays to the supernatant concentration was not achieved due to time restraints.

Our data suggests that Δ*ompH1* has affected the arginine gingipain but not OmpA or FimA, this indicates a transport role more specific to the Type 9 secretion system (T9SS) of *Bacteroides* (Mark and Zhu, 2013) which transports proteins with a CTD signal peptide including the gingipain proteases. The role of the T9SS in gingipain transport was initially discovered by Sato *et al* (2005) who found that a *P. gingivalis* mutant lacking one of the membrane transport proteins of the T9SS PorT, produced a white pigment on Blood agar plates, and that inactive gingipain proenzymes were accumulating in the periplasm of the mutant. The potential of *ompH1* being involved with the T9SS was also suggested by Taguchi *et al* (2015) as they investigated the presence of multiple CTD containing proteins. They found in the Δ*ompH1* mutant immature CTD bound proteins were present in the culture medium, indicating incorrect implementation by the T9SS. They also found that PorU, a key enzyme in the cleaving of the CTD and correct maturation of CTD containing proteins by the T9SS was not present in the outer membrane of Δ*ompH1*. Taguchi *et al* conclude that PorU maybe a chaperone client of *ompH1* and therefore have a role in CTD protein transport.

It is worth noting that some of the inconsistencies seen in the study by Taguchi *et al* (2015) may be due to multiple mutations in their *ompH1* mutant, this was not mentioned or checked

in their study. However, we have checked the full genome of our mutant for mutations and have shown that the mutation has only occurred at the intended site of the *ompH1* gene.

It would also be interesting to analyse the outer membrane protein fractions using western blot for CTD containing proteins such as gingipains. Although this work was started during this study, the optimisation to normalise the amount of protein was not achieved due to time restraints caused by the Coronavirus pandemic.

4.4 Conclusion

Our investigation into the SKP like chaperone proteins *ompH1* and *ompH2* has provided further evidence to support the essentiality of *ompH2* for *P. gingivalis* viability. We have also shown that *ompH1* does indeed play an important role in the adhesion and invasion of H357 cells by *P. gingivalis*, supporting the previous findings by Suwannakul *et al* (2010). Our data has also shown conflicting results to current literature findings, as we show Δ*ompH1* specifically affects arginine gingipain activity but not lysine contrary to the findings by (Taguchi *et al.*, 2015). Although these contradictions exist, the combination of our data and Taguchi *et al* provides strong evidence that *ompH1* is involved with translocation of CTD tagged proteins and therefore plays a role in the T9SS.

Chapter 5. Characterisation of the *rfbB* gene in *P. gingivalis* virulence

5.1 Introduction

As mentioned in section 1.6, previous work by Suwannakul *et al,* (2010) identified multiple overexpressed genes in an invasive subpopulation of *P. gingivalis*. One of these genes was rfbB. The *rfb* operon of *P. gingivalis* (Figure 5.1.1) is responsible for enzymes involved with the biosynthesis of dTDP-rhamnose, like rfb operons found in other Gram negative bacteria such as *E. coli* and *Streptococcus mutans* (Marolda and Valvano, 1995; Tsukioka *et al.*, 1997). The dTDP-rhamnose is used as the most abundant sugar of the O-antigen of *P. gingivalis* LPS (Bramanti *et al.*, 1989). The production of dTDP-rhamnose begins with glucose-1-phosphate which through the transfer of thymidine triphosphate by a thymidyl transferase (*rfbA)* to become dTDP-glucose. This precursor then interacts with a dehydratase (*rfbB*) and is changed to dTDP-4-keto-6-deoxy-D-glucose. The position of the OH and CH_3 groups are altered by an epimerase producing dTDP-4-keto-L-rhamnose, which is then reduced (by *rfbD*) by the addition of hydrogen to become dTDP-L-rhamnose (Figure 5.1.2). This dTDP-L-rhamnose is then attached to the O-antigen precursor by a rhamnosyltransferase (*gtfD*) (Swietnicki and Caspi, 2021).

Figure 5.1.1 Rhamnose synthesis operon sequences in *P. gingivalis*. Like other rhamnose synthesis systems, *P. gingivalis* contains four genes named *rfbABCD* that are required for the synthesis of dTDP-L-rhamnose from glucose-1-phosphate.

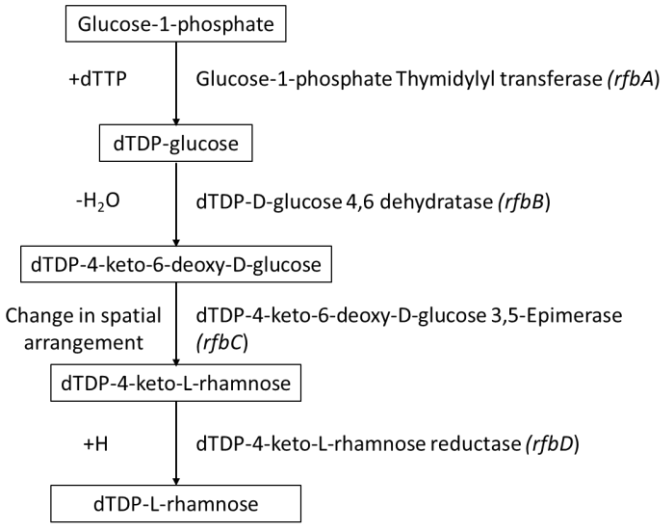

Figure 5.1.2 Rhamnose biosynthesis pathway. The synthesis of dTDP-L-rhamnose begins with glucose-1-phosphate, which is sequentially modified by the *rfbABCD* enzymes to produce dTDP-L-rhamnose.

The lipopolysaccharide (LPS) layer is a crucial part of all Gram negative bacteria virulence. For *P. gingivalis,* this is even more crucial as the progression of the immune response and inflammation is a vital part of dysbiosis and creating a favourable niche (Hajishengallis, Darveau and Curtis, 2012; Kinane, Stathopoulou and Papapanou, 2017). LPS is an immunoreactive molecule which is recognised by host cells through the Toll like receptor TLR4, this triggers a cascade which activates NF-κB and upregulates the production of inflammatory cytokines such as TNFα, IL-1, and IL-6 (Sweet and Hume, 1996). This inflammation of host tissues provide anaerobic periodontal pockets and a nutrient rich environment for assacharolytic bacteria through bleeding, allowing the progression of periodontitis. (Olczak *et al*, 2005; Kinane, Stathopoulou and Papapanou, 2017).

This section focusses on the characterisation and investigation of the *rfbB* gene. Previous attempts to investigate the *rfb* operon have proven difficult. A study by Shibata *et al*, (1999) gave evidence that trying to knockout any of the *rfb* genes resulted in lethality indicating the importance and perhaps essentiality for the *rfb* operon. However, in this study a knockout mutant was made that has displayed many phenotypical changes from the wild type. Indicating the potential roles of *rfbB*.

This chapter will explore the mutation and characterisation of a *rfbB* knockout mutant, specifically focussing on the virulence phenotype and an investigation in the LPS of the *rfbB* mutant.

5.1.1 Aims

The aim of this chapter was to explore the role of the *rfbB* gene in host-pathogen interactions and virulence. This was achieved through mutation and characterisation of a mutant in which the *rfbB* gene is disrupted, specifically focussing on the virulence phenotype and an investigation in the LPS of the *rfbB* mutant.

5.2 Results

5.2.1 Knockout mutagenesis of *rfbB*

To investigate the role of *rfbB,* first a knockout mutant had to be produced. The strategy employed was to attempt to replace the *rfbB* gene with an erythromycin antibiotic resistance cassette, in this case ErmF, as outlined in previous work in the lab (Naylor *et al.*, 2017). To achieve this, a gene construct with *rfbB* replaced with an erythromycin resistance cassette

surrounded by 1000bp of upstream and downstream DNA was synthesised by Genesynth. The gene sequence was then blunt cloned into a pJET1.2 holding vector (CloneJET), which is a blunt holding vector which does not have an origin of replication for *P. gingivalis* and will not replicate. The pJET: Δ*rfbB* was transformed into *E. coli* DH5α for storage and further upscaling of extractions for higher concentration of plasmid DNA.

Circular plasmid DNA (>1000 ng) was used to transform the wild type *P. gingivalis*. The transformation method used was natural competency (outlined in section 2.4.1.2), previously described by Tribble *et al* (2012) and applied successfully in the lab by Naylor *et al* (2017). Briefly, 3-day old *P. gingivalis* was used to make an overnight liquid culture. The culture was pelleted and resuspended in fresh equilibrated broth supplemented with a full plasmid extraction, where it was incubated for one day to allow transformation to occur and the expression of the erythromycin resistance cassette. Positive transformed bacteria were selected for by spreading the culture on erythromycin FA blood agar selection plates and incubating for at least one week. After many attempts only a single colony was identified for Δ*rfbB,* but a visual phenotype was observed as the colony was of a lighter cream colour than the usual brown/black colonies of *P. gingivalis*. This positive colony was subcultured onto another erythromycin selection plate and incubated to check if the resistance was retained. The mutant was checked for the mutation using PCR and gene sequencing with Eurofins.

5.2.1.1 PCR confirmation of rfbB knockout mutagenesis

Two separate PCR experiments were performed to confirm the presence of the mutation. The first PCR experiment used an upstream and downstream flanking primers of the *rfbB* gene. This shows that the erythromycin resistance cassette is positioned in the correct area of the gene as a different size band should be observed. The second PCR reaction used both a forward and reverse primer of the erythromycin resistance cassette to show the presence of the cassette in the mutant (Figure 5.2.1).

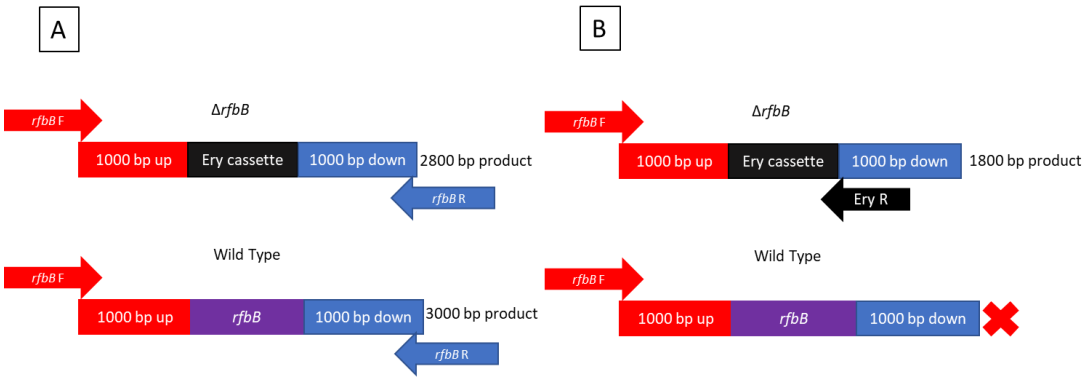

Figure 5.2.1 PCR reactions to confirm the erythromycin resistance cassette insertion. (A) A PCR reaction which will produce a gene sequence that encompasses the rfbB gene and the upstream and downstream flanking regions, producing a 3000bp product for the wild type and a 2800bp product for the mutant due to the shorter Ery cassette. (B) A PCR reaction which will produce a gene product with the upstream flanking region of rfbB and the erythromycin cassette if correctly inserted, this will not give a product for the wild type.

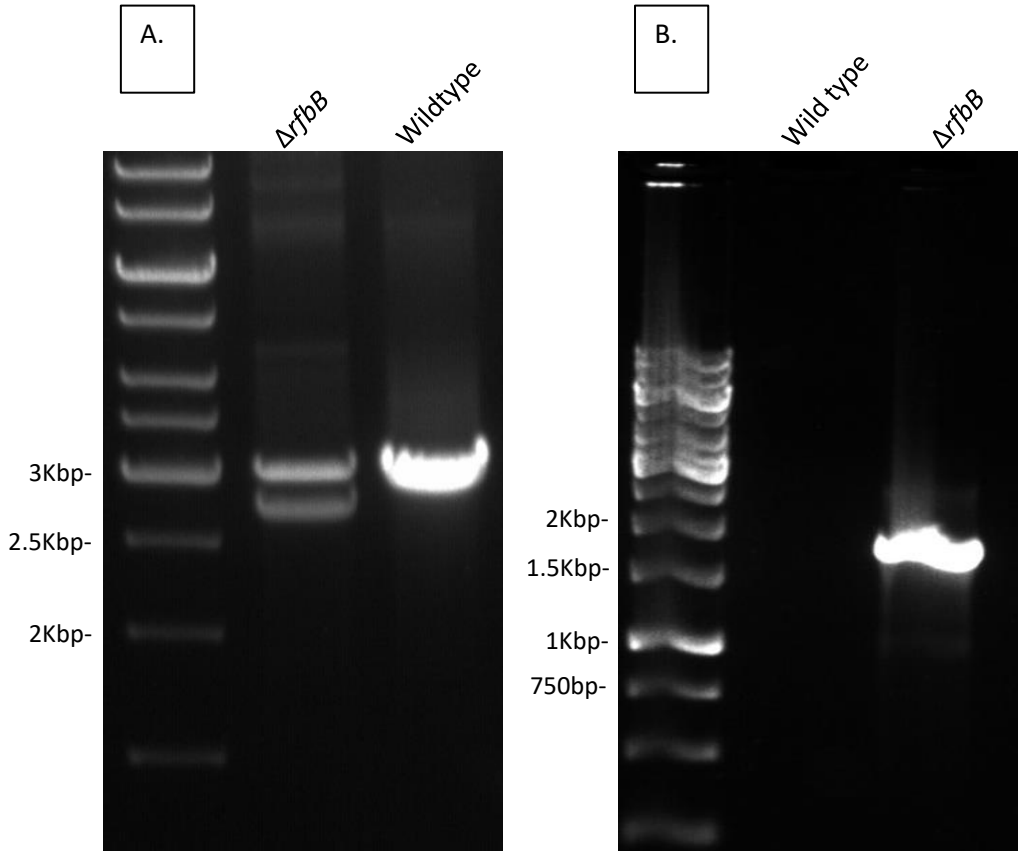

Figure 5.2.2 Confirmation PCR of Wild type and ΔrfbB Chromosomal DNA. (A) Chromsomal DNA of Wild type and ΔrfbB was amplified by PCR using upstream and downstream flanking primers as described in figure 5.2.1A. (B) Chromosomal DNA was amplified using an upstream flanking primer and an erythromycin reverse primer as described in figure 5.2.1B.

Figure 5.2.2 shows the results of the confirmation PCR experiments. In the upstream and downstream flanking PCR reaction (Figure 5.2.1A) a single band of 3Kbp was observed for the

wild type. However, for Δ*rfbB* two bands were observed, one at the expected size of 2.8Kbp indicating the presence of the erythromycin resistance cassette and one unexpected band at 3Kbp. This unexpected band could indicate the presence of both the wild type DNA and the mutant DNA both being present, potentially from a single crossover event. The second PCR experiment using the upstream flanking forward primer and the erythromycin reverse primer (Figure 5.2.1B) supports the presence of the erythromycin resistance cassette, showing a band of expected size of 1.8Kbp in the Δ*rfbB* but not in the wild type.

This double band seen in *ΔrfbB* suggests a single cross over event has occurred similar to that seen in *ΔompH2.* Unlike Δ*OmpH2* (section 4.2.1.2) which also had a single crossover event, multiple phenotypic changes have been observed in Δ*rfbB* indicating disruption to the gene. This disruption could be potentially due to a polar effect if the erythromycin cassette has been inserted upstream of *rfbB*.

The true mutation is further investigated in this chapter by full genome sequencing to identify what has occurred in the genome. However, there are many phenotypic changes in comparison to the wild type which will be shown in this chapter.

5.2.1.2 Genomic analysis of ΔrfbB by nanopore genomic sequencing

Genomic sequencing was performed to analyse the mutation that has occurred in the genomic DNA of *rfbB* to understand the double band observed during the PCR of Δ*rfbB*. Nanopore genomic sequencing was performed using chromosomal DNA from Δ*rfbB* as described in section 2.6.8 and briefly explained in section 4.2.1.2.

As seen in figure 5.2.3, there are individual reads that show the erythromycin cassette has integrated itself in the correct area, however there are also reads still showing the wild type *rfbB* gene. Unlike Δ*ompH2* there is no presence of the plasmid DNA in this mutant. Genomic alignments were attempted through multiple alignment software such as PATRIC and a galaxy workflow, however each alignment conflicted with each other, and neither were possible considering the data presented here. Therefore, we have looked at multiple of the individual reads and noticed that the reads containing the erythromycin cassette place it at the end of the rhamnose synthesis operon after *rfbD*. This indicates that the erythromycin cassette has been integrated just upstream of the *rfbB* gene (figure 5.2.4).

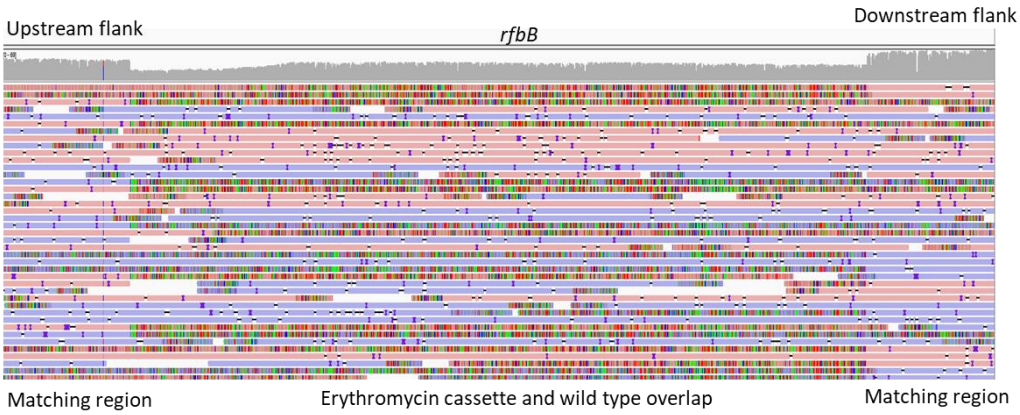

Figure 5.2.3 Change in the *rfbB* gene in chromosomal sequencing of Δ*rfbB*. Nanopore chromosomal sequencing was performed on a chromosomal DNA extract of Δ*rfbB*. All the reads were aligned and compared to a previously generated full genomic sequence of *P. gingivalis* ATCC 33277 taken from NCBI. The aligned sequences and the reference sequence were viewed in the Integrative genomics viewer (IGV). Total matching reads are shown in the top bar as grey peaks, with the read data just underneath. Pink or blue bars indicate reads that match the reference genome, whereas multicoloured bars indicate differences to the reference genome.

Figure 5.2.4 Predicted single crossover event resulting in incorrect insertion of erythromycin cassette and plasmid DNA. *rfbB* and the erythromycin cassette are shown to have both been inserted into the genome, this indicates a single crossover. Individual reads show the erythromycin cassette at the end of the rhamnose synthesis operon. Therefore, this is the sequence predicted from the individual reads.

5.2.2 QPCR of *rfbB* reveals expression by both wild type and Δ*rfbB*, with potentially less expression in Δ*rfbB*

To investigate whether *rfbB* expression had been disrupted by the mutation in Δ*rfbB* QPCR was performed as described in section 2.6.5. In brief, RNA was extracted from overnight samples of both wild type and Δ*rfbB* and concentration normalised before being converted into cDNA through reverse transcription (as described in section 2.6.4). QPCR was performed on the cDNA using *rfbB* specific primers and *P. gingivalis* ATCC 33277 16s gene primers as an internal control to normalise for the quantity of cDNA loaded. The results from the 16s primers were unfortunately too low of a C value to be quantified accurately, and therefore the data shown is not normalised to the internal quantity control. The data in figure 5.2.5, clearly show expression of *rfbB* by both the wild type and Δ*rfbB* samples, with statistically less expression by Δ*rfbB* with a mean of 0.6 fold compared to the wild type. However, as the internal control could not be achieved this difference may be due to a different amount of overall cDNA to begin with rather than a difference in expression.

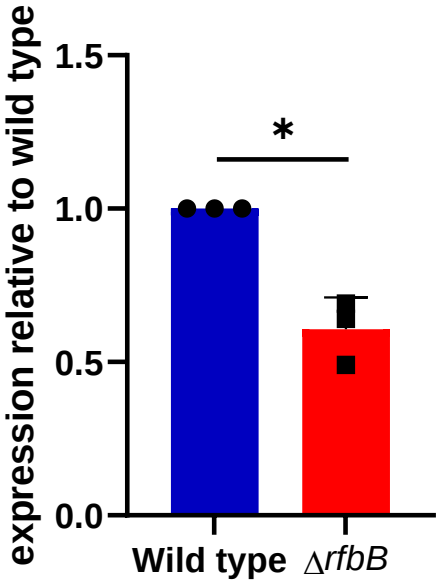

Figure 5.2.5. Expression of *rfbB* by wild type and Δ*rfbB P. gingivalis*. RNA was extracted from wild type and Δ*rfbB* before being converted to cDNA through reverse transcription. The cDNA was used for QPCR with *rfbB* specific primers as described in section 2.6.5. The C values were calculated and compared to that of the wild type. N=3 with 3 technical repeats, error bars indicate +/- SEM created on GraphPad Prism. Statistical significance was analysed through a paired students T-test. *P<0.05

5.2.3 The mutation of *rfbB* has reduced the growth of *P. gingivalis* in supplemented BHI

Knockout mutations are often detrimental to bacteria as unless a gene has redundancy within the genome it provides a function that will be lost. As *rfbB* has previously been described as essential by Shibata *et al* (1999) it was important to investigate whether the mutation has had any effect on the mutants ability to grow in comparison to the wild type. To achieve this growth curves were performed as described in section 2.8.7. In brief, both wild type and Δ*rfbB* were grown in overnight cultures before being prepared at OD_{600} 0.01 with equilibrated supplemented BHI. The samples were then placed into a 96 well plate and incubated in anaerobic conditions for up to 3 days without shaking, with the OD_{600} being measured every 30 minutes.

Our data suggest the Δ*rfbB* has had a clear disruption to its growth that is significantly lower than that of the wild type as can be seen in figure 5.2.6. Δ*rfbB* not only grows slower than the wild type over the 72-hour period, the mutant also never reaches a similar stationary phase OD600. Whereas the wild type reaches between OD600 0.8-0.9 by 31 hours with a generation time of 240 hours, Δ*rfbB* reaches a maximum OD600 of 0.6 by 42 hours with a generation

time of 312 hours. These data indicate that Δ*rfbB* has a reduced ability to grow and a slower overall speed of growth compared to the wild type.

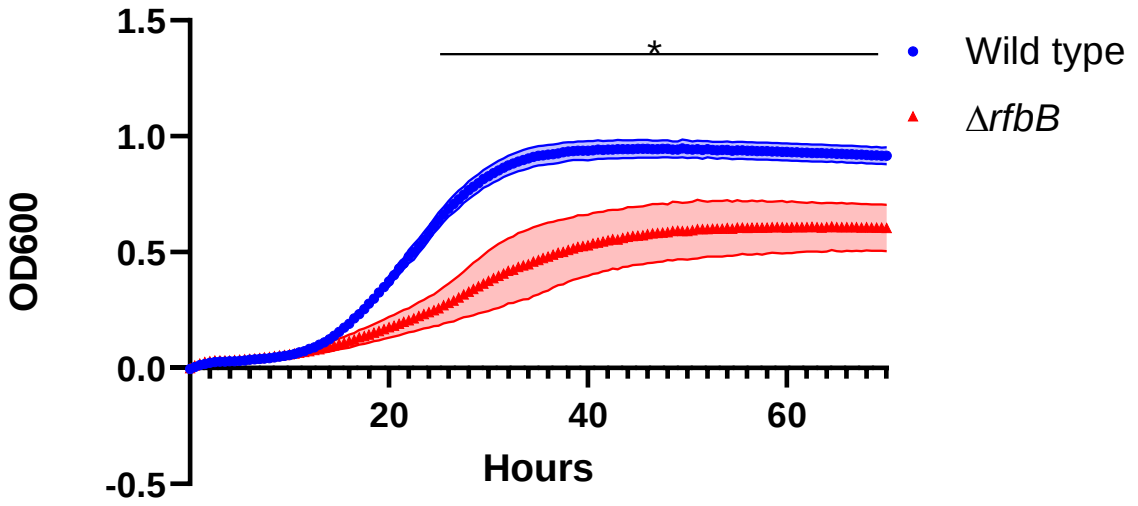

Figure 5.2.6. 3-day growth curve of Wild type and Δ*rfbB*. Wild type and Δ*rfbB P. gingivalis* were prepared at OD_{600} 0.01 before being incubated at 37°C in anaerobic conditions within a Cerillo stratus plate reader as described in section 2.8.7. OD_{600} was first blanked before being read every 30 minutes for 72 hours. N=3 with 9 technical replicates per biological repeat, shaded areas represent +/- SEM created on Graphpad Prism. Statistical analysis was analysed by 2-way ANOVA comparing the difference of each time point. *p <0.05.

Δ*rfbB* also has an altered pigmentation when compared to the wild type (Figure 5.2.7). This is a common phenotype of *P. gingivalis* with disrupted gingipain proteases.

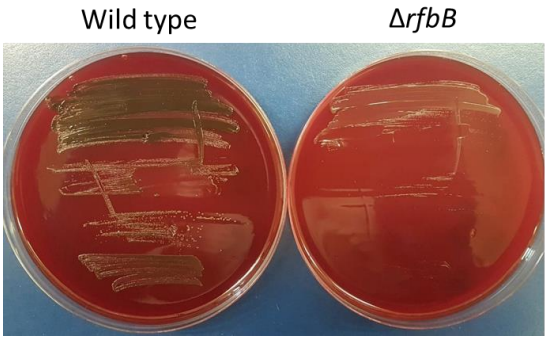

Figure 5.2.7 Δ*rfbB* and wild type *P. gingivalis* growth on fastidious anaerobic agar supplemented with horse blood. Wild type and Δ*rfbB P. gingivalis* were cultured on FA agar supplemented with horse blood for 3 days. Black pigmentation was presented by the wild type but not Δ*rfbB*.

5.2.4 Biofilm formation is reduced in Δ*rfbB* compared to Wild type *P. gingivalis*

To investigate the biofilm formation of wild type and Δ*rfbB P. gingivalis* a crystal violet biofilm staining method described in section 2.8.5 and explained briefly in section 4.2.3 was applied.

Our data suggests that Δ*rfbB* had a significantly reduced biofilm formation capability (p= 0.0172) resulting in a 56% reduction compared to the wild type. This result is also supported by the qualitative reduction of biofilm seen under light microscopy (figure 5.2.8). These results indicate that the mutation of *rfbB* is involved in the ability *P. gingivalis* has to form monoculture biofilms.

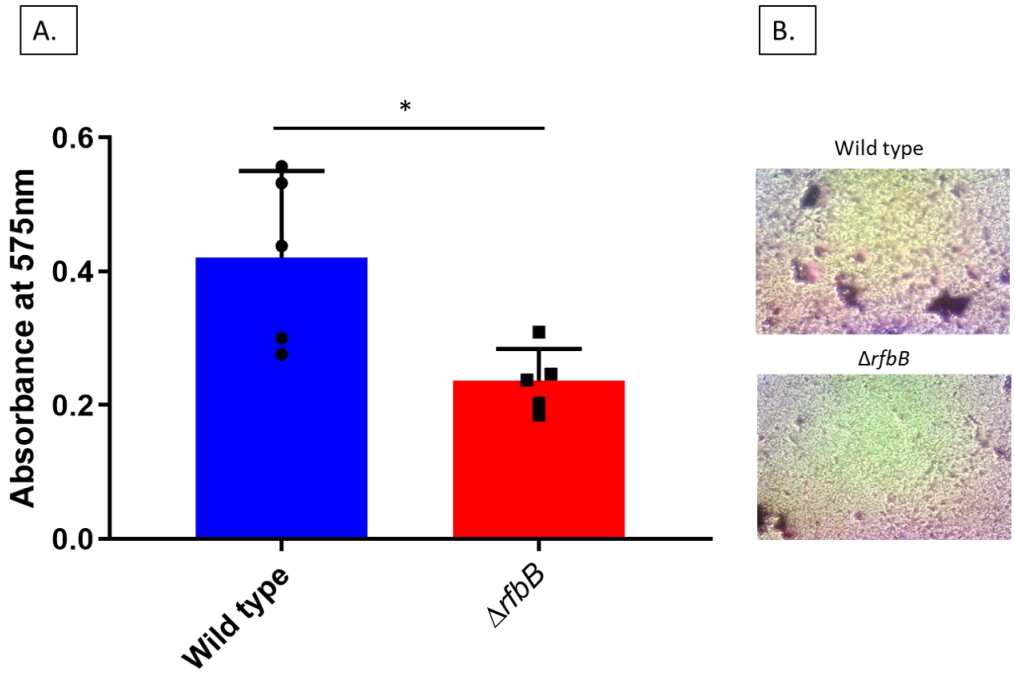

Figure 5.2.8. 5-day Biofilm formation of Wild type and ΔrfbB. (A) Crystal violet was extracted from 5-day old biofilms and quantified by absorption at 575nm using the TECAN plate reader before being normalised to growth. The average of 5 biological repeats (containing 9 technical repeats each) were quantified with error bars representing +/_ SEM. Statistical significance was assessed using a student's T-test. *p <0.05. (B) Light microscopy of stained 5-day old biofilms from wild type and ΔrfbB P. gingivalis using an Olympus light microscope with a camera attachment.

5.2.5 Antibiotic protection assay of Wild type and Δ*rfbB P. gingivalis* reveals reduced adhesion and invasion in the mutant.

As *rfbB* was over expressed in the hyper invasive subpopulation of *P. gingivalis* in the study by Suwannakul *et al* (2010), antibiotic protection assays were performed to investigate the host-pathogen interactions of the Δ*rfbB* mutant compared to the wild type. This was achieved through the methodology described in section 2.8.9 and briefly explained in section 4.2.4. As can be seen in figure 5.2.9 Δ*rfbB* had significant reductions of at least 50% in all three results,

indicating that the binding and invasive capabilities of this mutant have been affected. These results indicate that *rfbB* has a role in host-pathogen interactions and supports the previous findings by Suwannakul *et al* (2010), showing that *rfbB* can specifically affect the ability of *P. gingivalis* to attach and invade H357 human cells.

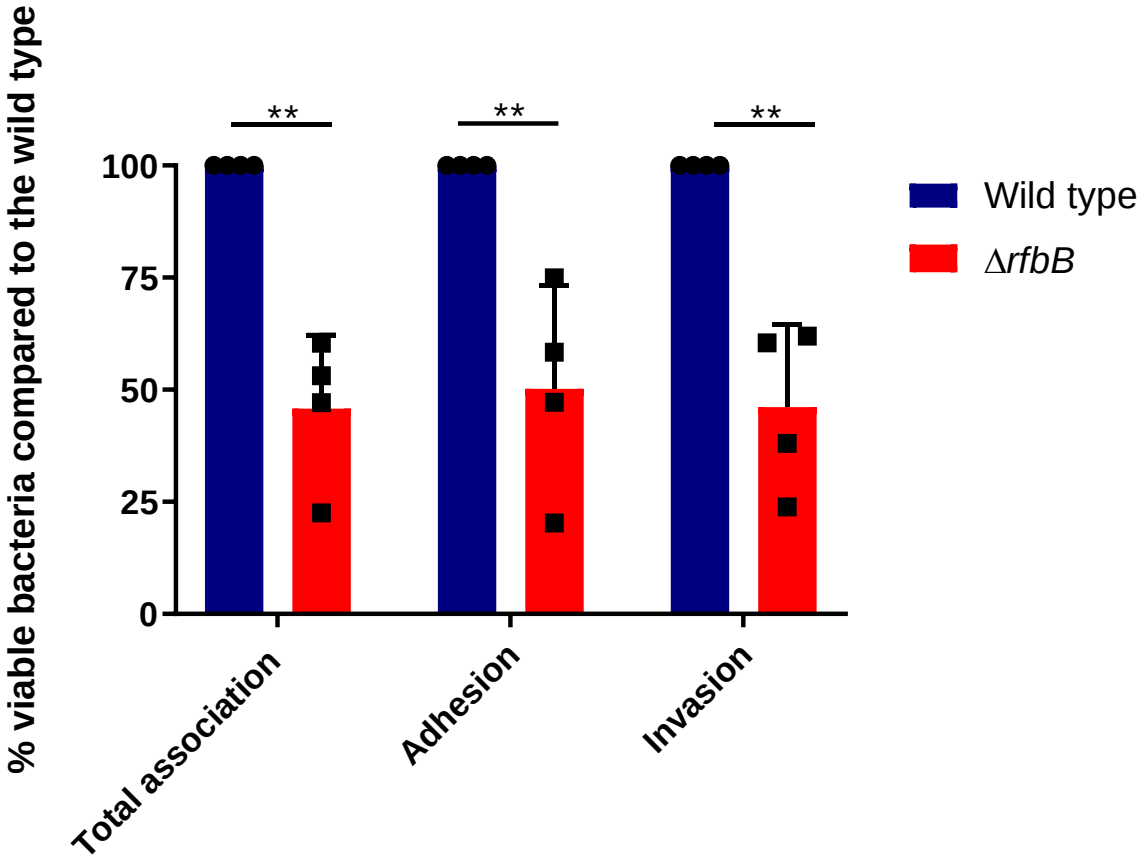

Figure 5.2.9 Antibiotic protection assays of wild type and ΔrfbB. Invasion and adhesion were determined using the antibiotic protection assays as described in section 2.8.9 Invasion was determined by the bacteria that survived the metronidazole treatment, as a percentage of overall viable wild type P. gingivalis. Total association was determined by admitting the metronidazole killing, therefore counting the number of bacteria that had invaded the cells but also the bacteria that is attached to the surface. Adhesion was calculated by subtracting the invasion data from the total association. All results were then compared to the wild type in each individual experiment to demonstrate the trend seen within the individual experiments that is obscured by the variability between experiments. Error bars are +/- SEM. Statistical analysis was performed using multiple T tests. **p <0.005. Antibiotic protection assays were performed with four biological repeats, each containing 3 technical replicates.

As *rfbB* is predicted to affect the production of *P. gingivalis* LPS, the results seen here could be due to the disruption of the LPS and outer membrane of *P. gingivalis*. The mutation of Δ*rfbB* has produced colonies with an altered pigment indicating the disruption of the gingipain

proteases. Therefore, we investigated the presence and proteolytic activity of the gingipain proteases.

5.2.6 Whole cell gingipain activity is reduced in Δ*rfbB in* comparison to wild type *P. gingivalis*

Colony pigmentation of Δ*rfbB* is different to the wild type, as Δ*rfbB* produces colonies with a cream-coloured pigment in comparison to the black pigment normally seen in *P. gingivalis*. The pigmentation of *P. gingivalis* is due to the function of the gingipain proteases and therefore Δ*rfbB* potentially has disrupted gingipains.

Figure 5.2.10 shows a clear reduction in arginine and lysine specific protease activity by Δ*rfbB* in comparison to the wild type. Our data show a statistically significant 5.9-fold reduction of arginine specific protease activity and a 3-fold reduction in lysine cleavage in comparison to the wild type. These results indicate that the whole cell arginine and lysine gingipain activity has been reduced by the Δ*rfbB* mutation, which supports the change in pigment seen in the colonies of Δ*rfbB* and potentially the reduced growth as the gingipains play an important role in nutrient acquisition and the presentation of protoporphyrin-IX (Smalley *et al.*, 2007).

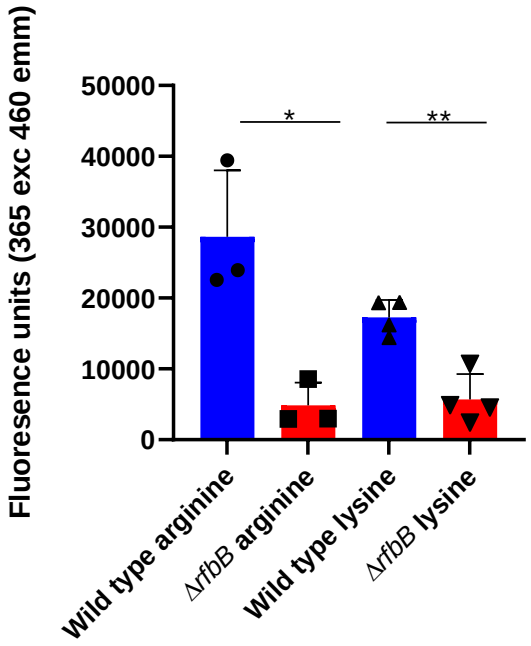

Figure 5.2.10 Arginine and lysine gingipain activity of Wild type and Δ*rfbB* P. gingivalis. Overnight cultures of P. gingivalis were made to OD_{600} 0.01 before being pelleted and resuspended in PBS, the bacteria were incubated with 100 µl of the arginine or lysine bound methylcoumarin for 5 minutes before the reaction was quenched and the fluorescence was read at 365 excitation and 460 emission. Error bars represent +/- SEM Statistical analysis was performed using a T-Test. *p<0.05 **p <0.005. N=3 for arginine and N=4 for lysine, each including triplicates of technical repeats.

It is also important to note that there are multiple studies that have linked the potential for gingipains to influence *P. gingivalis'* ability to adhere and invade host cells. Gingipains have been shown to process fimbriae to provide mature fimbriae on the bacteria surface (Nakayama *et al.*, 1996), and expose ligands on host cells to which the fimbriae can bind (Kato *et al.*, 2007). Further work in this chapter looks at a comparison of total arginine protein gingipain presence by western blot.

5.2.7 Western blot for arginine gingipain proteins

As the activity of gingipains were reduced in *ΔrfbB* a western blot technique was used comparing the wild type to Δ*rfbB* to identify if the presence of gingipains has been changed. To accomplish this the MAb1b5 antibody was used, this antibody was provided by Professor Mike Curtis. The MAb1b5 antibody was successfully used in previous studies by Curtis *et al* (1999), in this study it was found that Mab1b5 binds to RgpA, RgpB and LPS. This binding can be disrupted by chemical deglycosylation, indicating that the antibody binds to a carbohydrate epitope present on the gingipains and in the LPS. Figure 5.2.11 shows a clear reduction in the gingipain profile between the wild type and Δ*rfbB* indicating that the whole cell quantity of gingipains in Δ*rfbB* has been disrupted which supports the reduction of activity found in previous experiments. It is also worth noting that in Figure 5.2.11 B the total protein profile of Δ*rfbB* and wild type *P. gingivalis* are shown as a control for equal protein loading. At the same time differences can be seen in the protein profile of Δ*rfbB* with multiple bands being more prominent whilst others are lost, indicating a change to multiple proteins within Δ*rfbB*.

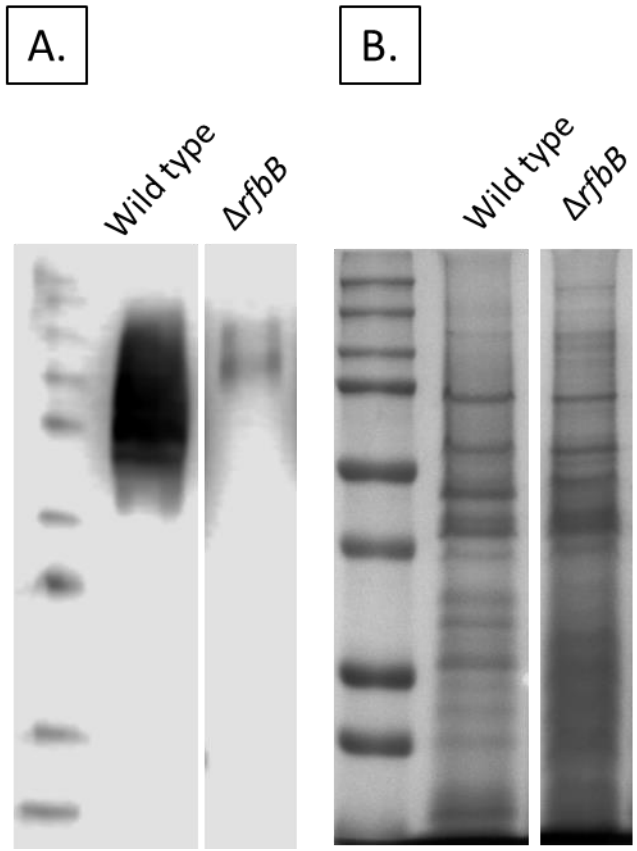

Figure 5.2.11 Western blot for gingipain proteins in whole protein samples of wild type and ΔrfbB P. gingivalis. (A) Total protein samples were separated by SDS-PAGE and transferred to nitrocellulose paper which underwent western blot using the MAb1b5 primary antibody, the blot was visualised via fluorescence of HRP-conjugated secondary antibodies using the LICOR. (B) Total protein samples were also separated via SDS-PAGE and stained using an Instant Blue Coomassie protein stain top show equal loading.

5.2.8 Western blot for major fimbriae component FimA

P. gingivalis has two types of fimbriae, major fimbriae composed of fimbrillin encoded by the *fimA* gene and minor fimbriae encoded by mfA1. Previous studies have shown an important role of the arginine specific gingipains in fully maturing fimbriae by processing fimbrillin (Nakayama *et al.*, 1996; Kadowaki *et al.*, 1998). The lack of this processing by gingipain null mutants result in no fimbriation. Therefore, as Δ*rfbB* has had a decrease in gingipain activity we investigated the presence of FimA in comparison to the wild type. However, figure 5.2.12 shows that there is no difference in the amount of FimA with both bands at 40 KDa being the same in the whole protein samples between the wild type and Δ*rfbB*. There is a potential that the amount of FimA may be similar in the whole protein, however the amount of processed FimA on the surface of *ΔrfbB* could be different to the wild type. This was investigated using outer membrane protein fractions as the sample to perform the western blot. However, there were issues normalising the amount of protein in these samples for fair quantification whilst

still having enough sample to visualise through staining. Due to reduced lab time because of the Covid 19 pandemic this problem was not solved, though if a larger sample was used to extract the outer membrane protein fraction it would be possible to solve this issue using a Bicinchoninic acid assay (BCA) to determine protein concentration of a larger sample and still visualise the bands on a protein gel.

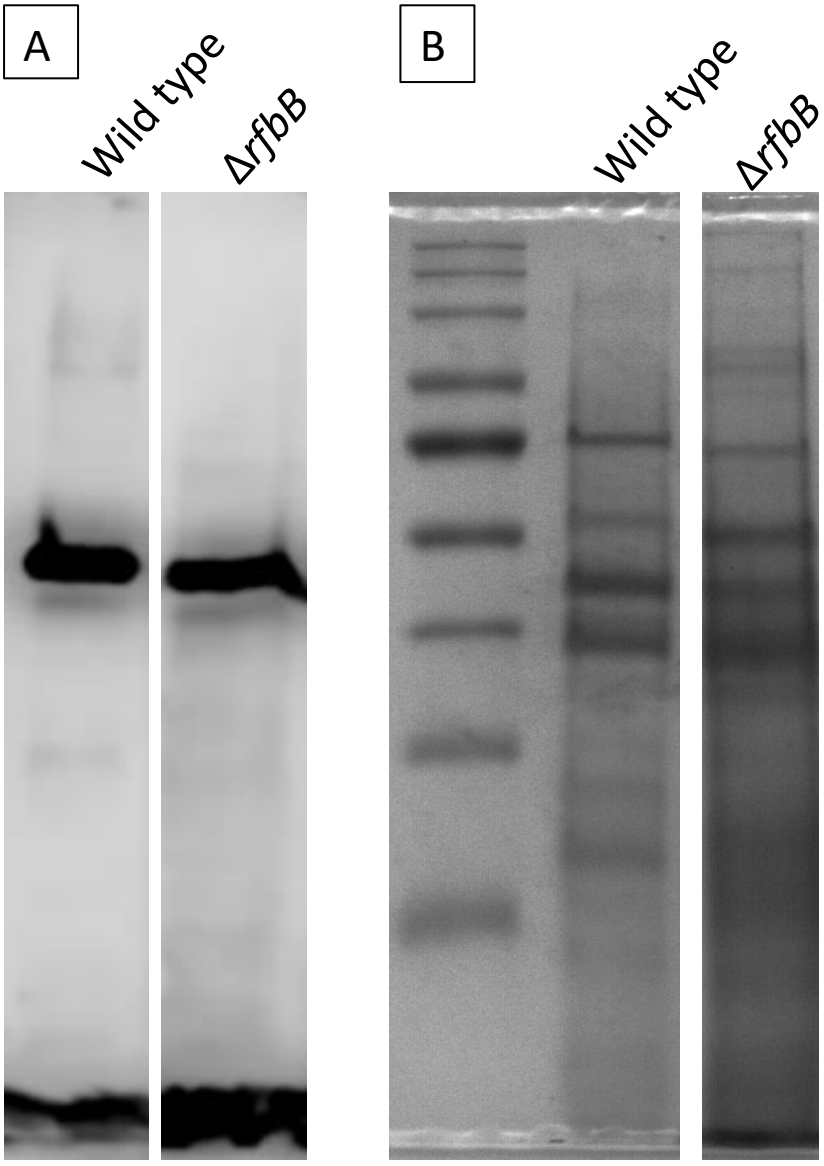

Figure 5.2.12. Western blot for FimA proteins in whole protein samples of wild type and ΔrfbB P. gingivalis. (A) Total protein samples were separated by SDS-PAGE and transferred to nitrocellulose paper which underwent western blot using the anti-FimA primary antibody, the blot was visualised via fluorescence of HRP-conjugated secondary antibodies using the LICOR. (B) Total protein samples were also separated via SDS-PAGE and stained using an Instant Blue Coomassie protein stain top show equal loading.

As Δ*rfbB* is predicted to have a mutation in genes involved with LPS production, the loss of gingipains may be due to a disruption of the LPS structure which is the underlying scaffold

which the gingipains are anchored too (Rangarajan *et al.*, 2017). To investigate this, we investigated the LPS profile of Δ*rfbB*.

5.2.9 The *rfbB* mutant has an altered LPS profile in comparison to the wild type

Δ*rfbB* is a mutant of the production of a major sugar structure in the LPS, therefore it is important to check if the overall structure of the LPS has been altered. To do this we investigated the LPS profile of Wild type and Δ*rfbB P. gingivalis*. This was achieved by isolating purified LPS and separating it by SDS-PAGE. To visualise the LPS periodate sensitive glycans are first oxidised by the addition of periodic acid which allows the fluorescent stain to bind to the oxidised carbohydrate groups (pro-Q emerald). The characteristic LPS ladder can then be visualised with UV light. In figure 5.2.13 it can be observed that there is a shift in the proportion of fluorescence from the bands at the top of the gel (high weight) to the bands at the bottom of the gel (low weight) in Δ*rfbB* when compared to the wild type. This therefore indicates that the disruption to the *rfbB* gene has shifted the LPS profile of *P. gingivalis* to include more light weight structures than high weight, causing a change in the structure in the LPS of the mutant. To evaluate if this change has influenced host-pathogen interactions we investigated the effect of Δ*rfbB* purified LPS on human macrophage cytokine production.

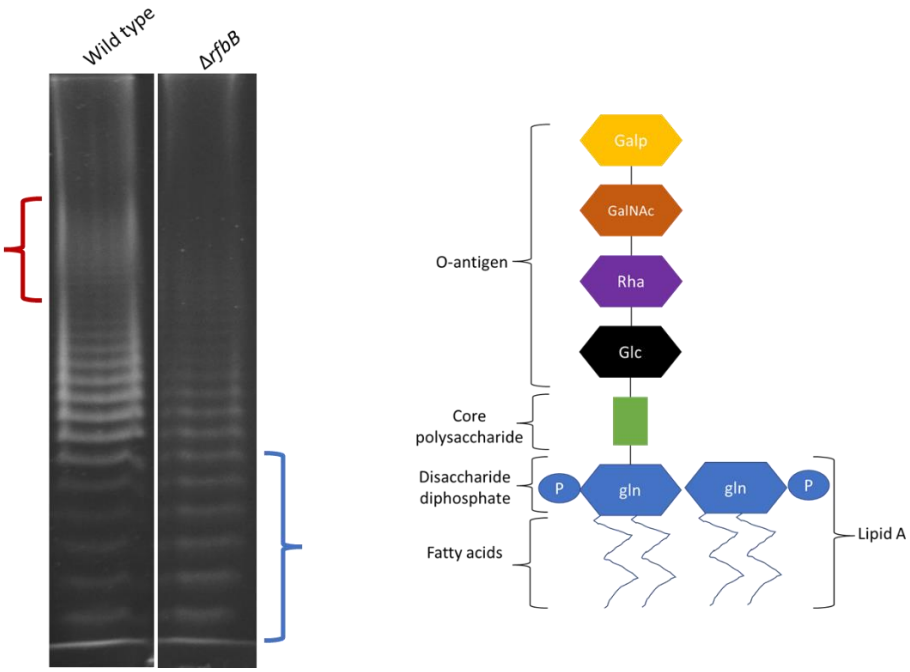

Figure 5.2.13 LPS profiles of wild type and ΔrfbB Porphyromonas gingivalis. Purified LPS was extracted and separated via SDS-PAGE before being stained with Pro-Q emerald LPS stain and visualised using UV light. Higher weight bands that are more present in the wild type have been highlighted with a red indicator. Whereas the lower weight bands more present in ΔrfbB have been highlighted with a blue indicator.

5.2.10 The effect of purified LPS from wild type and Δ*rfbB Porphyromonas gingivalis* on human macrophage cytokine production

LPS is recognised by host cells through Toll like receptors on cell surfaces which causes an immune response through increased expression of cytokines such as IL-6, IL-8 and other inflammatory markers such as TNFα (Ngkelo *et al.*, 2012). LPS can bind to the LPS binding protein (LBP) and CD14 to interact with TLR4 to stimulate an increase of inflammatory cytokines (Kopp, Kupsch and Schromm, 2016), however if the structure of the LPS has changed this could influence the affinity and therefore stimulation of cytokines. To investigate the effects of the Δ*rfbB* LPS on inflammatory response of host cells, the quantity of known inflammatory cytokines and markers IL-6, IL-8 and TNFα from treated cells were assessed by ELISA (section 2.7.5). To do this, primary macrophages were isolated and grown from human blood samples before being seeded at a known density within tissue culture well plates. The macrophages were then treated with growth media containing purified LPS from either wild type, Δ*rfbB* or *E. coli*, one sample was untreated for a negative control. After a 24-hour incubation period with the LPS supplemented growth media, this conditioned media was taken and used in ELISA to assess the quantity of cytokines in the media. Our data show that there was no significant difference in expression of IL-6, IL-8 or TNFα between wild type and Δ*rfbB*, as can be seen in figure 5.2.14. These results indicate the change in the LPS structure of Δ*rfbB* has had no significant effect on the expression of the inflammatory cytokines IL-6, IL-8 and TNFα in MDM's.

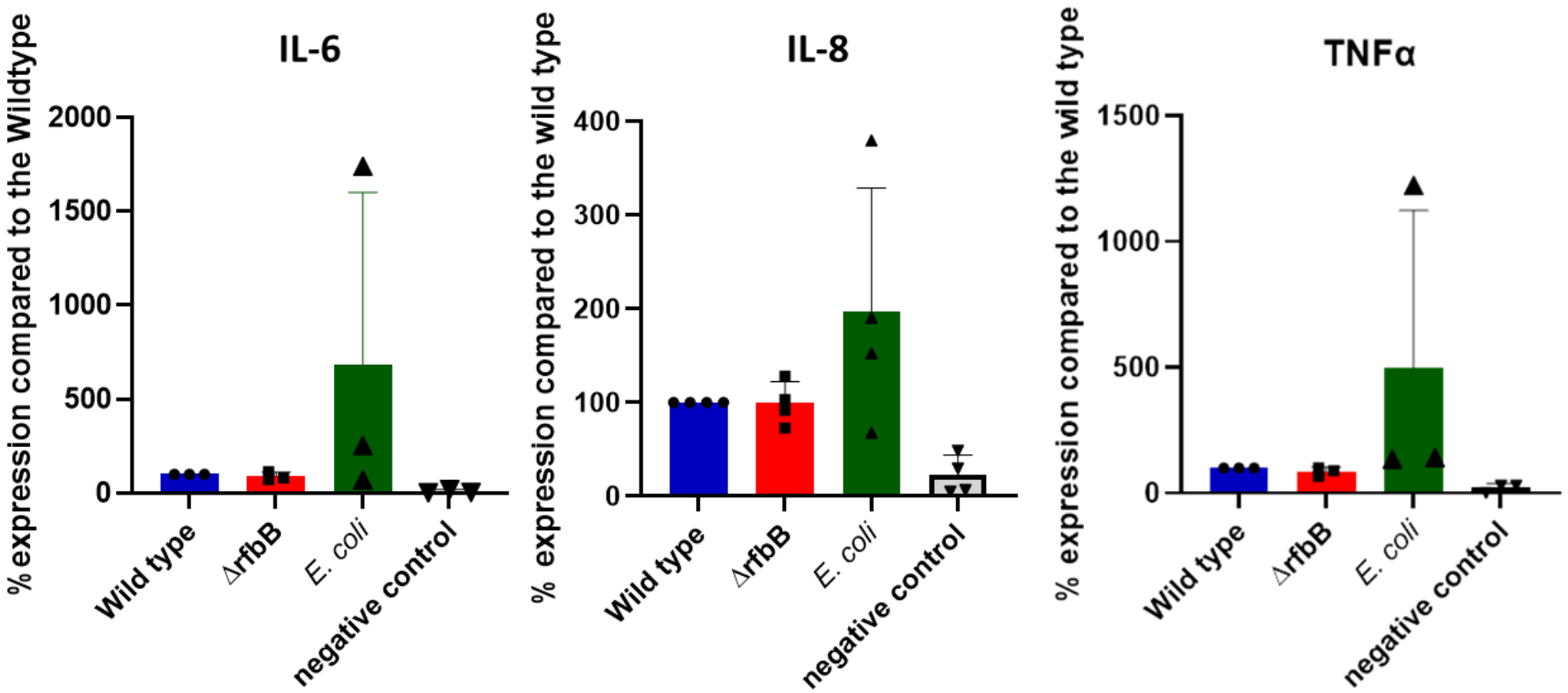

Figure 5.2.14 IL-6, IL-8 and TNFα expression from MDM after 24-hour incubation with LPS supplemented media. LPS was extracted from wild type and Δ*rfbB P. gingivalis* before being normalised to weight and incubated at 100ng/ml in growth media with MDM cells. The conditioned media was then assessed for the concentration of IL-6, IL-8 or TNFα using ELISA as described in section 2.7.5. The absorbance of the ELISA was measured at 450nm and normalised by subtracting the absorption at 570nm. Results are shown as a percentage of the wild-type results to indicate the expression compared to the wild type. Statistical analysis was performed by multiple comparisons ANOVA.

5.3 Discussion

The Lipopolysaccharide of Gram negative bacteria is an important structure in their outer membrane, not only structurally but also due to its role in host-pathogen interactions. The LPS consists of a conserved structure between Gram negative bacteria with variations in core oligosaccharide and more so in the O-antigen (Bertani and Ruiz, 2018). A hydrophobic lipid-A sits in the outer membrane, the core polysaccharide then attaches the lipid-A to the O-antigen which is a polysaccharide made up of repeating sub-units. Whilst the lipid A and core antigen are often required for the structural integrity, inflammation and are essential for growth, the role of the O-antigen has more varied roles with host-pathogen interactions (Raetz and Whitfield, 2002). *P. gingivalis* has been shown to be able to produce two heterogeneous types of LPS. Originally identified by Rangarajan *et al* (2008), they found that the LPS of *P. gingivalis* can exist in two forms. O-LPS which has an O-antigen structure consisting of a tetrasaccharide repeat of Glucose, rhamnose, acetyl galactosamine and galactose saccharides (Paramonov *et al.*, 2001). Whereas the second, the O-antigen has been replaced by an oligosaccharide chain of mannose sugars producing an anionic LPS termed A-LPS (Paramonov *et al.*, 2005). They also showed that each type may have different Lipid-A species with A-LPS uniquely having monophosphorylated penta-acylated lipid A at m/z 1,657 and monophosphorylated tetra-acylated Lipid A at m/z 1,449.

rfbB is the final gene in a putative rhamnose production operon, with a predicted role as a dTDP-glucose 4,6-dehydratase involved in the synthesis of dTDP-rhamnose for the O-antigen of Gram negative bacteria (Tsukioka *et al.*, 1997). Rhamnose is one of the most abundant sugar components in the O-antigen of *P. gingivalis* LPS, with a study by Bramanti *et al* (1989) showing a representation 35.6% of the overall sugar content of the O-antigen of ATCC 33277 *P. gingivalis*. Indicating the importance of rhamnose synthesis in the biogenesis of the O-antigen of *P. gingivalis*. Previous work by Suwannakul *et al* (2010) presented *rfbB* as the most over expressed gene in the invasive gene set from the hyper-invasive sub-population of *P. gingivalis*. Therefore, indicating an important role during invasion of host cells and host-pathogen interaction.

During our attempts to produce a knockout mutant of *rfbB* we only produced a single colony with erythromycin resistance, even though multiple attempts were conducted. Using PCR to

attempt to confirm the correct deletion/replacement mutation showed a double band indicating that *rfbB* had not been knocked out, but that our mutant gene sequence was also possibly incorporated into the genome. After further probing using full genome sequencing the results were unexpected. There seemed to be equal amounts of reads suggesting the *rfbB* gene was still present in the correct area, and that the erythromycin cassette had been inserted in the correct position. Although multiple attempts at sequence alignment were attempted to fully understand this problem, none of the alignments agreed, with either no erythromycin being present or no *rfbB* being present. Both of which are impossible given the results we have seen previously and the actual reads. What we can see in the reads is that the contigs containing the erythromycin cassette showed all the upstream genes in the operon and nothing past the erythromycin sequence. This indicates that the erythromycin cassette has positioned itself at the end of the operon. However, as the *rfbB* gene is still present in the genome this leads our current hypothesis to be that the erythromycin cassette has had a single crossover event placing it upstream of the *rfbB* gene. Unlike the *ompH2* mutant seen in chapter 4, multiple phenotypic changes have been observed in the *rfbB* mutant. There is also no evidence in the genome sequence that the erythromycin resistance cassette has been integrated anywhere else in the genome. Therefore, this upstream insertion of the erythromycin cassette has potentially had a polar effect on the *rfbB* gene disrupting its transcription resulting in the changes seen in this mutant. Multiple different approaches to test this hypothesis were started in this study. The first of which was to use QPCR of the *rfbB* gene to assess the expression of the gene in Δ*rfbB* and the wild type to identify if the *rfbB* gene had been disrupted in the mutant. This process took a lot of optimisations. To quantitatively assess if the gene has altered its expression, we needed to make sure we were normalising for the amount of RNA in the samples. To do this we used a 16s primer set as an internal control to assess the differences in RNA quantity, the difficulty came from the amount of expression seen from these primer sets. The threshold was so high for the 16s compared to the *rfbB* expression that accurate quantification was not achieved in this study. The other process was to produce an expression plasmid containing the wild type *rfbB* gene to be used to complement the mutant. This would allow us to see if the return of a functioning *rfbB* would revert the phenotypes seen in this mutant, confirming that the phenotypes were due to the disruption of the *rfbB* gene. Both approaches had the potential

to answer the questions surrounding the *rfbB* gene disruption, however due to time restraints caused by the coronavirus pandemic these were not achieved in this study.

It is important to note that the issues in producing this mutant through multiple attempts indicate that *rfbB* could potentially be essential to the survival of *P. gingivalis*. A study by Shibata *et al* (1999) attempted to create knockout mutants of all of the genes in the *rfbB* operon which they call rml. In this study *Shibata et al* found during the mutation of *P. gingivalis* that only mutants containing both the wild type and mutant *rml* genes were produced. This was the case for all the *rml* genes, they attempted the process three times with the same results, concluding that the dTDP-rhamnose synthesis pathway is essential for the viability of *P. gingivalis*. Unfortunately, no other data on the mutants were included so the phenotypes seen in our study are not mentioned in the study by *Shibata et al*. Interestingly, the essentiality of this pathway to *P. gingivalis* is not seen in other bacteria, as mutants of this pathway have been produced in other bacteria such as *Salmonella typhimurium* (Jiang *et al.*, 1991) and *Streptococcus mutans* (Tsukioka *et al.*, 1997). The likelihood that the production of dTDP-rhamnose is essential is even more interesting when you combine this with data that shows the O-antigen is not essential to *P. gingivalis*. An O-antigen ligase mutant (*Waal*) of *P. gingivalis* was produced by Rangarajan *et al* (2008), which had neither O-antigen or APS but was still viable. This indicates the role of the dTDP-rhamnose synthesis pathway in *P. gingivalis* is not only involved with O-antigen production but may have roles in other functions related to the viability of the bacteria and maybe even survival intracellularly. Potentially the glycosylation of other proteins important to *P. gingivalis* viability.

The potential of *rfbB* to be essential may be the reason behind the significant decrease seen in the rate of growth and overall OD_{600} of Δ*rfbB* in our laboratory conditions. There is strong evidence to suggest that if the *rfbB* gene is completely knocked out the bacteria is not viable, however if the genes transcription is only disrupted maybe this has led to the results seen in this study. In a study by Jorgenson and Young (2016), they investigated disrupting O-antigen synthesis in *E. coli* and its effect on the phosphate lipid carrier undecaprenyl phosphate (Und-P), a carrier involved in the attachment and transport of sugars to the O-antigen. In their study they created a *wbbl* mutant in *E. coli* that resulted in the formation of "dead end" Und-P attached O-antigen products which sequester the Und-P preventing its use in other systems

such as peptidoglycan synthesis needed for growth. However, the worst of these effects were seen in the Δ*Waal* mutant, a similar O-antigen ligase to the gene mutated in *P. gingivalis* by Rangarajan *et al* (2008) that did not see any problems with viability. Therefore, this may be a growth limiting factor for *E. coli,* however data in *P. gingivalis* suggests that Und-P sequestering may not be the underlying factor causing the problems with viability in Δ*rfbB*.

As mentioned previously gingipains play a role in the nutrition and growth of *P. gingivalis* and our data suggests that both gingipains have been disrupted in Δ*rfbB*. This may be a contributing factor to the reduced growth seen (Grenier *et al.*, 2001), however gingipain function has not been completely lost. In the future, it would be useful to compare a growth curve of a gingipain null mutants in our culture conditions to see how much a lack in gingipains effects the overall growth.

As *rfbB* was overexpressed in the hyper-invasive subpopulation of *P. gingivalis* we characterised multiple virulence factors to try to elucidate the gene's role in host-pathogen interactions. To start, we looked at monoculture biofilm formation and found that it had been significantly reduced in Δ*rfbB* in comparison to the wild type. Interestingly this is contrasting what is seen in other mutants of *P. gingivalis* that affect O-antigen biosynthesis. In a study by Nakao, Senpuku and Watanabe (2006), a knockout mutant of *galE* was created in *P. gingivalis*. *GalE* is conserved in Gram negative bacteria and is involved in the attachment of galactose to the O-antigen. The loss of this gene produced a mutant with a truncated LPS profile, very similar to the LPS profile of Δ*rfbB* with a reduction in intensity of higher weight bands and increase in the intensity of lower weight bands. However, in their study of Δ*galE* it was found that this mutant had a 4.5x greater effect on biofilm formation than the wild type, indicating that this change in LPS resulted in greater biofilm formation which is contradictory to our results. Similarly, in a study by Yamaguchi *et al* (2010), they produced a mutant in *P. gingivalis* of *gftB* which is a glycosyltransferase involved in the production of the O-antigen. In the study by Yamaguchi *et al* they found that Δ*gftB* had disrupted O-antigen and APS, whilst also having a greatly increased biofilm formation. This correlation between O-antigen disruption and increased biofilm formation is not only observed in *P. gingivalis*. In a different study by Nakao *et al* (2012) a mutant of *E. coli* was produced lacking O-antigen (rough LPS) which showed increased biofilm formation which was lost when the mutation was complemented. The literature therefore suggests that the disrupted O-antigen in Δ*rfbB* is not the cause of the

decreased biofilm formation and is the opposite of what is normally observed. This provides further evidence that the synthesis of dTDP-rhamnose does not only contribute to O-antigen production but may have other unknown roles within *P. gingivalis*.

It is important to note that in our study and the study by Nakao, Senpuku and Watanabe (2006) the LPS profiles of *P. gingivalis* with mutated O-antigen biosynthesis genes were similar. *RfbB* is predicted to be involved in the implementation of rhamnose into the O-antigen of *P. gingivalis,* whereas the *galE* gene is involved in the implementation of galactose. Both gene knockout mutants resulted in a truncated O-antigen with greater concentration of lower weight bands than higher weight bands. These results taken together indicate that the removal of a single sugar from the usual tetrasaccharide repeating unit does not completely abolish the O-antigen in *P. gingivalis* but produces a shorter O-antigen. The O-antigen of the LPS has been studied by nuclear magnetic resonance mass spectrometry previously to identify the sugars involved (Paramonov *et al.*, 2001), this would be a future step to further understand what has happened to the O- antigen structure of Δ*rfbB*.

The other important host-pathogen interaction predicted to be involved with *rfbB* by Suwannakul *et al* (2010) is adhesion and invasion. Through antibiotic protection assays we showed that Δ*rfbB* had a significant decrease in both adhesion and invasion supporting the findings of Suwannakul *et al*. However, this decrease in adhesion and invasion is unlikely to be caused by the truncation of the O-antigen. In a study by Soto *et al* (2016), they investigated the role of the O-antigen on multiple host-pathogen interactions including adhesion and invasion. Within the study by Soto *et al* an O-antigen ligase mutant (Δ*waaI*) was used that has no O-antigen present. They found that Δ*waaI* had no changes to its ability to adhere or invade gingival epithelial cells, indicating that the O-antigen does not play an important role in *P. gingivalis* adhesion or invasion of the host. Therefore, the reduction of adhesion and invasion seen in Δ*rfbB* is more likely to be due to a different factor that is not the alteration of the O-antigen. There is potential that the outer membrane of Δ*rfbB* has been disrupted due to the mutation, although the presence of the major fimbriae protein has not been lost. To investigate this further scanning electron microscopy could be used to investigate the morphology of Δ*rfbB* to see if any major changes have occurred to the outer membrane.

In the same study by Soto *et al*, they also demonstrated that a loss of O-antigen resulted in the decrease in expression of TLR4 in gingival epithelial cells, therefore indicating the O-antigen may play an important role in the promotion of an inflammatory response from the host. The process of TLR4 activation starts with the LPS binding protein (LBP) catalysing the interactions between the LPS, CD14 and TLR4 (Hailman *et al.*, 1994). The affinity between LBP, CD14 or even TLR4 and the LPS may be affected by the changes in O-antigen, resulting in a decrease in activation in an O-antigen absent LPS. We investigated the expression of known inflammatory markers in macrophage derived monocytes after exposure to LPS extracted from wild type *P. gingivalis* and Δ*rfbB* and saw no changes in expression. It is possible that the change in the O-antigen of Δ*rfbB* has been to minor to affect the recognition of the LPS, which would explain the lack of change in comparison to the complete removal of the O-antigen seen in the study by Soto *et al* (2016).

Our investigation into the presence of the gingipain proteases of Δ*rfbB* showed clear evidence to the disruption of both arginine and lysine gingipains. This was initially brought to our attention due to the very slow and incomplete pigmentation seen in Δ*rfbB* colonies on blood agar. Further investigation through proteolytic activity assays then displayed significant reduction in both arginine and lysine specific activity. This was also supported by the lack of signal detected in the western blot targeting the arginine gingipains. The study previously mentioned by Yamaguchi *et al* (2010) produced a glycosyltransferase knockout mutant (Δ*gtfB*) in *P. gingivalis* that resulted in the loss of both O-antigen and APS. The gingipain activity was greatly decreased in this mutant, the authors attribute this to the lack of A-LPS acting as an anchor point for the gingipain proteins in the outer membrane. There is accumulating evidence suggesting that gingipain proteases are anchored into the A-LPS once transported to the outer membrane via the T9SS (Shoji *et al.*, 2002; Yamaguchi *et al.*, 2010; Rangarajan *et al.*, 2017). Whether the A-LPS is disrupted in Δ*rfbB* is unknown, although the Mab1B5 antibody also detects A-LPS and has a very weak signal in the Δ*rfbB* total protein samples. The isolation of pure APS has been achieved by Paramonov *et al* (2005) during their study in which they analyse the structure of APS. Following the methodology of *Paramonov* et al purified APS could be isolated from Δ*rfbB* and wild type *P. gingivalis,* the isolated fractions could be probed using the Mab1B5 to investigate whether the A-LPS of Δ*rfbB* has been disrupted.

However, disrupting the dTDP-rhamnose synthesis in theory is unlikely to affect A-LPS. Unlike the O-antigen which rhamnose is the most abundant saccharide, the A-LPS is made up of mannose sugar chains and should not be disrupted by the lack of rhamnose. Multiple phenotypes of *ΔrfbB* seen in our study could also be due to a major disruption of the outer membrane caused by the mutation. To investigate this, we planned to conduct SEM as previously mentioned and membrane integrity studies. Previously in our lab thiazole orange has been used successfully to assess the permeability of bacterial membranes, with higher permeability being an indicator of disrupted membrane integrity (Naylor, 2017). Thiazole orange is a synthetic dye which when bound to DNA becomes fluorescent, this fluorescence can be detected and quantified in Δ*rfbB* and wild type *P. gingivalis* to investigate if the membrane integrity had been altered. This would give us an indication if the membrane integrity had been disrupted and if this is a possible reason for the loss of membrane bound proteins such as gingipains.

5.4 Summary

Although the knockout mutation of *rfbB* did not work as planned, the mutant we produced in this study has displayed multiple phenotypes like those of other O-antigen synthesis gene knockouts. The failure of complete knockout has been attributed by other studies and ours to be due to the dTDP-rhamnose synthesis pathway being essential for viability. Our theory is that a single crossover event has led to the implementation of the erythromycin cassette directly upstream of the *rfbB* gene in the chromosomal DNA, having a polar effect on the expression of *rfbB*. This polar affect has disrupted the gene enough to see phenotypic changes such as decreased growth, decreased adhesion and invasion, an altered LPS profile and reduced activity of gingipain proteins. However, the gene is still active enough to not have caused the bacteria to be unviable in our laboratory conditions. In this study we have provided evidence that *rfbB* is indeed essential for the growth of *P. gingivalis*. We also suggest that reason the dTDP-rhamnose synthesis pathway is essential is not due to disruption in the O-antigen of *P. gingivalis,* but an unknown role in other functions. This alternate role of dTDP-rhamnose is predicted to be the reason behind the reduction in biofilm formation, decreased adhesion and decreased invasion that is not seen in other O-antigen synthesis mutants of *P. gingivalis*.

Chapter 6. Characterisation of the putative metal specific TolC family pump PGN 2012 in *P. gingivalis* virulence

6.1 Introduction

The outer membrane of *P. gingivalis* holds many of the bacteria's virulence factors such as LPS, gingipains and fimbriae (Guo, Nguyen and Potempa, 2010; How, Song and Chan, 2016). These surface factors are well studied due to their role in host-pathogen interactions and the progression of infection. They are arguably the more "aggressive" virulence factors of *P. gingivalis*, with the ability to bind and invade host cells whilst eliciting an inflammatory response that can be destructive to the host and play roles in evading some of the host's natural defences.

In this chapter the work will focus on another one of the genes found by Suwannakul et al (2010) to be overexpressed in the hyper-invasive subpopulation of *P. gingivalis*. In this case the gene in question was referred to as *PG0063,* derived from the available W83 genome at the time. However, the full genome of the ATCC33277 strain that we use in the lab is now available, and this gene was reannotated as *PGN2012*. This gene is part of an operon that encodes what is predicted to be a putative copper, zinc, and cadmium ion efflux system (Figure 6.1). In Gram negative bacteria these and many other toxic compounds are exported from the cell across the periplasm from the cytoplasm likely in one step via the action of a tripartite system. This tripartite system is a combination of an efflux pump that interacts with a large trimeric channel protein by a periplasmic membrane fusion protein (MFP)(Daury *et al.*, 2016), this is illustrated in figure 6.1. The most well studied of these being the AcrAB-TolC tripartite system in *E. coli* with AcrB being the RND pump, and AcrA fusing this pump to the TolC channel membrane.

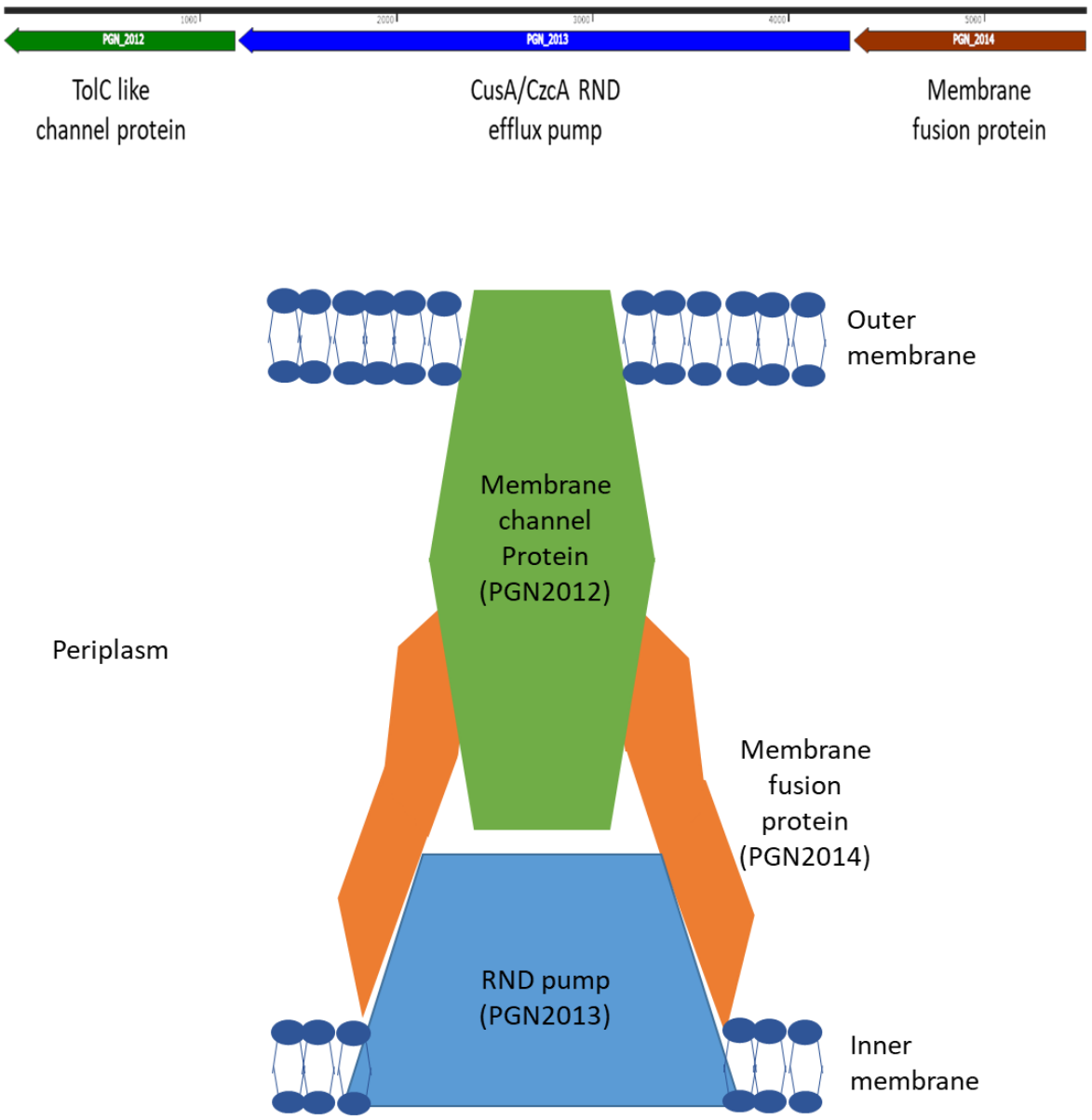

Figure 6.1 The PGN2012 operon and the basic structure of RND efflux tripartite pumps. The predicted RND metal ion efflux operon including the Resistance nodulation and division family membrane fusion protein, the metal ion efflux pump and the TolC membrane channel protein (PGN2012). The tripartite structure consists of the RND periplasm bound pump protein which is fused to a membrane channel protein by the membrane fusion proteins.

The Resistance, nodulation, and division (RND) efflux family is so-called as all known members are responsible for transport functions that are involved in export of toxic compounds involved in Resistance (to drugs or metals), nodulation (in soil bacteria) or Division. The most well studied Gram negative systems are the AcrAB-TolC system in *E. coli* and the MexAB-OprM system in *P. aeruginosa*. Both pumps have been shown to provide antibiotic resistance through the antiport of antibiotics/H^+ ions via proton motive force. Therefore, RND systems

in Gram negative bacteria produce a clinical challenge, as treatment such as antibiotics may no longer work (Venter *et al.*, 2015).

Although the most well studied RND systems are focussed on antibiotic resistance, there are multiple substrates that the RND efflux systems are involved in that are beneficial for the bacteria's survival. This is the case with heavy metal efflux (HME), these transporters are referred to as CBA transporters such as the CzcCBA system in *R. metallidurans* responsible for the efflux of Zn^{2+}, Co^{2+}, Cd^{2+} heavy metal ions (Saier *et al.*, 1994). As *PGN2012* is downstream of a putative CusA/CzcA efflux pump, the role of this gene in metal efflux will be explored in this chapter. It is worth noting that *P. gingivalis* has 7 different TolC homologues in separate efflux operons which will also be explored in this chapter.

The role of *PGN2012* is unclear, the gene was overexpressed in a hyper-invasive subpopulation indicating that its expression may influence and be beneficial to the bacteria as they invade H357 oral squamous carcinoma cells. In this chapter a bioinformatic and phenotypic analysis of the role of *PGN2012* and its role in physiology and virulence of *P. gingivalis* was investigated via a range of assays.

6.1.1 Aims

The aim of this chapter was to investigate the role of *PGN2012* in host pathogen interactions, virulence, and efflux. This was achieved through the production of a knockout mutant of *PGN2012* which was compared to the wild type. We specifically focus on characterising Δ*PGN2012*, investigating common virulence traits and investigating its role in the efflux of heavy metals.

6.2 Results

6.2.1 Bioinformatic analysis of *PGN2012* and related proteins in *P. gingivalis* efflux

To identify how many putative TolC family proteins the *P. gingivalis* genome may encode, a pfam scan of ATCC 33277 genome was completed and operons containing TolC homologues were identified and analysed as shown in figure 6.2.1. *P. gingivalis* has 7 potential TolC homologues as shown below in figure 6.2.1. Four of these are predicted to be involved in ATP fuelled transport via ABC transporters (PGN_0449, PGN_0715, PGN_1679, PGN_2041). Two of these operons putatively encode homologues of the haemolysin transport systems as characterised by having HlyD homologues (the hemolysin transport like periplasmic fusion

proteins)- indicated in red (Figure 6.2.1 PGN_1679, PGN_2041). Whereas the other three TolC homologues are in operons with predicted RND transport systems (Figure 6.2.1 PGN_1432, PGN_1539, PGN_2012). However, *PGN2012* is the only TolC family protein in an operon within a predicted HME-RND tripartite pump. From this analysis, we predicted that PGN2012 is the TolC like channel protein that interacts with PGN2013 the CusA/CzcA RND pump via further interactions with PGN2014 the predicted periplasmic membrane fusion protein. This would form a tripartite CBA transporter in *P. gingivalis*. The role and function of *PGN2012* will be investigated in this chapter by knockout mutagenesis, comparing the mutant to the wild type.

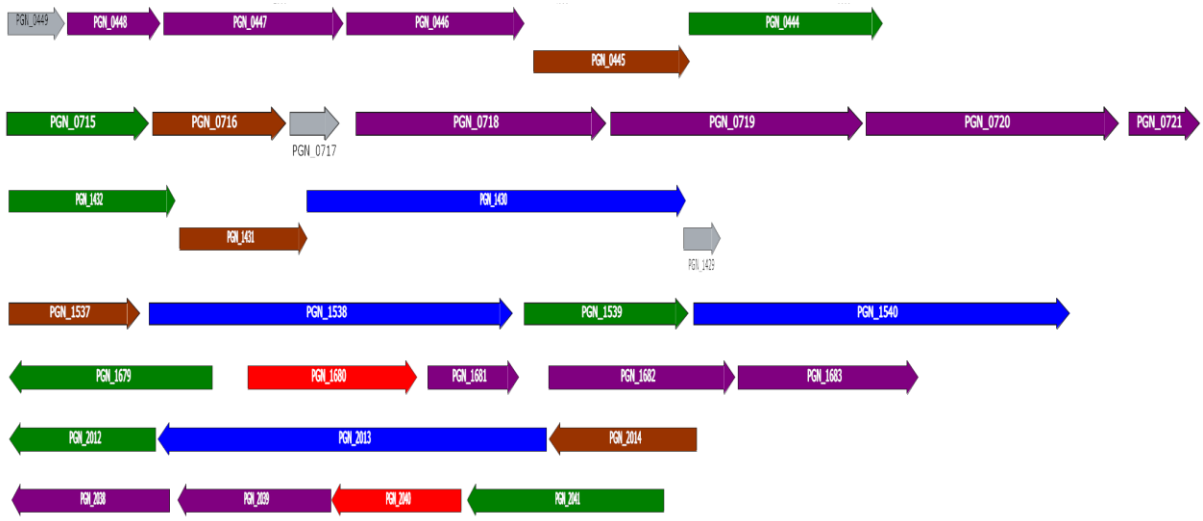

Figure 6.2.1 Bioinformatic alignment of TolC homologues and their operons in *P. gingivalis*. Seven TolC homologues and their related operons were identified by a Pfam screening of the full genome of *P. gingivalis* ATCC 33277. TolC channel protein homologues are colour coded green, periplasmic membrane fusion proteins are coloured brown, ABC transporters are coloured purple, HlyD proteins are coloured red and unclassified hypothetical proteins are coloured grey.

We also investigated PGN_2012 further by looking for protein family similarities and sequence similarities with the protein databases pFAM and Phyre. Figure 6.2.2 shows the result from the PGN_2012 amino acid sequence analysis using pFAM, where there are two distinct regions with high sequence similarities to outer membrane efflux proteins. Similarly, when running the sequence through the phyre database (Figure 6.2.3) there was multiple matches to RND outer membrane efflux proteins with >90% coverage.

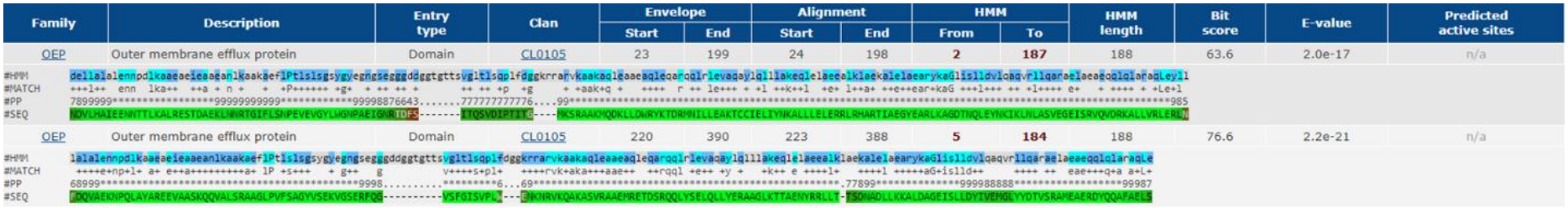

Family	Description	Entry type	Clan	Envelope		Alignment		HMM		HMM length	Bit score	E-value	Predicted active sites
				Start	End	Start	End	From	To				
OEP	Outer membrane efflux protein	Domain	CL0105	23	199	24	198	2	187	188	63.6	2.0e-17	n/a
OEP	Outer membrane efflux protein	Domain	CL0105	220	390	223	388	5	184	188	76.6	2.2e-21	n/a

Figure 6.2.2 PFAM alignment of the amino acid sequence of PGN2012. The amino acid sequence of *PGN2012* was analysed through the pFAM database to identify similarities to protein families.

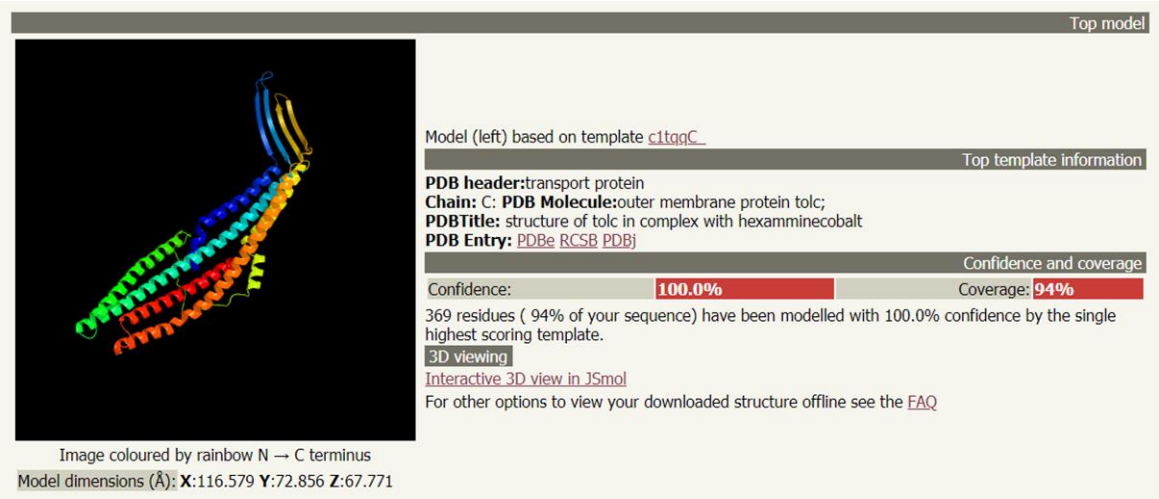

Figure 6.2.3 Phyre database prediction of PGN2012 in comparison to similar proteins. The amino acid sequence of *PGN2012* was analysed through the phyre database to identify structural coverage similarities to other known proteins.

6.2.2 Knockout mutagenesis of *PGN2012*

6.2.2.1 PCR confirmation of knockout mutagenesis

Similarly, to chapter 5, knockout mutagenesis was performed to produce a mutant in which *PGN2012* had been removed and the effects caused by this can be compared to the wild type to investigate the role of *PGN2012* in host-pathogen interactions. An altered gene sequence was commercially produced by genesynth, with PGN2012 replaced by a reverse complemented Erythromycin cassette (reverse complemented as the gene is read in 3'-5') surrounded by 500 bp of upstream and downstream DNA. This mutant sequence was then blunt cloned into pJET1.2 blunt cloning vector for replication and storage. The plasmid DNA was extracted and used to transform *P. gingivalis* ATCC 33277 by natural competency as described in section (2.4.1.2). Positive colonies grown on erythromycin supplemented FAB plates were subcultured and mutation was initially checked by PCR (Figure 6.2.4).

Two separate PCR experiments were performed to confirm mutation. The first used *PGN2012* forward and reverse flanking primers to check the mutation had occurred in the desired region. The second experiment used a forward flanking primer and a reverse erythromycin cassette primer to confirm the presence of the erythromycin cassette (Figure 6.2.5).

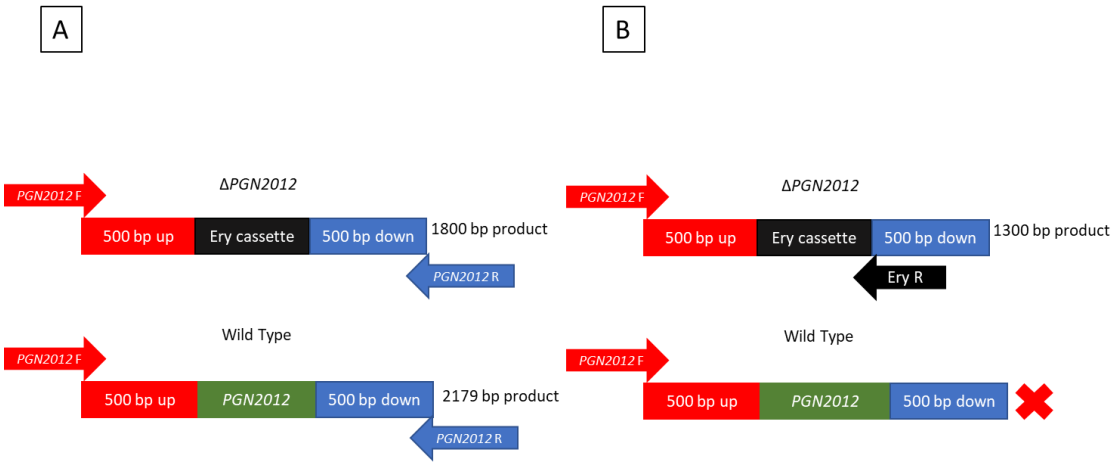

Figure 6.2.4 PCR reactions to confirm the erythromycin resistance cassette insertion for ΔPGN2012. (A) A PCR reaction which will produce a gene sequence that encompasses the rfbB gene and the upstream and downstream flanking regions, producing a 2179 bp product for the wild type and an 1800 bp product for the mutant due to the shorter Ery cassette. (B) A PCR reaction which will produce a gene product with the upstream flanking region of PGN2012 and the erythromycin cassette if correctly inserted, this will not give a product for the wild type.

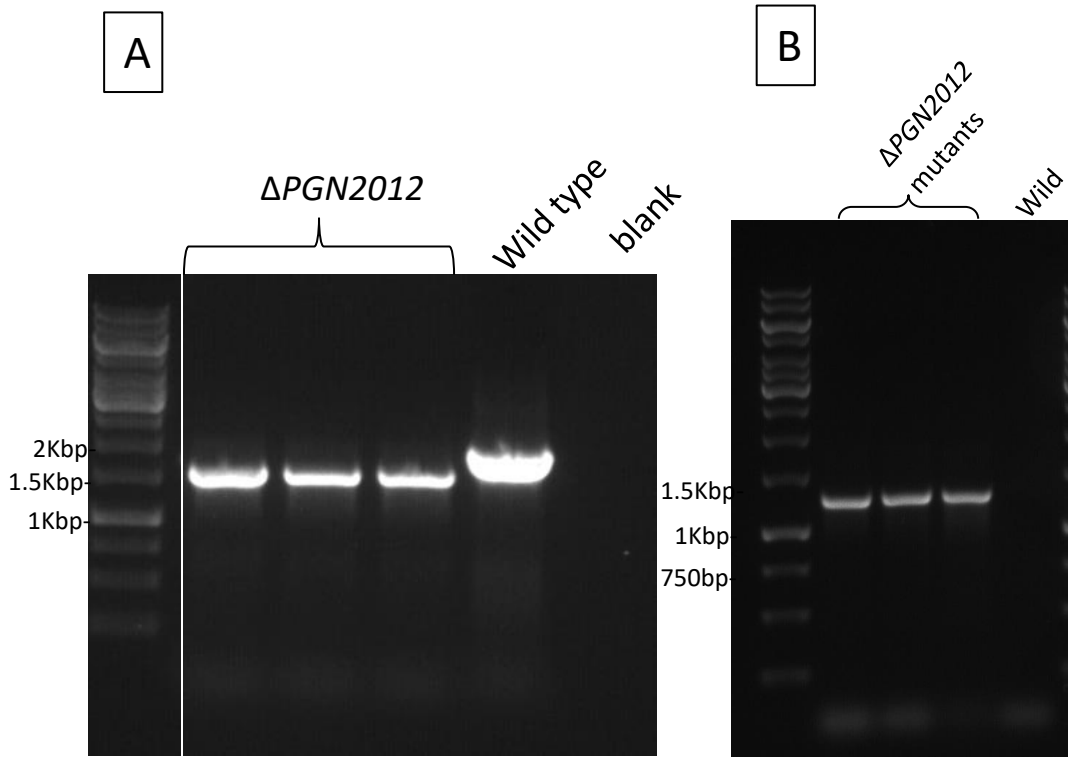

Figure 6.2.5 Confirmation PCR of Wild type and ΔPGN2012 Chromosomal DNA. (A) Chromosomal DNA of Wild type and three ΔPGN2012 was amplified by PCR using upstream and downstream flanking primers as described in figure 6.2.2A. (B) Chromosomal DNA was amplified using an upstream flanking primer and an erythromycin reverse primer as described in figure 6.2.2B.

Figure 6.2.5 shows the results of the PCR confirmation experiments. In figure 6.2.4A 3 single bands are seen in the Δ*PGN2012* DNA extracts at ~1800 bp which are smaller than the single band of the wild-type sample which is ~2179 bp. This result is expected as described in figure

6.2.5A as the erythromycin cassette is smaller than *PGN2012*. Figure 6.2.5B also presents a predicted result with 3 single bands in the Δ*PGN2012* samples at a size of ~1300 bp, which is the correct size of the erythromycin cassette and upstream fraction as shown in figure 6.2.4B. There is no band for the wild type as there is no erythromycin cassette.

These results indicate the presence of erythromycin in the chromosomal DNA and that is has inserted itself in the correct location, producing the desired knockout mutation. The mutation is unlikely to have polar effects on other genes in the operon due to it being the final gene in the operon. Further confirmation was achieved through full genomic sequencing as described below.

6.2.2.2 Confirmation of mutation through Nanopore genomic sequencing

To provide further evidence of correct knockout mutation and with the data from chapter 5 on rfbB in mind, full genomic sequencing, was performed to analyse the full sequence of the mutant and confirm mutation. Nanopore sequencing was performed with chromosomal DNA from *ΔPGN2012* as described in section 2.6.8 and explained in section 4.2.1.2.

Figure 6.2.6 shows the *PGN2012* gene region with upstream and downstream flanking areas in Integrative genomics viewer (IGV) as a comparison to the wild type reference. The amount of matching reads to the alignment can be seen by the grey peaks in the top bar in the upstream and downstream flanks, the matching reads can be seen underneath these grey bars as blue or pink bars indicating the direction of the reads. Whereas in the *PGN2012* region there is no evidence of matching reads to the alignment, and all reads in this section match the erythromycin resistance cassette. This data shows that Δ*PGN2012* is a clean knockout mutant, completely removing the original gene and replacing it with the erythromycin cassette.

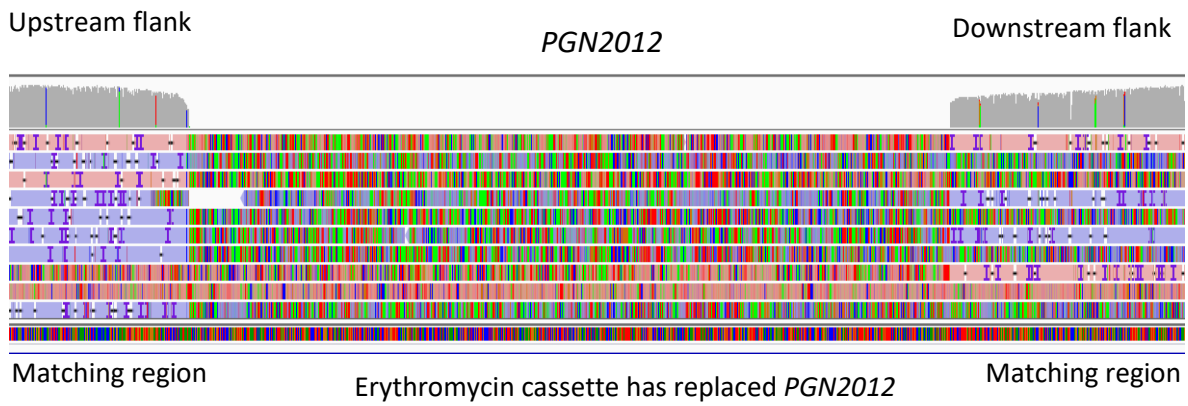

Figure 6.2.6 Change in the *PGN2012* gene in chromosomal sequencing of Δ*PGN2012*. Nanopore chromosomal sequencing was performed on a chromosomal DNA extract of Δ*PGN2012*. All the reads were aligned and compared to a previously generated full genomic sequence of *P. gingivalis* ATCC 33277 taken from NCBI. The aligned sequences and the reference sequence were viewed in the Integrative genomics viewer (IGV). Total matching reads are shown in the top bar as grey peaks, with the read data just underneath. Pink or blue bars indicate reads that match the reference genome, whereas multicoloured bars indicate differences to the reference genome.

6.2.3 Δ*PGN2012* has a reduced growth rate in supplemented BHI in comparison to wild type *P. gingivalis*

Efflux pumps are not only important for antibiotic resistance, but also the removal of toxins that can accumulate within bacteria (Blanco *et al.*, 2016), therefore a mutation to this system could potentially affect the growth and survivability of *P.* gingivalis. Anaerobic growth curves in supplemented BHI were performed to evaluate if the knockout mutation had any effects on the growth of the mutant in comparison to the wild type. In figure 6.2.7 the data show that Δ*PGN2012* has a slightly slower exponential phase growth rate with a mean generation time of 311 minutes whereas the wild type has a mean generation time of 305 minutes (approx. 2%, P <0.05, Fig 6.2.7). In addition, there is a small but statistically significant decrease in optical density for Δ*PGN2012* between 20 hours and 44.5 hours in comparison to the wild type with a p value <0.05. Finally, the final optical density is slightly lower (0.829) than wild type (0.907) but this is not statistically significant.

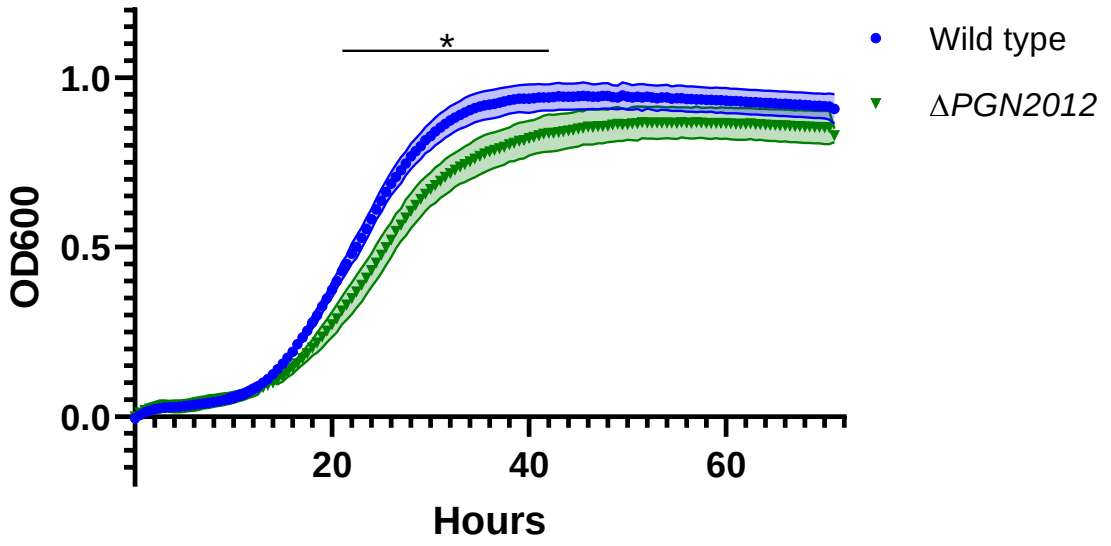

Figure 6.2.7 Anaerobic growth comparison of wild type and Δ*PGN2012 P. gingivalis*. Wild type and ΔPGN2012 *P. gingivalis* were prepared at OD600 0.01 before being incubated at 37°C in anaerobic conditions within a Cerillo stratus plate reader as described in section 2.8.7. OD600 was first blanked before being read every 30 minutes for 72 hours. N=3 with 9 technical replicates per biological repeat, shaded areas represent +/- SEM made in Graphpad prism. Statistical analysis was analysed by 2-way ANOVA comparing the difference of each time point. *p <0.05.

6.2.4 *PGN2012* knockout mutation does not change monoculture biofilm formation

Efflux pumps have been shown to influence biofilm formation in other bacteria through the efflux of quorum sensing inducers and or EPS (Alav, Sutton and Rahman, 2018). As biofilms are essential for the progression of periodontitis, we investigated the effect of knocking out *PGN2012* on the biofilm formation of *P. gingivalis*. To do this monoculture biofilm formation assays were performed using *ΔPGN2012* as described in section 2.8.5 and explained in 4.2.3.

As can be seen in figure 6.2.8A below, the biofilm formation of Δ*PGN2012* did not change significantly when compared to the wild type. There are also no obvious changes seen qualitatively in the microscope images in figure 6.2.8B.

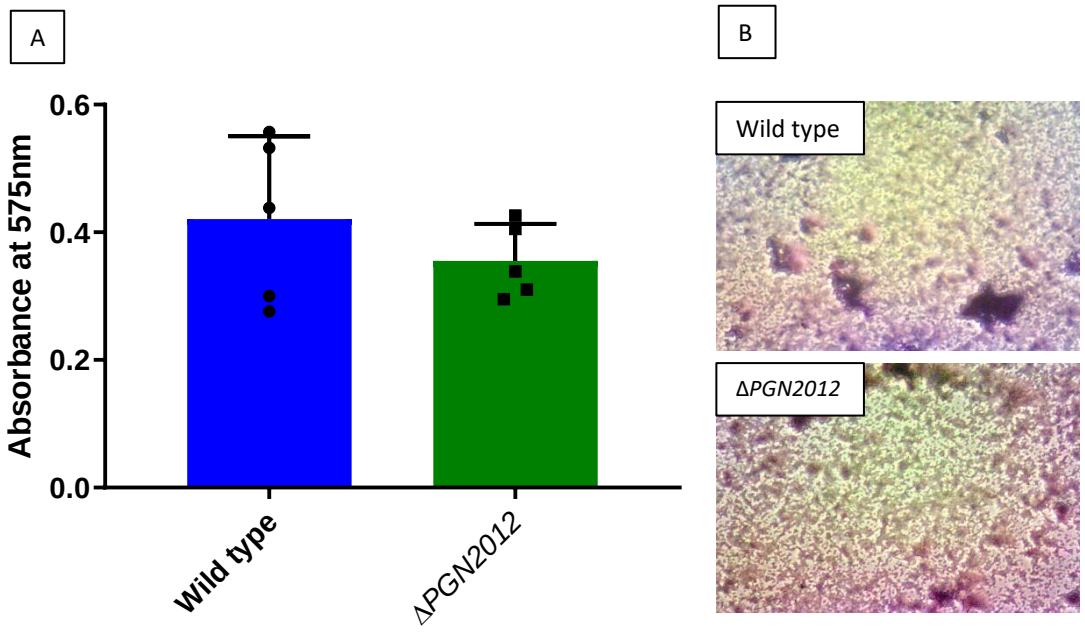

Figure 6.2.8. Biofilm formation assay after 5 days of growth. (A) Overnight cultures of *P. gingivalis* were made to OD_{600} 0.1 and incubated in a 96-well plate anaerobically at 37°C for 5 days. The OD_{600} was measured using a TECAN plate reader before the biofilms were washed and stained with crystal violet. The crystal violet in the biofilms was solubilised in ethanol: acetone (80:20) and the absorbance measured at 575nm using a TECAN plate reader. The results were normalised to growth by dividing the overall absorbance by the OD_{600} results. Statistical significance was determined by a Students T-test with a p value of <0.05 being significant, no statistical significance was observed. (B) Stained biofilms were washed and dried before images were taken at 100x magnification with an Olympus light microscope.

These results indicate that *PGN2012* does not have a significant role in the biofilm formation of *P. gingivalis*.

6.2.5 The effect of *PGN2012* knockout mutation on the Total protein profile of *P. gingivalis*

Protein profiles of whole cell protein samples were performed to investigate if the knockout mutation had a major effect on the proteins present in the *P. gingivalis*. To do this, liquid cultures of Δ*PGN2012* and wild type *P. gingivalis* were grown and normalised to an OD600 of 1 before being boiled in 2x SDS loading buffer. The protein samples were loaded equally into a 12% acrylamide gel before the proteins were separated by SDS-PAGE. Once separated the protein bands were stained using Coomassie instant blue™.

Figure 6.2.9 shows the analysed protein profiles of both wild type and Δ*PGN2012* total protein samples. There was no clear changes or differences in the protein profile of the mutant in

comparison to the wild type. This result shows that the knockout of *PGN2012* has not had any major effect on the presence of other major proteins of *P. gingivalis*.

After seeing a small change to growth but no substantial loss of other proteins, the gingipain activity of Δ*PGN2012* was investigated to see if the proteolytic activity of the mutant had been affected by the mutation.

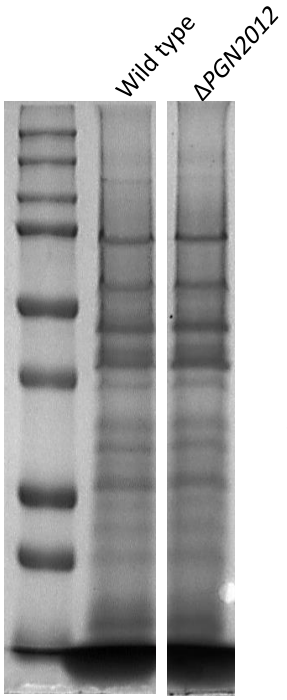

Figure 6.2.9 Total protein profiles of wild type and Δ*PGN2012*. Overnight liquid growth cultures from both samples were grown and normalised to OD600 1 before being pelleted and boiled in SDS-lysis buffer. The total protein samples were separated by SDS-PAGE on a 12% acrylamide gel. The protein bands were visualised by staining with Instant blue Coomassie staining.

6.2.6 Investigation in the gingipains of Δ*PGN2012* in comparison to the wild type.

As mentioned previously the gingipains of *P. gingivalis* are one of the bacteria's major virulence factors and play a role in growth and nutrient acquisition as well as host pathogen interactions (Guo, K. A. Nguyen and Potempa, 2010). To investigate whether the gingipains have been affected by the knockout of *PGN2012* we investigated the proteolytic activity of the mutant in comparison to the wild type, as well as the overall presence of gingipains via western blot.

6.2.6.1 Δ*PGN2012* has unaltered protease activity in comparison to the wild type

To investigate the proteolytic activity of the two different types of gingipains the same methodology was used as described in section 5.2.4. In brief, a substrate that can be specifically cleaved at either Arginine or Lysine was used that when cleaved releases fluorescent methyl coumarin (explained in detail in Section 2.8.10). This fluorescence is measured by a TECAN plate reader, and the proteolytic activity quantitatively analysed.

Figure 6.2.10 shows the results from the arginine and lysine gingipain assays, with no significant changes in activity between Δ*PGN2012* and wild type *P. gingivalis*. Therefore, demonstrating that the activity of arginine and lysine gingipains has not been disrupted by the knockout of *PGN2012*. These results show that the gingipain activity of Δ*PGN2012* has not been altered by the mutation. Western blot was performed to check if the overall amount of gingipains had been altered.

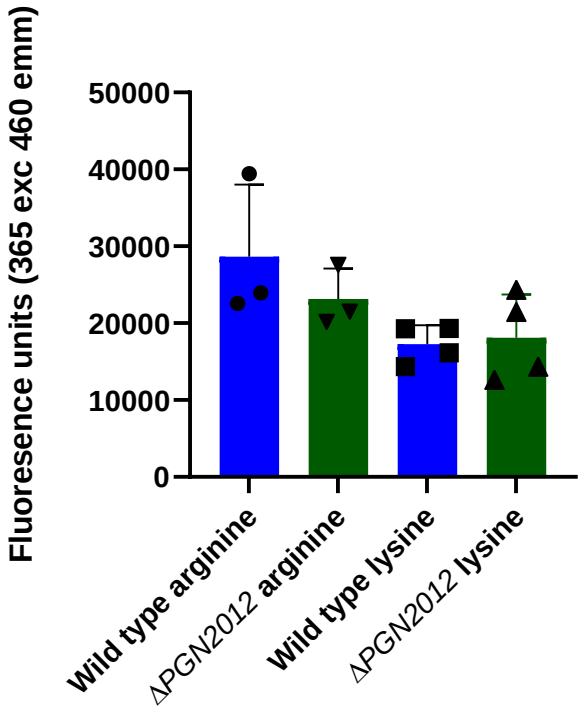

Figure 6.2.10 Arginine gingipain activity of Wild type and Δ*PGN2012* P. gingivalis. Overnight cultures of *P. gingivalis* were made to OD600 0.01 before being pelleted and resuspended in PBS, the bacteria were incubated with 100 µl of the arginine or lysine bound methylcoumarin for 5 minutes before the reaction was quenched and the fluorescence was read at 365 excitation and 460 emission. Error bars represent +/- SEM. Statistical analysis was performed using a T-Test. N=3 for arginine and N=4 for lysine each including triplicates of technical repeats.

6.2.6.2 Comparing *P. gingivalis* gingipain proteins between ΔPGN2012 and the wild type by western blot

The results from the gingipain activity assays indicated that there were no changes in activity between Δ*PGN2012* and the wild type, to investigate if the presence of gingipain proteins had been altered western blot was performed. To do this, whole cell protein samples were separated on a 12% acrylamide gel by SDS-PAGE. The protein gel was western blotted following the methodology described in section 2.7.3 using the mab1b5 primary antibody provided by Professor Mike Curtis. Figure 6.2.11 shows no clear changes in the presence of

gingipains when comparing Δ*PGN2012* to the wild type. The results from investigating the gingipains of Δ*PGN2012* again suggest that the gingipain proteases have not been affected by the knockout of *PGN2012*.

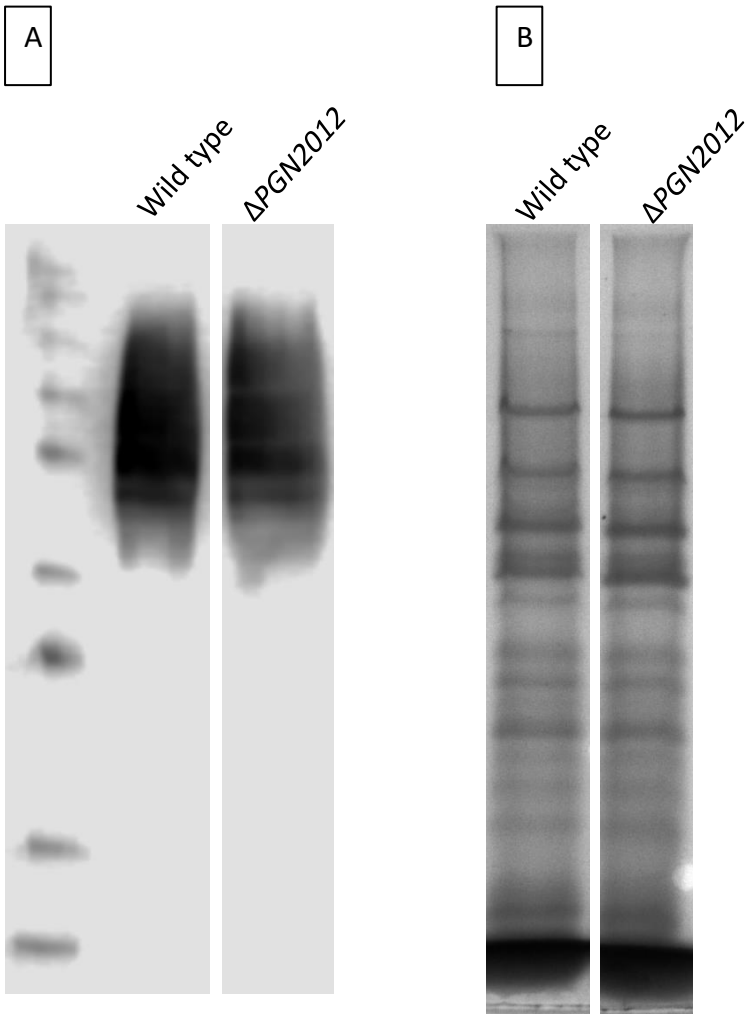

Figure 6.2.11. Western blot for gingipain proteins against wild-type and Δ*PGN2012* total protein samples. Overnight liquid growth cultures from both samples were pelleted and boiled in SDS-lysis buffer before the total proteins were separated by SDS-PAGE on a 12% acrylamide gel. (A) The proteins were transferred to nitrocellulose paper using semi-dry transfer before being blocked in TBS (5% milk powder). The paper was first probed with an anti-mouse Mab1b5 antibody, which was complemented with an HRP conjugated mouse antibody. ECL solution was incubated with the blot before visualising using a LICOR scanner. (B) The protein gel was stained with Coomassie instant blue to show equal loading, this is the same gel as seen in figure 6.2.9.

6.2.7 Antibiotic protection assay of Δ*PGN2012* in comparison to wild type *P. gingivalis* reveal no significant change in adhesion or invasion.

In the study by Suwannakul *et al* (2010) *PGN2012* was one of the genes found to be overexpressed in the hyper invasive subpopulation, indicating a role in the invasive capabilities of *P. gingivalis*. To

investigate this antibiotic protection assays were performed. The antibiotic protection assays were carried out as described in detail in section 2.8.9 and described in brief in section 5.2.4.

Figure 6.2.12 shows the results of the antibiotic protection assays, demonstrating no significant change in total association, adhesion, or invasion. Although a slight increase can be seen in the Δ*PGN2012* samples, these are not significant and possibly due to the amount of variation between biological repeats. Therefore, these results suggest that Δ*PGN2012* does not have a specific role in the adhesive and invasive abilities of *P. gingivali*s.

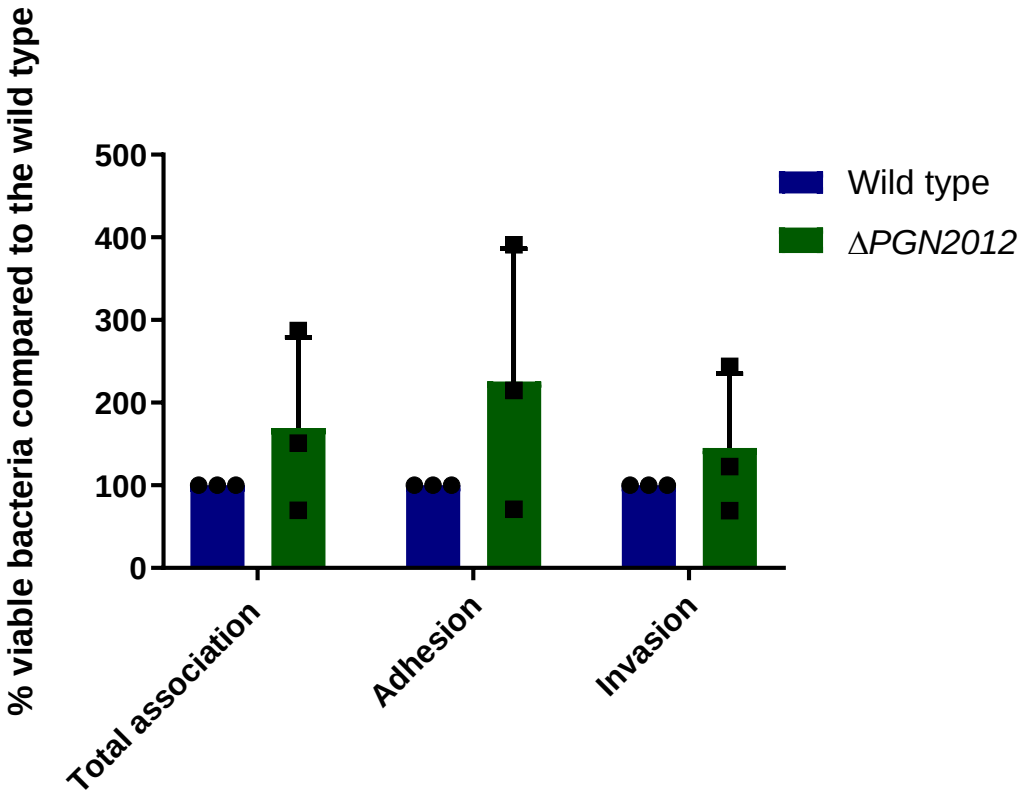

Figure 6.2.12. Antibiotic protection assays of wild type and ΔPGN2012. Invasion and adhesion were determined using the antibiotic protection assays as described in section 2.8.9. Invasion was determined by the bacteria that survived the metronidazole treatment, as a percentage of overall viable wild type P. gingivalis. Total association was determined by admitting the metronidazole killing, therefore counting the number of bacteria that had invaded the cells but also the bacteria that is attached to the surface. Adhesion was calculated by subtracting the invasion data from the total association. All results were then compared to the wild type in each individual experiment to demonstrate the trend seen within the individual experiments that is obscured by the variability between experiments. Error bars are +/- SEM. Statistical analysis was performed using multiple T tests. Antibiotic protection assays were performed with Three biological repeats, each containing 3 technical replicates.

It is important to note however that even though the role of *PGN2012* does not seem to specifically influence the mechanical adhesive and invasive abilities of *P. gingivalis*, its role

may be in the intracellular survivability of the bacteria. As an efflux gene, the role of *PGN2012* may be more related to the survivability of the bacteria once inside the host cells rather than the mechanisms behind invasion. Through the efflux of hazardous toxins the internalised bacteria may survive better inside the cells resulting in a greater internal viability that is seen in the hyper invasive subpopulation described by Suwannakul *et al* (2010). To investigate the effect of this mutation on efflux, minimal inhibitory concentration experiments were performed to investigate whether Δ*PGN2012* had become more susceptible to different metal ions.

6.2.8 Δ*PGN2012* has an increased metal sensitivity in comparison to wild type *P. gingivalis*

As seen in the figure 6.1 *PGN2012* is a TolC homologue in an operon with other components of a putative HME-RND efflux system with an efflux pump like that of CusA/CzcA in *E. coli* and *R. metallidurans* respectively. CusA is the efflux pump in the CusCFBA proteins that make up the copper efflux system in *E. coli*, with CusA being essential for copper resistance (Franke *et al.*, 2003). Whilst CzcA is the efflux pump in the CzcCBA set of proteins originally discovered to be related to heavy metal resistance in *R. metallidurans* (named at the time *Alcaligenes Eutrophicus*) (Saier *et al.*, 1994). CzcA has been shown to be involved in the resistance of the heavy metal cations Co^{2+}, Zn^{2+} and Cd^{2+} (Mergeay *et al.*, 1985; Diels, Mergeay and Regniers, 1988). Therefore, the knockout of *PGN2012* was predicted to influence the sensitivity to these metals. To investigate whether Δ*PGN2012* had an altered metal resistance MIC growth curves were performed with BHI supplemented with a range of metal salt solutions of Cu^{2+}, Zn^{2+}, Co^{2+} and Cd^{2+}. These metal ion salts were chosen due to their efflux in the CusA/CzcA systems, as PGN2013 is predicted to be a similar pump as well as the similar ionic radius'. In brief overnight cultures of Δ*PGN2012* and wild type *P. gingivalis* were grown before being normalised to OD_{600} 0.1 in supplemented BHI. The bacteria were pelleted and resuspended in BHI supplemented with a range of metal salt concentrations, with each concentration being tested in triplicate. These samples were incubated anaerobically at 37^{o}C in a 96 well plate, with the OD_{600} measured every 30 minutes by a Cerillo stratus plate reader. The growth curves were plotted, and differences analysed statistically by multiple comparisons ANOVA.

6.2.8.1 Zinc sensitivity of *ΔPGN2012* and wild type P. gingivalis

To evaluate any changes in sensitivity to zinc a range of zinc chloride supplemented BHI was used with a range of concentrations from 0.01 mM to 5 mM. Figure 6.2.13A shows the differences between the growth in the wild type and Δ*PGN2012* at all these concentrations, with no clear differences until a concentration of 0.5 mM was included in the media. A statistically significant reduction in growth was observed at the 3 day point with the wild type having a mean growth of 60% and ΔPGN2012 having a mean growth of 6.2% when compared to untreated growth. To analyse this further a growth curve was plotted using the data points from the 0.5 mM zinc chloride samples which can be seen in figure 6.2.13B. This growth curve clearly shows a statistically significant increase in sensitivity to Zinc ions, with the wild type having a mean generation time of 17.9 hours and reaching an average of OD_{600} 0.45 whilst Δ*PGN2012* does not grow above 0.11. Resulting in a statistically significant difference in growth between 91 hours and 132 hours where the p value <0.05. No statistical difference was observed in the 0.2M $ZnCl_2$ growth curve, with a mean generation time of 11.7 hours for the wild type and 13.7 hours for Δ*PGN2012* (Figure 6.2.14).

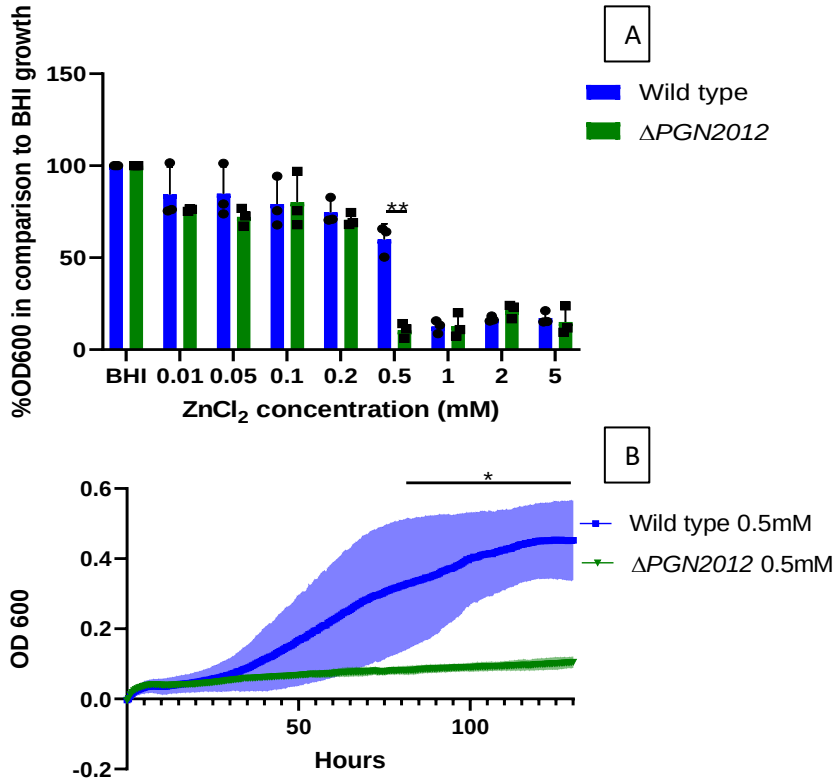

Figure 6.2.13 Zinc metal sensitivity of Δ*PGN2012* in comparison to wild type *P. gingivalis*. Overnight cultures of Δ*PGN2012* and wild type *P. gingivalis* were normalised to OD_{600} 0.1, pelleted, and resuspended in a range of zinc chloride supplemented BHI. The samples were incubated anaerobically at 37°C for 140 hours, with the OD600 being measured every 30 minutes by a Cerillo stratus plate reader. (A) OD_{600} values were taken at the 3 day point and normalised as a percentage of the growth of either wild type or Δ*PGN2012* in BHI to account for differences in growth between wild type and the mutant, the full range of zinc chloride concentrations is shown, and the point of sensitivity was then chosen to be shown as a growth curve. (B) A growth curve was plotted from using the concentration that indicated a difference in sensitivity between the wild type and Δ*PGN2012*. N=3 with 3 technical repeats to each biological repeat with shaded areas representing +/- SEM made in Graphpad prism. Statistical analysis was performed by T-test in (A) and multiple comparisons ANOVA in (B). P<0.05*.

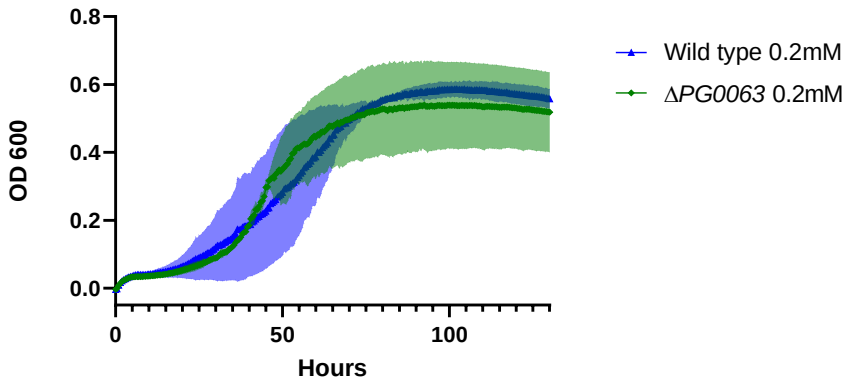

Figure 6.2.14 Zinc metal sensitivity of Δ*PGN2012* in comparison to wild type *P. gingivalis* at 0.2 mM. Overnight cultures of Δ*PGN2012* and wild type *P. gingivalis* were normalised to OD_{600} 0.1, pelleted, and resuspended in a range of zinc chloride supplemented BHI. The samples were incubated anaerobically at 37°C for 140 hours, with the OD600 being measured every 30 minutes by a Cerillo stratus plate reader. N=3 with 3 technical repeats to each biological repeat with shaded areas representing +/- SEM made in Graphpad prism. Statistical analysis was performed by T-test in (A) and multiple comparisons ANOVA in (B). P<0.05*.

6.2.8.2 Cobalt sensitivity of ΔPGN2012 and wild type P. gingivalis

To investigate cobalt sensitivity a range of cobalt chloride supplemented BHI was used between the concentrations of 1 mM to 10 mM. Figure 6.2.15A shows the full range investigated and the growth at the 3 day point, where a change can be seen in the average growth between wild type and Δ*PGN2012* at 2 mM cobalt chloride. At 3 days and in 2 mM cobalt chloride the wild type growth is 24% and Δ*PGN2012* is 10% the growth of the untreated samples. This concentration was then plotted as a growth curve seen in figure 6.2.15B. The growth curve shows a clear and statistically significant reduction in growth in Δ*PGN2012* from the 84.5 hour to the 119.5 hour time point in comparison to the wild type, where the wild type has a mean generation time of 21.5 hours while Δ*PGN2012* shows no real growth until 105 hours where a mean generation time of 21.6 hours is achieved. The exponential growth was still significantly slower in Δ*PGN2012* at 1 mM (Figure 6.2.16, $P<0.05$) with a generation time of 11.3 hours in comparison to the wild types 4.6 hours. However, Δ*PGN2012* can reach a stationary growth OD_{600} of 0.616 in 1 mM $CoCl_2$ showing a relatively high end point of growth. These data indicate an increased sensitivity to cobalt in Δ*PGN2012.*

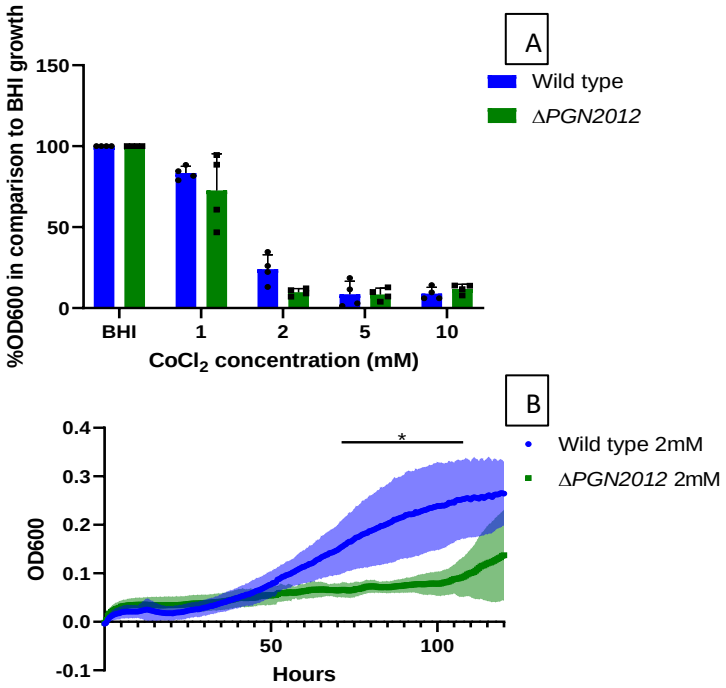

Figure 6.2.15 Cobalt metal sensitivity of Δ*PGN2012* in comparison to wild type *P. gingivalis*. Overnight cultures of Δ*PGN2012* and wild type *P. gingivalis* were normalised to OD_{600} 0.1, pelleted, and resuspended in a range of cobalt chloride supplemented BHI. The samples were incubated anaerobically at 37°C for 120 hours, with the OD600 being measured every 30 minutes by a Cerillo stratus plate reader. (A) OD_{600} values were taken at the 3 day point and normalised as a percentage of the growth of either wild type or Δ*PGN2012* in BHI to account for differences in growth between wild type and the mutant, the full range of cobalt chloride concentrations is shown, and the point of sensitivity was then chosen to be shown as a growth curve. (B) A growth curve was plotted from using the concentration that indicated a difference in sensitivity between the wild type and Δ*PGN2012*. N=4 with 3 technical repeats to each biological repeat with shaded areas representing +/- SEM created with Graphpad prism. Statistical analysis was performed by T-test in (A) and multiple comparisons ANOVA in (B). P<0.05*.

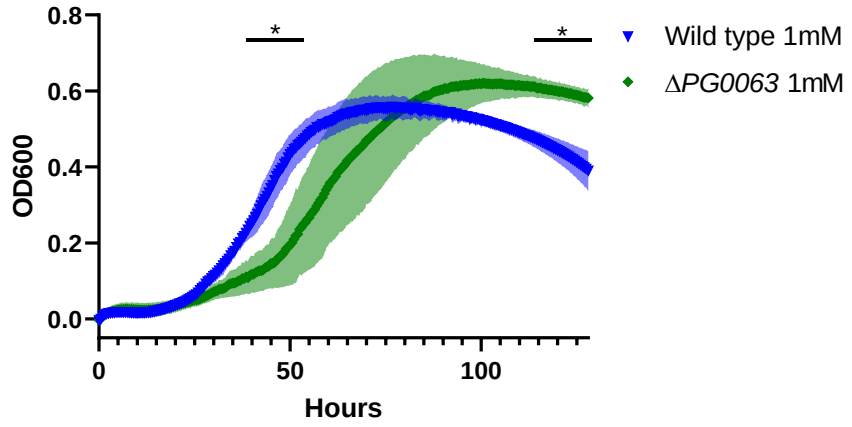

Figure 6.2.16 Cobalt metal (1 mM) sensitivity of Δ*PGN2012* in comparison to wild type *P. gingivalis*. Overnight cultures of Δ*PGN2012* and wild type *P. gingivalis* were normalised to OD_{600} 0.1, pelleted, and resuspended in cobalt chloride supplemented BHI (1 mM). The samples were incubated anaerobically at 37°C for 120 hours, with the OD600 being measured every 30 minutes by a Cerillo stratus plate reader. N=4 with 3 technical repeats to each biological repeat with shaded areas representing +/- SEM, created with Graphpad prism. Statistical analysis was performed by T-test in (A) and multiple comparisons ANOVA in (B). P<0.05*.

6.2.8.3 Cadmium sensitivity of ΔPGN2012 and wild type P. gingivalis

To investigate the cadmium sensitivity of Δ*PGN2012* a range of cadmium chloride concentrations were used in supplemented BHI, from a range of 0.05 mM to 2 mM. Figure 6.2.17A shows the differences in growth at the 3 day point of all the concentrations used. From this figure a decrease can be seen in the growth of Δ*PGN2012* in comparison to the wild type from 0.05 mM, however the only difference that is significant is at 0.1 mM. At 0.1 mM at the 3 day point the average growth for the wild type was 56% of untreated cultures whereas *ΔPGN2012* was 12.6%. Therefore, a growth curve was plotted from the 0.1 mM samples as can be seen in Figure 6.2.17B. Figure 6.2.17B shows a clear and statistically significant reduction in growth of Δ*PGN2012* in comparison to the wild type from the 51.5 hour time point onwards. Where the wild type had a mean generation time of 9.5 hours, *ΔPGN2012* had a mean generation time of 64.7 hours. The final OD_{600} were also significantly different with the wild type reaching 0.36 whilst *ΔPGN2012* only reached 0.135. A difference in mean growth rate is also observed in the 0.05mM growth curve (Figure 6.2.18), with the wild type generation time of 7.95 hours and Δ*PGN2012* being 17.5 hours. However, the SEM variation makes this difference not statistically significant. This data shows a clear increase in sensitivity to cadmium metal ions in Δ*PGN2012*.

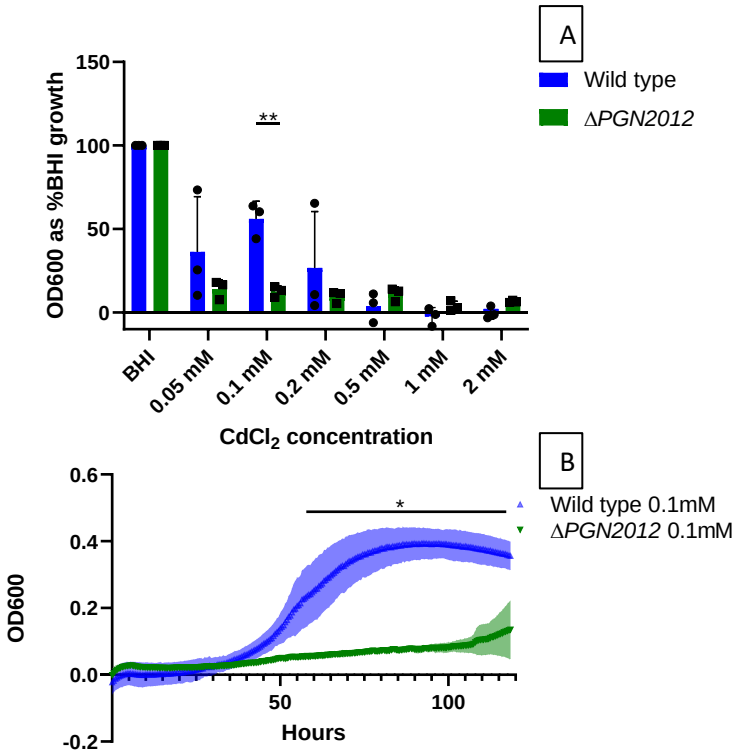

Figure 6.2.17 Cadmium metal sensitivity of Δ*PGN2012* in comparison to wild type *P. gingivalis*. Overnight cultures of Δ*PGN2012* and wild type *P. gingivalis* were normalised to OD_{600} 0.1, pelleted, and resuspended in a range of cadmium chloride supplemented BHI. The samples were incubated anaerobically at 37°C for 120 hours, with the OD_{600} being measured every 30 minutes by a Cerillo stratus plate reader. (A) OD_{600} values were taken at the 3 day point and normalised as a percentage of the growth of either wild type or Δ*PGN2012* in BHI to account for differences in growth between wild type and the mutant, the full range of cadmium chloride concentrations is shown, and the point of sensitivity was then chosen to be shown as a growth curve. (B) A growth curve was plotted from using the concentration that indicated a difference in sensitivity between the wild type and Δ*PGN2012*. N=3 with 3 technical repeats to each biological repeat with shaded areas representing +/- SEM. Statistical analysis was performed by T-test in (A) and multiple comparisons ANOVA in (B). P<0.05*.

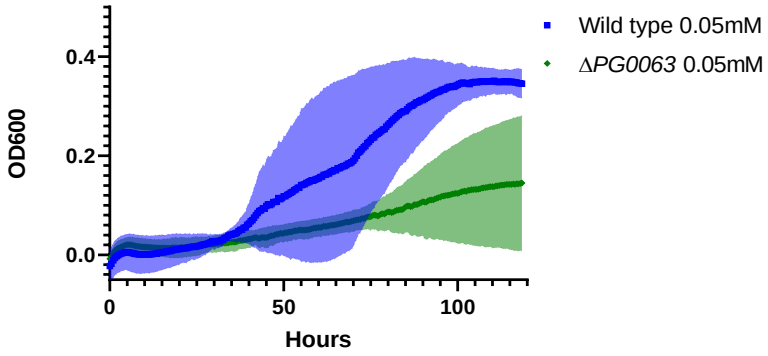

Figure 6.2.18 Cadmium metal (0.05 mM) sensitivity of Δ*PGN2012* in comparison to wild type *P. gingivalis*. Overnight cultures of Δ*PGN2012* and wild type *P. gingivalis* were normalised to OD_{600} 0.1, pelleted, and resuspended in cadmium chloride supplemented BHI (0.05 mM). The samples were incubated anaerobically at 37°C for 120 hours, with the OD_{600} being measured every 30 minutes by a Cerillo stratus plate reader. N=3 with 3 technical repeats to each biological repeat with shaded areas representing +/- SEM. Statistical analysis was performed by T-test in (A) and multiple comparisons ANOVA in (B). P<0.05*.

6.2.8.4 Copper sensitivity of ΔPGN2012 and wild type P. gingivalis

So far, the results of the metal sensitivity assays indicate that *PGN2012* is involved in Zn^{2+}, Co^{2+}, Cd^{2+} resistance pointing to *PGN2013* having a role more closely related to CzcA. As *PGN2013* is predicted to be similar to CusA we investigated the copper sensitivity of *ΔPGN2012.* To investigate the copper sensitivity of Δ*PGN2012* and wild type *P. gingivalis,* a range of copper chloride supplemented in BHI was used between 0.1 mM and 1 mM. Figure 6.2.19A shows the different growths at all of the ranges used at the 3 day time point. In this figure there is no significant changes between the growth of Δ*PGN2012* and the wild type. The greatest difference is at 0.2 mM where the wild type had a growth of 26% whilst *ΔPGN2012* had a growth of 11% in comparison to untreated growth, however there was too much variance to be significant. Therefore, this concentration was used to generate the growth curve seen in figure 6.2.19B. The growth curve further evidences the lack of change to the growth between Δ*PGN2012* and wild type *P. gingivalis*. This data suggests that there is no change in sensitivity to copper in Δ*PGN2012*. As no changes were seen here, we can conclude that Δ*PGN2012* does not have a greater sensitivity to copper nor chloride ions in comparison to the wild type. This is important as previous experiments were performed with metal chloride salts, this experiment excludes the effect of chloride as a factor in the increased sensitivity seen in Δ*PGN2012* to the other metals.

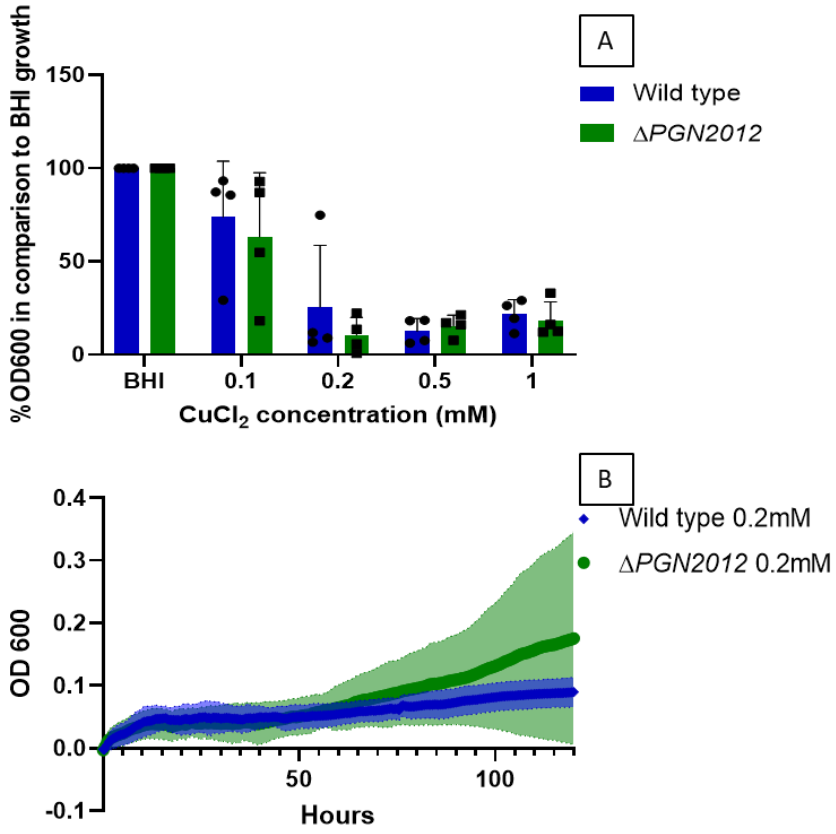

Figure 6.2.19 Copper metal sensitivity of Δ*PGN2012* in comparison to wild type *P. gingivalis*. Overnight cultures of Δ*PGN2012* and wild type *P. gingivalis* were normalised to OD600 0.1, pelleted, and resuspended in a range of copper chloride supplemented BHI. The samples were incubated anaerobically at 37°C for 120 hours, with the OD_{600} being measured every 30 minutes by a Cerillo stratus plate reader. (A) OD600 values were taken at the 3 day point and normalised as a percentage of the growth of either wild type or Δ*PGN2012* in BHI to account for differences in growth between wild type and the mutant, the full range of copper chloride concentrations is shown, and the point of sensitivity was then chosen to be shown as a growth curve. (B) A growth curve was plotted from using the concentration that indicated a difference in sensitivity between the wild type and Δ*PGN2012*. N=4 with 3 technical repeats to each biological repeat with shaded areas representing +/- SEM. Statistical analysis was performed by T-test in (A) and multiple comparisons ANOVA in (B). P<0.05*.

The data from these metal sensitivity experiments suggest that the knockout mutation of *PGN2012* has disrupted the efflux capabilities of the mutant and resulted in an increased sensitivity to Zn^{2+}, Co^{2+} and Cd^{2+} but not Cu^{2+}. This also indicates that *PGN2013* has a role more like CzcA than CusA. This data also shows that the role of *PGN2012* is not made redundant by the other TolC channel proteins present in *P. gingivalis* and is a key mechanism in the heavy metal resistance of *P. gingivalis*. It was also planned to investigate the sensitivity of nickel chloride to see if there is similarity in resistance of *PGN2012* to that of another HME-RND system Cnr, however due to time constraints brought on by the coronavirus pandemic this work was not completed.

6.2.9 *PGN2012* knockout mutation on reveals no changes in sensitivity to select antibiotics

As RND efflux systems are well documented for their role in multidrug resistance, it is important to investigate the role of *PGN2012* in antibiotic resistance. Previous work by Inoue *et al* (2015) investigated the knockout of *PGN2014* and its effect on antibiotic resistance to tetracycline, ampicillin, rifampicin and norfloxacin showing only a small difference in sensitivity to tetracycline dropping from 0.24 μg/ml in the wild type to 0.12 μg/ml in the *PGN2014* mutant. To investigate the role of *PGN2012* in antibiotic resistance antibiotic resistance, E-test strips were used to gain a general overview. Briefly, overnight cultures of *P. gingivalis* were grown and normalised to an OD_{600} of 0.2 before being spread onto a FA blood agar plate. Once dry an antibiotic ETEST strip was placed in the middle of the plate. The plate was incubated at 37^{o}C in anaerobic conditions for one week. The antibiotics chosen were ampicillin, amoxicillin, metronidazole, and vancomycin. Ampicillin and amoxicillin are penicillin derivatives which disrupt the cell wall of the bacteria, whilst metronidazole inhibits protein translation through DNA disruption. Vancomycin also disrupts bacterial cell walls but is often too large of a molecule to penetrate the outer membrane of Gram negative bacteria making it a good negative control. The range of antibiotic concentrations were between 256 and 0.016 μg/ml.

Figure 6.2.20 shows the results from the antibiotic strips used. All strips showed no changes between wild type and Δ*PGN2012 P. gingivalis*. Metronidazole had the greatest antibiotic effect with both wild type and Δ*PGN2012* being forced below the lowest concentration of 0.16 μg/ml. Ampicillin and amoxicillin had similar effects on both wild type and Δ*PGN2012* with both bacteria only growing at the bottom of 0.16 μg/ml. Whereas vancomycin had predictably the least effect on both wild type and Δ*PGN2012* with both bacteria growing up to 2 μg/ml. Therefore, these initial results suggest that the knockout of *PGN2012* has not majorly affected antibiotic resistance in Δ*PGN2012*. However, as these are broad range strips the accuracy is limited and would need to be further probed by MIC experiments like the metal salt MIC's seen above. Although this was planned, there was not enough time because of lack of lab access due to the coronavirus pandemic.

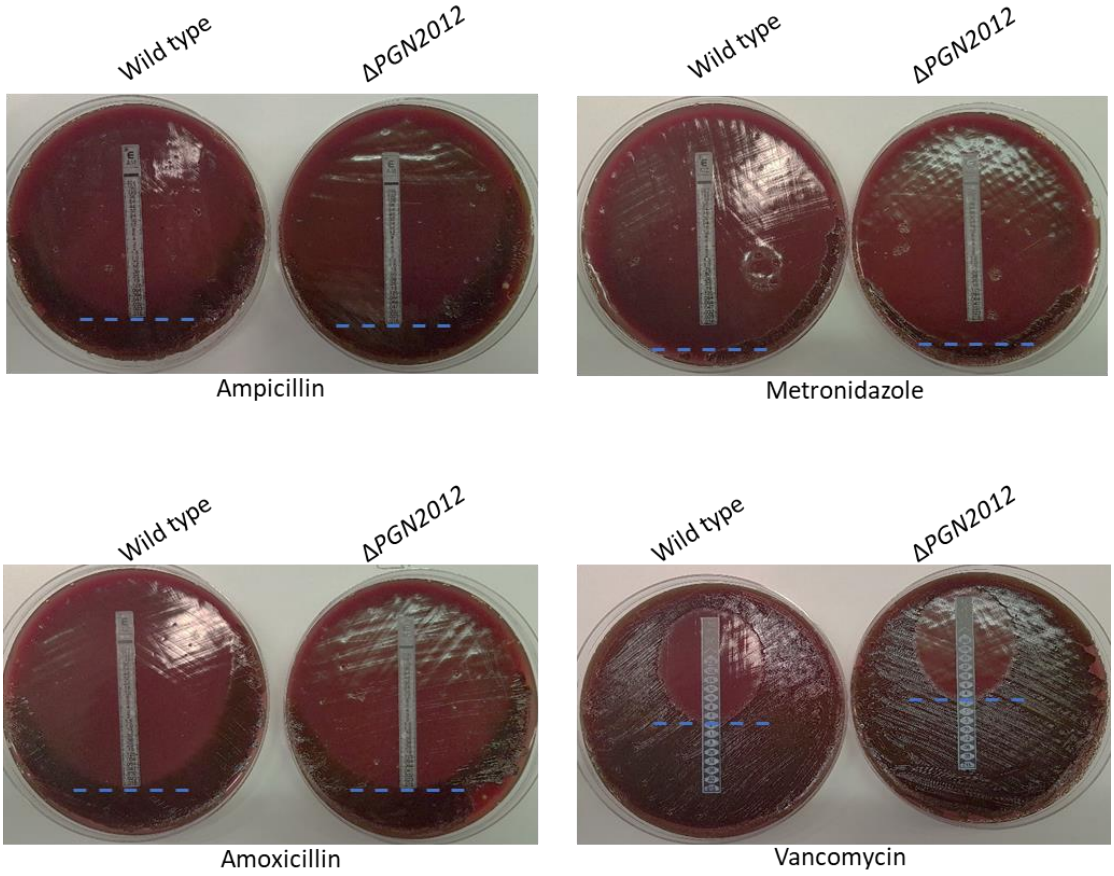

Figure 6.2.20 The effect of antibiotic ETEST strips on wild type *P. gingivalis* and Δ*PGN2012*. Wild type and Δ*PGN2012* overnight cultures were grown and normalised to OD_{600} 0.2 before being spread onto a FA blood agar plate. Once dry an ETEST antibiotic strip was placed onto the inoculated agar plate before being incubated at 37°C in anaerobic conditions for one week. Images were then taken of the growth and the halo indicating the point at which antibiotic susceptibility begins, shown by the blue dotted lines.

Initial work on oxidative stress was started to investigate whether knocking out *PGN2012* resulted in increased sensitivity to oxidation.

6.2.10 Initial investigation in the role of *PGN2012* in oxidative stress.

The role of HME-RND is the removal of hazardous heavy metal ions from inside the bacteria. One of the reasons it is beneficial to do this is that active metal ions such as Zn^{2+} can create oxygen free radicals which actively disrupt bacteria membranes, proteins and DNA resulting in death (Ezraty *et al.*, 2017). Therefore, we investigated the role of *PGN2012* in oxidative stress resistance using hydrogen peroxide as an active oxidiser. To do this, overnight cultures of wild type and Δ*PGN2012 P. gingivalis* prepared and normalised to OD_{600} 0.1. Samples were incubated in triplicate with BHI supplemented with H_2O_2 at a final concentration of 0.1 mM for 5 minutes before being serially diluted and spotted onto FA blood agar plates following

the Miles and Misra technique (Miles, Misra and Irwin, 1938). The plates were incubated at 37°C anaerobically for one week or until colonies could be counted. Colonies were counted and plotted as a percentage of the untreated wild type or Δ*PGN2012* respectively to account for differences in overall viability between the mutant and wild type.

Figure 6.2.21 shows preliminary results of a single biological experiment. The results indicate a greater effect on viability from oxidative stress in Δ*PGN2012* at 7% than in wild type *P. gingivalis* at 31%. However, it is important to note that this is only a single experiment with a large amount of variation. Therefore, further experiments would need to be conducted to be able to be confident in the changes seen and support the data statistically. The experiment took multiple attempts to optimise and unfortunately due to Covid time restraints, multiple optimised experiments were not able to be conducted.

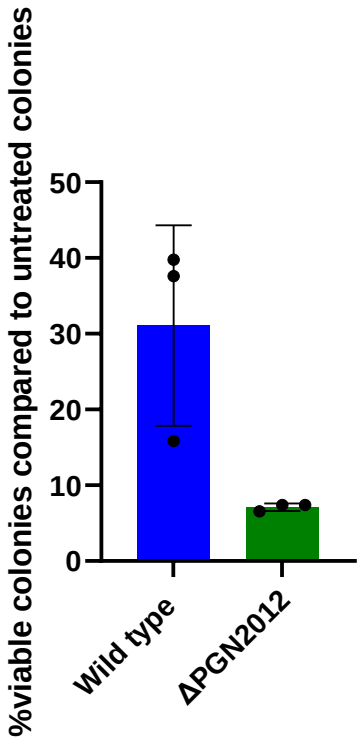

Figure 6.2.21 Oxidative stress resistance of wild type and ΔPGN2012 *P. gingivalis.* Overnight cultures of *P. gingivalis* were prepared and normalised to OD_{600} 0.1 before being incubated in BHI supplemented with 1 mM H_2O_2 at room temperature for 5 minutes. Samples were serially diluted and 10 µl dropped onto FA blood agar plates. The plates were incubated anaerobically for one week or until colonies could be counted. Colonies of treated samples were counted and shown as a percentage of untreated viable colonies. N=1 with three triplicates, error bars show +/- SD.

6.3 Chapter 6 discussion of results

Gram negative bacterial infections are often more difficult to treat than Gram positive infections due to a greater resistance to antibiotics. Partly due to the outer membranes' natural barrier to permeability, but also because of the presence of RND efflux pumps (Venter *et al.*, 2015). However, these RND efflux pumps are not limited to only transporting antibiotics. They have also been shown to transport multiple substrate types out of the bacterial cell into the environment such as bile salts in *E. coli's* well studied AcrAB efflux pump (Rosenberg *et al.*, 2003), quorum sensing ligands in *Burkholderia pseudomallei* (Ying *et al.*, 2007) and heavy metals in the case of CusA and CzcA (Mergeay *et al.*, 1985; Franke *et al.*, 2003). This efflux of hazardous toxins not only make the bacteria difficult to treat but also make them have a greater survivability in the niches they inhabit. Notably, export systems utilising TolC but alternative inner membrane transporters and adaptors are also able to secrete large protein substrates such as Haemolysin toxins (E.coli and others (Lenders *et al.*, 2015)) and entire enzymes like lipases in a range of bacteria (Duong *et al.*, 1994) indicating the adaptability of TolC based systems.

The focus of the experimental work in this chapter is *PGN2012,* a gene that encodes for a TolC like membrane channel protein that was predicted to be part of a tripartite CusA/CzcA like RND efflux pump system. The most researched TolC proteins are that of *E. coli* and *Pseudomonas* species. The importance of TolC in enterobacteria such as *E. coli* is uniquely significant as their genome only has one copy of TolC that has been shown to function as the channel membrane in multiple membrane transport systems. These transport systems consist of RND efflux pumps such as AcrAB (Du *et al.*, 2014) , major facilitator superfamily (MFP) (Lomovskaya, Lewis and Matin, 1995) and ATP binding cassette (ABC) transport such as hemolysin secretion (Kanonenberg, Smits and Schmitt, 2019). Whereas several other Gram negative bacteria have multiple TolC proteins that seem to be involved in specific export functions, for example *P. aeruginosa* which has 18 putative TolC like outer membrane efflux proteins (Jo, Brinkman and Hancock, 2003). Even though TolC like channel efflux proteins are ubiquitous in Gram negative bacteria, there is great variance between protein sequences with only two small coiled coil motifs being conserved (Johnson and Church, 1999), however structurally they are all predicted and modelled to form a trimeric channel that sits in the outer membrane and traverses the periplasm. This was the case for *PGN2012* as pfam

searches of protein alignment found two distinct regions with great similarity to other outer membrane efflux proteins, however when compared to TolC from *E. coli* there were only 9 matching amino acid sequences (Figure 6.3.1).

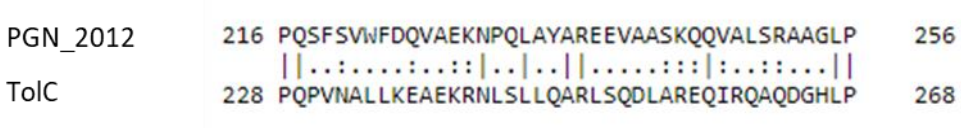

Figure 6.3.1 Protein sequence alignment of *PGN2012* from *P. gingivalis* and TolC from *E. coli*. *PGN2012* from *P. gingivalis* ATCC 33277 and TolC from *E. coli* K12 protein sequences were aligned using the EMBOSS matcher pairwise sequence alignment (EMBL-EBI).

Through Pfam scanning we discovered that there were 7 TolC like channel proteins in the genome of *P. gingivalis*. Of the 7 TolC channel proteins, 4 appear to be involved with ABC transport systems (Figure 6.2.1, PGN_0449, PGN_0715, PGN_1680 and PGN_2038) with two of these operons (Figure 6.2.1, PGN_1680 and PGN_2040) containing HlyD like fusion proteins. ABC transport systems can transport multiple types of substrates across the periplasmic and outer membrane using ATP as an energy source (Rees, Johnson and Lewinson, 2009). As PGN_1680 and PGN_2040 are both HlyD like periplasmic membrane fusion proteins, it is possible that the role of the operons they belong to is the transport of proteins such as haemolysin in the HlyABCD system (Lenders *et al.*, 2015). However, the other 3 operons found (Figure 6.2.1, PGN_1432, PGN_1539, PGN_2012) were more similar to RND specific transporters, containing the features of an RND efflux pump, MFP and TolC like channel protein. *PGN2013* is the only periplasmic protein with a predicted substrate, which was predicted to be like CusA/CzcA indicating a role in metal efflux like that found in those systems. The role of PGN_1432 may be linked to the removal of excess hemin to prevent toxicity, as a study by Veith et al (2018) found the PGN_1432 operon (PG0538 in their paper) to be overexpressed in excessive hemin conditions. The presence of multiple TolC genes in the genome of *P. gingivalis* each with their own efflux operon therefore points to a more specific role of each TolC like that seen in *P. aeruginosa* than the multiple roles seen in Enterobacteria.

The specific role of these TolC channel proteins have yet to be identified. A study by Ikeda and Yoshimura (2002) investigated the operon containing PGN_1430-1432 (named XepCAB

in the paper) by knocking out each gene in the operon separately to investigate the differences in sensitivity to multiple agents. Their results showed that each knockout mutant effected the sensitivity to multiple antibiotics and ethidium bromide. Furthermore, 6 of the 7 operons mentioned in our study have been investigated previously by Inoue *et al* (2015). In their study knockout mutants of the MFP gene from each of the operons in figure 6.2.1 except PGN_2038 operon was generated. The MICs of the knockout mutants were determined, and all the mutants had a 2-fold increase in sensitivity to tetracycline. However, only two of the mutants (Δ*PGN1431* and Δ*PGN1680*) showed an increased sensitivity to ampicillin, rifampicin and norfloxacin. This data indicates that only two of *P. gingivalis'* seven TolC efflux systems have been shown to have an effect on antibiotic resistance. However, this antibiotic resistance is likely due to substrate promiscuity rather than specificity to the antibiotics due to their previously mentioned upregulation in the presence of hemin.

PGN2012 was shown by Suwannakul *et al* (2010) to be upregulated by 6.3 fold in a hyperinvasive subpopulation, indicating a role in the invasive capabilities of *P. gingivalis*. However, the role of *PGN2012* in virulence, host pathogen interactions and heavy metal efflux was not researched until this study.

The knockout mutagenesis of *PGN2012* was successfully performed using the natural competency method previously described and well optimised in the study by Naylor (2017), which was adapted from the original study that used natural competency by Tribble *et al* (2012). The benefits of this methodology in comparison to other transformation methodologies such as electroporation are mainly in oxygen exposure time but also equipment requirements. Although multiple attempts were required for successful mutation, there was multiple Δ*PGN2012* mutants made and stored. PCR confirmation of this mutation showed that the erythromycin had been correctly incorporated into the chromosomal DNA by homologous recombination. Further evidence through nanopore genomic sequencing provided greater confidence showing a clean knockout in the correct orientation and position.

Once the mutation was proven successful, initial characterisation of Δ*PGN2012* begun. On an FAB plate the mutant grew with the same colony morphology as the wild type, accumulating a black pigment over the same time scale. However, during the growth curve experiments it was observed that the growth of Δ*PGN2012* was slightly slower than the wild type during the

exponential phase. Although this change is minor, there is evidence in the literature from other bacteria that suggest efflux pumps can play a role in the detoxification of bacteria through the efflux of metabolic substrates during growth. In a study by Aedekerk *et al* (2005) mutants of the MexGHI-OpmD efflux pump were made removing either the MexI efflux pump or the OpmD porin in *P. aeruginosa*. Both mutants resulted in stunted growth shown to be caused by the toxic accumulation of the metabolite anthranilate, which is a precursor to the *Pseudomonas* quinolone signalling (PQS) molecule. Therefore, there is a potential that *PGN2012* may also have a role in the efflux of toxic metabolites during growth, giving the bacteria a slower growth.

The biofilm formation of Δ*PGN2012* was investigated and showed no changes in comparison to the wild type. The role of efflux pumps and biofilm formation is a point of interest in the literature. There is evidence showing that bacteria in biofilms have greater expression of efflux pumps than in planktonic samples (Schembri, Kjærgaard and Klemm, 2003; Gillis *et al.*, 2005), and bacteria lacking efflux pumps have reduced biofilm formation (Matsumura *et al.*, 2011; Alav, Sutton and Rahman, 2018). There is also evidence of mechanistic roles in the export of quorum sensing molecules in *P. aeruginosa* (Pearson, Van Delden and Iglewski, 1999). Therefore, it was important to investigate the role of Δ*PGN2012* in biofilm formation, however no changes were observed indicating that this efflux system is not essential for biofilm formation under our growth conditions. As *PGN2012* has been shown to effect sensitivity to Zn^{2+}, Cd^{2+} and Co^{2+} ions it would be important to investigate its role in the biofilm growth in the presence of increased metal concentration. Further experimentation using growth media supplemented with metal ions slightly lower than identified MICs would give a greater indication for the role of *PGN2012* in the growth of biofilms in environments with higher metal concentrations.

Further characterisation was performed by looking at the protein profile of Δ*PGN2012* to investigate if the knockout had influenced the presence of any other major proteins. It was observed that there were no changes. As *PGN2012* is responsible for a membrane protein, the knockout could have potentially disrupted the membrane and the major proteins found there such as OmpA and the gingipains. Therefore, it was important to have an initial look at any potential changes in the proteins of Δ*PGN2012*.

As gingipains are major virulence factors and responsible for the nutrition and growth of *P. gingivalis* (Guo, K.-A. Nguyen and Potempa, 2010) the proteolytic activity of both arginine and lysine gingipains were investigated. In the case of both types of gingipains the activity was unaltered between Δ*PGN2012*. This was not surprising as the colonies of Δ*PGN2012* had no change in pigment, whereas *P. gingivalis* with disrupted gingipains are often pale as the lysine gingipain dependent accumulation of protoporphyrin IX on the cell surface is not present (Smalley *et al.*, 2004). Therefore, this further evidences that the growth issues seen in section 6.2.2 are not due to issues with gingipain related nutrient acquisition, and has a higher likelihood to be related to issues with efflux.

The overexpression of *PGN2012* in hyperinvasive sub-populations of *P. gingivalis* indicates a role for *PGN2012* in host invasion (S. Suwannakul *et al.*, 2010). The results from the antibiotic protection assays show that there was no change in overall association, adhesion, or invasion. However, this experimental procedure focuses more on adhesion and invasion than intracellular survivability. The experiment itself is indeed a viability experiment looking at the number of bacteria that survive at each stage. However, the experiment is designed to be as quick as possible as to not allow the bacteria to be exposed to oxygen for long periods of time. Therefore, giving us a snapshot of how many bacteria can bind to host cells and how many can initially invade host cells. As *PGN2012* was overexpressed in hyper-invasive *P. gingivalis* but did not have any effect on the binding or invading the cells, this leads us to believe it may have a role in intracellular survivability.

Much like how RND systems become more highly expressed in biofilms to provide a greater survivability, this may also be the case as a response to the intracellular environment. To investigate this in the future, long term invasion experiments could be performed allowing the invasion step to continue for longer time periods and surviving bacteria could be isolated and counted to see if intracellular survival has been affected by the knockout of *PGN2012*.

Another experiment we planned to complete was to investigate macrophage killing of Δ*PGN2012* in comparison to the wild type. One of the greatest trials to bacteria during infection is to resist the immune systems responses. During infection bacteria can be taken intracellularly into the phagosome organelle of phagocytes such as macrophages (Thakur, Mikkelsen and Jungersen, 2019). During phagocytosis, the bacteria will be exposed to many

toxins which can prove fatal such as reactive oxygen species, and enzymes such as lysozymes and proteases. The increased expression of *PGN2012* after invasion may indicate a role in the resistance to these strategies by this gene. To investigate the effect of macrophage killing on Δ*PGN2012* we planned to use a similar methodology to that of Nagl *et al* (2002), in which opsonised bacteria would be internalised by macrophages before isolating internalised bacteria and counting how many viable bacteria would survive over a period of time. Unfortunately, these follow up experiments to further investigate the roll of *PGN2012* in intracellular survivability were unable to be completed due to time constraints from the Covid-19 pandemic. The data does suggest however that PGN2012 does not have a role in the mechanism of adhesion and invasion by *P. gingivalis.*

The results from the metal salt MIC's provided us with useful data which evidences the role of *PGN2012* as a TolC protein in HME-RND efflux. There were significant reductions in overall growth and growth rate in both the Zn^{2+} and Cd^{2+} experiments for Δ*PGN2012*, as well as a reduction in growth rate for Co^{2+} indicating an increased sensitivity to these ions. The most sensitivity coming from Zn^{2+} and Cd^{2+} with sensitivities of 0.5 mM and 0.1 mM respectively. Whereas the sensitivity to cobalt was only seen at the higher concentration of 2 mM, indicating a greater sensitivity to zinc and cadmium than cobalt. In contrast to this, the initial studies of CzcCBA by Mergeay *et al* (1985) found that for *R. metallidurans* the resistance provided by the two plasmids containing CzcCBA and Cnr were highest for zinc and cobalt, with cadmium having the least resistance. This may be due to the enzyme kinetics of transport for each ion as a study by Goldberg *et al* (1999) investigated the activity of recombinant CzcA against each ion. In their study it was found that Zinc has the greatest V_{max} of 350 followed by cobalt at 100 and cadmium at 28. This increase in metal sensitivity of Δ*PGN2012* was not seen for copper as no changes occurred between the mutant and wild type. No differences seen in the copper chloride experiments provide evidence that the differences seen in the other metals were due to the metal ions and not the chloride ions. It was also planned to investigate the knockout mutations effect on nickel sensitivity, as the Cnr system is also involved with cobalt resistance, however we could not do this due to time restrains from the covid-19 pandemic.

Although known intracellular and plaque concentrations of all the metals tested are not fully known there has been previous work in the literature to investigate the concentration of zinc

in dental plaque. In an early study by Afseth (1983), they investigated the concentration of zinc and copper retained by dental plaque after mineral washes. The authors mention that before any treatment the base zinc concentration is 55 ppm (0.841 mM), indicating that our concentration range of zinc chloride is relevant to that found in dental plaque. This is further supported by Lynch (2011), who discuss multiple studies that also provide zinc concentrations in plaque with concentrations ranging between 7.86 ppm and 40 ppm (0.12 mM - 0.61 mM). Indicating our experimental range for Zinc is realistic to that seen in dental plaque.

As RND efflux pumps can be promiscuous in their substrates (Wong *et al.*, 2014) we also investigated the effect of knocking out *PGN2012* on the antibiotic resistance to commonly used antibiotics in periodontal treatment. Due to time constraints, we were only able to initially screen this with the use of antibiotic E-test strips for four antibiotics. Our data shows that there is no increase in sensitivity to any of the antibiotics used after the knockout of *PGN2012*. However, E-test strips are not very accurate, especially towards the lower end of the concentrations and are often used to see major differences. Better experiments could be performed to be check for subtle differences with higher accuracy. To do this, MIC experiments similar to the metal MIC's could be conducted with different concentrations of antibiotics, specifically focussed around known MIC's in the literature and our E-test data.

Metal ions can become toxic to bacteria in high quantities due to their ability to produce oxygen free radicals (Phaniendra, Jestadi and Periyasamy, 2015). Therefore, we planned to investigate whether *PGN2012* had a role in oxidative stress resistance outside of the removal of metal ions. Our preliminary data suggest that the loss of *PGN2012* has resulted in an increased sensitivity to oxidative stress. However, this experiment was only performed once and would need to be repeated multiple times for statistical significance before we could conclude this as being correct. There is evidence from other bacteria that RND efflux pumps can be induced by oxidative stress and reduce the effects. Expression of AcrAB in *E. coli* has been shown by White *et al* (1997) to be increased when SoxS is overexpressed in response to oxidative stress. The SoxRS oxidative stress response has also been shown to promote expression of AcrAB in other Enterobacteria such as *Klebsiella pnuemonieae* (Bratu *et al.*, 2009). This overexpression of RND in response to oxidative stress is not unique to single TolC Enterobacteria. A study by Fraud and Poole (2011) showed that PA5471, a gene overexpressed in oxidative stress conditions can induce MexXY RND efflux in *P. aeruginosa*.

In a study by Wu *et al* (2018) the expression of three genes from the SmeVWX RND transporter in *Stenotrophomonas maltophilia* increased between 5.6 to 12.4 fold in response to hydrogen peroxide treatment. In the same report they also show that overexpressing the SmeVWX operon increased resistance to menadione ROS killing but not hydrogen peroxide. Therefore, there is potential of *PGN2012* to have a role in oxidative stress resistance however more experiments would need to be completed before being confident in this.

Suwannakul *et al* (2010) have shown that *PGN2012* is overexpressed in invasion, however knowing what specifically induced this change would give a greater understanding of the role of *PGN2012*. Understanding the regulation of *PGN2012* is an important step in elucidating the genes' role in virulence. Our data suggests that *PGN2012* operon is like that of CzcCBA, with similar metal resistance. CzcCBA in *R. metallidurans* is regulated by CzcD and CzcR and has been shown to be expressed in response to Zn, Cd, Co, Cu, Ni, Hg, and Mn divalent cations (Nies, 1992). There are multiple expression experiments that could be completed in the future to investigate the regulation of *PGN2012* through quantitative real time PCR. The first factor to investigate would be Zn^{2+}, $Cd2^{+}$ and Co^{2+} induction through prolonged exposure to metal salts and analysing the expression of all three genes in the operon (*PGN2012-2014*) in comparison to an untreated control. This could also be done for oxidative stress through hydrogen peroxide treatment before QPCR. We also know for sure that at some point during invasion *PGN2012* becomes overexpressed, whether the cause is the expression of the other genes in the overexpressed gene set or if it is exposure to the intracellular environment is unknown. A potential experiment to see if it is exposure to the intracellular environment would be to do a time point intracellular survival assay. Conducting QPCR on bacteria at different time points within internalisation to see if the expression changes over time inside the host cells.

6.4 Summary

A *PGN2012* mutant was successfully produced and displayed changes in metal ion sensitivity. The sensitivity towards Zn^{2+}, Co^{2+} and Cd^{2+} but not Cu^{2+} suggests that *PGN2012* is involved in a CzcCBA like HME-RND transport system and not CusCBA. Although the regulation of this

gene is still unknown, our data suggests that *PGN2012* has a role in the survival of *P. gingivalis* and not the mechanism of cellular invasion.

Chapter 7. Final discussion and future prospects

7.1 Summary of major findings

The work of this study has provided a better understanding of three virulence genes of *P. gingivalis* through their characterisation and virulence assessment, whilst also investigating method optimisation for the receptor pulldown of the OmpA loop peptide 4 of *P. gingivalis*.

Previous work from our lab group by Suwannakul *et al* (2010), showed that *P. gingivalis* cultures had sub populations with a hyperinvasive phenotype. In this hyper-invasive subpopulation, there was a signature set of genes that were shown to be overexpressed, therefore indicating a potential role in the invasive capabilities of *P. gingivalis*. Carrying on from this work, Naylor *et al* (2017) investigated two of the overexpressed genes *ompA1* and *ompA2*, and found that the OmpA had a major effect on multiple virulence factors including adhesion and invasion of oral epithelial cells. Naylor *et al* went on to show that the four peptide loops on the outer surface of OmpA interacted with the surface of oral epithelial cells and were significant in their invasion by *P. gingivalis*.

The role of these peptide loops of OmpA in the adhesion and invasion of host cells is seen in other bacteria such as *E. coli* (Prasadarao *et al.*, 1996; Shin *et al.*, 2005). This interaction with host cells could be a potential therapeutic pathway if the receptors could be identified, this coupled with a greater understanding of *P. gingivalis* host-pathogen interactions is the rationale behind investigating these peptides.

The genes *ompH1*, *ompH2, rfbB* and *PGN2012* were all overexpressed in the hyperinvasive subpopulation identified by Suwannakul *et al* (2010) indicating potential roles in the host-pathogen interactions of *P. gingivalis.* Characterising these genes and their roles in host-pathogen interactions, provide a greater depth of understanding into the functions and mechanisms behind how *P. gingivalis* can survive in the niche of the oral cavity whilst infecting cells. The more we understand how the bacteria can interact with the host to cause disease, the better we can design treatments to prevent it.

Before the final discussion I have summarized the most important findings from each chapter of this thesis.

7.1.1 Chapter 3. Investigation into the human receptors of the *P. gingivalis* OmpA L4 loop peptide

The aim of this chapter was to attempt the isolation and identification of the receptor/s of the L4 peptide loop on the surface of the OmpA protein in *P. gingivalis*.

- Although multiple biotin-streptavidin pulldown assays were performed the receptors of the L4 peptide were not identified in this study. However, through optimisation we have seen that the L4 peptide potentially binds to multiple proteins on the surface of H357 cells through visible bands, however these were not able to be identified. The lack of bands at higher concentration could indicate that the affinity of the L4 peptide to its targets is weak, or that the target is not present in high quantities on the cell surface.

7.1.2 Chapter 4: Investigation of the role of the OmpH chaperone proteins

This chapter attempted to investigate the role of both skp like chaperon proteins of *P. gingivalis* through the knockout mutagenesis of Δ*ompH1* and Δ*ompH2*. After failing to produce Δ*ompH2* due to single crossover events, this gene was assumed to be essential and only Δ*ompH1* was characterised.

- Through knockout mutation through homologous recombination Δ*ompH1* was successfully produced. However, even with multiple attempts an *ompH2* knockout mutant was unable to be made. The single crossover event leading to the incorrect insertion of the erythromycin cassette into the genome of the *ompH2* mutant indicate that the *ompH2* gene is essential to the viability of *P. gingivalis.* This supports previous findings in the literature concluding that *ompH2* is essential (Taguchi *et al.*, 2015).
- Using anaerobic growth curves in supplemented BHI it was observed that Δ*ompH1* had a reduced growth rate in comparison to the wild type. However, the overall growth of Δ*ompH1* was not disrupted as there were no changes in final OD_{600} during the stationary phase.
- The role of *ompH1* in binding and invading oral epithelial cells was shown for the first time through antibiotic protection assays. The adhesion and invasion of H357 cells by Δ*ompH1* was significantly reduced in comparison to the wild type. This data indicates that the clients of *ompH1* are important for the adhesion and invasion of oral epithelial cells. This provides further evidence to support the reason for upregulation of these

genes in the hyper-invasive subpopulation of *P. gingivalis* found by Suwannakul *et al* (2010).

- Through proteolytic activity assays and western blot for arginine gingipains, we show a significant reduction in whole cell arginine gingipain presence and activity. In contrast to the literature (Taguchi *et al.*, 2015), we show that only the arginine gingipain has been disrupted and not the lysine gingipain. This data provides further evidence that *ompH1* is involved with the chaperoning of proteins involved with the type 9 secretion system.

7.1.3 Chapter 5. Characterisation of the *rfbB* gene in P. gingivalis virulence

rfbB is the dehydratase enzyme in the dTDP-rhamnose synthesis pathway involved in the production of the *P. gingivalis* O-antigen section of the Lipopolysaccharide. This chapter focused on the production and characterisation of a mutant in which *rfbB* has been disrupted. Despite multiple knockout mutagenesis attempts, a full knockout mutant was unable to be made. However, we show a mutant with multiple phenotypic changes which are indicated to be caused by the disruption of *rfbB,* probably via upstream polar effects of the erythromycin cassette insertion.

- Knockout mutagenesis of *rfbB* was attempted through homologous recombination mutagenesis techniques, however the gene was not replaced in the genomic DNA of the mutant. Through nanopore genomic sequencing it is suggested that the erythromycin has been integrated adjacent and upstream of *rfbB* (Figure 5.2.4), through a single crossover during homologous recombination. This indicates that like *ompH2*, *rfbB* is also essential for viability, this is also suggested in the literature (Shibata *et al.*, 1999). Unlike Δ*ompH2* in chapter 4, multiple phenotypic changes were observed in this *rfbB* mutant indicating the disruption of the *rfbB* gene expression potentially by gene expression effects due to polar effects.
- Using anaerobic growth curves in supplemented BHI, we observed that Δ*rfbB* had a significantly reduced growth rate, being slower to grow and reaching a lower final stationary growth. Also, we observed that the black pigment normally seen in *P. gingivalis* was changed to a creamy brown pigment on fastidious anaerobic agar plates supplemented with horse blood. This was the initial phenotypic change that prompted us to investigate this mutant further.

- Monoculture biofilm formation was assessed to investigate if *rfbB* had a role in production of biofilms on a surface, as this is an important virulence factor for oral bacteria that need to attach to the tooth surface and avoid saliva washing. Our results show that Δ*rfbB* had a significantly reduced biofilm formation which can be seen both quantitatively and qualitatively.
- The role of Δ*rfbB* was shown to be important in the adhesion and invasion of H357 oral epithelial cells using antibiotic protection assays. At least a 50% reduction was seen in both adhesion and invasion when compared to the wild type. This loss of adhesion and invasion is not seen when the O-antigen of *P. gingivalis* is absent (Soto *et al.*, 2016), indicating that *rfbB* has another role in *P. gingivalis* other than O-antigen production that is responsible for these changes.
- The presence and activity of gingipains were investigated in Δ*rfbB* by proteolytic activity assays and western blot. As suggested by the lack of black pigment, both types of gingipains have significantly reduced activity in Δ*rfbB* in comparison to the wild type. As rhamnose is not involved with the A-LPS that the gingipains are anchored too, this indicates that either the outer membrane has been disrupted or that rhamnose synthesis is involved in some way to the T9SS.
- As rhamnose is one of the major sugars in the O-antigen of *P. gingivalis* LPS, we investigated the LPS profile of Δ*rfbB*. Our data suggests that the LPS of Δ*rfbB* has become truncated, producing a higher quantity of lower weight bands whilst seeing a reduction in the amount of higher weight bands in comparison to the wild type. This change in LPS structure prompted us to investigate the effect of Δ*rfbB* LPS on the inflammatory response of human macrophages, although this was unchanged.

7.1.4 Chapter 6. Characterisation of the putative metal specific TolC family pump *PGN2012* in P. gingivalis virulence

PGN2012 is one of the 7 TolC proteins in *P. gingivalis*, it belongs to the operon of a resistance-nodulation-division (RND) with a putative CusA/CzcA efflux pump. *PGN2012* was overexpressed in the hyper invasive subpopulation of *P. gingivalis* indicating a role in the virulence of *P. gingivalis*. Therefore, in this chapter we produced a knockout mutant of *PGN2012* and characterised multiple virulence factors and the resistance of select heavy metals.

- The same type of homologous recombination mutagenesis that was used in the previous chapters was applied and successfully produced a knockout mutation of *PGN2012*. *ΔPGN2012* was confirmed through PCR and nanopore sequencing.
- The growth of Δ*PGN2012* was revealed to be slower in supplemented BHI in anaerobic conditions when compared to the wild type. Unlike the mutants of previous chapters, no disruption was seen to the gingipain activity of Δ*PGN2012* indicating this change in growth was specific to the role of the *PGN2012* operon.
- Unlike the other mutants produced of the overexpressed gene set in hyper invasive *P. gingivalis*, *PGN2012* had no significant effect on the adhesion and invasion to oral epithelial cells. The overexpression in the invasive subpopulation but no effect on adhesion and invasion indicates that the role of *PGN2012* is most likely intracellular survivability rather than the mechanism of invasion.
- Anaerobic growth experiments using BHI supplemented with a range of metal salt concentrations was used to investigate if the predicted role of *PGN2012* in metal resistance was correct. The operon to which *PGN2012* was suggested to be involved with heavy metal resistance, the prediction was a similar effect of CusA (copper)/CzcA (Zinc, cobalt, cadmium) therefore we investigated four metal divalent cations, Zn^{2+}, Co^{2+}, Cd^{2+} and Cu^{2+}. Our data has shown that *PGN2012* provides resistance to Zn^{2+}, Co^{2+}, Cd^{2+} but not Cu^{2+}. This suggests that *PGN2012-2014* is the CzcCBA homologue in *P. gingivalis*.

7.2 The potential to isolate the receptor/s of the L4 loop peptide

We have described the difficulty in isolating the unknown receptor/s of the L4 loop peptide from *P. gingivalis* OmpA. However, through the optimisation steps described in this thesis we have provided a better understanding of the further steps required to be successful in Identifying the receptor/s of the L4 peptide. Through multiple repeats of the biotin-streptavidin pulldown assays we eventually observed protein bands present in the L4 treated cells that were not present in the controls. However, due to the low protein abundance of these bands they were unable to be identified by mass spectrometry. These results suggest that either the L4 peptide receptor complex is weakly bound together, or that there are not high quantities of the receptor/s present. Although we attempted to trap the complex using

the 3,3'-Dithiobis(sulfosuccinimidylpropionate) (DTSSP) cross linker, this did not seem to be successful in our study. Continuing this method with a crosslinker with a smaller spacer arm, or one that is membrane soluble could potentially have more success as it is possible that the receptor is internalised upon binding. It would be interesting to perform a screening of crosslinkers to see which works the best via a western blot technique, using the L4 peptide as a primary antibody with different cross linkers to give a preliminary observation.

Alternatively, we had plans to use a Sulfo SBED biotin transfer reagent which could have been more efficacious for isolating the L4 receptor/s considering the weak interactions observed, unfortunately due to the covid-19 pandemic we were not able to perform these experiments. This Sulfo SBED biotin transfer reagent first crosslinks the bait peptide to the prey through primary amines, after which the biotin is transferred to the prey protein (in our case the receptor), where it can be isolated using streptavidin and analysed using mass spectrometry or visualized through western blot using a HRP conjugated streptavidin antibody. This process removes the problems caused by the complex disassociating during cell lysis, as it is the receptor which is biotinylated rather than the peptide.

Intracellular invasion is one of the virulence traits that allow *P. gingivalis* to survive the local host immune response and colonise the sub gingival niche (Lamont *et al.*, 1995). Naylor *et al* (2017) provided a step forward in understanding the role of OmpA in *P. gingivalis* host-pathogen interactions, by identifying the importance of the surface loop peptides in cell adhesion and invasion. The next important step is the identification of the receptor/s of these loops. Once the receptor/s have been identified, this will give a better understanding on how *P. gingivalis* invade cells and provide the potential for novel treatment options to be developed by interrupting this peptide-receptor interaction.

7.3 The *ompH* chaperone proteins: further understandings into their role and essentiality in *P. gingivalis*

The data from chapter four of this thesis provide a greater characterisation of *ompH1* with some conflicting results to other studies in the field, whilst also providing further evidence to support the theory that *ompH2* is essential for *P. gingivalis* viability. The importance of the *ompH* operon in host invasion interactions was first suggested by Suwannakul *et al* (2010), when the genes were overexpressed in a hyper invasive subpopulation of *P. gingivalis*. This was further evidenced by Taguchi *et al* (2015), when they showed a lack of virulence in mice

by a Δ*ompH1* mutant. Therefore, we began our study by attempting to investigate the full operon of *ompH1* and *ompH2* by making individual knockout mutants of each gene, with the plan to eventually produce a full knockout of the operon. Through attempting mutagenesis, we discovered that *ompH2* was unable to be replaced in our study, producing mutants with *ompH2* present alongside the erythromycin cassette. This single crossover event was not replicated in Δ*ompH1* indicating that *ompH2* is essential, supporting the similar claim by Taguchi *et al*.

The characterisation of Δ*ompH1* displayed multiple phenotypic changes in comparison to the wild type such as reduced growth rate, reduced adhesion and invasion and altered arginine gingipain activity. Taguchi *et al* suggest in their study that ompH1 is involved in the chaperoning of type 9 secretion system proteins such as PorU that is needed for cleavage of CTD groups and A-LPS anchoring. However, Taguchi *et al* show an almost complete loss of both gingipain proteases, whereas we only see the loss of arginine gingipain activity. With this difference in mind, it would be important to further investigate the potential role of *ompH1* in T9SS clients. Through western blot of outer membrane protein fractions using antibodies for known CTD containing proteins and T9SS pathway proteins, we could further understand the role of *ompH1* in protein chaperoning.

Interestingly the essentiality of *ompH2* is not seen in SKP protein mutants of other Gram negative bacteria such as *E. coli* and *S. typhirmurium* (Sklar *et al.*, 2007; Kapach *et al.*, 2020). In *E. coli* it is suggested by Sklar *et al* (2007), that the chaperone SurA has the most chaperone clients in *E. coli* with SKP being a more redundant system. This must not be the case for *P. gingivalis,* as viable *ompH2* mutants cannot be made. *P. gingivalis* has SurA and DegP homologues in its genome PGN_1552 and PGN_0637 (*htrA*) respectively. Knockout mutants of *htrA* have been investigated in the literature (Roy, Vanterpool and Fletcher, 2006; Yuan *et al.*, 2008), showing a role in resistance to oxidative stress. However, the outer membrane clients of SurA and DegP in *P. gingivalis* are relatively unknown. It would be interesting to investigate the client set of SurA, DegP and OmpH1 in *P. gingivalis* through individual and combined mutants. This would not only give a greater understanding of the outer membrane protein biogenesis of *P. gingivalis* but may also elucidate some of the clients of OmpH2 through the process of elimination.

As the *ompH* genes are overexpressed in the invasive sub-population of *P. gingivalis*, this indicates that their client set have important roles in invasion of host cells. Therefore, future work identifying more clients of these chaperones will point towards potentially novel virulence factors for *P. gingivalis* or give a greater understanding of the biogenesis of previously known factors.

7.4 The importance of the rhamnose biosynthesis pathway in *P. gingivalis*

The data from chapter 5 of this thesis provide strong evidence to suggest that not only is the rhamnose synthesis pathway essential to *P. gingivalis*, but it also has roles outside of the O-antigen biogenesis in the LPS.

Our work has demonstrated that disrupting the *rfbB* gene and therefore the dTDP-rhamnose synthesis in *P. gingivalis* results in the changes to multiple characteristics including virulence. Although presumed to be essential in *P. gingivalis* by Shibata *et al* (1999) who like our study, also failed to produce knockout mutants of *rfbB*, we provide evidence to suggest that we have produced a mutant with a disrupted *rfbB* gene due to upstream polar affects. Outside of the genomic sequencing we also observe that Δ*rfbB* has resulted in a truncated LPS profile, similar to a profile seen in another O-antigen sugar biosynthesis gene (*galE*) mutant of *P. gingivalis* (Nakao, Senpuku and Watanabe, 2006). However, optimally we would perform QPCR with *rfbB* primers to investigate the degree of disruption to *rfbB* expression in the mutant. QPCR and the production of a complement plasmid were started in this study and will be an important step for future work.

The disruption of *rfbB* has led to decreased growth in supplemented BHI and reduced biofilm formation, the lack of growth potentially being related to the part disruption of an essential pathway. Through antibiotic protection assays we demonstrate a clear and significant reduction in invasive capabilities of Δ*rfbB* to oral epithelial cells. Interestingly this is unlikely due to the changes in the O-antigen of *P. gingivalis,* as mutants lacking the O-antigen show no change in adhesion and invasion to gingival epithelial cells (Soto *et al.*, 2016). This indicates that there is another unknown role, potentially the rhamnose glycosylation of proteins that is causing this change in adhesion and invasion. We also observed a major reduction in the gingipain proteases of Δ*rfbB*, indicating a role of dTDP-rhamnose in the type 9 secretion system. This connection is unlikely to be caused by disrupting the anionic polysaccharide (APS) of the A-LPS, as this is composed of mannose sugars, therefore this disruption is more likely

due to disruption to the T9SS. Further investigation into this would provide a better understanding of why the gingipain proteins have been disrupted so significantly. The most important step would be to analyse the A-LPS of Δ*rfbB*, which has been achieved previously by other groups through isolation and mass spectrometry or western blot with Mab1B5 (Paramonov *et al.*, 2005).

Recently in a study by Soto *et al* (2016), they investigated the effect of the O-antigen on apoptosis in gingival epithelial cells. In the same study they showed that *P. gingivalis* isolates from patients with periodontitis had intact O-antigen, whereas strains from healthy patients lacked the O-antigen. It was observed that the O-antigen was required for the inhibition of gingival epithelial cell apoptosis, increasing the viability of the infected cells. This could be a reason for the overexpression of *rfbB* in the hyper-invasive *P. gingivalis*, producing the O-antigen during invasion to prevent the death of the infected cell. Experimentation on cell viability after infection with Δ*rfbB* would be useful to investigate whether this is the case and address another potential reason for its overexpression.

These results taken together show an importance of the rhamnose synthesis pathway in *P. gingivalis* virulence and viability that is not only specific its role in O-antigen biogenesis. The alternate role/s of dTDP-rhamnose in *P. gingivalis* are still unknown but are likely the reason for the rhamnose synthesis operon to be essential for *P. gingivalis* when it is not in other Gram negative bacteria(Jiang *et al.*, 1991; Tsukioka *et al.*, 1997).

7.5 PGN2012, the TolC channel protein of the CzcCBA heavy metal efflux operon of *P. gingivalis*

The final chapter of this thesis focused on the characterisation of *PGN2012,* predicted to be a TolC channel protein belonging to a putative heavy metal resistance RND tripartite pump. The roles of the TolC channel proteins of *P. gingivalis* are relatively undefined, with only a few studies investigating their role in antibiotic resistance (Ikeda and Yoshimura, 2002; Inoue *et al.*, 2015), or showing increased expression in the presence of hemin (Veith *et al.*, 2018). We show in this study novel characterisation of *PGN2012* focusing on virulence and heavy metal sensitivity. The initial reason for studying this gene, like the other genes investigated in this thesis is due to its overexpression in the previously mentioned hyper invasive subpopulation. However, when investigating known virulence factors of *P. gingivalis* such as biofilm formation, gingipain activity, adhesion, and invasion we saw no significant changes to the wild

type. This was not completely unexpected; the role of efflux proteins is often the removal of toxic compounds and therefore we were not surprised by the lack of effect on the mechanisms behind adhesion and invasion. Although the gene regulation was not determined in this study, we know from Suwannakul *et al* (2010) that *PGN2012* is overexpressed after being subjected to the intracellular environment indicating that during this time it is beneficial for *PGN2012* to be synthesized. Therefore, there is the potential that *PGN2012* is required for greater survivability in the intracellular environment. Testing this through multiple means would provide valuable insight into the role of *PGN2012* during cellular invasion. To do this, it would be best to look at long term internalization experiments with Δ*PGN2012* and wild type *P. gingivalis*. Doing this both the intracellular survival and the expression of *PGN2012* could be analysed giving a greater understanding of the regulation and role of *PGN2012*.

We show for the first time that the *PGN2012* operon is involved in the resistance of zinc, cobalt, and cadmium divalent cations. The current annotated genome of ATCC 33277 *P. gingivalis* labels *PGN2012* as being upstream of a CusA/CzcA RND efflux pump, referring to the copper resistance and cadmium, cobalt, zinc resistance RND operons in other bacteria respectively(Mergeay *et al.*, 1985; Franke *et al.*, 2003). However, our data suggests that *PGN2012* operon is representative of the CzcCBA system and not CusCBA, as we see no change to copper sensitivity in Δ*PGN2012* in comparison to the wild type. The substrate specificity of RND efflux pumps is notoriously promiscuous, which is often the reason for multi-drug resistance (Wong *et al.*, 2014). Therefore, we performed preliminary screening for multiple antibiotics, but found no changes. It would be beneficial to investigate this further with more antibiotics and more metals such as nickel, to see if there is substrate promiscuity in *PGN2012.*

If *PGN2012* was confirmed to be involved with intracellular survival and therefore be influential in the infection capability of *P. gingivalis*, it could prove useful as a target for therapeutic treatment when treating *P. gingivalis* infections and periodontal disease. The role of efflux pumps in antibiotic resistance has made them an important research topic for the future of bacterial infection treatments. There have been studies investigating the potential of co-treatment of bacteria with antibiotics and efflux pump inhibitors (EPI), thereby preventing the antibiotic resistance by inhibiting the pumps. An early study by Lomovskaya *et al* (2001), investigated potential EPI's of the three AcrAB-tolC like efflux pumps in

Pseudomonas aeruginosa. Lomovskaya *et al* discovered that one of the EPI's investigated MC-207,110 (later called Phe-Arg β-naphthylamide (PAβN)) inhibited Mex-AB-OprM efflux and produced increased sensitivity to levofloxacin, working as a competitive inhibitor. Similar results were shown by Kinana *et al* (2016), they demonstrated PaβN inhibits the AcrAB-TolC efflux system through competitively inhibiting the efflux pump AcrB, resulting in the decreased efflux of nitrocefin through AcrB. The potential of PaβN or similar EPIs to inhibit *PGN2012* efflux would be interesting to explore, if the increased intracellular survivability suspected to be provided by *PGN2012* could be inhibited by EPI's, this would be a potential co-treatment in periodontal disease therapy.

7.6 Hyper-invasive *P. gingivalis*: more pieces for the virulence puzzle

The initial work by Suwannakul *et al* (2010) presented evidence of 19 genes that were potentially influential in *P. gingivalis*' adhesion and invasion capabilities. This work and the role of *ompA* from other bacteria in adhesion and invasion of human cells prompted Naylor *et al* (2017) to investigate the *ompA* genes. Through combining the results from this study and the data from Naylor *et al* we now have a better understanding of the systems employed by *P. gingivalis* to effectively invade host cells.

First contact with host cells comes from the outer membrane of *P. gingivalis*, specifically the LPS and protein complexes present there. Through the work of Naylor *et al* the importance of ompA in host cell binding and invasion was demonstrated, with the peptide loops on the outer surface being influential on the interaction with host cells. OmpA is one of the outer membrane proteins predicted to be chaperoned by the Skp like chaperone proteins *ompH1* and *ompH2*. Our work on *ompH1* has displayed the importance of this chaperone in the adhesion and invasion of oral epithelial cells, indicating the biosynthesis of outer membrane proteins as an important factor during host-pathogen interaction. These results display the importance of outer membrane proteins as the first interaction for adhesion and invasion of human epithelial cells, which explains the reason *ompA1, ompA2, ompH1,* and *ompH2* are overexpressed in the invasive population. Further to this, our work on *rfbB* also demonstrated significant changes in the adhesion and invasion of human epithelial cells. As the O-antigen has been demonstrated by Soto *et al* (2016) to not be essential for *P. gingivalis* to bind and invade gingival epithelial cells, the change in invasion by *rfbB* is therefore more likely due to the changes of proteins in the outer membrane, as seen with the loss of the gingipain

proteases. Taken together, these results indicate the importance of the *ompA*, *ompH*, and *rfbB* genes in the initial adhesion and invasion of host cells, and the biosynthesis of outer membrane proteins in this interaction.

This is not the case for *PGN2012*, which showed no role in the mechanism of *P. gingivalis* invasion of human epithelial cells. We have demonstrated in this study the efflux ability of *PGN2012,* whilst also presenting preliminary data linked to oxidative stress resistance. Therefore, we predict the reason for the overexpression of *PGN2012* in the hyper invasive subpopulation is linked to intracellular survival.

Overall we are developing a greater understanding of the role of the overexpressed gene set identified by Suwannakul *et al* (2010), which will lead to further knowledge of the wider invasive process of *P. gingivalis*. We have demonstrated that although these genes are indicated to be influential of adhesion and invasion, some of the genes may have alternate roles that aid with maintaining *P.* gingivalis' viability during or after invasion.

7.7 Conclusion

The work in this thesis investigated the L4 peptide and multiple genes predicted to be involved in host-pathogen interactions, working to characterise common virulence factors whilst also delving into factors specific to each gene. Specifically showing that *ompH1* and *rfbB* have direct roles in the adhesion and invasion of oral epithelial cells, whilst indicating an ulterior role for *PGN2012* in survival. Each chapter has provided its own challenges and future questions to investigate. We have provided further evidence that suggest *ompH1* is involved with the type 9 secretion system through the loss of the arginine gingipains, however further investigation into its clients through screening for CTD and T9SS proteins in its outer membrane would elucidate this further. *rfbB* has seemingly been disrupted resulting in major phenotypic changes in growth, biofilm formation, LPS profile, adhesion, invasion and gingipain activity. Providing evidence to suggest that the rhamnose synthesis pathway is not only needed for O-antigen biogenesis, but also viability and host-pathogen interactions. We have also demonstrated for the first time that *PGN2012* is a TolC channel protein for the CzcCBA system in *P. gingivalis*, although why it is overexpressed in host-pathogen interactions remains unknown but could be due to intracellular survivability.

The results of this study taken together show the complexity of the invasion system used by *P. gingivalis*. Applying multiple genes in the effective adhesion and invasion of the host cell, whilst also making itself more suitable for the intracellular niche.

This thesis has contributed to a greater understanding of multiple genes in *P. gingivalis* that are linked to virulence. In the hope that the better we understand the virulence and invasion strategies of *P. gingivalis*, the better treatments and therapeutics can be developed to treat periodontal disease in the future.

References

Aedekerk, S. *et al.* (2005) 'The MexGHI-OpmD multidrug efflux pump controls growth, antibiotic susceptibility and virulence in *Pseudomonas aeruginosa* via 4-quinolone-dependent cell-to-cell communication', *Microbiology*. doi: 10.1099/mic.0.27631-0.

Afseth, J. (1983) 'Some aspects of the dynamics of Cu and Zn retained in plaque as related to their effect on plaque pH', *European Journal of Oral Sciences*, 91(3). doi: 10.1111/j.1600-0722.1983.tb00797.x.

Akiyama, T. *et al.* (2014) '*Porphyromonas gingivalis*-derived lysine gingipain enhances osteoclast differentiation induced by tumor necrosis factor-α and interleukin-1β but suppresses that by interleukin-17, *Journal of Biological Chemistry*. doi: 10.1074/jbc.M113.520510.

Al-Qutub, M. N. *et al.* (2006) 'Hemin-dependent modulation of the lipid A structure of *Porphyromonas gingivalis* lipopolysaccharide', *Infection and Immunity*. doi: 10.1128/IAI.01924-05.

Alav, I. *et al.* (2021) 'Structure, Assembly, and Function of Tripartite Efflux and Type 1 Secretion Systems in Gram-Negative Bacteria', *Chemical Reviews*. doi: 10.1021/acs.chemrev.1c00055.

Alav, I., Sutton, J. M. and Rahman, K. M. (2018) 'Role of bacterial efflux pumps in biofilm formation', *Journal of Antimicrobial Chemotherapy*. doi: 10.1093/jac/dky042.

Amano, A. *et al.* (1998) 'Binding of *Porphyromonas gingivalis* fimbriae to proline-rich glycoproteins in parotid saliva via a domain shared by major salivary components', *Infection and Immunity*, 66(5). doi: 10.1128/iai.66.5.2072-2077.1998.

Amano, A. *et al.* (1999) 'Molecular interactions of *Porphyromonas gingivalis* fimbriae with host proteins: Kinetic analyses based on surface plasmon resonance', *Infection and Immunity*. doi: 10.3189/172756408784700680.

Bainbridge, B. *et al.* (2010) 'Role of *Porphyromonas gingivalis* phosphoserine phosphatase enzyme SerB in inflammation, immune response, and induction of alveolar bone resorption in rats', *Infection and Immunity*. doi: 10.1128/IAI.00703-10.

Bassler, B. L., Wright, M. and Silverman, M. R. (1994) 'Multiple signalling systems controlling expression of luminescence in *Vibrio harveyi*: sequence and function of genes encoding a second sensory pathway', *Molecular Microbiology*, 13(2). doi: 10.1111/j.1365-2958.1994.tb00422.x.

Beikler, T. *et al.* (2003) 'Prevalence of *Porphyromonas gingivalis* fimA genotypes in Caucasians', *European Journal of Oral Sciences*. doi: 10.1034/j.1600-0722.2003.00065.x.

Bertani, B. and Ruiz, N. (2018) 'Function and Biogenesis of Lipopolysaccharides', *EcoSal Plus*, 8(1). doi: 10.1128/ecosalplus.esp-0001-2018.

Bingham, C. O. and Moni, M. (2013) 'Periodontal disease and rheumatoid arthritis: The evidence accumulates for complex pathobiologic interactions', *Current Opinion in Rheumatology*. doi: 10.1097/BOR.0b013e32835fb8ec.

Blanco, P. *et al.* (2016) 'Bacterial Multidrug Efflux Pumps: Much More Than Antibiotic Resistance Determinants', *Microorganisms*. doi: 10.3390/microorganisms4010014.

Bosshardt, D. D. (2018) 'The periodontal pocket: pathogenesis, histopathology and consequences', *Periodontology 2000*. doi: 10.1111/prd.12153.

Bradshaw, D. J. *et al.* (1998) 'Role of *Fusobacterium nucleatum* and coaggregation in anaerobe survival in planktonic and biofilm oral microbial communities during aeration.', *Infection and immunity*, 66(10), pp. 4729–4732.

Bramanti, T. E. *et al.* (1989) 'Chemical characterization and biologic properties of lipopolysaccharide from *Bacteroides gingivalis* strains W50, W83, and ATCC 33277', *Oral Microbiology and Immunology*. doi: 10.1111/j.1399-302X.1989.tb00250.x.

Bratu, S. *et al.* (2009) 'Correlation of the expression of acrB and the regulatory genes marA, soxS and ramA with antimicrobial resistance in clinical isolates of *Klebsiella pneumoniae* endemic to New York City', *Journal of Antimicrobial Chemotherapy*, 64(2). doi: 10.1093/jac/dkp186.

Brown, L. *et al.* (2015) 'Through the wall: Extracellular vesicles in Gram-positive bacteria, mycobacteria and fungi', *Nature Reviews Microbiology*. doi: 10.1038/nrmicro3480.

Carrion, J. *et al.* (2012) 'Microbial Carriage State of Peripheral Blood Dendritic Cells (DCs) in Chronic Periodontitis Influences DC Differentiation, Atherogenic Potential', *The Journal of Immunology*. doi: 10.4049/jimmunol.1201053.

Cecil, J. D. *et al.* (2017) 'Outer membrane vesicles prime and activate macrophage inflammasomes and cytokine secretion in vitro and in vivo', *Frontiers in Immunology*. doi: 10.3389/fimmu.2017.01017.

Cekici, A. *et al.* (2014) 'Inflammatory and immune pathways in the pathogenesis of periodontal disease', *Periodontology 2000*, 64(1). doi: 10.1111/prd.12002.

Chai, T. jyi and Foulds, J. (1977) 'Purification of protein A, an outer membrane component missing in *Escherichia coli* K-12 ompA mutants', *BBA - Protein Structure*, 493(1), pp. 210–215. doi: 10.1016/0005-2795(77)90274-4.

Chen, C. *et al.* (2018) 'Oral microbiota of periodontal health and disease and their changes after nonsurgical periodontal therapy', *ISME Journal*, 12(5). doi: 10.1038/s41396-017-0037-1.

Chen, H. A. *et al.* (1995) 'Immunodominant antigens of *Porphyromonas gingivalis* in patients with rapidly progressive periodontitis', *Oral Microbiology and Immunology*. doi: 10.1111/j.1399-302X.1995.tb00142.x.

Chen, T. *et al.* (2001) '*Porphyromonas gingivalis* gingipains and adhesion to epithelial cells', *Infection and Immunity*. doi: 10.1128/IAI.69.5.3048-3056.2001.

Chen, T. and Duncan, M. J. (2004) 'Gingipain adhesin domains mediate *Porphyromonas gingivalis* adherence to epithelial cells', *Microb.Pathog.*, 36(0882-4010 (Print)), pp. 205–209. Available at: pm:15001226.

Chung, W. O. *et al.* (2001) 'Signaling system in *Porphyromonas gingivalis* based on a luxS protein', *Journal of Bacteriology*, 183(13). doi: 10.1128/JB.183.13.3903-3909.2001.

Confer, A. W. and Ayalew, S. (2013) 'The OmpA family of proteins: Roles in bacterial pathogenesis and immunity', *Veterinary Microbiology*, pp. 207–222. doi: 10.1016/j.vetmic.2012.08.019.

Corgiat, B. A., Nordman, J. C. and Kabbani, N. (2014) 'Chemical crosslinkers enhance detection of receptor interactomes', *Frontiers in Pharmacology*. doi: 10.3389/fphar.2013.00171.

Cugini, C. *et al.* (2019) 'The Role of Exopolysaccharides in Oral Biofilms', *Journal of Dental Research*. doi: 10.1177/0022034519845001.

Curtis, M. A. *et al.* (1991) 'Identification of the major surface protein antigens of *Porphyromonas gingivalis* using IgG antibody reactivity of periodontal case-control serum', *Oral Microbiology and Immunology*. doi: 10.1111/j.1399-302X.1991.tb00502.x.

Curtis, Michael A *et al.* (1999) 'Variable carbohydrate modifications to the catalytic chains of the RgpA and RgpB proteases of *Porphyromonas gingivalis* W50.', *Infection and immunity*, 67(8), pp. 3816–3823. doi: 10.1111/j.1365-2958.2005.04871.x.

Curtis, Michael A. *et al.* (1999) 'Variable carbohydrate modifications to the catalytic chains of the RgpA and RgpB proteases of *Porphyromonas gingivalis* W50', *Infection and Immunity*. doi: 10.1128/iai.67.8.3816-3823.1999.

Curtis, M. A., Diaz, P. I. and Van Dyke, T. E. (2020) 'The role of the microbiota in periodontal disease', *Periodontology 2000*. doi: 10.1111/prd.12296.

Darveau, R. P. *et al.* (1998) 'Local chemokine paralysis, a novel pathogenic mechanism for *Porphyromonas gingivalis*', *Infect.Immun.*, 66(0019-9567 (Print) LA-eng PT-Journal Article PT-Research Support, U.S. Gov't, P.H.S RN-0 (Interleukin-8) RN-0 (RNA, Messenger) SB-IM), pp. 1660–1665. Available at: pm:9529095.

Darveau, R. P. *et al.* (2004) '*Porphyromonas gingivalis* lipopolysaccharide contains multiple lipid A species that functionally interact with both toll-like receptors 2 and 4.', *Infection and immunity*, 72(9), pp. 5041–5051. doi: 10.1128/IAI.72.9.5041-5051.2004.

Daury, L. *et al.* (2016) 'Tripartite assembly of RND multidrug efflux pumps', *Nature Communications*. doi: 10.1038/ncomms10731.

Deleon-Pennell, K. Y., Brï¿½s, L. E. d. C. and Lindsey, M. L. (2013) 'Circulating *Porphyromonas gingivalis* lipopolysaccharide resets cardiac homeostasis in mice through a matrix metalloproteinase-9-dependent mechanism', *Physiological Reports*. doi: 10.1002/phy2.79.

Diels, L., Mergeay, M. and Regniers, L. (1988) 'Structure and function of plasmids governing resistance to heavy metals in *Alcaligenes eutrophus* CH34', *MEDED. FAK. LANDBOUWWET. R. U. GENT*.

Dominy, S, S. *et al.* (2019) '*Porphyromonas gingivalis* in Alzheimer's disease brains: Evidence for disease causation and treatment with small-molecule inhibitors', *Science advances*, 5(1).

Dong, C. *et al.* (2003) 'A structural perspective on the enzymes that convert dTDP-D-glucose into dTDP-L-rhamnose', in *Biochemical Society Transactions*. doi: 10.1042/BST0310532.

Dong, H. *et al.* (2017) 'Structural and functional insights into the lipopolysaccharide ABC transporter LptB2FG', *Nature Communications*, 8(1). doi: 10.1038/s41467-017-00273-5.

Douglas, C W Ian *et al.* (2014) 'Physiological adaptations of key oral bacteria.', *Advances in microbial physiology*. Edited by R. K. Poole, 65, pp. 257–335. doi: 10.1016/bs.ampbs.2014.08.005.

Douglas, C. W.Ian *et al.* (2014) 'Physiological Adaptations of Key Oral Bacteria', *Advances in Microbial Physiology*. doi: 10.1016/bs.ampbs.2014.08.005.

Du, D. *et al.* (2014) 'Structure of the AcrAB-TolC multidrug efflux pump', *Nature*, 509(7501). doi: 10.1038/nature13205.

Du, D. *et al.* (2018) 'Multidrug efflux pumps: structure, function and regulation', *Nature Reviews Microbiology*. doi: 10.1038/s41579-018-0048-6.

Ducret, V. *et al.* (2020) 'The CzcCBA Efflux System Requires the CadA P-Type ATPase for Timely Expression Upon Zinc Excess in Pseudomonas aeruginosa', *Frontiers in Microbiology*, 11. doi: 10.3389/fmicb.2020.00911.

Duncan, L. *et al.* (2004) 'Loss of lipopolysaccharide receptor CD14 from the surface of human macrophage-like cells mediated by *Porphyromonas gingivalis* outer membrane vesicles', *Microbial Pathogenesis*. doi: 10.1016/j.micpath.2004.02.004.

Duong, F. *et al.* (1994) 'The *Pseudomonas fluorescens* lipase has a C-terminal secretion signal and is secreted by a three-component bacterial ABC-exporter system', *Molecular Microbiology*, 11(6). doi: 10.1111/j.1365-2958.1994.tb00388.x.

Economou, A. and Wickner, W. (1994) 'SecA promotes preprotein translocation by undergoing ATP-driven cycles of membrane insertion and deinsertion', *Cell*, 78(5). doi: 10.1016/S0092-8674(94)90582-7.

Enersen, M., Nakano, K. and Amano, A. (2013) '*Porphyromonas gingivalis* fimbriae', *Journal of Oral Microbiology*. doi: 10.3402/jom.v5i0.20265.

Entzminger, K. C. *et al.* (2012) 'The Skp chaperone helps fold soluble proteins in vitro by inhibiting aggregation', *Biochemistry*. doi: 10.1021/bi300412y.

Ezraty, B. *et al.* (2017) 'Oxidative stress, protein damage and repair in bacteria', *Nature Reviews Microbiology*. doi: 10.1038/nrmicro.2017.26.

Farid, S. S., Azizi, G. and Mirshafiey, A. (2013) 'Anti-citrullinated protein antibodies and their clinical utility in rheumatoid arthritis', *International Journal of Rheumatic Diseases*. doi: 10.1111/1756-185X.12129.

Farrugia, C., Stafford, G. P. and Murdoch, C. (2020) '*Porphyromonas gingivalis* Outer Membrane Vesicles Increase Vascular Permeability', *Journal of Dental Research*, 99(13). doi: 10.1177/0022034520943187.

Franke, S. *et al.* (2003) 'Molecular analysis of the copper-transporting efflux system CusCFBA of Escherichia coli', *Journal of Bacteriology*. doi: 10.1128/JB.185.13.3804-3812.2003.

Franke S, Grass, G. and Nies, D. H. (2001) 'The product of the ybdE gene of the Escherichia coli chromosome is involved in detoxification of silver ions', *Microbiology*, 147(4). doi: 10.1099/00221287-147-4-965.

Fraud, S. and Poole, K. (2011) 'Oxidative stress induction of the MexXY multidrug efflux genes and promotion of aminoglycoside resistance development in *Pseudomonas aeruginosa*', *Antimicrobial Agents and Chemotherapy*, 55(3). doi: 10.1128/AAC.01495-10.

Frias-Lopez, J. and Duran-Pinedo, A. (2012) 'Effect of periodontal pathogens on the metatranscriptome of a healthy multispecies biofilm model', *Journal of Bacteriology*. doi: 10.1128/JB.06328-11.

Frias, J., Olle, E. and Alsina, M. (2001) 'Periodontal pathogens produce quorum sensing signal molecules', *Infection and Immunity*, 69(5). doi: 10.1128/IAI.69.5.3431-3434.2001.

Garib, B. T. and Qaradaxi, S. S. (2011) 'Temporomandibular joint problems and periodontal condition in rheumatoid arthritis patients in relation to their rheumatologic status', *Journal of Oral and Maxillofacial Surgery*. doi: 10.1016/j.joms.2011.02.131.

Ge, X. *et al.* (2014) 'DegP primarily functions as a protease for the biogenesis of β-barrel outer membrane proteins in the Gram-negative bacterium *Escherichia coli*', *FEBS Journal*, 281(4). doi: 10.1111/febs.12701.

Genco, R. J. and Borgnakke, W. S. (2013) 'Risk factors for periodontal disease.', *Periodontology 2000*, 62(1), pp. 59–94. doi: 10.1111/j.1600-0757.2012.00457.x.

Gerits, E., Verstraeten, N. and Michiels, J. (2017) 'New approaches to combat *Porphyromonas gingivalis* biofilms', *Journal of Oral Microbiology*, 9(1). doi: 10.1080/20002297.2017.1300366.

Gillis, R. J. *et al.* (2005) 'Molecular basis of azithromycin-resistant *Pseudomonas aeruginosa* biofilms', *Antimicrobial Agents and Chemotherapy*. doi: 10.1128/AAC.49.9.3858-3867.2005.

Goebel, W. and Hedgpeth, J. (1982) 'Cloning and functional characterization of the plasmid-encoded hemolysin determinant of *Escherichia coli*', *Journal of Bacteriology*, 151(3). doi: 10.1128/jb.151.3.1290-1298.1982.

Goldberg, M. *et al.* (1999) 'Energetics and topology of CzcA, a cation/proton antiporter of the resistance-nodulation-cell division protein family', *Journal of Biological Chemistry*, 274(37). doi: 10.1074/jbc.274.37.26065.

Gonzalez, M. R. *et al.* (2019) '*Pseudomonas aeruginosa* zinc homeostasis: Key issues for an opportunistic pathogen', *Biochimica et Biophysica Acta - Gene Regulatory Mechanisms*. doi: 10.1016/j.bbagrm.2018.01.018.

Gonzalez, S. M. *et al.* (2015) 'Alveolar Bone Loss Is Associated With Circulating Anti-Citrullinated Protein Antibody (ACPA) in Patients With Rheumatoid Arthritis', *Journal of Periodontology*. doi: 10.1902/jop.2014.140425.

Gorasia, D. G. *et al.* (2016) 'Structural Insights into the PorK and PorN Components of the *Porphyromonas gingivalis* Type IX Secretion System', *PLoS Pathogens*, 12(8). doi: 10.1371/journal.ppat.1005820.

Gorasia, D. G., Veith, P. D. and Reynolds, E. C. (2020) 'The type IX secretion system: Advances in structure, function and organisation', *Microorganisms*. doi: 10.3390/microorganisms8081173.

Grenier, D. *et al.* (2001) 'Role of gingipains in growth of *Porphyromonas gingivalis* in the presence of human serum albumin', *Infection and Immunity*, 69(8). doi: 10.1128/IAI.69.8.5166-5172.2001.

Grossman, A. *et al.* (2020) 'Description of a widespread bacterial secretion system with chemically diverse substrates', *biorXiv*.

Guo, Y., Nguyen, K.-A. and Potempa, J. (2010) 'Dichotomy of gingipains action as virulence factors: from cleaving substrates with the precision of a surgeon's knife to a meat chopper-like brutal degradation of proteins.', *Periodontology 2000*, 54(1), pp. 15–44. doi: 10.1111/j.1600-0757.2010.00377.x.

Hailman, E. *et al.* (1994) 'Lipopolysaccharide (LPS)-binding protein accelerates the binding of LPS to CD14', *Journal of Experimental Medicine*. doi: 10.1084/jem.179.1.269.

Hajishengallis, George *et al.* (2011) 'Low-abundance biofilm species orchestrates inflammatory periodontal disease through the commensal microbiota and complement', *Cell Host and Microbe*. doi: 10.1016/j.chom.2011.10.006.

Hajishengallis, G *et al.* (2011) 'Low-abundance biofilm species orchestrates inflammatory periodontal disease through the commensal microbiota and complement', *Cell Host and Microbe*, 10(5), pp. 497–506. Available at: http://www.scopus.com/inward/record.url?eid=2-s2.0-81755166205&partnerID=40&md5=e552580edbbaeacddb710573bc1e289c.

Hajishengallis, G., Darveau, Richard P. and Curtis, M. A. (2012) 'The keystone-pathogen hypothesis', *Nature Reviews Microbiology*. doi: 10.1038/nrmicro2873.

Hajishengallis, G. and Lamont, R. J. (2012) 'Beyond the red complex and into more complexity: the polymicrobial synergy and dysbiosis (PSD) model of periodontal disease etiology.', *Molecular oral microbiology*, 27(6), pp. 409–419. doi: 10.1111/j.2041-1014.2012.00663.x.

Hassan, M. e. T. *et al.* (1999) 'Identification of a gene cluster, czr, involved in cadmium and zinc resistance in *Pseudomonas aeruginosa*', *Gene*, 238(2). doi: 10.1016/S0378-1119(99)00349-2.

Hasturk, H. *et al.* (2006) 'RvE1 protects from local inflammation and osteoclastmediated bone destruction in periodontitis', *The FASEB Journal*, 20(2). doi: 10.1096/fj.05-4724fje.

Hasturk, H. *et al.* (2007) 'Resolvin E1 Regulates Inflammation at the Cellular and Tissue Level and Restores Tissue Homeostasis In Vivo', *The Journal of Immunology*, 179(10). doi: 10.4049/jimmunol.179.10.7021.

Haurat, M. F. *et al.* (2011) 'Selective sorting of cargo proteins into bacterial membrane vesicles.', *The Journal of biological chemistry*, 286(2), pp. 1269–1276. doi: 10.1074/jbc.M110.185744.

Hendrickson, E. L. *et al.* (2009) 'Pathway analysis for intracellular *Porphyromonas gingivalis* using a strain ATCC 33277 specific database', *BMC Microbiology*. doi: 10.1186/1471-2180-9-185.

Herath, T. D. K. *et al.* (2013) 'Tetra- and Penta-Acylated Lipid A Structures of *Porphyromonas gingivalis* LPS Differentially Activate TLR4-Mediated NF-κB Signal Transduction Cascade and Immuno-Inflammatory Response in Human Gingival Fibroblasts', *PLoS ONE*. doi: 10.1371/journal.pone.0058496.

Hobbs, E. C. *et al.* (2012) 'Conserved small protein associates with the multidrug efflux pump AcrB and differentially affects antibiotic resistance', *Proceedings of the National Academy of Sciences of the United States of America*, 109(41). doi: 10.1073/pnas.1210093109.

Horiyama, T. and Nishino, K. (2014) 'AcrB, AcrD, and MdtABC multidrug efflux systems are involved in enterobactin export in *Escherichia coli*', *PLoS ONE*, 9(9). doi: 10.1371/journal.pone.0108642.

Hounsome, J. D. A. *et al.* (2011) 'Outer membrane protein a of bovine and ovine isolates of *Mannheimia haemolytica* is surface exposed and contains host Species-Specific Epitopes', *Infection and Immunity*. doi: 10.1128/IAI.05469-11.

How, K. Y., Song, K. P. and Chan, K. G. (2016) '*Porphyromonas gingivalis*: An overview of periodontopathic pathogen below the gum line', *Frontiers in Microbiology*. doi: 10.3389/fmicb.2016.00053.

Huang, R., Li, M. and Gregory, R. L. (2011) 'Bacterial interactions in dental biofilm.', *Virulence*, 2(5), pp. 435–444. doi: 10.4161/viru.2.5.16140.

Hutcherson, J. A. *et al.* (2015) '*Porphyromonas gingivalis* RagB is a proinflammatory signal transducer and activator of transcription 4 agonist', *Molecular Oral Microbiology*. doi: 10.1111/omi.12089.

Ide, M. *et al.* (2016) 'Periodontitis and cognitive decline in Alzheimer's disease', *PLoS ONE*, 11(3). doi: 10.1371/journal.pone.0151081.

Ikeda, T. and Yoshimura, F. (2002) 'A resistance-nodulation-cell division family xenobiotic efflux pump in an obligate anaerobe, *Porphyromonas gingivalis*', *Antimicrobial Agents and Chemotherapy*. doi: 10.1128/AAC.46.10.3257-3260.2002.

Inomata, M., Horie, T. and Into, T. (2018) 'OmpA-like proteins of *Porphyromonas gingivalis* contribute to serum resistance and prevent Toll-like receptor 4-mediated host cell activation', *PLoS ONE*, 13(8), pp. 1–16. doi: 10.1371/journal.pone.0202791.

Inoue, T. *et al.* (2015) 'Characterization of the tripartite drug efflux pumps of *Porphyromonas gingivalis* ATCC 33277', *New Microbiologica*.

Ishida, N. *et al.* (2017) 'Periodontitis induced by bacterial infection exacerbates features of Alzheimer's disease in transgenic mice', *npj Aging and Mechanisms of Disease*, 3(1). doi: 10.1038/s41514-017-0015-x.

Jarchow, S. *et al.* (2008) 'Identification of potential substrate proteins for the periplasmic *Escherichia coli* chaperone Skp', *Proteomics*. doi: 10.1002/pmic.200800288.

Jiang, Q. *et al.* (2000) 'Cutting Edge: Lipopolysaccharide Induces Physical Proximity Between CD14 and Toll-Like Receptor 4 (TLR4) Prior to Nuclear Translocation of NF- B', *The Journal of Immunology*. doi: 10.4049/jimmunol.165.7.3541.

Jiang, X. -M *et al.* (1991) 'Structure and sequence of the rfb (O antigen) gene cluster of *Salmonella serovar typhimurium* (strain LT2)', *Molecular Microbiology*, 5(3). doi: 10.1111/j.1365-2958.1991.tb00741.x.

Jo, J. T. H., Brinkman, F. S. L. and Hancock, R. E. W. (2003) 'Aminoglycoside efflux in *Pseudomonas aeruginosa*: Involvement of novel outer membrane proteins', *Antimicrobial Agents and Chemotherapy*, 47(3). doi: 10.1128/AAC.47.3.1101-1111.2003.

Johnson, J. M. and Church, G. M. (1999) 'Alignment and structure prediction of divergent protein families: Periplasmic and outer membrane proteins of bacterial efflux pumps', *Journal of Molecular Biology*, 287(3). doi: 10.1006/jmbi.1999.2630.

Jorgenson, M. A. and Young, K. D. (2016) 'Interrupting biosynthesis of O antigen or the lipopolysaccharide core produces morphological defects in *Escherichia coli* by sequestering undecaprenyl phosphate', *Journal of Bacteriology*, 198(22). doi: 10.1128/JB.00550-16.

Kadowaki, T. *et al.* (1998) 'Arg-gingipain acts as a major processing enzyme for various cell surface proteins in *Porphyromonas gingivalis*', *J.Biol.Chem.*, 273(0021-9258 (Print)), pp. 29072–29076. Available at: pm:9786913.

Kajiya, M. *et al.* (2011) '*Aggregatibacter actinomycetemcomitans* Omp29 is associated with bacterial entry to gingival epithelial cells by F-actin rearrangement', *PLoS ONE*, 6(4). doi: 10.1371/journal.pone.0018287.

Kalynych, S., Morona, R. and Cygler, M. (2014) 'Progress in understanding the assembly process of bacterial O-antigen', *FEMS Microbiology Reviews*. doi: 10.1111/1574-6976.12070.

Kanonenberg, K., Smits, S. H. J. and Schmitt, L. (2019) 'Functional Reconstitution of HlyB, a Type I Secretion ABC Transporter, in Saposin-A Nanoparticles', *Scientific Reports*, 9(1). doi: 10.1038/s41598-019-44812-0.

Kapach, G. *et al.* (2020) 'Loss of the Periplasmic Chaperone Skp and Mutations in the Efflux Pump AcrAB-TolC Play a Role in Acquired Resistance to Antimicrobial Peptides in *Salmonella typhimurium*', *Frontiers in Microbiology*, 11. doi: 10.3389/fmicb.2020.00189.

Kato, Takahiro *et al.* (2007) 'Maturation of fimbria precursor protein by exogenous gingipains in *Porphyromonas gingivalis* gingipain-null mutant', *FEMS Microbiology Letters*. doi: 10.1111/j.1574-6968.2007.00779.x.

Kaye, E. K. *et al.* (2010) 'Tooth loss and periodontal disease predict poor cognitive function in older men', *Journal of the American Geriatrics Society*, 58(4). doi: 10.1111/j.1532-5415.2010.02788.x.

Kim, S. W. *et al.* (2009) 'Serum resistance of *Acinetobacter baumannii* through the binding of factor H to outer membrane proteins', *FEMS Microbiology Letters*, 301(2). doi: 10.1111/j.1574-6968.2009.01820.x.

Kinana, A. D. *et al.* (2016) 'Aminoacyl β-naphthylamides as substrates and modulators of AcrB multidrug efflux pump', *Proceedings of the National Academy of Sciences of the United States of America*, 113(5). doi: 10.1073/pnas.1525143113.

Kinane, D. F., Stathopoulou, P. G. and Papapanou, P. N. (2017) 'Periodontal diseases', *Nature Reviews Disease Primers*. doi: 10.1038/nrdp.2017.38.

Kitamura, Y. *et al.* (2002) 'Gingipains in the culture supernatant of *Porphyromonas gingivalis* cleave CD4 and CD8 on human T cells.', *Journal of periodontal research*, 37(6), pp. 464–468.

Kolenbrander, P. E. *et al.* (2006) 'Bacterial interactions and successions during plaque development.', *Periodontology 2000*, 42(5), pp. 47–79. doi: 10.1111/j.1600-0757.2006.00187.x.

Kontani, M. *et al.* (1996) 'Cysteine protease of *Porphyromonas gingivalis* 381 enhances binding of fimbriae to cultured human fibroblasts and matrix proteins', *Infection and Immunity*, 64(3). doi: 10.1128/iai.64.3.756-762.1996.

Kopp, F., Kupsch, S. and Schromm, A. B. (2016) 'Lipopolysaccharide-binding protein is bound and internalized by host cells and colocalizes with LPS in the cytoplasm: Implications for a role of LBP in intracellular LPS-signaling', *Biochimica et Biophysica Acta - Molecular Cell Research*. doi: 10.1016/j.bbamcr.2016.01.015.

Krishnan, S. and Prasadarao, N. V. (2012) 'Outer membrane protein A and OprF: Versatile roles in Gram-negative bacterial infections', *FEBS Journal*, pp. 919–931. doi: 10.1111/j.1742-4658.2012.08482.x.

Kulp, A. and Kuehn, M. J. (2010) 'Biological Functions and Biogenesis of Secreted Bacterial Outer Membrane Vesicles', *Annual Review of Microbiology*. doi: 10.1146/annurev.micro.091208.073413.

Kuramitsu, H. K. *et al.* (2001) 'Role for Periodontal Bacteria in Cardiovascular Diseases', *Annals of Periodontology*. doi: 10.1902/annals.2001.6.1.41.

Kuzminov, A. (2011) 'Homologous Recombination—Experimental Systems, Analysis, and Significance', *EcoSal Plus*. doi: 10.1128/ecosalplus.7.2.6.

Lamont, R. J. *et al.* (1995) '*Porphyromonas gingivalis* invasion of gingival epithelial cells', *Infect.Immun.*, 63(0019-9567 (Print) LA-eng PT-Journal Article PT-Research Support, U.S. Gov't, P.H.S RN-0 (Protease Inhibitors) SB-IM), pp. 3878–3885. Available at: pm:7558295.

Larsen, T. (2002) 'Susceptibility of *Porphyromonas gingivalis* in biofilms to amoxicillin, doxycycline and metronidazole.', *Oral microbiology and immunology*, 17(5), pp. 267–271. Available at: http://www.ncbi.nlm.nih.gov/pubmed/12354206.

Lasica, A. M. *et al.* (2017) 'The Type IX Secretion System (T9SS): Highlights and Recent Insights into Its Structure and Function', *Frontiers in Cellular and Infection Microbiology*. doi: 10.3389/fcimb.2017.00215.

Lebeaux, D., Ghigo, J.-M. and Beloin, C. (2014) 'Biofilm-Related Infections: Bridging the Gap between Clinical Management and Fundamental Aspects of Recalcitrance toward Antibiotics', *Microbiology and Molecular Biology Reviews*. doi: 10.1128/mmbr.00013-14.

Lenders, M. H. H. *et al.* (2015) 'Directionality of substrate translocation of the hemolysin A Type I secretion system', *Scientific Reports*, 5. doi: 10.1038/srep12470.

Lewis, J. P. *et al.* (1999) 'Hemoglobinase Activity of the Lysine Gingipain Protease (Kgp) of *Porphyromonas gingivalis* W83'.

Liang, S. *et al.* (2011) 'The C5a receptor impairs IL-12-dependent clearance of *Porphyromonas gingivalis* and is required for induction of periodontal bone loss.', *Journal of immunology (Baltimore, Md. : 1950)*, 186(2), pp. 869–877. doi: 10.4049/jimmunol.1003252.

Liccardo, D. *et al.* (2020) 'Potential Bidirectional Relationship Between Periodontitis and Alzheimer's Disease', *Frontiers in Physiology*. doi: 10.3389/fphys.2020.00683.

Lin, X., Wu, J. and Xie, H. (2006) '*Porphyromonas gingivalis* minor fimbriae are required for cell-cell interactions.', *Infection and immunity*, 74(10), pp. 6011–6015. doi: 10.1128/IAI.00797-06.

Lombardi, C. *et al.* (2019) 'Structural and functional characterization of the type three secretion system (T3SS) needle of *pseudomonas aeruginosa*', *Frontiers in Microbiology*, 10(MAR). doi: 10.3389/fmicb.2019.00573.

Lomovskaya, O. *et al.* (2001) 'Identification and characterization of inhibitors of multidrug resistance efflux pumps in *Pseudomonas aeruginosa*: Novel agents for combination therapy', *Antimicrobial Agents and Chemotherapy*, 45(1). doi: 10.1128/AAC.45.1.105-116.2001.

Lomovskaya, O., Lewis, K. and Matin, A. (1995) 'EmrR is a negative regulator of the *Escherichia coli* multidrug resistance pump emrAB', *Journal of Bacteriology*, 177(9). doi: 10.1128/jb.177.9.2328-2334.1995.

Lourbakos, A. *et al.* (2001) 'Arginine-specific protease from *Porphyromonas gingivalis* activates protease-activated receptors on human oral epithelial cells and induces interleukin-6 secretion', *Infection and Immunity*. doi: 10.1128/IAI.69.8.5121-5130.2001.

Lu, Y. C., Yeh, W. C. and Ohashi, P. S. (2008) 'LPS/TLR4 signal transduction pathway', *Cytokine*. doi: 10.1016/j.cyto.2008.01.006.

Ma, D. *et al.* (1995) 'Genes acrA and acrB encode a stress-induced efflux system of *Escherichia coli*', *Molecular Microbiology*, 16(1). doi: 10.1111/j.1365-2958.1995.tb02390.x.

Madej, M. *et al.* (2019) 'Dynamic oligopeptide acquisition by the RagAB transporter from *Porphyromonas gingivalis*', *Nature Microbiology*. doi: 10.1101/755678.

Madej, M. *et al.* (2021) 'Porz, an essential component of the type ix secretion system of *Porphyromonas gingivalis*, delivers anionic lipopolysaccharide to the poru sortase for transpeptidase processing of t9ss cargo proteins', *mBio*, 12(1). doi: 10.1128/mBio.02262-20.

Maekawa, T. *et al.* (2014) '*Porphyromonas gingivalis* manipulates complement and TLR signaling to uncouple bacterial clearance from inflammation and promote dysbiosis', *Cell Host and Microbe*. doi: 10.1016/j.chom.2014.05.012.

Majithia, V. and Geraci, S. A. (2007) 'Rheumatoid Arthritis: Diagnosis and Management', *The American Journal of Medicine*. doi: 10.1016/j.amjmed.2007.04.005.

Maresz, K. J. *et al.* (2013) '*Porphyromonas gingivalis* Facilitates the Development and Progression of Destructive Arthritis through Its Unique Bacterial Peptidylarginine Deiminase (PAD)', *PLoS Pathogens*. doi: 10.1371/journal.ppat.1003627.

Mark, B. M. and Zhu, Y. (2013) 'Gliding motility and por secretion system genes are widespread among members of the phylum bacteroidetes', *Journal of Bacteriology*, 195(2). doi: 10.1128/JB.01962-12.

Marolda, C. L. and Valvano, M. A. (1995) 'Genetic analysis of the dTDP-rhamnose biosynthesis region of the *Escherichia coli* VW187 (O7:K1) rfb gene cluster: Identification of functional homologs of rfbB and rfbA in the rff cluster and correct location of the rffE gene', *Journal of Bacteriology*. doi: 10.1128/jb.177.19.5539-5546.1995.

Marsh, P. D. (2003) 'Are dental diseases examples of ecological catastrophes?', *Microbiology (Reading, England)*, 149(Pt 2), pp. 279–294. Available at: http://www.ncbi.nlm.nih.gov/pubmed/12624191.

Martinez, E. *et al.* (2014) 'Identification of OmpA, a *Coxiella burnetii* Protein Involved in Host Cell Invasion, by Multi-Phenotypic High-Content Screening', *PLoS Pathogens*, 10(3). doi: 10.1371/journal.ppat.1004013.

Matsumura, K. *et al.* (2011) 'Roles of multidrug efflux pumps on the biofilm formation of *Escherichia coli* K-12', *Biocontrol Science*. doi: 10.4265/bio.16.69.

McGraw, W. T. *et al.* (1999) 'Purification, characterization, and sequence analysis of a potential virulence factor from *Porphyromonas gingivalis*, peptidylarginine deiminase.', *Infection and immunity*.

Meghil, M. M. *et al.* (2019) 'Disruption of Immune Homeostasis in Human Dendritic Cells via Regulation of Autophagy and Apoptosis by *Porphyromonas gingivalis*', *Frontiers in Immunology*, 10. doi: 10.3389/fimmu.2019.02286.

Mergeay, M. *et al.* (1985) '*Alcaligenes eutrophus* CH34 is a facultative chemolithotroph with plasmid-bound resistance to heavy metals', *Journal of Bacteriology*. doi: 10.1128/jb.162.1.328-334.1985.

Mikolajczyk-Pawlinska, J., Travis, J. and Potempa, J. (1998) 'Modulation of interleukin-8 activity by gingipains from *Porphyromonas gingivalis*: Implications for pathogenicity of periodontal disease', *FEBS Letters*. doi: 10.1016/S0014-5793(98)01461-6.

Miles, A. A., Misra, S. S. and Irwin, J. O. (1938) 'The estimation of the bactericidal power of the blood', *Journal of Hygiene*, 38(6). doi: 10.1017/S002217240001158X.

Miller, M. B. and Bassler, B. L. (2001) 'Quorum sensing in bacteria', *Annual Review of Microbiology.*

Mistou, M. Y., Sutcliffe, I. C. and Van Sorge, N. M. (2016) 'Bacterial glycobiology: Rhamnose-containing cell wall polysaccharides in gram-positive bacteria', *FEMS Microbiology Reviews*. doi: 10.1093/femsre/fuw006.

Miteva, Y. V., Budayeva, H. G. and Cristea, I. M. (2013) 'Proteomics-based methods for discovery, quantification, and validation of protein-protein interactions', *Analytical Chemistry*, pp. 749–768. doi: 10.1021/ac3033257.

Mombelli, A. (2018) 'Microbial colonization of the periodontal pocket and its significance for periodontal therapy', *Periodontology 2000*. doi: 10.1111/prd.12147.

Morita, Y. *et al.* (2001) 'Roles of MexXY- and MexAB-multidrug efflux pumps in intrinsic multidrug resistance of *Pseudomonas aeruginosa* PAO1', *Journal of General and Applied Microbiology*, 47(1). doi: 10.2323/jgam.47.27.

Murakami, Y. *et al.* (2002) 'Separation of the outer membrane and identification of major outer membrane proteins from *Porphyromonas gingivalis*.', *European journal of oral sciences*, 110(2), pp. 157–162.

Murray, G. L., Attridge, S. R. and Morona, R. (2003) 'Regulation of *Salmonella typhimurium* lipopolysaccharide O antigen chain length is required for virulence; identification of FepE as a second Wzz', *Molecular Microbiology*, 47(5). doi: 10.1046/j.1365-2958.2003.03383.x.

Na, H. S. *et al.* (2020) 'Identification of Potential Oral Microbial Biomarkers for the Diagnosis of Periodontitis', *Journal of Clinical Medicine*, 9(5). doi: 10.3390/jcm9051549.

Nagano, K. *et al.* (2005) 'Trimeric structure of major outer membrane proteins homologous to OmpA in *Porphyromonas gingivalis*', *Journal of Bacteriology*. doi: 10.1128/JB.187.3.902-911.2005.

Nagano, K. *et al.* (2012) '*Porphyromonas gingivalis* FimA fimbriae: Roles of the fim gene cluster in the fimbrial assembly and antigenic heterogeneity among fimA genotypes', *Journal of Oral Biosciences*. doi: 10.1016/j.job.2012.07.002.

Nagano, K. *et al.* (2015) 'A major fimbrilin variant of Mfa1 fimbriae in *Porphyromonas gingivalis*', *Journal of Dental Research*. doi: 10.1177/0022034515588275.

Nagl, M. *et al.* (2002) 'Phagocytosis and killing of bacteria by professional phagocytes and dendritic cells', *Clinical and Diagnostic Laboratory Immunology*, 9(6). doi: 10.1128/CDLI.9.6.1165-1168.2002.

Naito, M. *et al.* (2019) 'PGN_0297 is an essential component of the type IX secretion system (T9SS) in *Porphyromonas gingivalis*: Tn-seq analysis for exhaustive identification of T9SS-related genes', *Microbiology and Immunology*, 63(1). doi: 10.1111/1348-0421.12665.

Nakagawa, I. *et al.* (2002) 'Functional differences among FimA variants of *Porphyromonas gingivalis* and their effects on adhesion to and invasion of human epithelial cells', *Infection and Immunity*. doi: 10.1128/IAI.70.1.277-285.2002.

Nakamura, T. *et al.* (1999) 'Specific interactions between *Porphyromonas gingivalis* fimbriae and human extracellular matrix proteins', *FEMS Microbiology Letters*. doi: 10.1016/S0378-1097(99)00205-0.

Nakano, K. *et al.* (2004) 'Comparison of inflammatory changes caused by *Porphyromonas gingivalis* with distinct fimA genotypes in a mouse abscess model', *Oral Microbiology and Immunology*. doi: 10.1111/j.0902-0055.2004.00133.x.

Nakano, K. *et al.* (2009) 'Detection of oral bacteria in cardiovascular specimens', *Oral Microbiology and Immunology*. doi: 10.1111/j.1399-302X.2008.00479.x.

Nakao, R. *et al.* (2012) 'Enhanced Biofilm Formation by *Escherichia coli* LPS Mutants Defective in Hep Biosynthesis', *PLoS ONE*. doi: 10.1371/journal.pone.0051241.

Nakao, R., Senpuku, H. and Watanabe, H. (2006) '*Porphyromonas gingivalis* galE is involved in lipopolysaccharide O-antigen synthesis and biofilm formation', *Infection and Immunity*. doi: 10.1128/IAI.00261-06.

Nakayama, K. *et al.* (1996) 'Involvement of arginine-specific cysteine proteinase (Arg-gingipain) in fimbriation of *Porphyromonas gingivalis*', *J.Bacteriol.*, 178(0021-9193 (Print)

Nativel, B. *et al.* (2017) '*Porphyromonas gingivalis* lipopolysaccharides act exclusively through TLR4 with a resilience between mouse and human', *Scientific Reports*. doi: 10.1038/s41598-017-16190-y.

Naylor, K. L. *et al.* (2017) 'Role of OmpA2 surface regions of *Porphyromonas gingivalis* in host–pathogen interactions with oral epithelial cells', *MicrobiologyOpen*. doi: 10.1002/mbo3.401.

Ngkelo, A. *et al.* (2012) 'LPS induced inflammatory responses in human peripheral blood mononuclear cells is mediated through NOX4 and G iα dependent PI-3kinase signalling', *Journal of Inflammation*. doi: 10.1186/1476-9255-9-1.

Nies, D. *et al.* (1987) 'Cloning of plasmid genes encoding resistance to cadmium, zinc, and cobalt in *Alcaligenes eutrophus* CH34', *Journal of Bacteriology*, 169(10). doi: 10.1128/jb.169.10.4865-4868.1987.

Nies, D. H. (1992) 'CzcR and CzcD, gene products affecting regulation of resistance to cobalt, zinc, and cadmium (czc system) in *Alcaligenes eutrophus*', *Journal of Bacteriology*, 174(24). doi: 10.1128/jb.174.24.8102-8110.1992.

Nies, D. H. (2003) 'Efflux-mediated heavy metal resistance in prokaryotes', *FEMS Microbiology Reviews*. doi: 10.1016/S0168-6445(03)00048-2.

Noinaj, N., Gumbart, J. C. and Buchanan, S. K. (2017) 'The β-barrel assembly machinery in motion', *Nature Reviews Microbiology*. doi: 10.1038/nrmicro.2016.191.

O-Brien-Simpson, N. M. *et al.* (2003) '*Porphyromonas gingivalis* gingipains: the molecular teeth of a microbial vampire', *Current Protein & Peptide Science*. doi: 10.2174/1389203033487009.

Oido-Mori, M. *et al.* (2001) '*Porphyromonas gingivalis* gingipain-R enhances interleukin-8 but decreases gamma interferon-inducible protein 10 production by human gingival fibroblasts in response to T-cell contact', *Infection and Immunity*. doi: 10.1128/IAI.69.7.4493-4501.2001.

Okuda, K., Slots, J. and Genco, R. J. (1981) '*Bacteroides gingivalis, Bacteroides asaccharolyticus, and Bacteroides melaninogenicus subspecies*: Cell surface morphology and adherence to erythrocytes and human buccal epithelial cells', *Current Microbiology*. doi: 10.1007/BF01566718.

Olczak, T. *et al.* (2005) 'Iron and heme utilization in *Porphyromonas gingivalis*', *FEMS Microbiology Reviews*. doi: 10.1016/j.femsre.2004.09.001.

Oliveira, F. A. F. *et al.* (2015) 'Molecular Analysis of Oral Bacteria in Heart Valve of Patients With Cardiovascular Disease by Real-Time Polymerase Chain Reaction.', *Medicine*. doi: 10.1097/MD.0000000000002067.

Olsen, I., Lambris, J. D. and Hajishengallis, G. (2017) '*Porphyromonas gingivalis* disturbs host–commensal homeostasis by changing complement function', *Journal of Oral Microbiology*. doi: 10.1080/20002297.2017.1340085.

Palmer, T. *et al.* (2021) 'A holin/peptidoglycan hydrolase-dependent protein secretion system', *Molecular Microbiology*. doi: 10.1111/mmi.14599.

Palomino, C., Marín, E. and Fernández, L. Á. (2011) 'The fimbrial usher FimD follows the surA-BamB pathway for its assembly in the outer membrane of *Escherichia coli*', *Journal of Bacteriology*, 193(19). doi: 10.1128/JB.05585-11.

Papanikou, E. *et al.* (2004) 'Helicase Motif III in SecA is essential for coupling preprotein binding to translocation ATPase.', *EMBO reports*, 5(8), pp. 807–811. doi: 10.1038/sj.embor.7400206.

Paramonov, N. *et al.* (2001) 'Structural analysis of the polysaccharide from the lipopolysaccharide of *Porphyromonas gingivalis* strain W50', *European Journal of Biochemistry*, 268(17). doi: 10.1046/j.1432-1327.2001.02397.x.

Paramonov, N. *et al.* (2005) 'Structural analysis of a novel anionic polysaccharide from *Porphyromonas gingivalis* strain W50 related to Arg-gingipain glycans.', *Molecular microbiology*, 58(3), pp. 847–863. doi: 10.1111/j.1365-2958.2005.04871.x.

Park, Y. *et al.* (2005) 'Short Fimbriae of *Porphyromonas gingivalis* and Their Role in Coadhesion with *Streptococcus gordonii*', 73(7), pp. 3983–3989. doi: 10.1128/IAI.73.7.3983.

Pearson, J. P., Van Delden, C. and Iglewski, B. H. (1999) 'Active efflux and diffusion are involved in transport of *Pseudomonas aeruginosa* cell-to-cell signals', *Journal of Bacteriology*. doi: 10.1128/jb.181.4.1203-1210.1999.

Phaniendra, A., Jestadi, D. B. and Periyasamy, L. (2015) 'Free Radicals: Properties, Sources, Targets, and Their Implication in Various Diseases', *Indian Journal of Clinical Biochemistry*. doi: 10.1007/s12291-014-0446-0.

Plančak, D., Musić, L. and Puhar, I. (2015) 'Quorum sensing of periodontal pathogens', *Acta Stomatologica Croatica*, 49(3). doi: 10.15644/asc49/3/6.

Poole, S. *et al.* (2013) 'Determining the presence of periodontopathic virulence factors in short-term postmortem Alzheimer's disease brain tissue.', *Journal of Alzheimer's disease : JAD*, 36(4), pp. 665–677. doi: 10.3233/JAD-121918.

Prasadarao, N. V. *et al.* (1996) 'Outer membrane protein A of *Escherichia coli* contributes to invasion of brain microvascular endothelial cells', *Infection and Immunity*.

Prasadarao, N. V. (2002) 'Identification of *Escherichia coli* outer membrane protein A receptor on human brain microvascular endothelial cells', *Infection and Immunity*. doi: 10.1128/IAI.70.8.4556-4563.2002.

Preshaw, P. M. *et al.* (2012) 'Periodontitis and diabetes: A two-way relationship', *Diabetologia*. doi: 10.1007/s00125-011-2342-y.

Raetz, C. R. H. and Whitfield, C. (2002) 'Lipopolysaccharide Endotoxins', *Annual Review of Biochemistry*. doi: 10.1146/annurev.biochem.71.110601.135414.

Rangarajan, M. *et al.* (2008) 'Identification of a second lipopolysaccharide in *Porphyromonas gingivalis* W50.', *Journal of bacteriology*, 190(8), pp. 2920–2932. doi: 10.1128/JB.01868-07.

Rangarajan, M. *et al.* (2017) 'Hemin binding by *Porphyromonas gingivalis* strains is dependent on the presence of A-LPS', *Molecular Oral Microbiology*. doi: 10.1111/omi.12178.

Rees, D. C., Johnson, E. and Lewinson, O. (2009) 'ABC transporters: The power to change', *Nature Reviews Molecular Cell Biology*. doi: 10.1038/nrm2646.

Rôças, I. N. *et al.* (2001) '"Red complex" (*Bacteroides forsythus, Porphyromonas gingivalis, and Treponema denticola*) in endodontic infections: A molecular approach', *Oral Surgery, Oral Medicine, Oral Pathology, Oral Radiology, and Endodontics*. doi: 10.1067/moe.2001.114379.

Roier, S. *et al.* (2016) 'A novel mechanism for the biogenesis of outer membrane vesicles in Gram-negative bacteria', *Nature Communications*. doi: 10.1038/ncomms10515.

Rollauer, S. E. *et al.* (2015) 'Outer membrane protein biogenesis in Gram-negative bacteria', *Philosophical Transactions of the Royal Society B: Biological Sciences*. doi: 10.1098/rstb.2015.0023.

Rosenberg, E. Y. *et al.* (2003) 'Bile salts and fatty acids induce the expression of *Escherichia coli* AcrAB multidrug efflux pump through their interaction with Rob regulatory protein', *Molecular Microbiology*. doi: 10.1046/j.1365-2958.2003.03531.x.

Roy, F., Vanterpool, E. and Fletcher, H. M. (2006) 'HtrA in *Porphyromonas gingivalis* can regulate growth and gingipain activity under stressful environmental conditions.', *Microbiology (Reading, England)*, 152(Pt 11), pp. 3391–3398. doi: 10.1099/mic.0.29147-0.

Ruoslahti, E. (1996) 'RGD AND OTHER RECOGNITION SEQUENCES FOR INTEGRINS', *Annual Review of Cell and Developmental Biology*. doi: 10.1146/annurev.cellbio.12.1.697.

Ryder, M. I. *et al.* (2012) 'Periodontal disease in HIV/AIDS', *Periodontology 2000*. doi: 10.1111/j.1600-0757.2012.00445.x.

Säemann, M. D. *et al.* (2009) 'The multifunctional role of mTOR in innate immunity: Implications for transplant immunity', *American Journal of Transplantation*. doi: 10.1111/j.1600-6143.2009.02832.x.

Saier, M. H. *et al.* (1994) 'Two novel families of bacterial membrane proteins concerned with nodulation, cell division and transport', *Molecular Microbiology*. doi: 10.1111/j.1365-2958.1994.tb00362.x.

Sato, K. *et al.* (2005) 'Identification of a new membrane-associated protein that influences transport/maturation of gingipains and adhesins of *Porphyromonas gingivalis*.', *The Journal of biological chemistry*, 280(10), pp. 8668–8677. doi: 10.1074/jbc.M413544200.

Schaefer, A. L. *et al.* (1996) 'Quorum sensing in Vibrio fischeri: Probing autoinducer-LuxR interactions with autoinducer analogs', *Journal of Bacteriology*, 178(10). doi: 10.1128/jb.178.10.2897-2901.1996.

Schembri, M. A., Kjærgaard, K. and Klemm, P. (2003) 'Global gene expression in *Escherichia coli* biofilms', *Molecular Microbiology*. doi: 10.1046/j.1365-2958.2003.03432.x.

Scheres, N. *et al.* (2011) 'Periodontal ligament and gingival fibroblasts from periodontitis patients are more active in interaction with *Porphyromonas gingivalis*', *Journal of Periodontal Research*. doi: 10.1111/j.1600-0765.2011.01353.x.

Schiffrin, B. *et al.* (2016) 'Skp is a multivalent chaperone of outer-membrane proteins', *Nature Structural and Molecular Biology*, 23(9), pp. 786–793. doi: 10.1038/nsmb.3266.

Schulze, W. X. and Mann, M. (2004) 'A Novel Proteomic Screen for Peptide-Protein Interactions', *Journal of Biological Chemistry*. doi: 10.1074/jbc.M309909200.

Scott, D. A. and Krauss, J. L. (2011) 'Neutrophils in periodontal inflammation', in *Periodontal Disease*. doi: 10.1159/000329672.

Seers, C. a *et al.* (2006) 'The RgpB C-terminal domain has a role in attachment of RgpB to the outer membrane and belongs to a novel C-terminal-domain family found in *Porphyromonas gingivalis*.', *Journal of bacteriology*, 188(17), pp. 6376–6386. doi: 10.1128/JB.00731-06.

Shah, H. N. and Collins, M. D. (1988) 'Proposal for Reclassification of *Bacteroides asaccharolyticus*, *Bacteroides gingivalis, and Bacteroides endodontalis* in a New Genus, Porphyromonas', *International Journal of Systematic Bacteriology*. doi: 10.1099/00207713-38-1-128.

Shahan, T. A. *et al.* (1999) 'Identification of CD47/integrin-associated protein and alpha(v)beta3 as two receptors for the alpha3(IV) chain of type IV collagen on tumor cells.', *Cancer Research*, 59(18), pp. 4584–4590.

Sharma, D., Misba, L. and Khan, A. U. (2019) 'Antibiotics versus biofilm: An emerging battleground in microbial communities', *Antimicrobial Resistance and Infection Control*. doi: 10.1186/s13756-019-0533-3.

Shi, X. *et al.* (2007) 'The rag locus of *Porphyromonas gingivalis* contributes to virulence in a murine model of soft tissue destruction.', *Infection and immunity*, 75(4), pp. 2071–2074. doi: 10.1128/IAI.01785-06.

Shi, Y. *et al.* (1999) 'Genetic analyses of proteolysis, hemoglobin binding, and hemagglutination of *Porphyromonas gingivalis*: Construction of mutants with a combination of rgpA, rgpB, kgp, and hagA', *Journal of Biological Chemistry*, 274(25). doi: 10.1074/jbc.274.25.17955.

Shibata, Y. *et al.* (1999) 'Isolation and characterization of the rml gene homologs from Porphyromonas gingivalis', *Oral Microbiology and Immunology*. doi: 10.1034/j.1399-302X.1999.140602.x.

Shields, P. A. and Farrah, S. R. (1983) 'Influence of salts on electrostatic interactions between poliovirus and membrane filters', *Applied and Environmental Microbiology*, 45(2). doi: 10.1128/aem.45.2.526-531.1983.

Shin, S. *et al.* (2005) '*Escherichia coli* outer membrane protein A adheres to human brain microvascular endothelial cells', *Biochemical and Biophysical Research Communications*, 330(4). doi: 10.1016/j.bbrc.2005.03.097.

Shoji, M. *et al.* (2002) 'Construction and characterization of a nonpigmented mutant of *Porphyromonas gingivalis*: cell surface polysaccharide as an anchorage for gingipains The GenBank/EMBL/DDBJ accession number for the sequences reported in this paper is D64132.', *Microbiology*, 148(4). doi: 10.1099/00221287-148-4-1183.

Silhavy, T. J., Ruiz, N. and Kahne, D. (2006) 'Advances in understanding bacterial outer-membrane biogenesis', *Nature Reviews Microbiology*. doi: 10.1038/nrmicro1322.

Siqueira, J. F., Alves, F. R. F. and Rôças, I. N. (2011) 'Pyrosequencing analysis of the apical root canal microbiota.', *Journal of endodontics*, 37(11), pp. 1499–1503. doi: 10.1016/j.joen.2011.08.012.

Sklar, J. G. *et al.* (2007) 'Defining the roles of the periplasmic chaperones SurA, Skp, and DegP in *Escherichia coli*', *Genes and Development*, 21(19). doi: 10.1101/gad.1581007.

Smalley, J. W. *et al.* (1998) 'The periodontopathogen Porphyromonas gingivalis binds iron protoporphyrin IX in the μ-oxo dimeric form : an oxidative buffer and possible pathogenic mechanism', *Biochem. J*. doi: http://dx.doi.org/10.1016/j.jconrel.2011.10.036.

Smalley, J. W. *et al.* (2004) 'A combination of both arginine- and lysine-specific gingipain activity of *Porphyromonas gingivalis* is necessary for the generation of the micro-oxo bishaem-containing pigment from haemoglobin.', *The Biochemical journal*, 379(Pt 3), pp. 833–840. doi: 10.1042/BJ20031221.

Smalley, J. W. *et al.* (2007) 'Sequential action of R- and K-specific gingipains of *Porphyromonas gingivalis* in the generation of the heam-containing pigment from oxyhaemoglobin', *Archives of Biochemistry and Biophysics*. doi: 10.1016/j.abb.2007.05.011.

Smani, Y. *et al.* (2014) 'Role of OmpA in the multidrug resistance phenotype of *Acinetobacter baumannii*', *Antimicrobial Agents and Chemotherapy*, 58(3). doi: 10.1128/AAC.02101-13.

Smith, S. G. J., Mahon, V., Lambert, M. a, *et al.* (2007) 'A molecular Swiss army knife: OmpA structure, function and expression.', *FEMS microbiology letters*, 273(1), pp. 1–11. doi: 10.1111/j.1574-6968.2007.00778.x.

Socransky, S. S. *et al.* (1998) 'Microbial complexes in subgingival plaque', *Journal of Clinical Periodontology*. doi: 10.1111/j.1600-051X.1998.tb02419.x.

Soto, C. *et al.* (2016) 'The *Porphyromonas gingivalis* O antigen is required for inhibition of apoptosis in gingival epithelial cells following bacterial infection', *Journal of periodontal research*. doi: 10.1111/jre.12331.

Spiess, C., Beil, A. and Ehrmann, M. (1999) 'A temperature-dependent switch from chaperone to protease in a widely conserved heat shock protein', *Cell*, 97(3). doi: 10.1016/S0092-8674(00)80743-6.

Stafford, P. *et al.* (2013) 'Gingipain-dependent degradation of mammalian target of rapamycin pathway proteins by the periodontal pathogen *Porphyromonas gingivalis* during invasion.', *Molecular oral microbiology*, 28(5), pp. 366–378. doi: 10.1111/omi.12030.

Sulavik, M. C. *et al.* (2001) 'Antibiotic susceptibility profiles of *Escherichia coli* strains lacking multidrug efflux pump genes', *Antimicrobial Agents and Chemotherapy*, 45(4). doi: 10.1128/AAC.45.4.1126-1136.2001.

Suwannakul, S *et al.* (2010) 'Identification of bistable populations of *Porphyromonas gingivalis* that differ in epithelial cell invasion.', *Microbiology (Reading, England)*, 156(Pt 10), pp. 3052–3064. doi: 10.1099/mic.0.038075-0.

Sweet, M. J. and Hume, D. A. (1996) 'Endotoxin signal transduction in macrophages', *Journal of Leukocyte Biology*. doi: 10.1002/jlb.60.1.8.

Swietnicki, W. and Caspi, R. (2021) 'Prediction of selected biosynthetic pathways for the lipopolysaccharide components in *porphyromonas gingivalis*', *Pathogens*, 10(3). doi: 10.3390/pathogens10030374.

Taguchi, Y. *et al.* (2015) 'Involvement of an Skp-like protein, PGN_0300, in the type IX secretion system of *Porphyromonas gingivalis*', *Infection and Immunity*. doi: 10.1128/IAI.01308-15.

Tam, V. *et al.* (2009) 'The RgpA-Kgp proteinase-adhesin complexes of *Porphyromonas gingivalis* Inactivate the Th2 cytokines interleukin-4 and interleukin-5.', *Infection and immunity*, 77(4), pp. 1451–1458. doi: 10.1128/IAI.01377-08.

Thakur, A., Mikkelsen, H. and Jungersen, G. (2019) 'Intracellular pathogens: Host immunity and microbial persistence strategies', *Journal of Immunology Research*. doi: 10.1155/2019/1356540.

Theilade, E. *et al.* (1966) 'Experimental gingivitis in man: II. A Longitudinal Clinical and Bacteriological Investigation', *Journal of Periodontal Research*, 1(1). doi: 10.1111/j.1600-0765.1966.tb01842.x.

Thurlow, L. R. *et al.* (2011) ' *Staphylococcus aureus* Biofilms Prevent Macrophage Phagocytosis and Attenuate Inflammation In Vivo ', *The Journal of Immunology*. doi: 10.4049/jimmunol.1002794.

Tonetti, M. S., Greenwell, H. and Kornman, K. S. (2018) 'Staging and grading of periodontitis: Framework and proposal of a new classification and case definition', *Journal of periodontology*, 89. doi: 10.1002/JPER.18-0006.

Tribble, Gena D. *et al.* (2012) 'Natural competence is a major mechanism for horizontal DNA transfer in the oral pathogen *Porphyromonas gingivalis*', *mBio*. doi: 10.1128/mBio.00231-11.

Tsuda, K. *et al.* (2005) 'Molecular Dissection of Internalization of *Porphyromonas gingivalis* by Cells using Fluorescent Beads Coated with Bacterial Membrane Vesicle', 91, pp. 81–91.

Tsuda, K. *et al.* (2008) 'Functional analysis of alpha5beta1 integrin and lipid rafts in invasion of epithelial cells by *Porphyromonas gingivalis* using fluorescent beads coated with bacterial membrane vesicles', *Cell Struct.Funct.*, 33(1347-3700 (Electronic)), pp. 123–132. Available at: pm:18388398.

Tsukioka, Y. *et al.* (1997) 'Biological function of the dTDP-rhamnose synthesis pathway in *Streptococcus mutans*', *Journal of Bacteriology*. doi: 10.1128/jb.179.4.1126-1134.1997.

Varela, J. C. and Tomlinson, S. (2015) 'Complement. An Overview for the Clinician', *Hematology/Oncology Clinics of North America*. doi: 10.1016/j.hoc.2015.02.001.

Veith, Paul D *et al.* (2014) '*Porphyromonas gingivalis* Outer Membrane Vesicles Exclusively Contain Outer Membrane and Periplasmic Proteins and Carry a Cargo Enriched with Virulence Factors.', *Journal of proteome research*. doi: 10.1021/pr401227e.

Veith, P. D. *et al.* (2018) 'Outer Membrane Vesicle Proteome of *Porphyromonas gingivalis* Is Differentially Modulated Relative to the Outer Membrane in Response to Heme Availability', *Journal of Proteome Research*. doi: 10.1021/acs.jproteome.8b00153.

van Venrooij, W. J. and Pruijn, G. J. M. (2000) 'Citrullination: A small change for a protein with great consequences for rheumatoid arthritis', *Arthritis Research*. doi: 10.1186/ar95.

Venter, H. *et al.* (2015) 'RND-type drug efflux pumps from Gram-negative bacteria: Molecular mechanism and inhibition', *Frontiers in Microbiology*. doi: 10.3389/fmicb.2015.00377.

Walton, T. A. *et al.* (2009) 'The cavity-chaperone Skp protects its substrate from aggregation but allows independent folding of substrate domains', *Proceedings of the National Academy of Sciences of the United States of America*, 106(6). doi: 10.1073/pnas.0809275106.

Wandersman, C. and Delepelaire, P. (1990) 'TolC, an *Escherichia coli* outer membrane protein required for hemolysin secretion', *Proceedings of the National Academy of Sciences of the United States of America*, 87(12). doi: 10.1073/pnas.87.12.4776.

Wang, X. *et al.* (2020) '*Stenotrophomonas maltophilia* outer membrane protein A induces epithelial cell apoptosis via mitochondrial pathways', *Journal of Microbiology*, 58(10). doi: 10.1007/s12275-020-0235-9.

Wang, Z. *et al.* (2017) 'An allosteric transport mechanism for the AcrAB-TolC multidrug efflux pump', *eLife*, 6. doi: 10.7554/eLife.24905.

White, D. G. *et al.* (1997) 'Role of the acrAB locus in organic solvent tolerance mediated by expression of marA, soxS, or robA in *Escherichia coli*', *Journal of Bacteriology*, 179(19). doi: 10.1128/jb.179.19.6122-6126.1997.

Wong, K. *et al.* (2014) 'Towards understanding promiscuity in multidrug efflux pumps', *Trends in Biochemical Sciences*. doi: 10.1016/j.tibs.2013.11.002.

World Health Organization (WHO) (2016) 'WHO | Antimicrobial resistance: global report on surveillance 2014', *Antimicrobial resistance: global report on surveillance 2014*.

Wu, C. J. *et al.* (2018) 'Role of smeU1VWU2X operon in alleviation of oxidative stresses and occurrence of sulfamethoxazole-trimethoprim-resistant mutants in *stenotrophomonas maltophilia*', *Antimicrobial Agents and Chemotherapy*, 62(2). doi: 10.1128/AAC.02114-17.

Wyss-Coray, T. and Rogers, J. (2012) 'Inflammation in Alzheimer disease-A brief review of the basic science and clinical literature', *Cold Spring Harbor Perspectives in Medicine*, 2(1). doi: 10.1101/cshperspect.a006346.

Xie, H. (2015) 'Biogenesis and function of *Porphyromonas gingivalis* outer membrane vesicles', *Future Microbiology*. doi: 10.2217/fmb.15.63.

Yamaguchi, M. *et al.* (2010) 'A *Porphyromonas gingivalis* mutant defective in a putative glycosyltransferase exhibits defective biosynthesis of the polysaccharide portions of lipopolysaccharide, decreased gingipain activities, strong autoaggregation, and increased biofilm formation', *Infection and Immunity*. doi: 10.1128/IAI.00071-10.

Yilmaz, O., Watanabe, K. and Lamont, R. J. (2002) 'Involvement of integrins in fimbriae-mediated binding and invasion by *Porphyromonas gingivalis*', *Cell Microbiol.*, 4(1462-5814 (Print)), pp. 305–314. Available at: pm:12027958.

Ying, Y. C. *et al.* (2007) 'Control of quorum sensing by a *Burkholderia pseudomallei* multidrug efflux pump', *Journal of Bacteriology*. doi: 10.1128/JB.00003-07.

Yuan, L. *et al.* (2008) '*Porphyromonas gingivalis* HtrA is involved in cellular invasion and in vivo survival', *Microbiology*, 154(4). doi: 10.1099/mic.0.2007/015131-0.

Zeituni, A. E. *et al.* (2009) 'Targeting of DC-SIGN on Human Dendritic Cells by Minor Fimbriated *Porphyromonas gingivalis* Strains Elicits a Distinct Effector T Cell Response', *The Journal of Immunology*. doi: 10.4049/jimmunol.0901030.

Zgurskaya, H. I. *et al.* (2011) 'Mechanism and function of the outer membrane channel TolC in multidrug resistance and physiology of enterobacteria', *Frontiers in Microbiology*. doi: 10.3389/fmicb.2011.00189.

Zhang, W. *et al.* (2013) 'Integrin α5β1-fimbriae binding and actin rearrangement are essential for *Porphyromonas gingivalis* invasion of osteoblasts and subsequent activation of the JNK pathway.', *BMC microbiology*, 13. doi: 10.1186/1471-2180-13-5.

Zheng, C., Wu, J. and Xie, H. (2011) 'Differential expression and adherence of *Porphyromonas gingivalis* FimA genotypes', *Molecular Oral Microbiology*. doi: 10.1111/j.2041-1014.2011.00626.x.

Zhou, L. *et al.* (1998) 'On the origin of membrane vesicles in Gram-negative bacteria', *FEMS Microbiology Letters*. doi: 10.1016/S0378-1097(98)00147-5.